

**GEOCHEMICAL CHARACTERISATION OF THE LATE
CRETACEOUS COAL AND MUDSTONES FROM GOMBE
FORMATION, GONGOLA SUB-BASIN, NORTHERN BENUE
TROUGH, NIGERIA**

AYINLA HABEEB AYOOLA

**FACULTY OF SCIENCE
UNIVERSITY OF MALAYA
KUALA LUMPUR**

2018

**GEOCHEMICAL CHARACTERISATION OF THE
LATE CRETACEOUS COAL AND MUDSTONES FROM
GOMBE FORMATION, GONGOLA SUB-BASIN,
NORTHERN BENUE TROUGH, NIGERIA**

AYINLA HABEEB AYOOLA

**THESIS SUBMITTED IN FULFILMENT OF THE
REQUIREMENTS FOR THE DEGREE OF
DOCTOR OF PHILOSOPHY IN PETROLEUM
GEOLOGY**

**DEPARTMENT OF GEOLOGY
FACULTY OF SCIENCE
UNIVERSITY OF MALAYA
KUALA LUMPUR**

2018

UNIVERSITY OF MALAYA
ORIGINAL LITERARY WORK DECLARATION

Name of Candidate: **Ayinla Habeeb Ayoola**

Name of Degree: **Doctor of Philosophy**

Title of Project Paper/Research Report/Dissertation/Thesis ("this Work"):

**GEOCHEMICAL CHARACTERISATION OF THE LATE CRETACEOUS
COAL AND MUDSTONES FROM GOMBE FORMATION, GONGOLA SUB-
BASIN, NORTHERN BENUE TROUGH, NIGERIA.**

Field of Study: **Petroleum Geology**

I do solemnly and sincerely declare that:

- (1) I am the sole author/writer of this Work;
- (2) This Work is original;
- (3) Any use of any work in which copyright exists was done by way of fair dealing and for permitted purposes and any excerpt or extract from, or reference to or reproduction of any copyright work has been disclosed expressly and sufficiently and the title of the Work and its authorship have been acknowledged in this Work;
- (4) I do not have any actual knowledge nor do I ought reasonably to know that the making of this work constitutes an infringement of any copyright work;
- (5) I hereby assign all and every rights in the copyright to this Work to the University of Malaya ("UM"), who henceforth shall be owner of the copyright in this Work and that any reproduction or use in any form or by any means whatsoever is prohibited without the written consent of UM having been first had and obtained;
- (6) I am fully aware that if in the course of making this Work I have infringed any copyright whether intentionally or otherwise, I may be subject to legal action or any other action as may be determined by UM.

Candidate's Signature

Date:

Subscribed and solemnly declared before,

Witness's Signature

Date:

Name:

Designation:

**GEOCHEMICAL CHARACTERISATION OF THE LATE CRETACEOUS
COAL AND MUDSTONES FROM GOMBE FORMATION, GONGOLA SUB-
BASIN, NORTHERN BENUE TROUGH, NIGERIA**

ABSTRACT

The discovery of proven coal reserve of about 4.5 million tons and recent exploration activities at the Maiganga coal mine uncover some missing gaps in the stratigraphy of the Upper Cretaceous Gombe Formation. Therefore, there is a need to further investigate this sequence, including the organic and inorganic facies variations and distributions of the coals, mudstones and sandy-shaly sediments in the Gombe Formation, Gongola Sub-basin, Northern Benue Trough of Northeastern Nigeria. Organic and inorganic geochemical methods were used to assess the organic matter source input, paleodepositional conditions, thermal maturity, kerogen type, hydrocarbon generation potential, tectonic setting and paleoclimatic condition of the analysed Maiganga and Yaya-Ngari samples. Field observations showed four coal seams interbedded with mudstones and shales deposited in coarsening upward sequence of a deltaic environment. Evaluation based on the source rock analyses (SRA) and organic petrography reveal that Maiganga sedimentary facies is dominated by terrestrial source input of Type III kerogen. This is supported by the biomarker study suggesting land plant origin (dominance of $n\text{-C}_{27}$, $n\text{-C}_{29}$ and $n\text{-C}_{31}$) for the organic matter with minor lacustrine and marine influences, in Maiganga, that grades into predominantly mixed organic matter input of a transitional (terrestrial to marine) environment in the Yaya-Ngari area. This shows a progressive movement towards marine source input. Paleodepositional conditions of organic matters were suboxic to oxic in Maiganga, while the mixed organic matters in Yaya-Ngari were deposited in suboxic conditions. Based on organic petrology and bitumen extraction data, the Maiganga coal was distinctly observed to be immature of pre-oil generation window, while the Yaya-Ngari is in early

oil generation window. These analysed sediments are mainly gas prone based on the dominance of Type III kerogen, although the presence of Type II/III kerogen supported by the PY-GC data and relatively higher HI may indicate gas/oil potential for the Maiganga coal. On the other hand, Type IV kerogen dominated the Yaya-Ngari samples. This suggests that these shales are gas prone or do not possess any hydrocarbon generation potential as indicated by the very low HI values. The ICPMS result indicates predominantly semi-arid paleoclimatic condition and a passive continental margin setting based on the binary plots of SiO_2 versus $(\text{Al}_2\text{O}_3 + \text{K}_2\text{O} + \text{Na}_2\text{O})$ and $\log \text{SiO}_2$ versus $(\text{K}_2\text{O}/\text{Na}_2\text{O})$ for the Gongola sub-basin (shales and mudstones) samples. This is in accordance with the tectonic events of in the West and Central Africa during the Cretaceous period due to separation of South America plate. The predominating force controlling the separation of the West African plates is opening of the Atlantic Ocean in the Early Cretaceous. This data therefore, could be used as a guide for future exploration campaigns in the coal and coal bearing Formations in the Northern Benue Trough and the world at large.

Keywords: Benue Trough; Maiganga coal; Gombe Formation kerogen type; Biomarkers; Paleodepositional condition; thermal maturity; Hydrocarbon potential; Tectonic setting.

**PENILAIAN CIRI-CIRI GEOKIMA TERHADAP BATUAN ARANG DAN
BATUAN LUMPUR PADA ZAMAN AKHIR KRITASUS DARIPADA
FORMASI GOMBE, SUB-LEMBANGAN GONGOLA, PALUNG UTARA
BENUE, NIGERIA**

ABSTRAK

Penemuan rizab arang sebanyak 4.5 juta tan dan aktiviti penerokaan di kuari arang di Maiganga telah menemukan kehilangan jurang lapisan stratigrafi pada Formasi Gombe pada Kretaceous Awal. Oleh yang demikian, penyelidikan mendalam terhadap turutan ini perlu dijalankan termasuklah melibatkan organik dan bukan organik terhadap variasi fasis, taburan arang, batuan lumpur dan sedimen shal pasir di Formasi Gombe, sub-basin Gongola, palung Utara Benue, Nigeria. Kaedah geokimia organik dan bukan organik telah digunakan untuk menilai bahan organik yang terkandung, sejarah keadaan pembentukan, kematangan terma, jenis kerogen terhadap potensi pembentukan hidrokarbon, penetapan tektonik, sejarah keadaan cuaca terhadap analisis sampel di Maiganga dan Yaya-Ngari. Pemerhatian lapangan menunjukkan empat lapisan arang melapisi di antara batuan lumpur dan shal telah termendap di keadaan urutan kasar keatas di kawasan persekitaran delta. Penilaian terhadap analisis batuan sumber (SRA) and petrografi organik menunjukkan bahawa fasis sedimentari Maiganga telah didominasi oleh sumber kawasan daratan kerogen Type III. Ini disokong oleh biomarker yang menunjukkan kawasan tumbuhan (didominasi oleh $n\text{-C}_{27}$, $n\text{-C}_{29}$ and $n\text{-C}_{31}$) untuk bahan organik dengan sedikit pengaruh dari daratan dan lautan, di Maiganga, yang boleh digredkan kepada sebahagian besarnya adalah campuran bahan organik (daratan ke lautan) di persekitaran di Yaya-Ngari. Ini menunjukkan pergerakan progresif terhadap sumber lautan. Sejarah pemendapan terhadap bahan organik pula menunjukkan ianya termendap di kawasan suboxic. Berdasarkan data daripada organik petrografi dan pengekstrakan bitumen, arang Maiganga telah dikategorikan sebagai tidak matang di

tingkap penghasilan minyak, sementara itu Yaya-Ngari di kategorikan di peringkat tingkap awal penghasilan minyak. Analisis terhadap sedimen ini menunjukkan ianya cenderung kepada gas dengan didominasi oleh Type III kerogen, walaupun dengan kehadiran Type II/III kerogen telah disokong oleh data daripada PY-GC telah menunjukkan kandungan HI yang tinggi dan boleh dinyatakan sebagai potensi gas/minyak terhadap arang Maiganga. Tambahan pula, kerogen Type IV telah mendominasi sampel di Yaya-Ngari. Ini mencadangkan bahawa shal ini cenderung kepada gas dan tidak berkemungkinan berpotensi menghasilkan kerogen yang mana telah dinyatakan dengan nilai HI yang rendah. Keputusan daripada ICPMS menyatakan bahawa sebahagian besarnya berada di keadaan semi-arid dan pasif margin benua berasaskan terhadap plot binary SiO_2 lawan $(\text{Al}_2\text{O}_3 + \text{K}_2\text{O} + \text{Na}_2\text{O})$ and $\log \text{SiO}_2$ lawan $(\text{K}_2\text{O}/\text{Na}_2\text{O})$ terhadap sampel sub-basin Gongola (shal dan batuan lumpur). Ini telah mengikut terhadap kesan tektonik yang berlaku di barat dan tengah Afrika semasa zaman Kretaceous akibat daripada pemisahan plat Amerika Selatan. Daya pengawalan yang mendominasi pemisahan plat Afrika Barat telah membuka lautan Atlantik pada awal Kretaceous. Untuk itu data ini boleh digunakan sebagai petunjuk kepada aktiviti eksplorasi di masa hadapan terhadap arang dan lapisan arang di formasi di palung utara Benue dan di sekitar dunia.

Katakunci: Palung Benue; Arang Maiganga; Jenis Kerogen Formasi Gombe; Biomarker; Keadaan Sejarah Pemendapan; Kematangan Termal; Potensi Hidrokarbon; Penetapan Tektonik.

ACKNOWLEDGEMENTS

All praises and adorations are due to Almighty Allah the Creator, the Cherisher and the Protector of the entire Universe. I thank Him immensely for sparing my life and giving me a sound health to carry out this study. Undoubtedly, His mercy has no bound.

With all sense of gratitude, I acknowledge the great guidance and motherly, brotherly and friendly advice, help and support of my supervisors Prof. Dr. Wan Hasiah Abdullah and Dr. Yousif Mohammed Makeen. Their contribution as Teachers/Mentors as well as facilitating collaboration with the National Centre for Petroleum Research and Development, A.T.B.U., Bauchi, Nigeria, to get samples used for this research worth mentioning. My pen cannot adequately express my appreciation to both of you; nonetheless, I pray that Almighty Allah will reward you with perfect happiness here and in the hereafter. In the same way, I thank my collaborators Prof. M.B. Abubakar, Prof. Aliyu Jauro and their team for the fieldwork to Gongola Sub-basin and Dr. Babangida Mohammed Sarki Yandoka for being a friend and link to the centre.

I am profoundly grateful to the management and staff of Federal University Lokoja, Nigeria, especially the Geology department, for granting me the study leave and financial support through TETFUND to undergo further training at the University of Malaya, Malaysia. My appreciation goes to Department of Geology, University of Malaya for providing the organic geochemistry facilities. The financial supports by the IPPP grant from University of Malaya (grants No. PG1712015A), Ministry of Higher Education in Malaysia (FP042 2013A) are gratefully acknowledged.

I sincerely thank Dr. Khairul Azlan Mustapha, Mrs. Nor Syazwani Zainal Abidin, Mr. Zamri Rashid, Mrs. Zeleha, Mr Zaharudeen, Mr. Yusri, Mr. Nadzmiand Mrs. Fasya for

their supports during my laboratory analyses. My gratitude also goes to the staff and visiting consultants of the Department of Geology, University of Malaya such as Head of Department Prof. Dr. Azman Abdul Ghani, Prof. Dr. Ismail Yousif, Associate Prof. Dr. Ng Tham Fatt, Dr. Mohamad Tarmizi Mohamad Zulkifley, Dr. Meor Amir Hakif, Dr. Ralph L. Kugler, Dr. Nur Iskandar Taib for their motivations and supports throughout the research.

Special thanks to my father and mentor (Alh. Musa A. Ayinla), mother (Late Alhaja Rayhanah O. Ayinla), brothers and sisters (Dr. Abubakar O. Ayinla, Alhaja Risikat Ayinla, Associate Prof. Lukman A. Ayinla, Barr. Balqees Ayinla, Mrs. Titilayo Ayinla, Mrs. Rabiya Ayinla, Mr. Yaqub Ayinla, Mr. Daud Ayinla, Mr Adam Ayinla and Mrs Hadeezah Ayinla). I will not forget to thank the respective family members and my In-laws who deservingly, worth my recognition and appreciations for their prayers and priceless words of encouragement. The unalloyed and dedicated support, prayers and understanding of my wife (Nur. Balqees Abubakar), and children (Sheikh-Ahmad, Nana Aishah and Nurul Hikmah) are highly acknowledged and appreciated. I will continue to remember your endurance and perseverance when I needed to be away from home for a span of hours in a day while you continue to pray for my return and success. This list will not be completed without mentioning the supports of my friends - Alh. Is-haq Abulsalam, Dr. Abdul-Razaq Nafiu, Dr. Adam Shehu Usman and Dr. Saheed Adebayo as well as other members of Nigerian students' community in UM (NiSCUM). May the Almighty Allah reward you with endless bliss. Despite putting in immense efforts and being dedicated, it is with all your motivations, supports and prayers that I have been able to complete this research timely and successfully. I say Jazakumullahu khayran to you all.

Table of Contents

Abstract-----	iii
Abstrak-----	v
Acknowledgements-----	vii
Table of Contents-----	ix
List of Figures-----	xiv
List of Tables -----	xviii
List of Appendices-----	xix
CHAPTER 1: INTRODUCTION	
1.1 General Introduction-----	1
1.2 Location of study area-----	4
1.2.1 Climate and vegetation-----	4
1.3 Problem statement-----	5
1.4 Aims and objectives of this study-----	6
1.5 Scope of the study-----	7
1.6 Outline of the thesis-----	7
CHAPTER 2: REVIEW OF STRATIGRAPHICAL FRAMEWORK OF THE BENUE TROUGH AND ORGANIC GEOCHEMICAL APPLICATION	
2.1 Review on research gap in Gongola sub-basin-----	9
2.2 General Geology and tectonic evolution of the Benue Trough-----	10
2.2.1 Tectonic models of the Benue Trough-----	11
2.2.2 Northern Benue Trough-----	14
2.3 General lithostratigraphy of the Northern Benue Trough-----	15
2.3.1 Bima Sandstone-----	16
2.3.2 Yolde Formation-----	16
2.3.3 Pindiga Formation-----	17

2.3.4 Gombe Sandstone-----	18
2.3.5 Kerri-Kerri Formation-----	19
2.4 Organic geochemical overview-organic facies concept-----	21
2.4.1 Kerogen type-----	21
2.4.2 Hydrocarbon formation-----	24
2.4.3 Palynofacies (kerogen typing) -----	27
2.4.4 Coal rank-----	29
2.4.5 Maceral concept-----	32
2.4.5.1 Maceral group-----	33
2.4.5.2 Petrographic paleoenvironmental Indices (TPI and GI) -----	36
2.4.6 Biological marker and sedimentary settings-----	37
2.4.6.1 Normal and branched alkanes-----	38
2.4.6.2 Acyclic isoprenoids-----	39
2.4.6.3 Tricyclic and tetracyclic terpanes-----	40
2.4.6.4 Hopanes-----	41
2.4.6.5 Steranes-----	43
2.4.7 Pyrolysis gas chromatography (Py-GC) -----	44
2.5 Inorganic geochemical overview-----	45
2.5.1 Major elements-----	45
2.5.2 Trace elements-----	46
CHAPTER 3: METHODOLOGY	
3.1 Introduction-----	48
3.2 Fieldwork and sampling-----	49
3.3 Laboratory analyses-----	51
3.3.1 Organic geochemical methods-----	54
3.3.1.1 Source rock analysis SRA-----	54

3.3.1.2 Total organic matter content (TOC) determination-----	55
3.3.1.3 Bitumen extraction method-----	56
3.3.1.4 Liquid column chromatography-----	58
3.3.1.5 Gas chromatography-mass spectrometry (GC-MS) analysis-----	59
3.3.1.6 Pyrolysis-gas chromatography (Py-GC) -----	60
3.3.1.7 Bulk kinetic pyrolysis analysis-----	61
3.3.1.8 Elemental (CHNSO) analysis -----	61
3.3.2 Inorganic geochemical analysis -----	62
3.3.2.1 X-ray diffraction (XRD) analysis-----	62
3.3.2.2 X-ray fluorescence (XRF) analysis-----	63
3.3.2.3 Trace and major elemental (ICPMS) analyses-----	64
3.3.3 Organic petrographic analysis-----	65
3.3.3.1 Polished block preparation-----	65
3.3.3.2 Vitrinite reflectance measurements and maceral identification-----	67
3.3.3.3 Maceral analysis (point counting) -----	68
3.3.3.4 Materials for kerogen isolation-----	69
3.3.3.5 Kerogen isolation procedure-----	69
3.3.3.6 Glass slide mount-----	70
 CHAPTER 4: RESULTS OF ANALYSES	
4.1 General Statement-----	72
4.2 Stratigraphic succession-----	72
4.2.1 Coal-----	74
4.2.2 Mudstones (claystones and siltstones) -----	76
4.2.3 Shales-----	77
4.2.3.1 Mainganga Shales-----	77
4.2.3.2 Yaya-Ngari Shales-----	77

4.2.4 Sandstones-----	79
4.2.4.1 Poorly laminated sandstones-----	79
4.2.4.2 Laminated sandstones-----	79
4.2.4.3 Coarse sandstones-----	79
4.3 Bulk organic geochemical data-----	80
4.4 Extractable organic matter - EOM (or bitumen)-----	84
4.5 Molecular geochemical analysis-----	87
4.5.1 n-Alkanes and acyclic isoprenoids-----	87
4.5.2 Terpanes and steranes-----	91
4.6 Kerogen pyrolysis (Py-GC)-----	96
4.7 Ultimate analysis-----	99
4.8 Organic petrographic analysis-----	101
4.8.1 Vitrinite/ulminite reflectance measurements-----	101
4.8.2 Maceral analysis-----	101
4.8.3 Palynofacies-----	107
4.9 Bulk kinetics for hydrocarbon generation-----	109
4.10 Bulk elemental analysis-----	110
4.10.1 Geochemistry of major oxides-----	110
4.10.2 Geochemistry of trace elements-----	114
4.10.3 Geochemistry of clay minerals-----	117
CHAPTER 5: DISCUSSION	
5.1 Source rock characterisation-----	121
5.2 Stratigraphic succession-----	121
5.3 Total organic matter (richness)-----	123
5.4 Type of organic matter (quality)-----	126
5.4.1 Type of organic matter based on SRA-----	126

5.4.2 Type of organic matter based on Py-GC-----	128
5.4.3 Type of organic matter based on organic petrography-----	130
5.5 Origin of organic matter-----	132
5.6 Paleodepositional environment and preservation condition during sedimentation-	137
5.7 Thermal maturity-----	148
5.8 Hydrocarbons generation potential-----	152
5.9 Bulk kinetics and predictions for hydrocarbon generation-----	154
5.10 Tectonic setting-----	157
5.11 Paleoclimatic conditions-----	158
CHAPTER 6: CONCLUSION AND RECOMMENDATION	
6.1 Conclusion-----	162
6.2 Recommendation-----	165
REFERENCES -----	166
LIST OF PUBLICATIONS AND PAPERS PRESENTED -----	184
APPENDICES -----	185

LIST OF FIGURES

Figure 1.1: Map of Nigeria showing the sedimentary basins and study area, Maiganga coal mine (modified after Obaje, 2009) -----	3
Figure 2.1: Opening of the South Atlantic associated with a triple junction during the Early Cretaceous which subsequently formed the Benue Trough (modified after Burke et al., 1970).-----	13
Figure 2.2: Tectonic map of the Early Cretaceous in the Northern Benue Trough. 1, regional fault; 2, sinistral fault; 3, normal fault; 4, anticline axis; 5, $\delta 1$ trajectories; 6, $\delta 3$ trajectories; 7, compressive strike-slip tensors; 8, extensional tensors (Adapted from Guiraud, 1990) -----	14
Figure 2.3: Paleogeographic stages in the separation of Africa and South America during the Cretaceous (adapted after Tissot et al., 1980). -----	15
Figure 2.4: Stratigraphy of the Northern Benue Trough (modified after Abubakar, et al., 2006, Ayinla et al 2017b).-----	20
Figure 2.5: The three successive transformation stages of kerogen distinguished as diagenesis, catagenesis and metagenesis (modified after Tissot and Welte, 1984; Rojas et al., 2011)-----	27
Figure 2.6: Illustration of gradual formation of coal from millions of years ago upto present day retrieved from Coal-Formation of Coal-Types of Coal https://goo.gl/images/8mBoc8 -----	31
Figure 3.1: Illustration of source rock evaluation parameters-----	49
Figure 3.2: Flow chart showing the laboratory analyses used for source rock evaluation-----	53
Figure 3.3: Weatherford source rock analyser (equivalent of Rock-Eval equipment) used for screening the whole rock samples-----	55
Figure 3.4: A Multi N/C 3100 analyser produced by Analytik Jena used to determine the total organic matter contents (richness) of sedimentary facies from the Gombe Formation-----	56
Figure 3.5: (a) Bitumen extraction set-up (Soxhlet procedure) showing thimbles containing samples, covered with cotton in a Soxhlet apparatus, round bottom flask for extracted EOM, water source and inlet connected to the condenser as well as the hot plate (heat source) (b) Buchi rotary evaporator-----	57
Figure 3.6: Liquid column chromatography set-up to separate the EOM into its different components (saturated aromatic and NSO compounds). -----	58
Figure 3.7: Agilent 6890N Series gas chromatography- mass spectrometer (GCMS) and GC attached to Py-2020iD model pyrolysis gas chromatograph (Py-GC)-----	60
Figure 3.8: Elementar Analysensysteme GmbH (vario MICRO cube) with simultaneous determination of carbon, hydrogen, nitrogen, and total sulfur (CHNS) used study. This analysis was carried-out at University of Technology PETRONAS (UTP)-----	62
Figure 3.9: SIEMENS5000 X-RAY diffractometer at the Department of Geology University of Malaya-----	63
Figure 3.10: PANanalytical AxiosmAX 4KW sequential XRF spectrometer at the Department of Geology University of Malaya. -----	64
Figure 3.11: Polished blocks and materials used during the preparation-----	66

Figure 3.12: LEICA DM6000M microscope CTR6000 photometry system equipped with fluorescence illuminator at the Department of Geology, University of Malaya-----	68
Figure 3.13: Flow chart of the kerogen isolation procedure for palynofacies studies---	71
Figure 4.1: Panoramic view of Maiganga coalfield showing the four coal seams interbedded with mudstones, and shales, while sandstones cap the sequence-----	73
Figure 4.2: Illustration of: (a) the laterally extensive and thicker seams B compared with seam A ₃ and A ₂ which gradually thin out towards the south and (b) peats associated with seam A ₃ .-----	75
Figure 4.3: (a) Mudstone interbed within coal seams (b) rootlets on mudstone as evidence of terrigenous source input-----	76
Figure 4.4: (a) Fine to medium-grained shales characterised by varying degree of fissility which overlie coal facies, (b) dark grey shales interbedded with coal showing rootlets which suggest terrigenous source input for the sediments, (c) Yaya-Ngari shale often associated with some sandy materials-----	78
Figure 4.5: (a) poorly laminated fine-grained sandstone, (b) normal fault associated with parallel laminated, fine to medium-grained sandstones interbedded with iron stones, while clay and silty materials fill the fault plain, (c) medium to coarse-grained sandstones and (d) pebbly coarse-grained sandstones with trace fossils of horizontal burrowing organisms (<i>Thalassinoides</i>), with their molds filled with iron material-----	80
Figure 4.6: The mass fragmentograms of <i>m/z</i> 85 of saturated hydrocarbon fractions of representative samples from Maiganga and Yaya-Ngari-----	88
Figure 4.7: The mass fragmentograms of <i>m/z</i> 191 (left; a, c, e, g) and 217 (right; b, d, f, h) of saturated hydrocarbon fractions of the analysed Maiganga and Yaya-Ngari samples-----	92
Figure 4.8: The mass fragmentograms of Phenanthrenes (<i>m/z</i> 178), Methylphenanthrenes isomers (<i>m/z</i> 192) and aromatic Dibenzothiophenes (<i>m/z</i> 184) for aromatic hydrocarbon fractions of the analysed Maiganga and Yaya-Ngari samples-----	94
Figure 4.9: The Py-GC trace of the analysed samples-----	97
Figure 4.10: Photomicrographs of identified liptinites (a-j), huminites and inertinites macerals (k-r) in Maiganga coal -----	105
Figure 4.11: Photomicrographs of identified palynomorphs (P), phytoclast (Ph) and amorphous organic matter (AOM) in the studied Yaya-Ngari shale (a and b) and Maiganga mudstones (c-h) -----	108
Figure 4.12a: Identified clay minerals on the diffractogram of Maiganga shale are kaolinite, chlorite, montmorillonite, illite, and corrensite often associated with calcite and quartz-----	118
Figure 4.12b: Identified clay minerals on the diffractogram of Maiganga mudstone are kaolinite, chlorite, montmorillonite, illite, and corrensite often associated with calcite and quartz-----	119
Figure 4.12c: Identified clay minerals on the diffractogram of Yaya-Ngari shale are kaolinite, chlorite, montmorillonite, illite, and corrensite often associated with calcite and quartz-----	120

Figure 5.1: Stratigraphy of the studied coal bearing formation in the Northern Benue Trough as exposed at the Maiganga coalfield-----	122
Figure 5.2: The cross plot of S ₂ (mg HC/g rock) versus TOC (wt.%) showing the hydrocarbon potential for the analysed Maiganga and Yaya-Ngari samples-----	124
Figure 5.3: The cross plot of Total organic carbon content (TOC, wt. %) versus Bitumen content (ppm) showing the hydrocarbon potential for the analysed Maiganga and Yaya-Ngari samples-----	125
Figure 5.4: The bar plot of hydrocarbons concentration (aliphatic+aromatic fraction) of the extractable organic matter (ppm) showing the hydrocarbon potential of analysed Maiganga and Yaya-Ngari samples-----	125
Figure 5.5: The plot of the Hydrogen Index (HI, mg HC/gTOC) versus pyrolysis T _{max} (°C) showing the kerogen type of the analysed Maiganga and Yaya-Ngari samples-----	127
Figure 5.6: The Ternary plot based on compounds, m(+p)-xylene, <i>n</i> -octene (<i>n</i> -C ₉) and phenol, showing the kerogen type of the analysed Maiganga coal (modified after Larter, 1984)-----	131
Figure 5.7: The cross plot of atomic H/C versus atomic O/C on the Van Krevelen diagram showing the kerogen type of the analysed coal samples (adapted after Peters and Cassa, 1994).-----	131
Figure 5.8: The cross plot of Pr/ <i>n</i> -C ₁₇ versus Ph/ <i>n</i> -C ₁₈ showing the organic matter source input for the analysed Maiganga and Yaya-Ngari samples-----	135
Figure 5.9: The cross plot of C ₂₃ /C ₂₄ tricyclic terpane versus C ₂₄ tetracyclic/C ₂₆ tricyclic indicating significant terrigenous source input with more marine contribution in Yaya-Ngari compared to Maiganga facies. -----	135
Figure 5.10: Ternary plot of C ₂₇ , C ₂₈ and C ₂₉ regular steranes indicating organic matter source input for the analysed Maiganga and Yaya-Ngari samples-----	136
Figure 5.11: The cross plot of C ₂₇ /C ₂₉ regular sterane versus pristane/phytane showing the redox condition during deposition of Maiganga and Yaya-Ngari sediments-----	136
Figure 5.12: Bivariant plot of GI versus TPI showing the paleodepositional condition of Gombe Formation (modified after Diessel, 1986; Kalkreuth and Leckie, 1989; Wan Hasiyah, 2002) -----	139
Figure 5.13: Cross plot of aromatic Dibenzothiophenes/phenanthrenes (DBT/P) ratio (<i>m/z</i> 184 and 178) versus Pr/Ph ratio for discriminating the source rock depositional environment (after Hughes et al., 1995)-----	146
Figure 5.14: Bivariant plot of vanadium versus nickel showing the suboxic to oxic depositional condition for the analysed samples (adapted after Galarraga et al., 2008) -----	146
Figure 5.15: Trace element ratios of V/(V + Ni) versus total sulfur content (wt.%) of the analysed samples (adapted after Hakimi et al., 2017).-----	147
Figure 5.16: Bivariant plot showing the negative correlation between the total organic carbon content and uranium concentration during sedimentation of the analysed samples-----	147
Figure 5.17: Bivariant plot of V/Ni ratio versus Sr/Ba ratio for the analysed sediments of the Gombe Formation (adapted after Jia et al., 2013). -----	148

Figure 5.18: The bar plot of the analysed sedimentary succession versus average vitrinite reflectance showing the thermal maturity and maturation direction of organic matter in Maiganga and Yaya-Ngari areas. -----	149
Figure 5.19: Ternary plot of saturated, aromatic and nitrogen-sulphur-oxygen compounds showing their relative concentration in the analysed Maiganga and Yaya-Ngari samples -----	150
Figure 5.20: The cross plot of $20S/(20S+20R)$ C_{29} steranes versus $22S/(22S+22R)$ C_{32} homohopanes showing the thermal maturity of the organic matter in the analysed Maiganga and Yaya-Ngari samples.-----	152
Figure 5.21: Activation energy distributions of selected coal samples from Gombe Formation. -----	156
Figure 5.22: Bivariate plots of K_2O/Na_2O versus SiO_2 showing the tectonic setting of Gombe Formation based on analysed samples (adapted after Roser and Korsch, 1986) -----	158
Figure 5.23: Binary SiO_2 versus $(Al_2O_3 + K_2O + Na_2O)$ showing the paleoclimatic condition during sedimentation of the analysed samples (adapted after Suttner and Dutta, 1986) -----	159
Figure 5.24: Ga/Rb ratio versus K_2O/Al_2O_3 plot showing the paleoclimatic condition during sedimentation of the analysed samples (adapted after Roy and Roser, 2013) -----	161

LIST OF TABLES

Table 2.1: Geochemical parameters describing kerogen type, expected hydrocarbon products and associated depositional environments (modified after Larter and Douglas 1980; Stach et al, 1982, Peter and Cassa, 1994) -----	23
Table 2.2: Geochemical parameters used in describing organic matter richness of a potential source rock (after Peter and Cassa, 1994) -----	25
Table 2.3: Geochemical parameters used in describing thermal maturity of organic matter in source rock (after Tissot and Welte, 1984; Peter and Cassa, 1994; Peters et al 2005) -----	35
Table 4.1: TOC content, pyrolysis parameters and vitrinite reflectance data of the studied samples-----	82
Table 4.2: Extractable organic matter and relative percentages of saturates, aromatics and nitrogen-sulfur-oxygen (NSO) compounds of EOM-----	85
Table 4.3: Biomarker ratios based on m/z 85 and 191 mass chromatograms for selected samples-----	89
Table 4.4: Biomarker ratios based on m/z 191, 217, 184 and 178 mass chromatograms for selected samples-----	95
Table 4.5: Py-GC parameters of the analysed samples-----	98
Table 4.6: Ultimate Analysis showing CHNSO concentration of the analysed coal samples-----	100
Table 4.7: Maceral composition of the analysed coal samples-----	104
Table 4.8: Bulk kinetic parameters for hydrocarbon generation of the selected samples-----	109
Table 4.9: Major oxides composition of the analysed samples-----	112
Table 4.10: Trace elements composition of the analysed samples-----	115

LIST OF APPENDICES

Appendix A1: Histograms of some of the measured vitrinite/huminite reflectance (%Ro)-----	185
Appendix A2: Photomicrographs of some identified macerals in Maiganga coals under reflected white light and UV light-----	188
Appendix B: The GC-MS peak abbreviations and definitions from mass fragmentograms of the saturated hydrocarbon fraction in the <i>m/z</i> 191 (I) and 217 (II)-----	189
Appendix C1: Correlation matrix for major oxides and geochemical parameters-----	191
Appendix C2: Correlation matrix for trace elements and geochemical parameters----	192

University of Malaya

CHAPTER 1: INTRODUCTION

1.1 General Introduction

Nigeria is located at the bend of West African Gulf of Guinea (Figure 1.1). It is not only the major oil producer in Africa, but also one of the 10 top oil producers in the world (Solarin and Ozturk, 2016). Thus, oil and natural gas form the economic backbone of Nigeria's economy, accounting for more than 90% of her foreign earnings (Abubakar, 2014). Although there is potential for oil generation in the six sedimentary basins in Nigeria (Figure 1.1) including the Benue Trough and Bornu (Chad) basin, efforts on oil exploration are mainly concentrated in the Niger-Delta (Obaje, 2009; Abubakar, 2014). This is possibly due to earlier oil discovery at Oloibiri area of Niger-Delta in 1956. Thus, subsequent explorations gave access to its subsurface geology compared to other basins (Obaje, 2009; Nwajide, 2013; Ayinla et al., 2017a). In an effort to sustain the hydrocarbon production in Nigeria, attention is now focused on the search for oil and gas in the Nigeria's frontier inland basins. This includes Bida basin, Sokoto basin, Dahomey, Anambra Basin, Bornu (Chad) basin and Benue Trough (focus of this research) which shares the same evolutionary history with the prolific Muglad basin (Sudan), Termit basin (Niger republic) as well as Doba, Dosco and Bongor basin (Chad republic).

The Benue Trough is geographically divided into northern, central and southern parts. Similarly, the Northern Benue Trough (see Figure 1.1) is sub-divided into Gongola and Yola Sub-basins (Obaje, 2009; Nwajide, 2013; Abubakar, 2014; Ayinla et al., 2017a). The Gongola Sub-basin of the Northern Benue Trough (Figure 1.1) is one of the hydrocarbon exploration frontier inland basins in Nigeria where to date; minimal data is still available for adequate assessment of its organic and inorganic facies distributions. Previous exploration activities in the Gongola Sub-basin recorded success

for gas generation potential in 1999. As at that time, estimated reserve was about 33 bcf in the *Kolmani River-1* well drilled by Shell Nigeria Exploration and Production Company – SNEPCO.

Ever since then, there has been increasing interest to search for hydrocarbons in the Gongola Sub-basin. Thus, the basin consists of two major petroleum systems – the Lower Cretaceous petroleum system and the Upper Cretaceous petroleum system (Lawal and Moullade, 1986; Abubakar, 2014; Sarki Yandoka et al., 2016). The Maastrichtian sediments of the Gombe Formation are part of the Upper Cretaceous petroleum system of the Gongola Sub-basin (Abubakar et al., 2008). The formation consists of mudstones, sandstone, coal, shale and sandy-shaly sediments deposited in lacustrine to deltaic settings (Obaje et al, 1999; Jauro et al., 2008; Adedosu, 2009; Ayinla et al., 2017a).

The Gombe Formation coals (Maiganga and Yaya-Ngari areas) are part of the 17 % coal reserves in the world, which are lignite. As the world's hydrocarbon reserves keep falling, alternative sources have to be explored. This leads to a sustained interest in investigating the source rock potential of coal and coaly sediments in Nigerian sedimentary basins. The Gombe Formation coals and organic rich mudstones were found in two localities; Yaya-Ngari and Maiganga areas. The coalfields fall within the N-S trending Gongola sub-basin of the Northern Benue Trough, northeastern Nigeria (Figure 1.1).

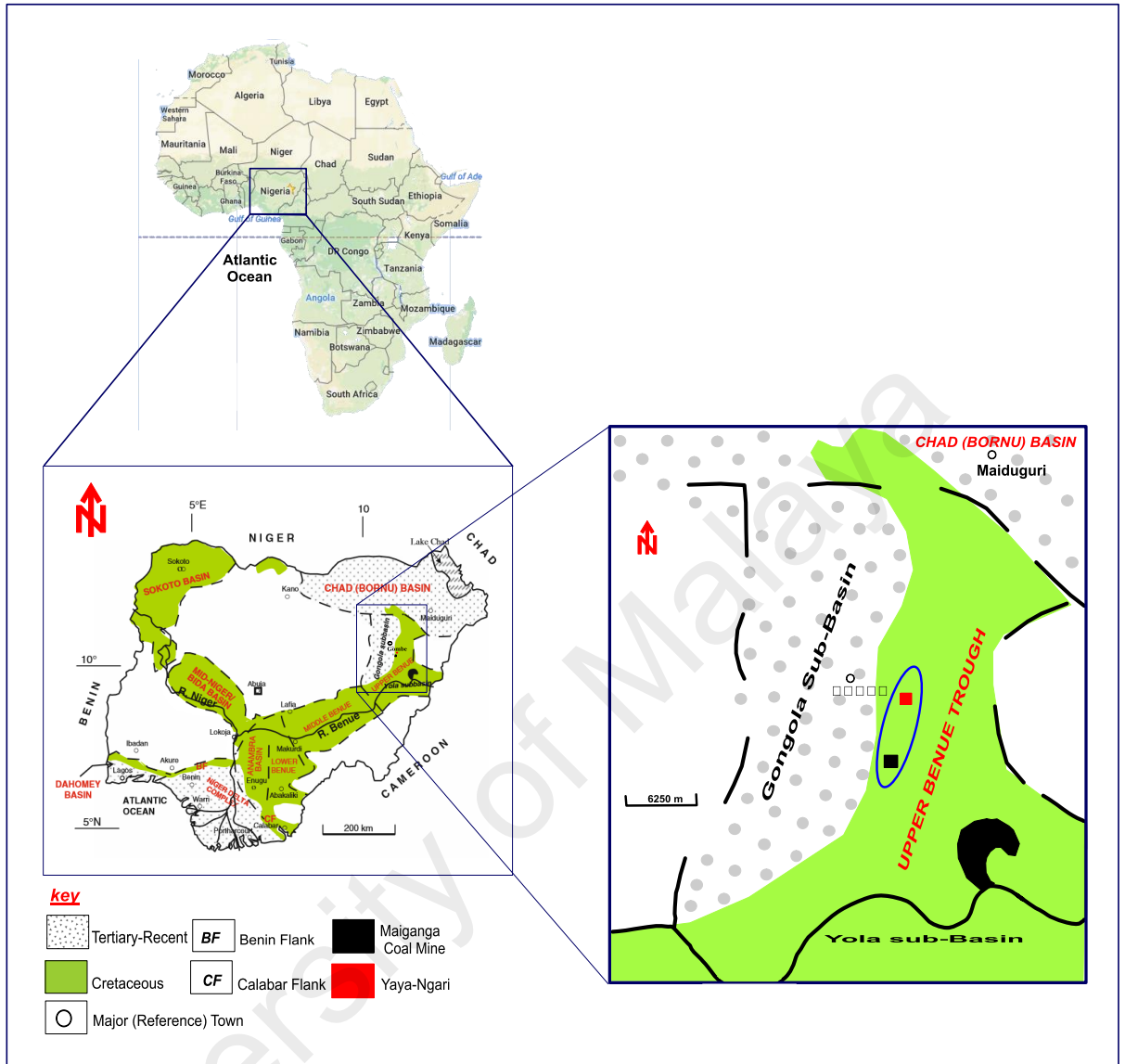


Figure 1.1: Map of Nigeria showing the sedimentary basins and study area, Mainganga coal mine (modified after Obaje, 2009).

Onoduku and Okosun (2014) and Aynla et al. (2017a) observed that, there are still some stratigraphic gaps that are linked to non-availability of subsurface data which give room for further research in the Gongola Sub-basin. These gaps include the non-inclusion of the coal facies in the stratigraphy of the Gombe Formation. The discovery of 4.5 million tons of coal at Mainganga coalfield exposes the need for detail study of these coal beds.

Detailed organic and inorganic geochemical investigation based on kerogen pyrolysis, organic petrography, biomarker distributions and inorganic studies of this area is also lacking. Prior to this research, Sarki Yandoka et al. (2015a) characterised coal facies from Yola sub-basin using the geochemical methods. Geochemical analyses employed in this research were: source rock analysis (pyrolysis), total organic carbon (TOC) determination, organic petrography, bitumen extraction, gas chromatography mass spectrometry (GC-MS) of extractable organic matter, pyrolysis gas chromatography (Py-GC), elemental CHNS(O), XRD, XRF and Inductively-coupled plasma mass spectrometer (ICPMS) analyses.

This study will provide organic and inorganic geochemical assessment of coals and organic rich mudstone from the Gombe Formation, part of the Gongola sub-basin, in an effort to further investigate the hydrocarbon potential of the Northern Benue Trough of Nigeria. It also aimed to determine the organic matter origin, paleodepositional conditions (preservation), thermal maturity, hydrocarbon generation potential, paleoclimatic conditions and tectonic setting. The data in this research could be used as a guide for future coal, oil and gas exploration campaigns in the Nigeria basins and the surrounding regions.

1.2 Location of study area

The study area is located in the N-S trending Gongola Sub-basin of the Northern Benue trough Nigeria. The basin represents the second bifurcated arm in the Northern Benue Trough (Figure 1.1). Maiganga coal mine falls within longitude 10⁰ E and 12⁰ E, and latitude 009⁰ N and 12⁰ N.

1.2.1 Climate and vegetation

The climate of the Gongola sub-basin is bi-seasonal with predominance of hot semi-arid climate which is typical of Northern Nigeria region and North-Central Africa.

The climate is characterised by a long period of dry season (November-March) and a short rainy season (mid-May–September). Usually, there is little or no rainfall in January (0 mm of precipitation) while August has the highest precipitation (average of 254 mm). The yearly average rainfall, between the two seasons, is 907 mm. The two seasons are both related to two seasonal winds; the North-Eastern Trade Wind and the South-Western Monsoon wind. During the dry season, the northeastern, cool nights and warm days. In the rainy season, moisture-laden monsoon winds blow temperatures. Yearly extremes temperature varies between the warmest in March and April (36.7 °C) and coolest in December and January (13.4 °C). On average, the monthly average temperature varies from 18.5 °C to 32.4 °C.

The vegetation cover in the Gongola sub-basin is typical of the Sahel savannah, which composed mainly of grasses, isolated huge trees, and shrubs. The type of vegetation cover in the area contributes significantly to the organic matter type in the analysed sedimentary facies. This in turn depends mainly on the rainfall distribution as well as topography and ground water condition in the area (Falconer, 1911).

1.3 Problem statement

The discovery of proven coal reserve of about 4.5 million tons and recent exploration activities at the Maiganga coalmine uncover some missing gaps in the stratigraphy of the Gombe Formation. Therefore, there is a need to further understand the organic and inorganic facies variations and distributions of the coals and sandy-shaly sediments in the Maiganga coalfield from Gombe Formation in the Northern Benue Trough, Northeastern, Nigeria. This study is one out of many of such research works that are much needed at this point in time. Moreso, when attention is now being focused on the search for hydrocarbon in the Nigeria inland basins such as Bornu (Chad) Basin, Benue trough, Bida basin, Sokoto basin and Anambra Basin.

In line with the problem statement, this research will provide the required and all-embracing answers to the following questions addressed in this study:

- a) Are the coal beds in the Gombe Formation actually thin as previously reported by earlier workers?
- b) Are the organic matters well preserved and mature enough to generate and expel liquid hydrocarbon in the basin?
- c) What is the extent of the relationship between the organic matter type, source input and depositional setting within the basin that can be interpreted based on the geochemical composition of the sediments?

1.4 Aims and objectives of this study

The central point of this study is to assess the organic and inorganic geochemical characteristics of the Gombe Formation coals, mudstones and sandy-shaly sediments for its suitability as potential hydrocarbon source rocks in Gongola sub-basin. The following measures were used in achieving this aim;

- a) Determining the amount, type and source inputs of the organic matter in coals, mudstones and the sandy-shaly sediments from the Gombe Formation, Gongola-sub-basin.
- b) Identification of the macerals and palynofacies in the sedimentary facies within the Gombe Formation.
- c) Determining the paleodepositional environment/conditions (preservation) and stratification of water column during sedimentation in the area.
- d) Assessing the thermal maturity and hydrocarbon potentials of the coals, mudstones and the sandy-shaly sediments in the Gombe Formation of the Gongola-sub-basin.

- e) Determining the bulk kinetics to predict the hydrocarbon generation in Gongola sub-basin.
- f) Delineating the bulk chemical composition of coals, mudstones and sandy-shaly sediments in the area.
- g) Determining the paleoclimatic condition of the area based on the bulk geochemical composition.
- h) Determining the tectonic setting of the Gongola sub-basin.

1.5 Scope of the study

To ensure that all the stated aims and objectives are met, the scope of this study covers field investigation of outcrops for samples collection, sedimentary logging/lithological descriptions and laboratory analyses of the collected outcrop samples. Detailed laboratory analyses performed are organic petrography (maceral point count and vitrinite reflectance measurements) and organic geochemical analyses (e.g. Rock-Eval pyrolysis, TOC, Py-GC, GC-MS, CHNS(O)) which were complemented by inorganic geochemical analyses (ICP-MS, XRD and XRF) to determine the suitability of the analysed Gongola sub-basin samples as potential hydrocarbon source rocks. Similarly, a sedimentary log of the study area was produced to fill the missing gap in the stratigraphy of the Northern Benue Trough. Qualitative and quantitative interpretation based on organic and inorganic geochemical composition of the sediments were made so as to determine the source rocks characteristics, paleodepositional environment/condition during deposition and hydrocarbon generation potential of the area.

1.6 Outline of the thesis

This thesis is divided into six chapters. Chapter 1 is the introduction which provides background information on the study area, problem statement as well as the

motivation for the research, aims and objectives, scope of the study and the outline of the thesis in a chronological order. Since the study area (Gongola sub-basin) falls within the Northern Benue Trough, Nigeria. Chapter 2 covers the literature review on the previous work done in the area as well as overview of the methods used in this study. This is followed by the description of the sample collection and methods employed in this study in Chapter 3.

The results of the various analyses performed so as to determine the source rock characteristics (organic matter quality, quantity, thermal maturity and prediction of hydrocarbon potentials) of the area are presented in Chapter 4. Chapter 5 provides detailed discussion of the results of the analyses carried out and their implications on the organic matter quantity, quality, source input, palaeodepositional environment, preservation condition during sedimentation, thermal maturity, hydrocarbons generation potential, tectonic setting and paleoclimatic condition. The major findings of this study are summarized in Chapter 6 while recommendations are made for further research in the area so as to complement this work. This is followed by the list of references used for this study.

In an effort to fill the missing gap in the stratigraphy of the Gombe Formation, this study provides vital information on the organic facies variations and distributions of the coals, mudstones and sandy-shaly sediments for hydrocarbon generation. These results would add to the existing knowledge on the sedimentary facies and organic facies characteristics of the Cretaceous Gongola sub-basin. Thus, main aspects of this work have been published in ISI/WoS indexed Journals. These can serve as guides for future oil exploration campaigns in the Northern Benue Trough of Nigeria as well as other coal and coal bearing source rocks around the world.

CHAPTER 2: REVIEW OF STRATIGRAPHICAL FRAMEWORK OF THE BENUE TROUGH AND ORGANIC GEOCHEMICAL APPLICATION

2.1 Review on research gap in Gongola sub-basin

The focus of this chapter is to review literatures on the studied basin and organic geochemical methods adopted in this research. Following the review of previous works done in the Gongola sub-basin of the Northern Benue trough, it becomes crystal clear that there are still some missing gaps in the stratigraphy as well as lack of description of the sedimentary and organic facies variation and distribution in the Gombe Formation (e.g. Carter et al., 1963; Grant, 1971; Olade, 1975; Kogbe, 1976; Lawal and Moullade, 1986; Benkhelil, 1982; 1989; Zaborski et al., 1997; Akande et al., 1998; Ojo, and Akande, 2004; Jauro et al., 2007; Abubakar et al., 2008; Jauro et al., 2008; Obaje, 2009; Onoduku et al., 2013; Nwajide, 2013; Onoduku and Okosun, 2014; Abubakar, 2014). The need for further research becomes more obvious and evident from the ongoing exploration activity at the Maiganga coal mine in the Gombe Formation which exposed about 4.5 million tons of Cretaceous coal interbedded with organic rich shales and mudstones that has not been duly investigated (Jimoh and Ojo, 2016; Ayinla et al., 2017a). Therefore, integrated organic and inorganic geochemical characterisation based on pyrolysis, organic petrography, biomarker distributions and trace/major elements studies were carried out to fill the missing gap and contribute to the pool of existing knowledge on the Geology of the area and hydrocarbon prospects in the coal bearing strata around the world.

Earlier researchers have made effort in assigning age (e.g. Carter et al., 1963; Lawal and Moullade, 1986; Zaborski et al., 1997; Onoduku and Okosun, 2014), stratigraphic description and hydrocarbon potential (Akande et al., 1998; Ojo, and Akande, 2004; Obaje, 2009; Onoduku et al., 2013; Nwajide, 2013; Abubakar, 2014; Jimoh and Ojo, 2016).

However, some key elements relating to potential source rock (organic matter quantity, quality and thermal maturity) have not been captured in detail. This is probably associated with sampling an incomplete sequence, not being aware of the Maiganga coal discovery or completion of the research before the discovery (e.g. Carter et al., 1963; Lawal and Moullade, 1986). Other limitations of some of the previous researches (e.g. Lawal and Moullade, 1986; Benkhelil, 1982; 1989; Zaborski et al., 1997; Akande et al., 1998; Ojo, and Akande, 2004; Obaje, 2009; Onoduku et al., 2013; Nwajide, 2013; Abubakar, 2014; Jimoh and Ojo, 2016). include lack of biomarker studies, Py-GC, detailed maceral point counting, ICP-MS studies in order to have an integrated approach in determining the source rock rich, kerogen type, thermal maturity and paleodepositional condition. These were identified from the literature search and, thus, incorporated in this study. Knowing full well that some of the earlier methods used also have inherent limitations such as problem of correct identification of vitrinite due to mud additive and caving, condition of preparation (scratched polished surface) as well as low number of measurements.

2.2 General Geology and tectonic evolution of the Benue Trough

Detailed literature search revealed that sedimentary basins in Nigeria can be grouped into six (from the oldest to the youngest): Benue Trough (location of the study area), Chad basin, Nupe/Bida basin, Sokoto basin, Dahomey basin and Niger delta (Obaje, 2009, Nwajide, 2013; Abubakar, 2014). Just like other basins, the Benue Trough (1000 km long and 150 km wide) is an intracratonic basin formed during the Cretaceous period as a result of the tensional opening of the South Atlantic Ocean equatorial domain and subsequent complex interplate movement within the African plate (Thomas, 1996). It is filled with about 6000 m of Cretaceous–Palaeogene sediments associated with volcanics and those before the Mid-Santonian were folded,

faulted and uplifted in several places (Benkhelil, 1989). This leads to formation of >100 anticlines and synclines in the three geographic sub-divisions of the Benue Trough: Northern, Central and Southern Benue Trough (Nwajide, 2013; Abubakar, 2014).

These new geographical sub-divisions are now preferred over the former arbitrarily subdivisions (Obaje, 2009) into a lower (Southern Benue Trough), middle (Central Benue Trough) and upper (Northern, Benue Trough). The Southern Benue has the Abakaliki anticlinorium and the Afikpo syncline, while the Central Benue is known for the Giza anticline and the Obi syncline. As for the Northern Benue Trough, it is characterised by the Lamurde anticline and the Dadiya syncline. Similarly, “Dumbulwa-Bage” High (an important anticline) marks the boundary between the Benue Trough and the Chad (Bornu) basin (Zaborski et al, 1997).

2.2.1 Tectonic models of the Benue Trough

Although a number of models have been proposed for the evolutionary history of the Benue Trough, the rift system and pull-apart are the two fundamental models (Abubakar, 2014). A number of researchers agreed that the separation of Africa and South America plates in the early Cretaceous best explains the evolution of the Benue Trough as well as the entire West and Central African Rift System (WCARS) (Benkhelil, 1989; Genik, 1992; Guiraud and Maurin, 1992). Based on the rift system model which suggests presence of a triple junction underneath the prolific Niger Delta, King (1950) proposed tensional movements resulting in a rift as the main mechanism in the Benue Trough. This model was strengthened by the observed axial zone of positive gravity anomalies associated with linear negative anomalies usually found in the rifted basin (Carter, et al., 1963; Cratchley and Jones, 1965; Cratchley, 1984).

Furtherance to the efforts of these researchers, Stoneley (1966) proposed a graben-like structure. In the contrary, Burke et al., 1970 suggested a spreading ridge

(Figure 2.1) that was active from Albian to Santonian (RRR triple junction), while to Grant (1971) proposed the presence of an unstable ridge–ridge-fault (RRF) triple junction resulted in plate dilation and the opening of the Gulf of Guinea. Finally, Olade (1975) put forward the aulocogenic perspective for the origin of the Benue Trough. Nonetheless, a basic limitation of this model is lack of prominent rifted fault at the Trough's margin (Popoff et al., 1983).

On the other hand, the pull-apart model based on wrenching was being proposed as a predominant tectonic process in the Benue Trough (e.g. Benkhelil, 1989 and Guiraud, 1990). This model relies on the fact that transcurrent faults rather than normal faults are the major faults observed in the Benue Trough which is not usually the case in rift systems (Figure 2.2).

University of Malaya

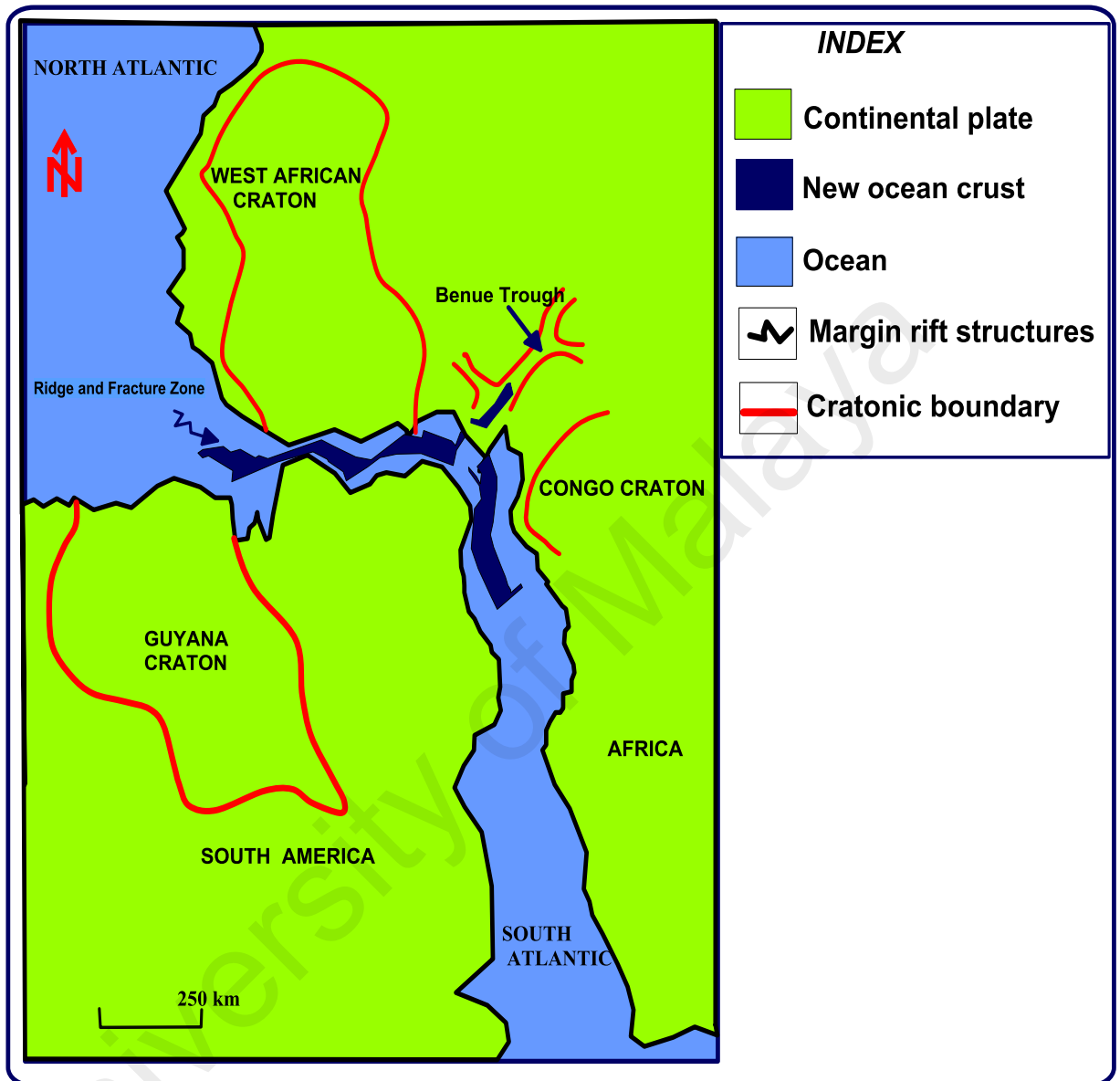


Figure 2.1: Opening of the South Atlantic associated with a triple junction during the Early Cretaceous, which subsequently formed the Benue Trough (modified after Burke et al., 1970).

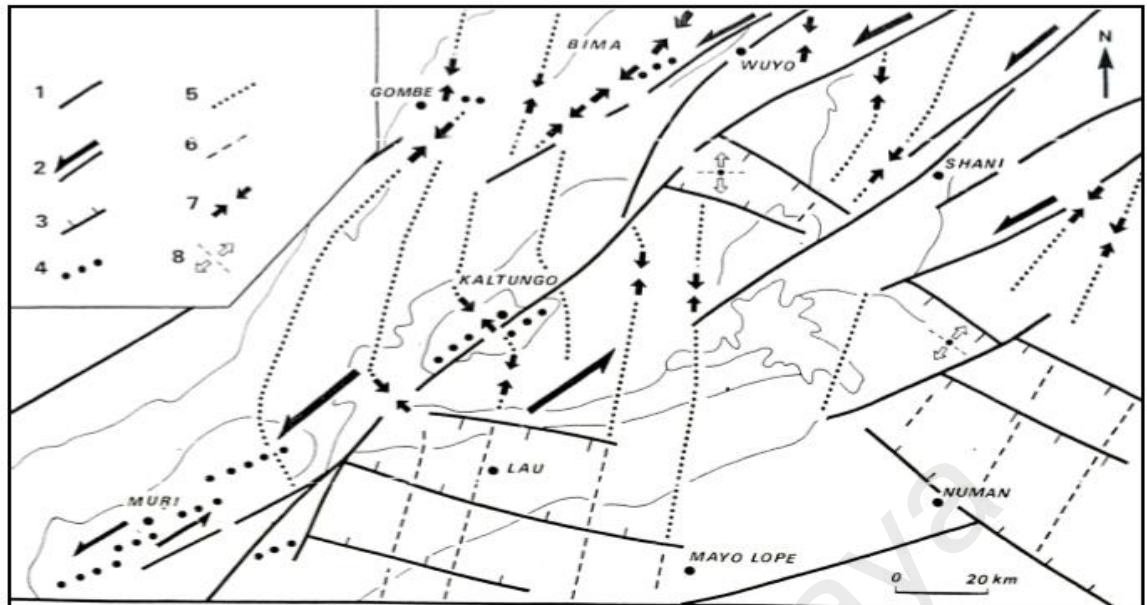


Figure 2.2: Tectonic map of the Early Cretaceous in the Northern Benue Trough. 1, regional fault; 2, sinistral fault; 3, normal fault; 4, anticline axis; 5, δ_1 trajectories; 6, δ_3 trajectories; 7, compressive strike-slip tensors; 8, extensional tensors (adapted from Guiraud, 1990).

2.2.2 Northern Benue Trough

The Northern Benue Trough extends from the Bashar–Mutum Biyu up to the southern boundary of the Borno Basin around the ‘Dumbulwa-Bage High’. It is divided into two major sub-basins; the N-S trending Gongola sub-basin and the E-W trending Yola sub-basin (Ojo and Akande, 2004; Abubakar, 2014). Northern Benue Trough belongs to the northeast-southwest trending Chad basin – Benue Trough – Niger delta region (Figure 2.1) which represents series of tectonic episodes leading to formation of megastructures in the west and central African that is associated with the WCARS (Ojo, 1982; Ayinla et al., 2013; Abubakar, 2014). Therefore, stratigraphic, tectonic and geochemical evidences in the Northern Benue Trough indicate similar evolutionary history with the adjoining basins in Chad, Niger and Sudan within the same rift trend termed West and Central African Rift System (Abubakar, 2014). Tissot et al. (1980) illustrated the paleogeographic stages in the separation of Africa and South America during the Cretaceous (Figure 2.3) which also affected the Benue Trough.

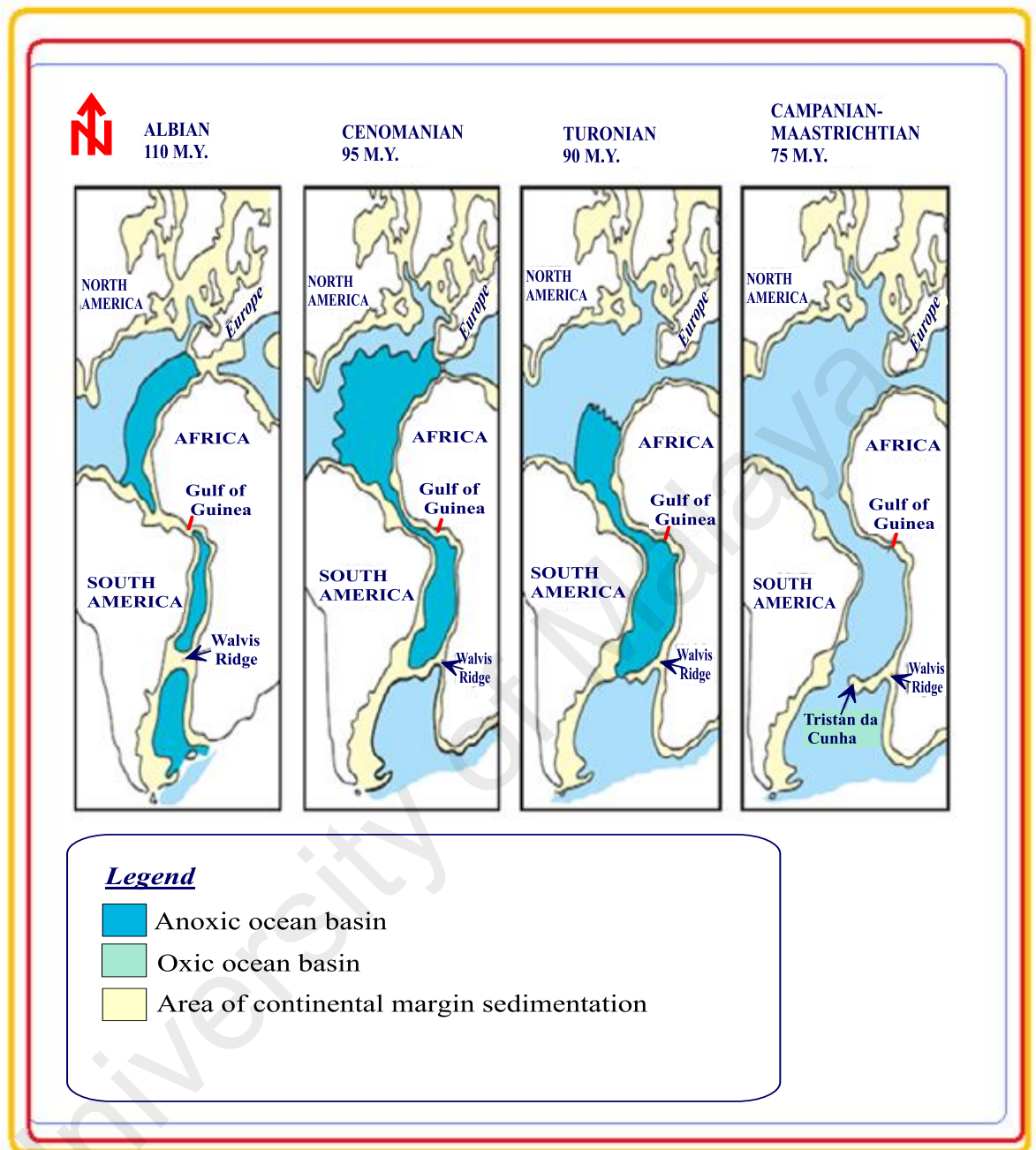


Figure 2.3: Paleogeographic stages in the separation of Africa and South America during the Cretaceous (adapted after Tissot et al., 1980).

2.3 General lithostratigraphy of the Northern Benue Trough

The Northern Benue trough, just like other parts of Nigeria, has no record of sedimentation between the Precambrian and Late Mesozoic times (Carter et al., 1963). Unlike the Niger-delta area where many exploratory wells have been drilled, outcrops and boreholes have proved useful in identifying the stratigraphic units in the Northern

Benue trough (Reyment, 1965; Olade, 1975; Kogbe, 1976; Lawal and Moullade, 1986; Guiraud et al., 1989; Zaborski et al., 1997; Zaborski, 2003; Ojo, and Akande, 2004; Jauro et al., 2007; Abubakar et al., 2008; Obaje, 2009; Nwajide, 2013; Jimoh and Ojo, 2016; Ayinla et al, 2017a). According to these authors, the five stratigraphic units that have been described in the Northern Benue Trough are Bima Formation, Yolde Formation, Pindiga Formation (Kanawa, Gulani, Deba-Fulani, Dumbulwa and Fika shale member), Gombe Formation, and Kerri-Kerri Formation (Figure 2.4). The following are the brief descriptions of each the formation.

2.3.1 Bima Sandstone

This is an Upper Albian to Lower Turonian formation known as the oldest stratigraphic unit in the whole of Benue Trough. The origin of Bima Formation has been associated with a granitic terrain and directly overlies the Lower Palaeozoic-Precambrian Basement (Carter et al., 1963; Guiraud, 1990). It is characterised by alluvial fan through lacustrine to fluvial sediments that are sparsely fossiliferous, poorly sorted, and medium to coarse grained feldspathic sandstone. The formation shows varied sedimentary structures such as current bedding (Okosun, 1995), trough cross bedding, planar cross bedding, groove mark and soft sediments deformation (Guiraud, 1990, Sarki Yandoka, 2014). Bima Formation has three distinct members (from oldest to youngest): Lower (B1), Middle (B2) and Upper (B3) Bima member (Kogbe, 1976; Guiraud et al., 1989; Zaborski et al., 1997; Abubakar et al., 2008; Sarki Yandoka et al., 2014). This falls below the Yolde Formation (see Figure 2.4).

2.3.2 Yolde Formation

This Formation is a Cenomanian transitional sequence between the continental Bima sandstone and marine Pindiga Formation (Figure 2.4) in the Northern Benue

trough (Carter et al., 1983; Avbovbo et al., 1986; Lawal and Moullade, 1986). Although, Falconer (1911) and Barber et al, (1954) had earlier recognized this formation, it was Carter et al, (1963) that named it “Yolde” Formation. It is characterised by fluvial sandstone-mudstone at the lower boundary which gradually changes to more thinly and regularly bedded bioturbated sandstones at the upper boundary representing shallow marine. This formation is poorly exposed in Gongola sub-basin but a type section occurs at Yolde stream in the Yola sub-basin (Barber et al, 1954, Abubakar et al., 2006; Sarki Yandoka et al., 2015b).

2.3.3 Pindiga Formation

Pindiga Formation (Figure 2.4) was first named by Barber et al, (1954) and later by Carter et al. (1963) to represent a set of Cenomanian to Santonian sediments consisting of calcareous limestones, sandstones and shales in Pindiga area. This includes five members (Zaborski et al., 1997):(a) the marine shales and intercalated limestones of Kanawa Member dated Late Cenomanian to Early Turonian which was deposited during transgression (Thompson, 1958; Ayok et al., 2016; Aliyu et al., 2017; Ayinla et al., 2017b), It is characterised by alternating beds of massive to nodular limestones (lower boundary), marly bed (about 3 m) and thick shale units, intercalated with thin limestone beds at the upper part boundary (Carter et al., 1983; Akande et al., 1998) (Figure 2.4). The limestones are bioturbated and consist of both non-fossiliferous and shelly limestone varieties. Presence of this calcareous lithologic units associated with non-terrestrial microflora suggests marine environment for the Formation.

(b) This is followed by the regressive fluvial and littoral sandy facies of the Gulani Member characterised by thinly bedded coarse to very coarse-grained pebbly sandstones with purple, brown and white laminated mudstone interbeds. (c) The Deba-Fulani Member which is mainly sandy beds occurring at the central part of the Pindiga

Formation, (d) while the Dumbulwa Member is known for its sandstone and shale sequence. (e) The open marine Fika Member caps this sequence. It consists of bluish-black, ammonite-rich shale which is locally gypsiferous and contains one or two thin impersistent limestone beds. The Fika shale is diachronous and has been assigned a Turonian-Maastrichtian age (Carter et al., 1963; Lawal, 1982). Its thickness varies from 100 m at the southwestern margins near Potiskum to about 500 m near Maiduguri in the northeast (Avbovbo et al., 1986).

2.3.4 Gombe Sandstone

An estuarine/deltaic progradational sequence comprising of sandstone, siltstone, shales, clays, thin coal beds and oolitic ironstone intercalations that overlain the Fika shale (Figure 2.4) is known as Gombe Sandstone (Carter et al., 1963; Dike, 1995). This depositional environment was supported by Lawal (1982) who observed rapid decrease in marine microfossils at the boundary between Pindiga and Gombe Formation. The Gombe Formation had been assigned a Campanian to Maastrichtian age based on the palynological evidence (Carter et al., 1963; Lawal and Moulade, 1986; Abubakar, 2014). The base of the formation is characterised by alternation of thin beds of silty shales with the middle part composed of well-defined beds of sandstone and mudstones associated with coal beds. Cross-bedded sandstone is present towards the top of the sequence. Occasionally, sedimentary facies of the Gombe Formation have plant remains and *Thalassinoides* type of bioturbation (horizontal feeding burrows). This formation is restricted to the western side of the Gongola Basin where a thickness of about 350 m had been recorded. The area is characterised with series of folding and faulting due to igneous activity, which perhaps can be responsible for the observed maturity difference within the Formation. Following a marked angular unconformity, the Kerri-Kerri

Formation overlies the Gombe Formation (Carter et al., 1963; Nwajide, 2013; Abubakar, 2014, Ayinla et al., 2017a, 2017b).

2.3.5 Kerri-Kerri Formation

Kerri-Kerri Formation consists of mainly continental (fluvial and lacustrine) sandstones with shale and coaly shale intercalations. It rests unconformably on the Cretaceous Gombe Formation to mark the end of sedimentation (at western side) in the Gongola sub-basin, while the basalts of Biu plateau concealed the Gongola stratigraphy to the extreme east. The Kerri-Kerri Formation (> 320 m) has been dated Tertiary (Paleocene-Eocene) based on palynomorph assemblage (Adegoke et al., 1986; Dike, 1995). The Kerri-Kerri Formation and Bima sandstone share some similarities in both lithology and structures; the latter however, have more feldspartic and coarser grades sandstone (Carter et al., 1963; Ayinla et al., 2013; Abubakar, 2014).

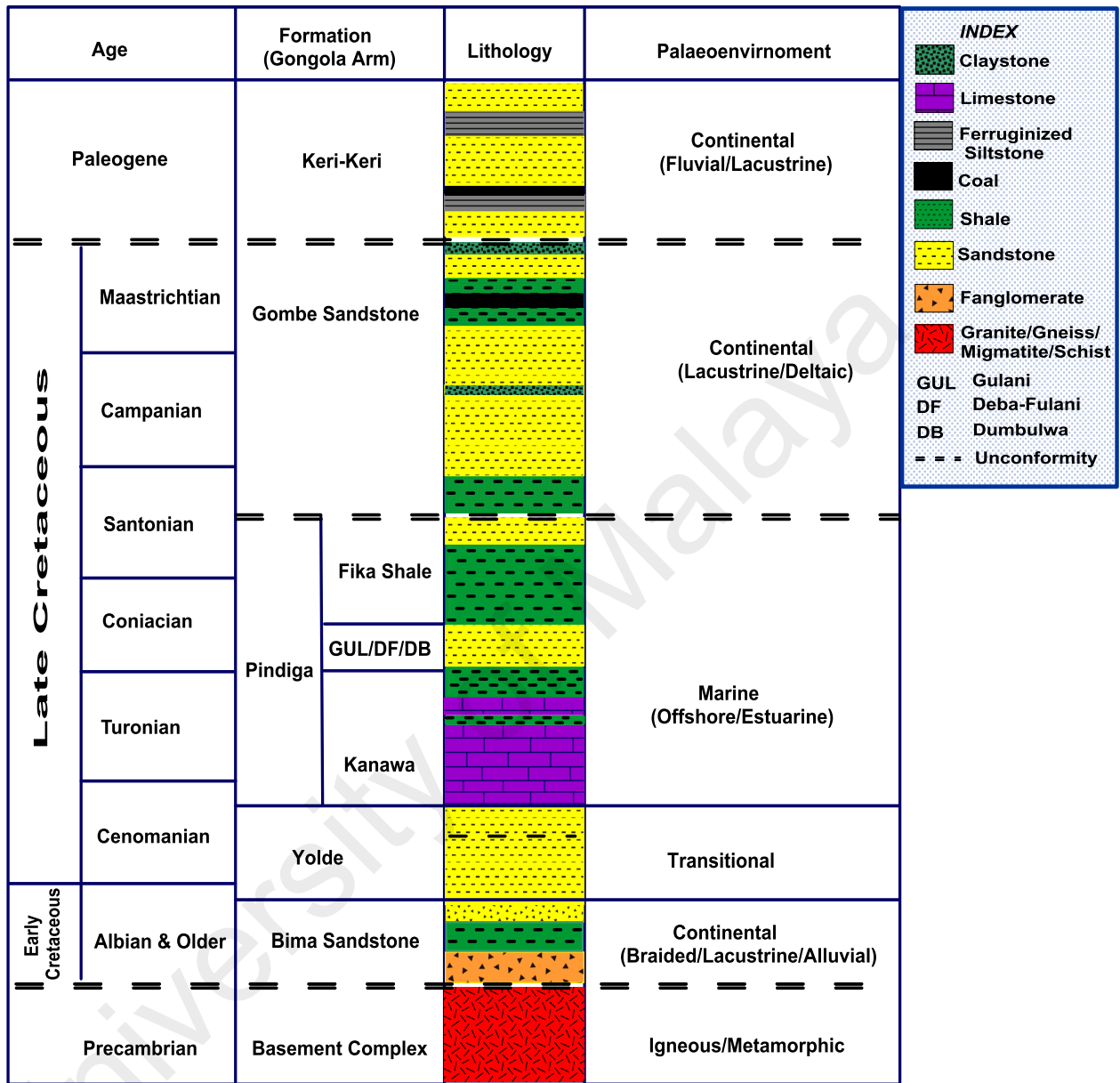


Figure 2.4: Stratigraphy of the Northern Benue Trough (modified after Abubakar, et al., 2006, Ayinla et al 2017b).

2.4 Organic geochemical overview-organic facies concept

This is an important perspective of characterising sedimentary organic matter (soluble bitumen and insoluble kerogen) by integration of organic petrology and organic geochemical tools to interpret the paleoenvironment, source rock evaluation as well as hydrocarbon exploration in a sedimentary basin (Jones, 1987; Peters and Cassa, 1994). According to Peters and Cassa (1994), many authors had used different terms such as kerogen facies, palynofacies, maceral facies to describe organic facies, it can be succinctly described as a mappable subdivision of a stratigraphic unit which can be distinguished from adjacent units based on only its organic constituents (Jones, 1987). In geologic record, primary producers of organic matter (before Devonian) are the blue-green algae, photosynthetic bacterial, while high molecular weight land plants joined the leagues in Devonian as the third major producer (Tissot and Welte, 1984; Peters et al., 2005). Detail maceral and palynofacies analyses carried out were complemented by bulk geochemical analyses performed in this study.

Organic matters (OM) + minerals = Sedimentary rock

Organic matters = bitumen (soluble) and kerogen (insoluble component)

NOTE

In coal: OM >>>> mineral

In other sedimentary rocks (e.g. mudstone) Mineral >>>> OM

(Tissot and Welte, 1984; Peters et al., 2005).

2.4.1 Kerogen type

Kerogen is particulate organic constituents of sedimentary rocks that is insoluble in organic solvent because of its high molecular weight constituent compounds made up of elemental C, H, O, N and S (Forsman and Hunts, 1958; Peters and Moldowan, 1993). Although, kerogen accounts for > 95% of the total organic

matter, it represents small portion when compared to the mineral matrix, in sedimentary rock (Tyson, 1995). Kerogen has no specific chemical formula, its components are well described using geochemical methods such as Py-GC, GC, GC-MS, GC-MS-MS, elemental analysis (CHNSO), Rock-Eval pyrolysis/source rock analyser and organic petrographic studies (under reflected, fluorescence and transmitted light).

Parameters resulting from the aforementioned method (among others) are employed in identifying and discriminating kerogen types (Table 2.1). This include hydrogen index (HI), oxygen index (OI), atomic ratios of H/C and O/C, dominant maceral composition (see Table 2.1 for kerogen Type parameters). Similarly, useful bivariant (e.g. T_{max} vs. HI, HI vs. OI, Pr/*n*-C₁₇, Ph/*n*-C₁₈) and ternary plots (e.g. oxylene, *n*-C₉ and phenol) as well as kerogen “type index” have been proposed for the four kerogen types and their level of thermal maturity (e.g Van Krevelen, 1961; Tissot and Welte, 1984; Mukhopadhyay et al., 1995; Larter and Douglas 1980; Dembicki, 2009). It is noteworthy, that there exist intermediates between the kerogen types. A typical example is Type II/III kerogen characterised by predominantly vitrinite (with some liptinite and inertinites), HI of 200-300 mg HC/g TOC, OI of 5-10, H/C of 1-1.2 with mixed hydrocarbon potential (oil and gas). All these are articulated in discriminating the kerogen type in the studied Gombe Formation samples (see Chapter 5).

Table 2.1: Geochemical parameters describing kerogen type, expected hydrocarbon products and associated depositional environments (modified after Larter and Douglas 1980; Stach et al, 1982, Peters and Cassa, 1994).

Kerogen Type	HI(mg HC/g TOC)	OI	Atomic Ratio		Type Index	Dominant maceral	Expected Hydrocarbon	Depositional Environments
			H/C	O/C				
Type I	>600	>15	>1.5	< 0.1	< 0.4	Liptinite	Oil	Lacustrine
Type II	300-600	10-15	1.2-1.5	0.2	0.4-1.3	Liptinite	Oil	Marine
Type III	50-300	1-10	0.7-1.2	< 0.3	1.3 -20	Vitrinite/some liptinite	Gas/Little oil	Terrestrial/Paralic/ Deltaic setting
Type IV	< 50	<1	<0.7	> 0.3	>20	Inertinites	Little gas or None	Reworked/Oxidized setting

2.4.2 Hydrocarbon formation

The main contributors of organic matter (from which hydrocarbon is formed) are the phytoplankton, zooplankton, land plants and bacterial. Some of the organic matters are consumed, recycled or decayed by bacterial activities while the remaining are buried and preserved under favourable condition in sedimentary rocks. Geologically, organic matter is composed of organic molecules derived directly or indirectly from the organic part of organisms except the mineralized skeletal part such as shells and bones. According to Tissot and Welte, (1984), petroleum hydrocarbons are formed when buried sedimentary organic matters are subjected to progressively increasing pressure and temperature for millions of years. During the process, series of physical and geochemical reactions gradually transform the organic matters to kerogen and finally changed to petroleum hydrocarbon (oil and gas). This process is called organic matter transformation.

However, since certain threshold of organic matter (expressed as TOC) must be reached for hydrocarbon generation (see Table 2.2), its high productivity and preservation (under either oxic, suboxic or anoxic condition) is essential. Although, oxygen is required by living organic matters, oxygen-deficient (marine) environment supports its preservation than terrestrial setting. Factors enhancing OM productivity include light, oxygen, nitrogen phosphorous, temperature and saline water condition. Fine grained sediment enhance preservation than coarse grain, thus, source rocks are usually shale, mudstones and coal (Wilkins and George, 2002; Peters et al., 2005). Rapid sedimentation and high rate of burial also supports preservation (Sia and Abdullah, 2012; Makeen et al., 2015a).

Table 2.2: Geochemical parameters used in describing organic matter richness of a potential source rock (after Peters and Cassa, 1994).

Interpretation	TOC (wt %)	EOM/Bitumen (ppm)	Hydrocarbons (ppm)	S1 (mgHC/g)	S2 (mgHC/g)
Poor	< 0.5	0 - 500	0 - 300	< 0.5	<2.5
Fair	0.5 - 1.0	500 - 1000	300 - 600	0.5 - 1.0	2.5 - 5.0
Good	1.0 - 2.0	1000 - 2000	600 - 1200	1.0 - 2.0	5.0 - 10.0
Very Good	2.0 - 4.0	2000 - 4000	1200 - 2400	2.0 - 4.0	10.0 - 20.0
Excellent	> 4.0	> 4000	> 2400	> 4.0	> 20.0

A potential source rock must be rich in organic matter which has passed through the petroleum hydrocarbon formation stages (Peters, 1986). The three successive transformation stages (diagenesis, catagenesis and metagenesis) are briefly discussed below (Tissot and Welte, 1984; Hunt, 1996; Peters et al., 2005; Mendonça Filho et al., 2012):

a) **Diagenesis:** This is the early process of organic matter transformation occurring at shallow depth (< 1000 m), relatively low temperature (< 60 °C) and pressure where the system tries to attain equilibrium. It involves decarboxylation, deamination, polymerization, reduction and decomposition of organic matter through bacterial activity resulting in production of CH₄, CO₂, and H₂O. Thus, there is decrease in oxygen and increase carbon content which corresponds with decrease of H/C and a notable decrease of O/C ratios on the van Krevelen diagram (Figure 2.5). Although, this is a stage of thermally immature kerogen (< 0.6% vitrinite reflectance); little hydrocarbon can be generated in the source rocks (Tissot and Welte, 1984). Similarly, it is the quantity and quality of organic matter preserved and transformed at this stage that

define the hydrocarbon potential of a basin below (Tissot and Welte, 1984; Peters et al., 2005; Mendonça Filho et al., 2012).

b) Catagenesis: This is the second stage of kerogen degradation at greater depth (1000-6000 m) higher temperature (60-175°C) and pressure which leads to a marked decrease in hydrogen content and H/C ratio (e.g 1.2-1.5 in type-II kerogen). Since the effect of temperature on the buried organic matter is the dominant transformation force during catagenesis, the vitrinite reflectance value increases gradually and later rapidly (0.6-2%). This is followed by generation and expulsion of petroleum hydrocarbons. Thus, catagenesis is the main zone of oil generation (from kerogen to petroleum) and commencement of the cracking to produce "wet gas" (Tissot and Welte, 1984; Peters et al., 2005; Mendonça Filho et al., 2012).

c) Metagenesis: This is the last but the main stage of thermal cracking of kerogen occur at greater depth of burial (> 6000 m) and high temperature (> 180°C) as deposition continues, prior to metamorphism. During the transformation of the kerogen (in this case oil and wet gas), dry gas (> 98% methane) is the main product formed at a considerably high vitrinite reflectance value (2.0-4.0%) (Tissot and Welte, 1984; Peters and Cassa, 1994; Peters et al., 2005; Mendonça Filho et al., 2012).

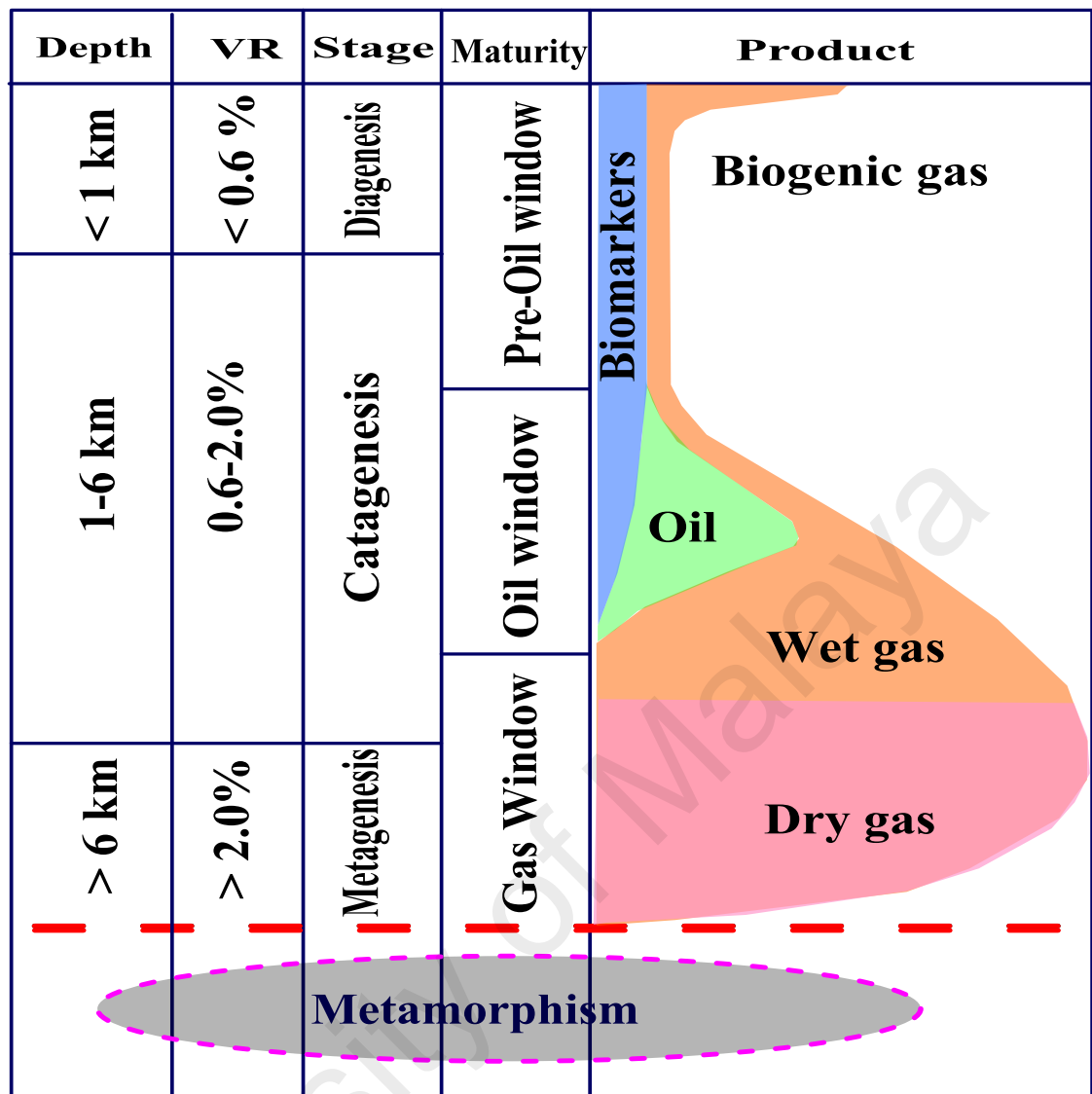


Figure 2.5: The three successive transformation stages of kerogen distinguished as diagenesis, catagenesis and metagenesis (modified after Tissot and Welte, 1984; Rojas et al., 2011).

2.4.3 Palynofacies (kerogen typing)

Kerogens assemblages can be categorized into three palynofacies groups based on their shape and morphology determined by degree of translucency and fluorescence properties under transmitted normal light and fluorescence UV light microscopy. These are phytoclast (fragment of tissue of higher plant), palynomorph (organic walled remains), and amorphous organic matter (structureless derived algae and plant resin) (Tyson, 1995; Mendonça Filho et al., 2012). The translucency and morphology of an organic particle represents the extent of their thermal alteration, botanical affinity,

depositional environments and degree of terrigenous input. Thus, palynofacies analysis gives useful information about organic particles provenance, biological affinity, paleoenvironment, redox condition, preservation, hydrocarbon potential and thermal maturity (Tyson, 1995; Zulkefley et al., 2015; Mendonça Filho et al., 2012; Mustapha et al., 2017).

a) Phytoclast group: Phytoclasts are the clay to fine-grained sand size fragments of tissues derived from higher plants or fungi. They can be translucent or opaque (black) and their autofluorescence depends on the plant source (Tyson, 1995; Mendonça Filho et al., 2012; Zulkefley et al., 2013). Phytoclast display varying morphology thus can be biostructured, non-biostructured, structured or "pseudoamorphous". They are usually derived from the highly lignified support tissue in higher plants such as xylem (wood), and since lignin is highly resistant to decay, tends to become preferentially preserved and therefore concentrated during decay. Gymnosperm wood contains more lignin than angiosperm (flowering plant) wood, hence, often more well preserved compared to angiosperm wood (Mendonça Filho et al., 2012; Mustapha et al., 2017).

b) Palynomorph group: Palynomorphs are organic-walled microfossils, which range in size between 5 and 500 μm including pollen, spores, dinoflagellates (dinocysts), acritarchs, chitinozoans and scolecodonts together with particulate organic matter (POM) and kerogen found in sedimentary rocks. These are commonly concentrated from sediments using chemical digestion (HCl acid to remove carbonates and HF acid to remove silicates). Palynomorphs can occur as unicellular, multicellular or colonial form and can be subdivided into terrestrial (sporomorphs) and aquatic (marine and fresh water) subgroups (Tyson, 1995). Therefore, palynomorphs are widely used as indicators of paleoenvironment, paleoclimate, redox conditions as well as age determination. High

concentration of pollens and spores is an indication of terrigenous organic matter from Bryophyte, Pteridophyte (fern type) plants and their primitive ancestors. While high dinoflagellates typify a marine setting, the presence of fungal spores may suggest redeposition from active fluvio-deltaic source areas, whereas high concentration of dinocysts and foraminiferal linings can indicate upwelling areas. Botryococcus genus usually characterises Carboniferous to Recent Freshwater sedimentary facies (Mendonça Filho et al., 2012; Mustapha et al., 2017).

c) Amorphous organic matter (AOM): Amorphous group represents all structureless particulate organic, under light microscope scale, derived from phytoplankton, bacteria, higher plant resins, and diagenetic product of macrophyte tissues (Mendonça Filho et al., 2012). Their colour ranges from yellow through orange to brown or grey with angular to rounded particles. AOM is a known hydrocarbon associated kerogen group in source rocks (Tyson, 1995; Mendonça Filho et al., 2012; Mustapha et al., 2017).

2.4.4 Coal rank

Coal is a combustible brown-black sedimentary rock composed of lithified remains of prehistoric vegetation (average of 50% organic matter content) deposited in swampy and peat bog depositional environments (Figure 2.6). Based on coal depositional origin and maceral-mineral composition, sapropelic (from organic mud) and humic coal (from peat) have been discriminated as the main two types of coal which can be allocthonous or autochthonous (O'keefe et al., 2013). Before any peat mire will lead to formation of coal rather than organic-rich shale, accumulation of organic matter must exceed the rate of decay and there must be limited clastic influx into the peat-forming environment (Zulkefley et al., 2015; O'keefe et al., 2013).

Aquicludes can be developed by the presence of impermeable clay that can also aid organic matter accumulation. Over time, under the effect of temperature and pressure, the plant remains are converted to peat (brown) which marks the beginning of coal formation. The progressive degree of diagenesis and metamorphism of the plant materials (coalification), which depends on temperature, pressure, time, depth of burial and geothermal gradient determines coal rank or thermal maturity (Taylor et al., 1998; Zulkefley et al., 2015; O'keefe et al., 2013). It is important to note that coal experiences series of physical and chemical changes (e.g colour, increase in the carbon content, vitrinite reflectance and calorific value, while decrease in moisture and volatile matter) which are not uniform throughout the coalification stages and are used in measuring coal rank (van Krevelen, 1961). In low-rank coals, vitrinite reflectance measurements are complemented with moisture and heating value for coal rank determination. The four main ranks of coal are: lignite, subbituminous, bituminous and anthracite (O'keefe et al., 2013).

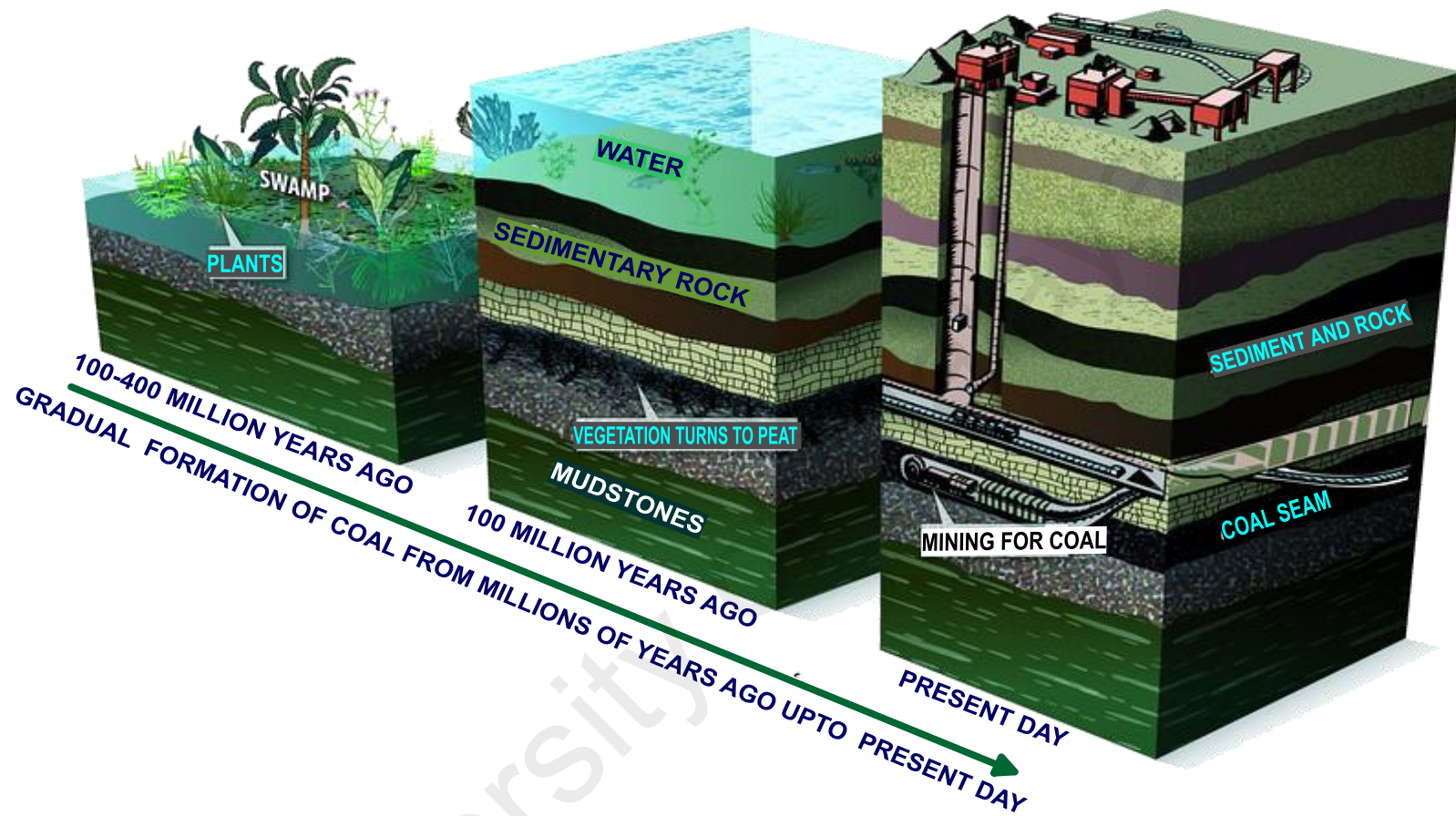


Figure 2.6: Illustration of gradual formation of coal from millions of years ago upto present day retrieved from Coal – Formation of Coal – Types of Coal <https://goo.gl/images/8mBoc8>.

a) Lignite is the softest and lowest rank of coal ($< 0.4\% R_o$) composed of about 50% – 73% carbon with evidence of pre-existing plants tissues. Being subjected to low temperature and pressure, it has highest moisture content and consequently lowest calorific value (10-20 MJ/kg). It is brownish-black and appears dull with submetallic listre, accounting for about 17% of total coal reserve in the world (Stach et al., 1982; Yi et al., 2017).

b) Subbituminous coal is soft and crumbly rank of coal (0.4-0.7% R_o) forming an intermediate between lignite and bituminous coal (about 68-83% carbon). It has higher moisture content and lower calorific value (about 19-26 MJ/kg) compared to bituminous coal. It is dark brownish-black and accounts for about 30% of total coal reserve in the world (Stach et al., 1982; Yi et al., 2017).

c) Bituminous coal is a black coal (0.7-2.0% R_o) composed of about 78%–88% carbon, which is relatively soft, compared to anthracite but harder than other rank of coal. It has high moisture content and moderate calorific value (24-35 MJ/kg) compared to anthracite. It accounts for about 52 % of total coal reserve in the world (Stach et al., 1982; Yi et al., 2017).

d) Anthracite is the hardest and highest rank of coal ($> 2.0\% R_o$) composed of about 79–91% carbon, very low moisture content and the highest calorific value (> 35 MJ/kg). It is black and display submetallic listre. It accounts for $< 1\%$ of total coal reserve in the world (Stach et al., 1982; Yi et al., 2017).

2.4.5 Maceral concept

Coal is a combustible brown-black sedimentary rock composed of lithified remains of prehistoric vegetation (average of 50% organic matter content) deposited in

swampy and peat bog depositional environments. Although, White and Thiessen (1913) had earlier observed organic constituents of coal (maceral), it was Stopes (1935) who introduced the term maceral to describe the basic organic building blocks of coal. This concept of maceral was later presented in a more encompassing manner by Spackman (1958) as naturally occurring heterogeneous aggregates of organic matter that are optically distinguishable based on their chemical and physical properties. However, there are two limitations (difficulty in separating coal maceral and detail of each maceral change during maturation). Today, with the development of powerful petrographic instruments, the term has now been standardized and succinctly described as the microscopically observable basic unit of coal, which is synonymous to mineral in rock (ICCP 1963, 1993; Stach et al., 1982).

Petrographic observation using reflected, transmitted and fluorescent light has made it possible to have better information and discover more macerals (ICCP, 1998; 2001; Sykorova et al., 2005; Pickel et al., 2017). The macerals are characterised by their distinguishing morphology (shape and structure), reflectance, colour, fluorescence and relief of the polished surface which in turn determines their geochemical characteristics, petroleum potential, industrial and economic values (Teichmuller, 1989; ICCP, 1998; 2001; Sykorova et al., 2005; Sia and Abdullah, 2012; Hakimi and Abdullah, 2014; Pickel et al., 2017).

2.4.5.1 Maceral group

Despite the existence of many classification nomenclatures for coal macerals, the ICCP classification system has gained prominence among the coal petrologists over the years. It is, therefore, adopted as the standard classification system for maceral identification and point count of the studied Gombe Formation samples (see Ayinla et al., 2017a, 2017b). Based on petrographic characteristics, the three maceral groups are

vitrinite/huminite, liptinite and inertinite (Teichmuller, 1989; ICCP, 1998; 2001; Sykorova et al., 2005; Sia and Abdullah, 2012; Hakimi and Abdullah, 2014; Pickel et al., 2017).

a) Vitrinite/huminite macerals are low-gray coloured maceral formed from thermal alteration of polymer, lignin and cellulose in the cell wall (woody-tissue) of plants which can be used as a measure of thermal maturity of organic matter. This is especially for hydrocarbon generation and expulsion (see Figure 2.5) from pre-oil generation window ($< 0.6\% R_o$) through oil window ($0.6-2\% R_o$) to gas window ($> 2\% R_o$). Vitrinite is the most abundant group of macerals. Most often, it accounts for 50-90% of maceral composition (Tissot and Welte, 1984; Peters and Cassa, 1994; Rojas et al., 2011; Makeen et al., 2015b).

b) Liptinite maceral originates from non-humifiable waxy and resinous part of plants, which are relatively rich in hydrogen content, such as spore, pollens, cuticles and resin. They are usually plant fossils or phyterals characterized by the highest aliphatic content among the maceral groups; thus, they have high potential for generating liquid hydrocarbon. Liptinites are classified based on this phyteral nature into sporinite, cutinite, resinite, suberinite, alginites, exsudatrinites, liptodatininites, chlorophyllinite and bitumeninites (Teichmuller, 1989; Taylor et al., 1998; ICCP, 2001; Pickel et al., 2017). Among all the maceral groups, liptinite macerals have the lowest relectance but highest fluorescence (under UV light) which makes it easily distinguishable. Usually, the liptinite content is high in sapropelic coal ($> 10\%$) than humic coal ($< 10\%$) (Peters and Cassa, 1994). Coal seams with average liptinite content between 15-20% have potential to generate oil (Hunt, 1991),

c) **Inertinite maceral** is derived from plant that has been strongly altered and degraded in the peat stage of coal formation as a result of forest fire or biochemical degradation. The inertinite macerals has the highest carbon content and reflectance of all the macerals and are distinguished by their relative reflectance and structures into fusinite, semifusinite, macrinite, macrinite and sclerotinites (ICCP, 2001; Sykorova et al., 2005).

Integration of organic petrography results such as vitrinite reflectance, %R_o, pyrolysis T_{max} (°C) and biomarker parameters such as CPI values, C₃₂ homohopane ratio (22S/22S+22R) and sterane ratio C₂₉ ββ/(ββ+αα) can provide reliable information about thermal maturity of source rock. Just the same way, cross plot of Pr/n-C₁₇ vs. Ph/n-C₁₈, 20S/(20S+20R) and steranes vs. C₃₂ 22S/(22S+22R) homohopanes have been useful for maturity determination (Seifert and Moldowan, 1986; Peters and Moldowan, 1993; Peters et al., 2005). According to Seifert and Moldowan (1986), the C₃₂ 22S/(22S + 22R) homohopane ratio has values between 0.0 to 0.6 with increasing thermal maturity; below 0.50 to 0.54 corresponds to just beginning of “oil window”, while 0.57 to 0.62 implies “oil window” (Table 2.3).

Table 2.3: Geochemical parameters used in describing thermal maturity of organic matter in source rock (after Tissot and Welte, 1984; Peters and Cassa, 1994; Peters et al., 2005).

Interpretation	Vitrinite reflectance (% R _o)	T _{max}	PI (S1 +S2)	CPI	C ₃₂ 22S/(22S + 22R)
Pre-oil window	< 0.6	< 435	< 0.1	> 1	< 0.50 -0.54
oil window	0.6-2.0	435-470	0.1-0.4	1	0.57-0.62
Gas window	> 2.0	> 470	> 0.4		>0.62

2.4.5.2 Petrographic paleoenvironmental Indices (TPI and GI)

Tissue preservation index (TPI) and gelification index (GI) are important petrographic paleodepositional indices that have been widely used in deciphering the paleoenvironmental condition of coals. Diessel (1986) proposed TPI and GI indices for high-rank coals, which was later modified for low-rank coals such as lignite by Kalkreuth et al. (1991), Markic and Sachsenhofer (1997), Kalaitzidis et al. (2000) and Sia and Abdullah, (2012). TPI is used in defining the degree of tissue preservation versus destructive tissue breakdown compared to the amount of woody plants in the original peat forming facies (Diessel, 1992; Singh et al., 2012). High TPI (>1) suggests high degree of tissue preservation in a wet forest raised bog paleomire with balance ratio between plant growth/peat accumulation and rise in groundwater column. This can be associated with high subsidence rate in acidic medium that can inhibit bacterial decay of the organic matter. In the case of low TPI (<1), it indicates presence of herbaceous plants in the mire or large-scale destruction of wood due to extensive humification and mineralization. Most often, large scale of wood destruction is associated with reasonable amount of liptinite macerals such as sporinite and resinite with some inertodetrinites (Diessel, 1992; Singh et al., 2012; Oikonomopoulos et al, 2015). This is commonly found in alkaline medium characterised by high bacterial activity resulting in decay of organic matter.

GI reflects the degree of dryness or wetness (i.e. moisture conditions) of a peatland. High GI ($> 1\%$) is typical of wet conditions which enhance high huminite formation by preventing oxidation to preserve more huminite than inertinite, whereas low GI (<1) suggests presence of low water table during coal formation (Diessel, 1992, Wan Hasiah, 2002; Sia and Abdullah, 2012; Singh et al., 2012; Oikonomopoulos et al, 2015; Sen et al., 2016). High TPI and GI values ($> 1\%$) are indicators of low levels of aerobic decomposition, which will result in a low content of inertinite (Diessel, 1992,

Oikonomopoulos et al, 2015). In this study, the formulae described by Sia and Abdulah, 2012 are adopted for TPI and GI calculation as follows:

$$\text{TPI} = \text{Telohuminite} + \text{Semifusinite} / (\text{Detrohuminite} + \text{Macrinite} + \text{Inertodetrinite})$$

$$\text{GI} = \text{Huminite} / \text{Inertinite}$$

2.4.6 Biological marker and sedimentary settings

Biological markers (biomarker) are molecular geochemical fossils of traceable organic matter origin in coal and other sedimentary rocks (Tissot and Welte, 1984; Philp, 1985). Its chemical compositions are carbon, hydrogen and other petroleum associated elements which form the basic unit of most biomarker isoprene subunit (methylbutadien). Since their chemical structures can be linked to a known organic matter/compound especially lipid, they have potential to serve as useful tools in evaluating sedimentary organic matters in source rock (Peters et al., 2005; Han et al., 2017). Thus, biomarkers provide information about biological precursor of an organic matter and consequently organic source input, the prevailing environmental conditions and the stratification of water column as at the time of deposition (Peters and Moldowan, 1993; El-Diasty and Moldowan, 2012). They are also useful in determining the degree of thermal maturity, extent of microbial biodegradation and geologic age (Grantham et al., 1983; Tissot and Welte, 1984; Brooks, 1986; Ekweozor and Telnaes, 1990; Peters et al., 2005; El-Diasty and Moldowan, 2013).

Biomarkers are also widely used in petroleum industries to identify group of genetically related oils, to correlate oil with source rock and describe the most likely source rock, depositional environment for migrated oil of certain origin (e.g. Peters and Moldowan, 1993; Peters et al., 2005; Han et al., 2017). This study employed gas chromatography-mass spectrometry (GC-MS) to evaluate the source rock generation potential of coal and mudstones from the Gombe Formation based on the biomarker

assemblages. Below are examples of common biomarkers often applied in assessing oil and source rock extracts.

2.4.6.1 Normal and branched alkanes

Naturally, *n*-alkanes (acyclic and saturated hydrocarbon) accounts for highest percentage concentration of hydrocarbon in organic matter and organism in sedimentary facies. The discovery of their high concentration in geochemical material and ease of detection with GC make them the most exploited class of biomarkers (Philp, 1985). Therefore, *n*-alkanes have been studied from different depositional environment and source input ranging from primitive aquatic organism such as benthic and pelagic algae to higher organism of terrigenous origin (Philp, 1985). Brassell et al. (1978) gave useful insight on the chromatographic distribution of *n*-alkanes in plants, algae and bacterial while Philp (1985) compiled series of informative mass spectra of compounds to aid their identification. Predominance of high molecular weight *n*-alkanes (*n*-C₂₇ to *n*-C₃₁) especially *n*-C₂₇, *n*-C₂₉ and *n*-C₃₁ over other *n*-alkanes are typical of terrestrial higher plant, where they form the main component of plant waxes i.e. leaf cuticles, spores, pollens and resins (Bray and Evans, 1961; Eglinton and Hamilton, 1967; Tissot and Welte, 1984). On the other hand, algae and micro-organism are characterised by low molecular weight *n*-alkanes with odd-to-even predominance in the *n*-C₁₁ to *n*-C₁₇ region (Peters et al., 2005).

For more than 5 decades, the ratio of odd to even carbon has been a complementary tool in the geochemical determination of thermal maturity of organic facies. This is known as carbon preference index (CPI) (Bray and Evans, 1961). Scalan and Smith (1970) later modified it as odd- to-even predominance (OEP). Thus, values of CPI and OEP significantly above 1 reflect thermally immature extract. Values of 1.0 suggests, but do not prove, thermal maturity, while below 1.0 is unusual and typify low

maturity extracts from carbonate or hypersaline settings (Peters et al., 2005). Tissot and Welte (1984) observed that although the formulae are useful, they are influenced by organic matter type and extent of maturation, thus applied with caution (Peters et al., 2005).

The *n*-alkanes can be identified as the dominant peaks on total ion current chromatogram (TIC), *m/z* 99 and *m/z* 85 chromatograms (Philp, 1985; Peters et al., 2005; Zulkefley et al., 2015; Ayinla et al., 2017a). Biodegradation in oil and rock extracts can be read on the GC trace by the superimposition of *n*-alkanes over a hump of unresolved components (Philp, 1985). Thus, the CPI values in this study were calculated using the formula proposed by Bray and Evans (1961).

$$\text{CPI} = \frac{2(\text{C}_{23} + \text{C}_{25} + \text{C}_{27} + \text{C}_{29})}{(\text{C}_{22} + 2(\text{C}_{24} + \text{C}_{26} + \text{C}_{28}) + \text{C}_{30})}$$

2.4.6.2 Acyclic isoprenoids

Although, several acyclic isoprenoids have been widely employed in the geochemical evaluation of sedimentary depositional environment, Philp (1985) described three major types. These are the head-to-tail type such as pristane (C₁₉) and phytane (C₂₀); tail-to-tail linkage such as lycopane (C₄₀) and head-to-head linkage with a parent C₄₀ compound (biphtane). Pristane (Pr) and phytane (Ph) are the most important isoprenoids found in sedimentary rocks, crude oils and coals, and are mostly sourced from phytol side chain of chlorophyll (Powell and McKirdy, 1973; Didyk et al., 1978).

Over the years, the Pr/Ph have proved useful in determining the paleoredox conditions (i.e. oxic, su-oxic and anoixic) of sedimentary facies during deposition (Didyk et al., 1978). Anoxic depositional conditions are indicated by low Pr/Ph ratio (< 0.6), from 0.6 to 3 typify sub oxic and > 3 denote terrigenous organic matter inut under oxic conditions (Peters and Moldowan, 1993). On the other hand, the cross relationship

between Pr/n-C₁₇ and Ph/n-C₁₈ are widely used as indicator of kerogen type, thermal maturity, redox conditions and degree of biodegradation of organic matter ((Peters et al., 2005; Ayinla et al., 2017a; Makeen et al., 2015c). For immatured samples, supporting maturity determination parameters (e.g vitrinite/huminite reflectance measurements and T_{max}) are always advisable for more reliable and dependable results (Ayinla et al., 2017a).

2.4.6.3 Tricyclic and tetracyclic terpanes

Frequent occurrence of tricyclic and tetracyclic terpanes in oil and rock extract from marine environment had been employed in geochemical discrimination of sedimentary environment (Aquino Neto et al., 1983). Although, there are other sources of tricyclic terpanes, its high concentrations are usually associated with Prasinophyte algae (Tasmanites) origin (Simoneit et al., 1993). Tasmanites are usually found in high latitude, nutrient-rich, marginal marine settings. Apart from the algal origin, partial aerobic oxidation of bacterial membrane has been suggested as tricyclic terpane origin as well as terrigenous plants origin as in the case of extended tricyclic terpanes (> C₂₀) (Peters et al., 2005). The abundance of C₁₉ to C₃₀ tricyclic terpane is useful in evaluating organic matter source input and depositional settings (De Grande et al., 1993; Peters et al., 2005).

It is noteworthy that most often, tricyclic terpane series lacks or has low concentrations of C₂₂, C₂₇, C₃₂, C₃₇, and C₄₂ homologs due to methyl substitution of every fourth carbon atom. Nevertheless, tricyclic terpanes have proved useful in oil-to-source correlation, determining source rock characteristics, degree of thermal maturity and biodegradation of organic facies (Peters and Moldowan, 1993). El-Diasty and Moldowan (2012) illustrated the relevance of high ratios of C₂₃/C₂₄ tricyclic terpane and C₂₄ tetracyclic/C₂₆ tricyclic terpane in marking terrestrial organic matter source input. This was further buttressed by the cross plot of C₂₃/C₂₄ tricyclic terpane versus C₂₄

tetracyclic/C₂₆ tricyclic to differentiate organic facies (as marine and non-marine) and depositional conditions (as oxic, suboxic, dysoxic and anoxic).

The relative high abundance of C₁₉-C₂₀ tricyclic terpanes compared to other tricyclic terpanes is typical of terrigenous oils, while dominance of C₂₃ tricyclic terpane homologue is common in marine oils (Peters and Moldowan, 1993; Tao et al., 2015). The tricyclic terpanes ratios (C₂₂/C₂₁ and C₂₄/C₂₃) can be used in identifying extract and oil derived from carbonates source rocks whereas C₂₆/C₂₅ can be used to differentiate lacustrines from marine source rock extract and oil with C₂₆/C₂₅>1 typifying lacustrine (Peters et al., 2005). Similarly, high concentration of tricyclic terpanes compared to hopanes with dominance of 24-methyl- and 24-ethylcholestanes (C₂₈ and C₂₉) with few cholestanes (C₂₇) characterised brackish water environment (Peters et al., 2005).

Tetracyclic terpanes such as C₂₄ is common in carbonate sedimentary rock and is perhaps derived from microbial or thermal of hopanes (Peters et al., 2005). C₂₅-C₂₇ Tetracyclic terpanes have been identified in oil and bitumen showing more resistance to biodegradation than hopanes (Killops and Killops, 2005; Peters et al., 2005). Therefore, high concentration of C₂₄ as well as C₂₅-C₂₇ tetracyclic terpanes in oil and bitumen indicate carbonate and evaporite source input especially from marine settings (Peters et al., 2005). In this study, tricyclic and tetracyclic terpanes are shown on the *m/z* 191 ion chromatogram (Figure 4.7).

2.4.6.4 Hopanes

Hopanes are pentacyclic triterpanes composed of four 6-member rings and one five-member ring within a C₂₇-C₃₅ naphthenic structure. They are derived from bacteriohopanoids in bacterial membranes and most often dominate the triterpanes in crude oil and source rock extract (Ourisson et al., 1984; Tissot and Welte, 1984; Killops and Killops, 2005; Peters et al., 2005; Kim and Rodchenko, 2016). Hopanes have series of isomeric form such as diahopanes, neohopanes, moretanes, demethylated hopanes,

and homohopanes. They are molecular indicators of organic matter origin, thermal maturity and paleo-redox condition during sedimentation (Peters et al., 2005; Kim and Rodchenko, 2016). Oleanane is an important plant-derived pentacyclic triterpenoids biomarker suggesting Late Cretaceous age and angiosperms origin for organic matter inputs in a sedimentary basin (Grantham et al., 1983; Brooks 1986; Ekweozor and Telnaes, 1990; Murray et al., 1997; Peters et al., 2005; Jauro et al., 2007; Adedosu, 2009).

Although, the $C_{31}R/C_{30}$ hopane ratio is a good molecular tool to differentiate marine (> 0.25) from lacustrine environmental influence (< 0.25) in the source input especially in shales and mudstones, low rank coals are known to show high values which limit the use of the ratio (Peters et al., 2005). In addition, high concentration of C_{34} and C_{35} hexacyclic hopanes having side chains with a pentacyclic or hexacyclic ring at C-22 are typical of lacustrine oils and bitumens whereas it is absent in marine oils. Homohopanes in stair-step pattern ($C_{31} > C_{32} > C_{33} > C_{34} > C_{35}$) indicate suboxic conditions while V-shaped ($C_{31} > C_{32} \geq C_{33} \leq C_{34} < C_{35}$) characterise saline lacustrine source rock deposited under anoxic conditions (Peters and Moldowan, 1993, Sarki Yandoka et al., 2015a; Makeen et al., 2015c).

Organic matter thermal maturity can be evaluated based on the relative distribution of hopanes. Predominance of the more thermally stable 22S over biologically derived 22R isomer of homohopanes C_{31} - C_{35} usually characterise mature samples while immature samples have dominance of the 22R isomer (Peters et al., 2005; Kilops and Kilops, 2005). In essence, the ratio of C_{32} ($22S/22S+22R$) are often employed in geochemical evaluation of thermal maturity. Although, the C_{31} homohopanes isomers ratio are usually measured, the C_{32} homohopanes have been suggested because of the possibility of co-elution of Gammacerane with 31 homohopanes (Farrimond et al., 1998; Peters et al., 2005). In furtherance, C_{27} , $18\alpha(H)$ -

22, 29, 30-Trisnorneohopane (Ts) and C₂₇, 17 α (H)-22, 29, 30-Trisnorhopane (Tm) ratio have been widely employed as a supporting maturity indicator.

It is worth noting that Tm Peak in immature samples may not be well developed and a 17 β (H)-22,29,30-trisnorhopane isomer perhaps developed instead, which explains the low abundance of Tm and an indication of immaturity (Abdullah and Abolins, 1999). Thus, as the maturity increases during the catagenetic stage, Ts displays a high concentration compared to Tm (Seifert and Moldowan, 1981). The relationship between the two parameters is expressed as Ts/(Ts+Tm), Ts/Tm or Tm/Ts ratio. This ratio is both related to both maturity and organic facies source input (Abdullah and Abolins, 1999; Peters et al., 2005; Adegoke et al., 2014). In this research, the hopanoids are monitored on the *m/z* 191 ion chromatograms (Figure 4.7).

2.4.6.5 Steranes

Sterane represents an important biomarker group which originated from sterols in higher plants and algae but rare or absent in prokaryotic organisms (Huang and Meinschein, 1979; Tissot and Welte, 1984). They are good indicators of organic matter source input, paleodepositional environment and thermal maturity. Based on relative abundance of the “regular steranes” (C₂₇, C₂₈ and C₂₉), Huang and Meinschein, (1979) proposed a classification system based on the predominance of C₂₇ steranes being source input of marine phytoplankton, C₂₉ steranes are evidence of terrigenous matter, while C₂₈ steranes suggest contribution from lacustrine algae. The ratio of C₂₉/C₂₇ > 1 has been reported for terrestrial organic matter input (Czochanska et al., 1988; Harouna and Philp, 2012).

It ought to be noted that, exceptions occur where some marine organisms contribute to C₂₉ regular steranes such as diatoms (Volkman, 1986, 1988). Thus, supporting evidences such as petrographic studies are always recommended for

paleoenvironmental interpretation (e.g. Abdullah and Abolins, 1999; Ayinla et al., 2017a).

Moreover, high sterane/hopane ratio close to 1 characterised planktonic marine source, while a low ratio of sterane/hopane typifies terrestrial organic matter (Tissot and Welte, 1984). Holba et al. (2003) observed that high values of hopane/(hopane + sterane) > 0.7 characterise terrigenous-rich oils which can be of marine and nonmarine deltaic or coal source.

Sterane ratios of C₂₉ (20S/20S + 20R) and C₂₉ ββ/(ββ + αα) are commonly used as maturity indicators (Farrimond et al., 1998). It has been reported that (20S/20S + 20R) C₂₉ sterane ratio usually increases from 0 until equilibrium (0.52-0.55), while C₂₉ ββ/(ββ + αα) vary from 0 to equilibrium around 0.67-0.71. However, coelution of the ααα isomer with the αββ isomers is a known problem in immature samples (Seifert and Moldowan, 1986; Peters et al., 2005). Thus, integration of other thermal maturity parameters is recommended. For the analysed samples, steranes are monitored on the *m/z* 217 ion chromatograms (Figure 4.7).

2.4.7 Pyrolysis gas chromatography (Py-GC)

Py-GC of kerogen is an important geochemical development in the late sixties as a means to elucidate structural composition of kerogen (Giraud, 1970; Larter and Douglas, 1980, Dembicki et al., 1983). It gives a direct indicator of the qualitative and quantitative kerogen composition as well as type of hydrocarbon that can be generated by the kerogen during the thermal maturation process (Dembicki et al., 1983; Horsfield, 1989; Eglinton et al., 1990). Py-GC is often used with Rock-Eval parameters for more accurate assessments of kerogen type (Dembicki, 1993).

The chromatogram, of the oil-prone Types I and II kerogens usually display *n*-alkanes and *n*-alkenes doublet (>*n*-C₁₅) extending to the high molecular weight compounds (C₃₀₊). Chromatogram of gas-prone Type III kerogen are characterised by

n-alkanes and *n*-alkenes doublet confined to $<n-C_{10}$. A typical Type IV kerogen with little gas or no hydrocarbons potential show few or no chromatographic peak. Marine organic matters are characterised by more *n*-alkane/*n*-alkene doublet compared to terrigenous organic matter with high aromatic compounds, xylene and phenol. On the other hand, *n*-alkyl derived from lipids and aliphatic biopolymers are incorporated into the marine organic matter (Tissot and Welte, 1984; Dembicki, 2009).

2.5 Inorganic geochemical overview

2.5.1 Major elements

Major elements (e.g. Si, Al, Fe, Mg, Ca, Na and K) are elemental component of major oxides such as SiO₂, Al₂O₃, FeO, MgO, CaO, Na₂O and K₂O whose composition in rocks are usually greater than 1%/. Major oxides composition can be determined using Inductively-coupled plasma mass spectrometer (ICP-MS) analysis as well as X-ray fluorescence, XRF, (Peters et al., 2005; Roy and Roser, 2013; Tao et al., 2013; Makeen et al., 2015a).

Al₂O₃ and SiO₂ are important oxides in sediment which often show reasonable correlation with each other and the organic matter content in sedimentary rocks. Usually, coarse sediments are characterised by significant SiO₂ concentration, whereas Al₂O₃ is the characteristic component of clay minerals. Thus, the oxides display negative correlation with each other (Fu et al. 2011). Similarly, K₂O and TiO₂ are also associated with clay minerals (Fu et al., 2011). Roser and Korsch (1986) discriminate tectonic settings based on the bivariate plot of log (K₂O/Na₂O) versus SiO₂. Hence, three or four sedimentary origins and tectonic settings have been suggested i.e. oceanic island arc, continental island arc, active continental margin and passive margin (Maynard et al., 1982, Bhatia, 1983, Bhatia and Crook, 1986 and Roser and Korsch, 1986, Tao et al., 2013).

Climatic conditions of a sedimentary basin play an important role in organic matter input, (Suttner and Dutta, 1986; Hieronymus et al., 2001; Ratcliffe et al., 2004; Beckmann et al., 2005; Roy and Roser, 2013; Makeen et al., 2015a). This means that, paleoclimatic condition of a basin can be inferred from the concentration of constituting elements/oxides such as SiO_2 versus $\text{Al}_2\text{O}_3 + \text{K}_2\text{O} + \text{Na}_2\text{O}$ as well as $\text{K}_2\text{O}/\text{Al}_2\text{O}_3$ versus trace elements ratio of Ga/Rb (Suttner and Dutta, 1986; Roy and Roser, 2013). Warm-humid climate enhance mineral nutrient supply and phytoplankton growth (Talbot, 1988; Makeen et al., 2015a). Therefore, organic carbon and total sulphur content in the sedimentary rocks can give useful information about the paleodepositional environment and activities of microbial sulphate reduction (Berner and Raiswell, 1983; Berner, 1984; Mohialdeen and Raza, 2013).

2.5.2 Trace elements

Trace elements such as V, Ni, Cr, U, Th, Co and Mn are elemental components of rocks (e.g coal, mudstones and shale) whose composition are less than 0.1% thus expressed in part per million (ppm) or part per billion (ppb) (Swaine, 1990). The distinguishing physical and chemical properties of coal, mudstones and shale are associated with their organic and inorganic component (Wilkins and George, 2002; Peters et al., 2005; Sia and Abdullah, 2012). The organic components of these sedimentary rocks can give useful information about the kerogen type/origin, hydrocarbon potential and paleodepositional environments (Peters and Cassa, 1994). On the other hand, inorganic constituents such as major and trace element composition are good indicators of provenance, redox conditions during sedimentation and/or the effect of preservation of organic matter, water salinity, paleoclimate and tectonic setting (Tribovillard et al., 2005; Moosavirad et al., 2011, Mohialdeen and Raza, 2013; Shu et al., 2013, Jia et al., 2013; Makeen et al., 2015a). Trace element composition can be

determined using Inductively-coupled plasma mass spectrometer (ICP-MS) analysis (Adegoke et al., 2014).

The term “clark” (= Clarke, in English) was introduced in 1923 by A.E. Fersman (the famous Russian geochemist) in honor of the former Chief Chemist at U.S. Geol. Survey, F.W. Clarke, who first calculated average composition of various rocks, and later, the Earth's crust (Ketriss and Yudovich, 2009). Today, Clarkes' represents the average content of given chemical element in the Earth's crust and also in the hydrosphere. For example, “coal Clarkes” means the average trace element composition in the World coals. Others include “Clarkes of sedimentary rocks”, “Clarkes of granites”, etc. (Ketriss and Yudovich, 2009).

Concentration of trace elements such as V, Ni Cr, U, Th, Co and Mn in sediments are indicators of paleo-redox conditions of sedimentary basin (e.g. Algeo and Maynard, 2004; Yang et al., 2004; Harris et al., 2004; Tribovillard et al., 2005; MacDonald et al., 2010; Fu et al., 2011, Adegoke et al., 2014). Similarly, seawater can be differentiated from fresh water based on the concentration of trace elements such as Ba, Ga, Rb, Sr and V (Reimann and De-Caritat, 1998, Makeen et al., 2015a).

CHAPTER 3: METHODOLOGY

3.1 Introduction

A thorough literature search was carried out in order to determine the best approach to be adopted in assessing the organic and inorganic geochemical characteristics of the Gombe Formation coals, mudstones and shales for its suitability as potential hydrocarbon source rock. This revealed that, usually, geochemical characterisation of source rock involves assessment of three important parameters (organic matter quality, quantity and thermal maturity; Figure 3.1) among others (e.g. Peters and Cassa, 1994, Peters et al., 2005). Based on this fact, a careful selection of methods (Figure 3.2) which is up to state-of-the-art and will produce valid and reliable information were made. These parameters were adopted in this study (e.g. Espitalié et al., 1977; Peters et al., 2005; Teichmuller, 1989; ICCP, 2001; Sykorova et al., 2005; Hakimi and Abdullah, 2014; Pickel et al., 2017). A total of 81 samples were used for this study. During the analyses, systematic errors were avoided by calibrating, running blank GC column and ensuring proper functioning of the equipment. In the course of doing these, random errors were avoided by taking repeated measurements, calculating the average and standard deviation (quality control). Therefore, this chapter discusses the two approaches employed in this research: fieldwork (sampling) and laboratory analyses.

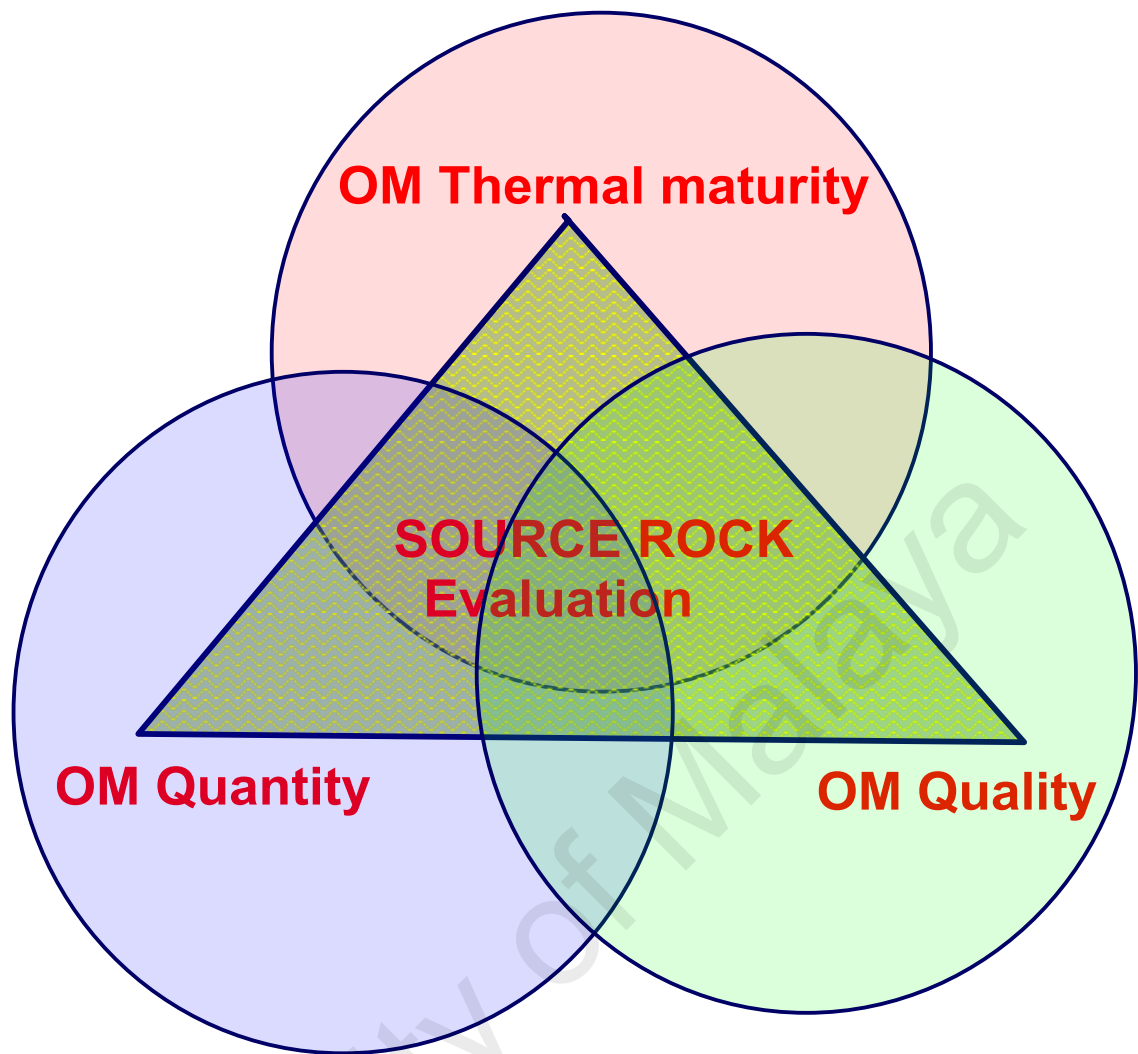


Figure 3.1: Illustration of source rock evaluation parameters.

3.2 Fieldwork and sampling

Fieldwork was conducted in the active mining sites hosting the Gombe Formation following the report of discovery of about 4.5 million tons of coal (proven reserve). The mining operation started in October 2007 at Maiganga coalfield. This provided access to subsurface samples and data of the Gongola sub-basin. Four coal seams from the Maiganga and Yaya-Ngari areas of the Gongola Sub-basin were identified and studied in detail. The following are the steps involved in this fieldwork:

i. Literature review for fieldwork

Before the fieldwork was conducted, several papers regarding Geology of the Gongola sub-basin were reviewed to gain insight into general Geology of the area and have bigger picture on its lithology and structural orientation (e.g Jauro et al., 2007, 2008; Obaje, 2009; Abubakar, 2014). Among others, relevant literatures on geochemical studies were consulted to determine what to target during the fieldwork to obtain useful samples for the intended analyses (Peters and Cassa, 1994; Peters et al., 2005).

ii. Data acquisition methods used in this trip are:

- a) Reconnaissance using Google Earth
- b) Sedimentary logging and sample collection
- c) Acquisition of samples from Ashaka Cement Company operational site at Maiganga.

iii. Tools used:

- a) Bruton GPS: to determine the co-ordinates of the study location
- b) Clinofom compass.
- c) Measuring tap: to measure bed true thickness.
- d) Sedimentary logging sheet: recording lithology, grain size, sedimentary structures, trace fossils etc.
- e) Hand lens and grain size comparator: to determine the sandstone grain size.
- f) Geological hammmer and chisel: to obtain fresh samples.
- g) Samples bag, masking tape amd permernet marker: to bag the samples and label them accordingly.
- h) Protective wears: body and head protector, eye protective glass, nose mask and foot wear.

iv. Sampling

Eighty-one outcrop samples (coal, mudstones and shales) collected from both Maiganga and Yaya-Ngari areas were used for this study. In the course of the fieldwork, sedimentary characteristic of the rocks including the colour, grain size, shape arrangement, orientation, bed attitudes, sedimentary structures, fossils were observed, described and measured. A systematic sampling was carried out based on variation in lateral and vertical succession of the sedimentary facies. The lithologic changes (e.g. colour, grain size, shape and arrangement) within the area were considered in the choice of sampling interval (about 1 m) after removing weathered surfaces (about 5 cm). Thereafter, a lithologic log of the sedimentary facies in the area was produced (see Figure 4.1). The samples collected were bagged and labelled accordingly in readiness for laboratory preparation and subsequent analyses.

3.3 Laboratory analyses

The laboratory analyses employed for organic and inorganic facies characterisation involve standard methods which can be grouped into three:

1. Organic geochemical method:

- i. Source rock analyses using SRA.
- ii. Total organic carbon content (TOC) determination.
- iii. Bitumen extraction using Soxhlet apparatus.
- iv. Column chromatography.
- v. GC/GCMS & biomarker studies.
- vi. Py-GC
- vii. Bulk kinetics.
- viii. Ultimate analysis.

2. Inorganic geochemical method:

- i. XRF analysis (clay mineral).

- ii. XRD (major oxides) analysis.
 - iii. ICPMS (major and trace element).
3. Petrographic method:
- i. Vitrinite reflectance measurement.
 - ii. Maceral point count
 - iii. Visual kerogen typing.

University of Malaya

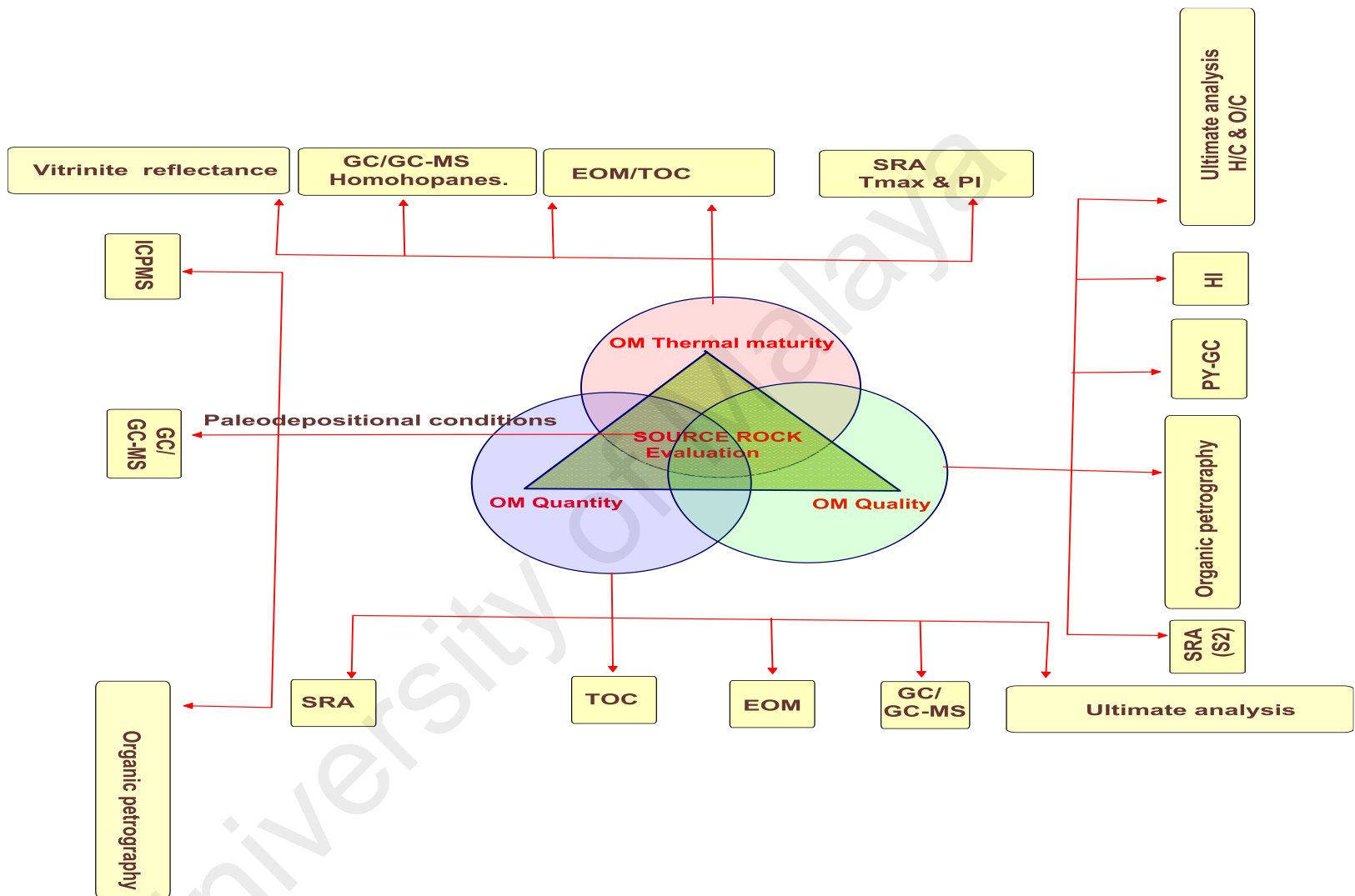


Figure 3.2: Flow chart showing the laboratory analyses used for source rock evaluation.

3.3.1 Organic geochemical methods

An array of geochemical methods was carried out to characterise the organic facies in order to determine the source rock potential, thermal maturity, source input and paleoenvironmental condition during deposition. The methods are:

3.3.1.1 Source rock analysis SRA

Weatherford source rock analyser (equivalent of Rock-Eval equipment, Figure 3.3) was used for screening of whole rock samples (pyrolysis) of the studied sedimentary facies (Espitalié, 1977; Peters and Cassa, 1994; Peters et al., 2005). This method was employed to evaluate the bulk composition of organic matter (S_1 , S_2 and T_{max}) as well as their derivatives: which will be used to determine the source rock hydrocarbon potential (OM quantity and quality) and thermal maturity. About 30 mg of coal and 90 mg of non-coaly samples were crushed to fine powder ($< 150 \mu\text{m}$) and screened by source rock analyser (SRA) which pyrolysed the samples to $600 \text{ }^\circ\text{C}$ in a helium atmosphere. The SRA machine used for this analysis has two components: The basic unit is the SRA-TPH (total petroleum hydrocarbon) which provides the amount of free hydrocarbon (S_1), the amount of hydrocarbon generated after thermal cracking of non-volatile organic matter (S_2) as detected by the flame ionization detector (FID) as well as T_{max} which represents the maximum temperature of S_2 -peak. The other component is the SRA-TPH/TOC which is used for determining the S_3 and TOC. In this study, only the SRA-TPH component was used to determine S_1 , S_2 , and T_{max} . Hence, oxygen index (OI) values were not obtained. Other parameters such as hydrogen index (HI), production index (PI), production yield (Py) were derived from the SRA data as follows:

Hydrogen Index (HI) = $(S_2 \times 100)/\text{TOC}$ (mg HC/ g TOC).

Production Index (PI) = $S_1/(S_1+S_2)$.

Production yield (PY) = S_1+S_2 (mg HC/g rock).

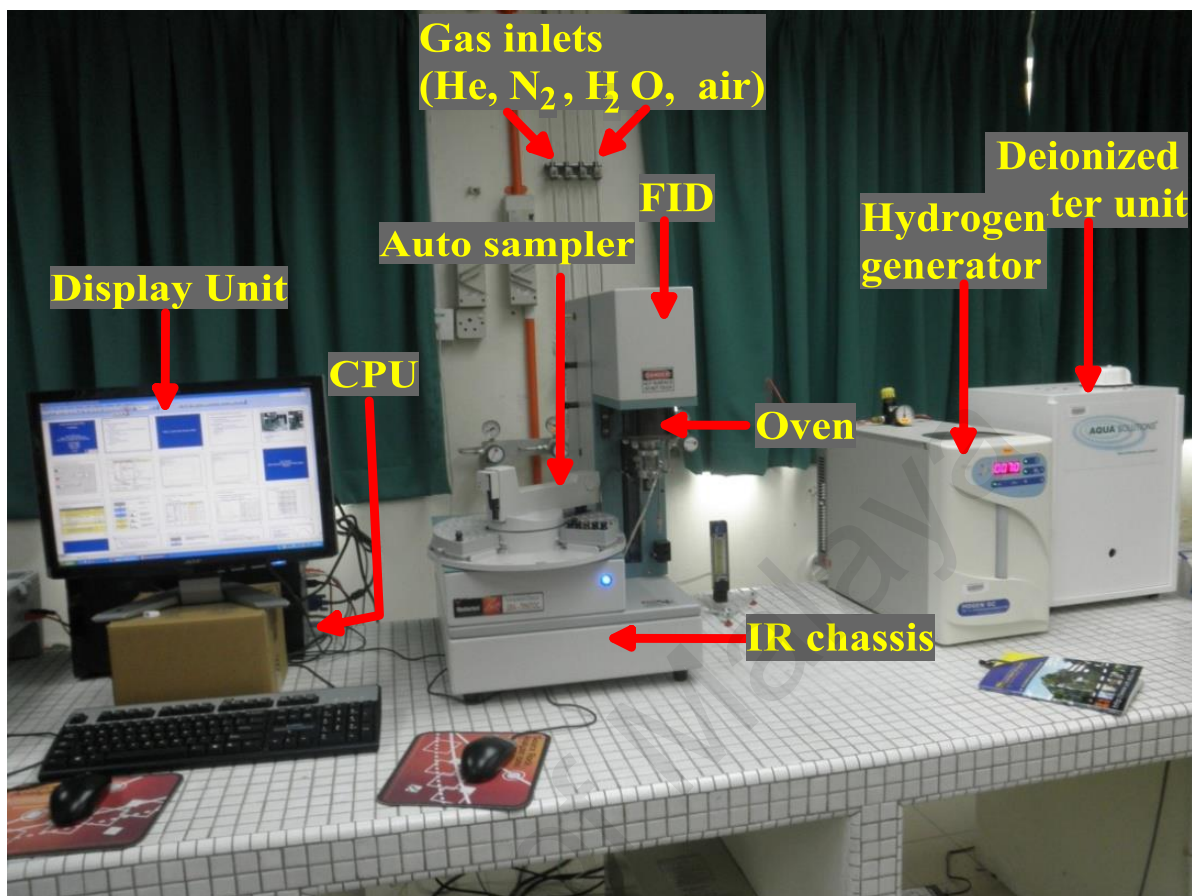


Figure 3.3: Weatherford source rock analyser (equivalent of Rock-Eval equipment) used for screening the whole rock samples.

3.3.1.2 Total organic matter content (TOC) determination

A Multi N/C 3100 analyser produced by Analytik Jena (Figure 3.4) was used to determine the total organic matter content (richness) of coals and other organic rich sediments of the Gombe Formation. All the samples were treated with HCl to remove CaCO_3 and dried at about 25°C for 24 hours. Subsequently 100 mg of each sample was subjected to TOC analysis using the multi N/C 3100 analyser (Figure 3.4) that was carried-out at university of technology PETRONAS (UTP). The total organic carbon values obtained is used alongside other parameters such as S_2 (from SRA), extractable organic matter (EOM) and hydrocarbon yields (from bitumen extraction method) to determine the quantity of organic matter and the generative potential of the source rock.

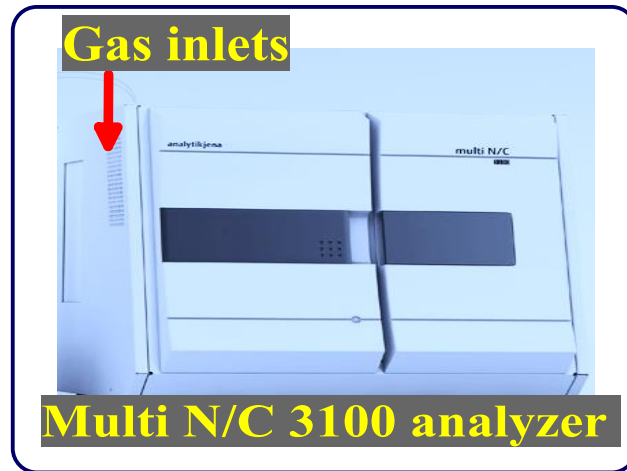


Figure 3.4: A Multi N/C 3100 analyser produced by Analytik Jena used to determine the total organic matter contents (richness) of sedimentary facies from the Gombe Formation.

3.3.1.3 Bitumen extraction method

Bitumen extraction using Soxhlet procedure is an excellent way of determining the bitumen contents and hydrocarbons concentration (saturates + aromatics). The result provides complementary data which can be compared with the S_1 , S_2 and TOC while evaluating the source richness (OM quantity) and hydrocarbon generation potential. This method involves subjecting fresh whole rock samples to bitumen extraction procedure using a Soxhlet apparatus in order to obtain the extractable organic matter (EOM) or bitumen which is precursor of oil.

In carrying this out, about 10 g of coal and 20 g of shales/mudstones samples were pulverized to less than 75 microns' grain size and were put into thimble, subsequently covered with cotton, and then placed in a Soxhlet apparatus (Figure 3.5a). 200 ml of azeotropic mixture of 93% dichloromethane (DCM) and 7% methanol were used in 250 ml flat bottom flask, connected to the Soxhlet apparatus with attachment to a condensing chamber. Anti-bumping granules and copper sheets were added to the solvent in the flask, while the condensing chamber is connected to water inlet and outlet to cool the system. This reflux procedure lasted for 72 hours to ensure exhaustive

extraction. The EOM collected in the flask were evaporated, using Buchi rotary evaporator (Figure 3.5b). Thereafter, a concentrated EOM was transferred to a clean, labelled and weighed vial and allowed to dry. The difference between the weight of the empty vial and weight of the vial + EOM after drying gives the EOM contents.

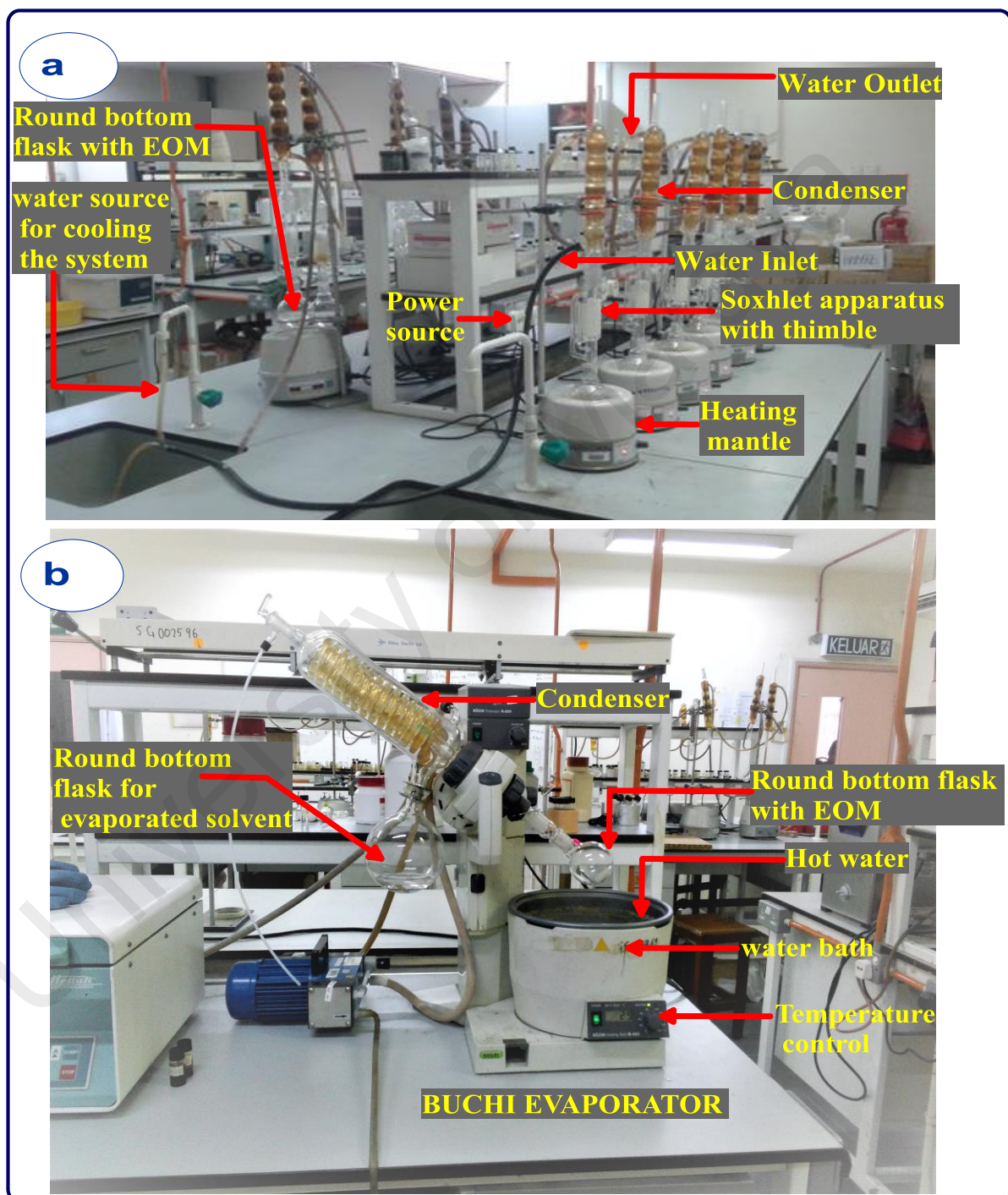


Figure 3.5: (a) Bitumen extraction set-up (Soxhlet procedure) showing thimbles containing samples, covered with cotton in a Soxhlet apparatus, round bottom flask for extracted EOM, water source and inlet connected to the condenser as well as the hot plate (heat source) (b) Buchi rotary evaporator.

3.3.1.4 Liquid column chromatography

Liquid column chromatography was performed in order to separate the EOM into its different components (saturated, aromatic and NSO compounds). Prior to the commencement of this analysis, alumina and silica, which will form the stationary phase during the separation, were activated by keeping them in the oven at 110°C. Thereafter, a mixture of silica gel and petroleum ether (petroleum benzene) was prepared and poured into a chromatographic column (30 x 0.72 cm) with small cotton at its lower end (Figure 3.6). Similarly, alumina (2-3 cm) was added above the silica. The EOM was separated using solvents of increasing polarity in sequential order of petroleum ether (100 ml), DCM (100 ml) and methanol (50 ml) to obtain saturated, aromatic and NSO compounds respectively. After concentrating the eluents in the Buchi rotary evaporator and drying, weights of the different fractions were determined and recorded. The saturated fraction of the EOM is now ready for GCMS analysis and biomarker studies to determine the organic matter type/source input, thermal maturity and paleodepositional condition during sedimentation of the organic facies.

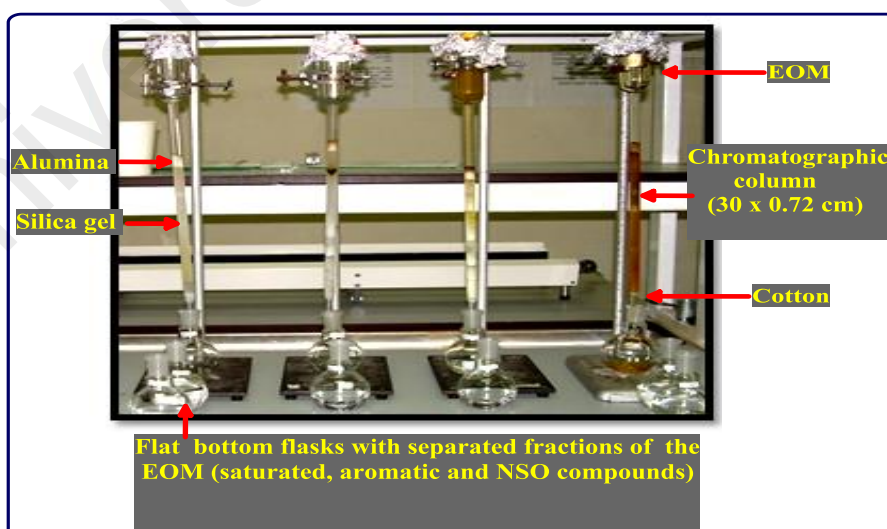


Figure 3.6: Liquid column chromatography set-up to separate the EOM into its different components (saturated, aromatic and NSO compounds).

3.3.1.5 Gas chromatography-mass spectrometry (GC-MS) analysis

GCMS analysis and biomarker studies were carried-out to determine the organic matter type/source input, thermal maturity and paleodepositional condition during sedimentation of the organic facies. The analysis was performed on about 1 μ l of aliphatic hydrocarbon fraction (mixed with *n*-hexane) and injected with the aid of a standard golden syringe into the gas fragmentogram inlet. Fused silica and helium are the stationary and mobile phase respectively employed during the separation. An Agilent GC-MS HP 5975B MSD mass spectrometer with gas chromatograph coupled to its ion source, operating at 70eV ionization voltage, 100 milliamperere filament emission current, 230 °C interface temperature (Figure 3.7), was used for detail analysis of the saturated component of the extractable organic matter. The HP-5MS column GC instrument (column length: 30 m, internal diameter: 0.32 mm, film thickness: 0.25 μ m) was programmed from 40 to 300 °C at 4 °C/min, and then held for 30 min at 300 °C. After fragmentation of the samples in the column, the eluents are recorded on the detector in form of peaks (chromatogram). *n*-Alkanes and linear isoprenoids were identified from fragmentograms ion *m/z* 85, terpanes from *m/z* 191 and steranes from *m/z* 217. These chromatograms were used to study the biomarkers as well as interpret the provalance and depositional setting of the organic matter.

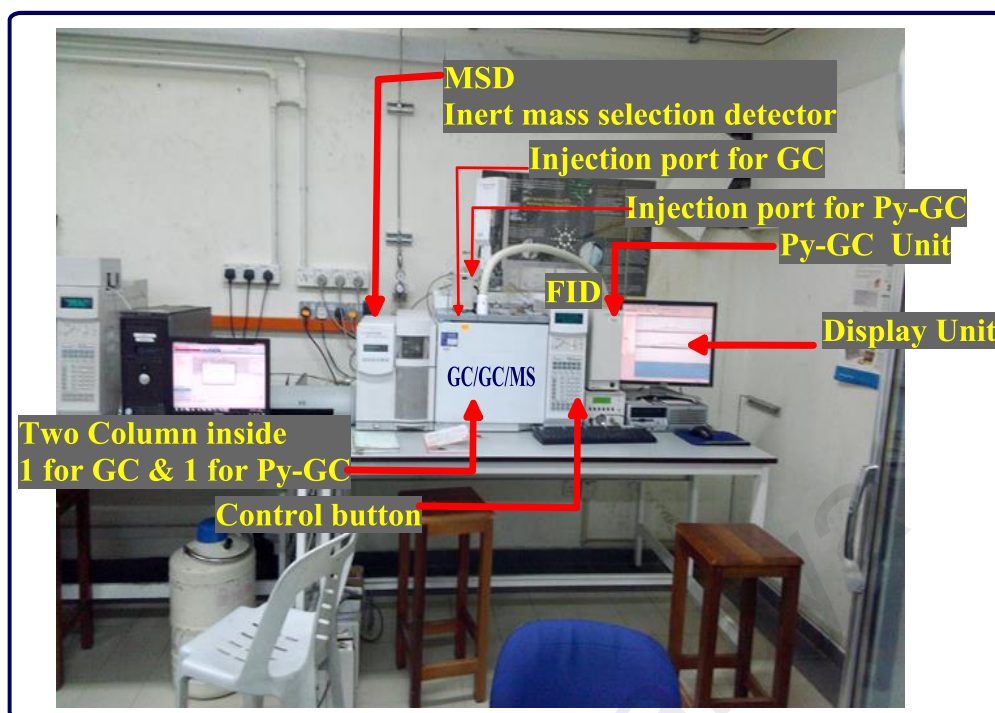


Figure 3.7: Agilent 6890N Series gas chromatography- mass spectrometer (GCMS) and GC attached to Py-2020iD model pyrolysis gas chromatograph (Py-GC).

3.3.1.6 Pyrolysis-gas chromatography (Py-GC)

Pyrolysis-gas chromatography (Py-GC) is a detail S_2 -peak analysis performed to determine the kerogen generative potential and type of petroleum that can be produced during maturation of the Gombe Formation samples. About 4 mg of each sample were subjected to an open system pyrolysis with a flame ionisation detector (FID). This pyrolysis-gas chromatography (Py-GC) analysis uses an Agilent GC chromatograph (HP-Ultra1, 50 m 32 mm i.d., dimethylpoly-siloxane-coated column of 0.52 mm film thickness). During the process, the pyrolysate were monitored between 300-600 °C (25 °C/min). Generated peaks were manually identified using the standard chromatograms on the Agilent ChemStation software together with reference to chromatograms in published literatures (e.g. Larter and Douglas, 1980, Dembicki et al., 1983; Horsfield, 1989; Eglinton et al., 1990; Dembicki, 2009).

3.3.1.7 Bulk kinetic pyrolysis analysis

About 10 mg of selected coal samples were subjected to open system kinetic pyrolysis analysis using Weatherford SRA machine with helium as carrier gas. The samples were heated at different heating rates of 1, 5, 10, 25 and 50°C/min. The bulk petroleum formation curves measured at the five heating rates served as input for the kinetic model. The activation energy distribution (E_a) and frequency factor (A) were evaluated using KINETICS 2000 and KMOD software. The strenuous mathematical model used for kinetic analysis is as suggested by Burnham et al., (1987).

3.3.1.8 Elemental (CHNSO) analysis

Elementar Analysensysteme GmbH (vario MICRO cube; Figure 3.8) with simultaneous determination of carbon, hydrogen, nitrogen, and total sulfur (CHNS) was used for the ultimate analysis carried out on selected coal samples. The oxygen content was calculated based on the difference in the percentage composition of the CHNS. Other calculated parameters are atomic ratio of H/C and O/C using the following formulae:

$$\text{Calculated oxygen content (O)} = 100 - (\text{C} + \text{H} + \text{N} + \text{TS})$$

$$\text{Atomic ratio H/C} = (\text{H}/1.00794)/(\text{C}/12.0107)$$

$$\text{Atomic ratio O/C} = (\text{O}/15.994)/(12.0107)$$

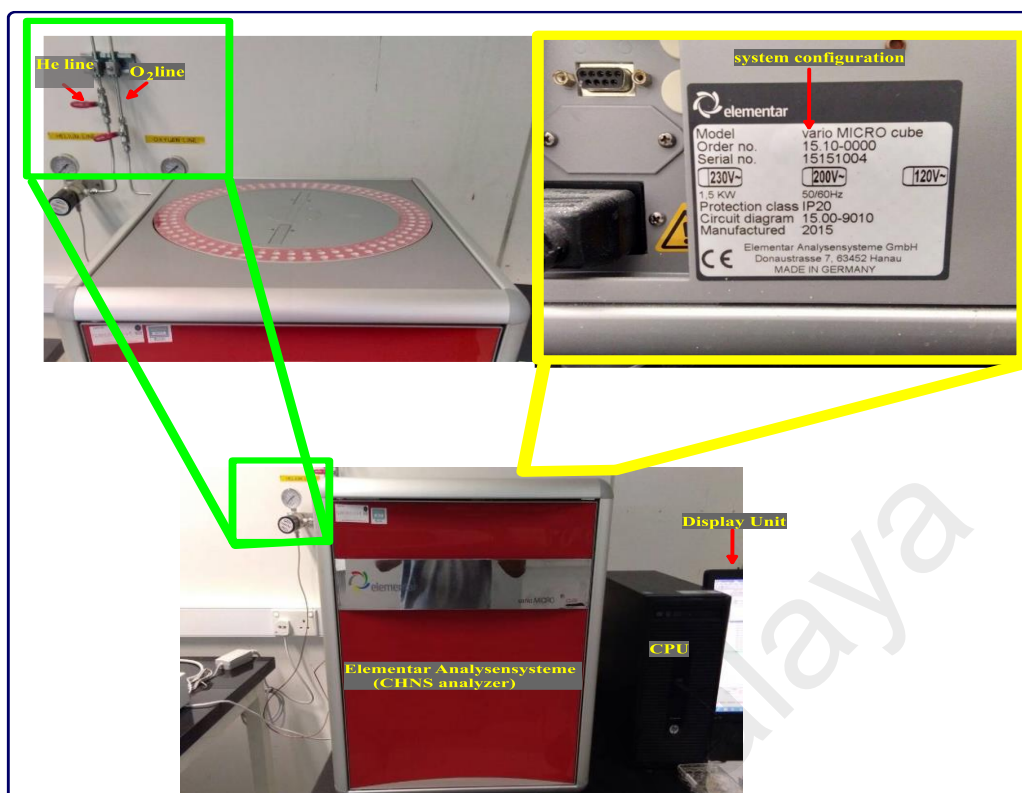


Figure 3.8: Elemental Analyzersysteme GmbH (vario MICRO cube) with simultaneous determination of carbon, hydrogen, nitrogen, and total sulfur (CHNS) used study. This analysis was carried-out at University of Technology PETRONAS (UTP).

3.3.2 Inorganic geochemical analysis

The following are the inorganic geochemical analyses carried out to further elucidate the source rock characteristics:

3.3.2.1 X-ray diffraction (XRD) analysis

X-ray powder diffraction XRD analysis was performed on powdered samples using SIEMENS5000 X-RAY diffractometer with Cu K α radiation (Figure 3.9), run from 5 to 60° 2 θ with step increment of 0.02° and counting time of 2 s per step. Similarly, the clay minerals in the studied samples were further distinguished by analysing the sample under four different conditions: normal (without glycol or heating), after treating with glycol, after heating at 350 °C and 550 °C. The minerals were identified by referencing the ICDD powder Diffraction.

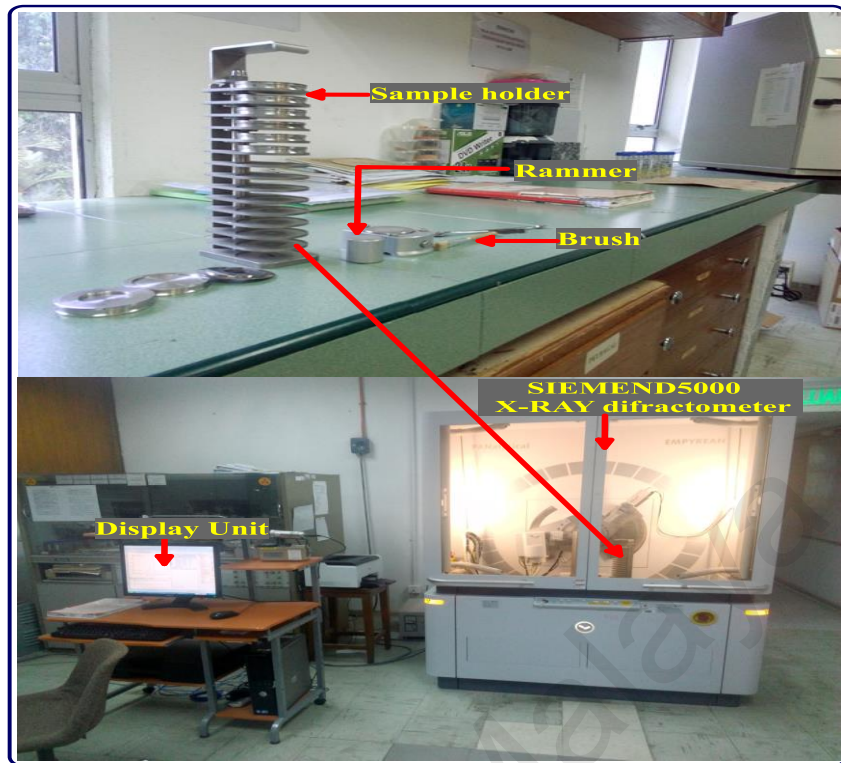


Figure 3.9: SIEMENS5000 X-RAY diffractometer at the Department of Geology University of Malaya.

3.3.2.2 X-ray fluorescence (XRF) analysis

X-ray fluorescence (XRF) analysis was carried out to determine the concentrations of oxides of major elements such as SiO_2 , Al_2O_3 , K_2O , Na_2O , Fe_2O_3 , MnO , MgO , TiO_2 and P_2O_5 . To prepare the pellets used for the analysis, about 3 g of representative sample was thoroughly mixed with about 1 g of cellulose powder using mechanical shaker. The mixture was poured in a metal cast and rammered. Subsequently, Boric acid powder was added to it and the mixture was compressed at 4000 ton using mechanical compactor. The pellet formed was subjected to a non-destructive X-ray fluorescence analysis using PANalytical AxiosmAX 4KW sequential XRF spectrometer (Figure 3.10).

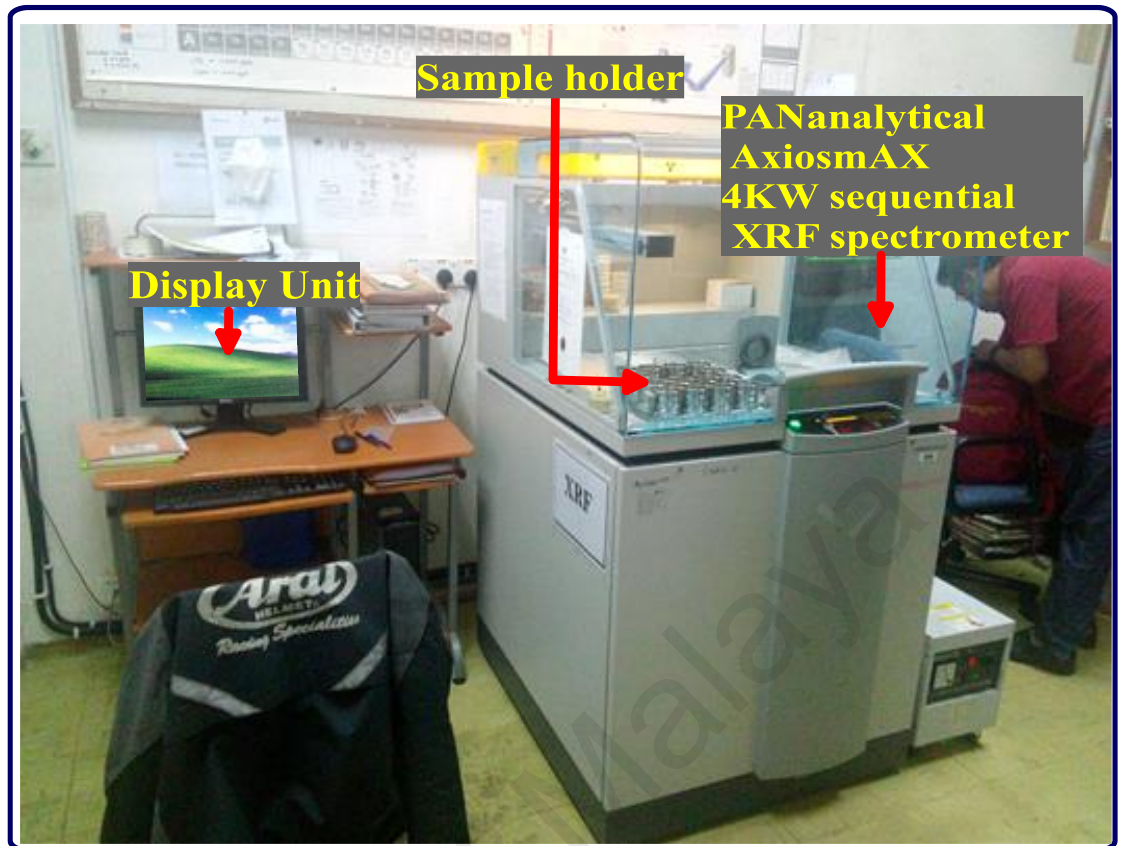


Figure 3.10: PANanalytical AxiosmAX 4KW sequential XRF spectrometer at the Department of Geology University of Malaya.

3.3.2.3 Trace and major elemental (ICPMS) analyses

Inductively-coupled plasma mass spectrometer (ICP-MS) analysis was carried out on about 0.5g of whole rock samples (pulverised) to determine the concentration of major and trace element in Gongola sub-basin. The representative samples were made to pass through digestion process so as to dissolve the constituting elements in liquid medium in readiness for ICP-MS analysis. In order to get total digestion, the samples were heated in HNO_3 - HClO_4 - HF to fuming and taken to dryness. The residue was dissolved in HCl . The minimum and maximum detection limits of the equipment are 0.5 ppb and 100% respectively.

3.3.3 Organic petrographic analysis

Three organic petrographic methods were employed for quantitative and qualitative characterisation and interpretation of the analysed organic facies. These are vitrinite reflectance measurements, maceral identification including maceral analysis (point counting) and visual kerogen typing. The first two methods require production of polished “coal” block, while isolated kerogens mounted on glass slide were used for the later,

3.3.3.1 Polished block preparation

Polished blocks were made in order to have an excellent reflecting maceral surface which can be studied under reflected and Ultra-violet lights for organic facies characterisation and interpretations. Representative samples were crushed, using mortar and pestle to about 0.3 cm grains and carefully arranged in a moulding cup (Figure 3.11). Mounting was done by pouring a densification mixture of hardener (< 2%) and Serifix resin on the “coal grains” in the cups and, allowed to dry for about 48 hours at 30°C. The “blocks” formed were carefully grounded with coarse (350 size), intermediate (550 size), fine (800 size) and very fine (1200 size) silicon carbide powder. Initial polishing was done with agglomerated alpha alumina powder of 1 µm followed by 0.3 µm using water as lubricant during the process, while 0.04 µm colloidal silica (OP-S) suspension was used for final polishing. The polished blocks produced (Figure 3.11) were used for maceral identification, vitrinite reflectance measurements and maceral point counting using organic petrographic microscope equipped with reflected (white) and UV light (Figure 3.12).



Figure 3.11: Polished blocks and materials used during the preparation.

3.3.3.2 Vitrinite reflectance measurements and maceral identification

Organic petrographic studies were performed on polished blocks to determine kerogen type and thermal maturity of the organic matter. This was carried out using LEICA CTR 6000 Orthoplan microscope with $\times 50$ oil immersion objectives (to enhance the component maceral reflectance difference) under immersion oil with a refractive index (n_e) of 1.518 at 23°C (Figure 3.12). Reflected white light was used for vitrinite reflectance measurement, while ultra-violet light was used for maceral identification and capturing of fluorescing macerals. Prior to commencement of vitrinite reflectance measurements, calibration was done with a standard sapphire glass (0.589% reflectance value). Reflectance measurements were carried out using DISKUS fossil software in the random mode (R_{rand}) on ulminites for Maiganga samples and vitrinites for Yaya-Ngari samples at a wavelength of 546 nm and the mean value is recorded. Reported vitrinite/ulminite reflectances (%Ro) are the arithmetic means of 50-100 measurements per sample (Table 4.1). Histograms of the measured reflectance are shown in the Appendix A1.

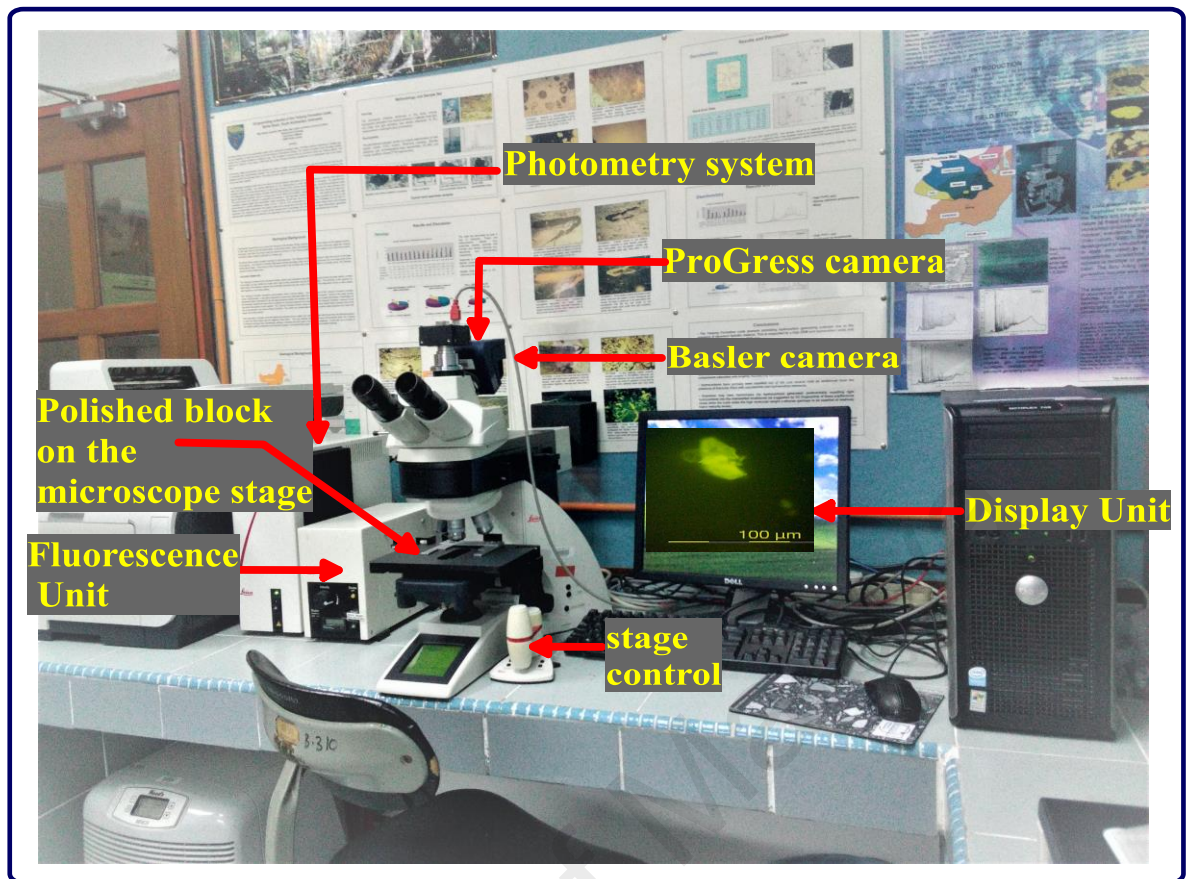


Figure 3.12: LEICA DM6000M microscope CTR6000 photometry system equipped with fluorescence illuminator at the Department of Geology, University of Malaya.

3.3.3.3 Maceral analysis (point counting)

Detailed maceral analysis was performed on selected coal samples based on lateral and vertical facies variation to determine the paleodepositional environment/conditions of the studied samples. Following the low vitrinite/huminite reflectance measurement and T_{max} recorded for the area (Ayinla et al., 2017a), the ICCP system classification of 1994 for low-rank coal was adopted in this study. The three groups of coal macerals (liptinite, vitrinite/humite and inertinite) were identified based on their different colours, relief of polished surface, morphology (shape and structure) reflectance and fluorescence under the microscope (Teichmuller, 1989; ICCP, 2001; Sykorova et al., 2005; Hakimi and Abdullah, 2014; Pickel et al., 2017).

Maceral identification and point count were carried out using a LEICA CTR 6000 reflected light microscope coupled with UV-light illumination using a $\times 50$ oil

immersion objective under immersion oil with a refractive index (ne) of 1.518 at 23 °C (Figure 3.12). An automatic stage adjustment method was used to ensure a systematic maceral count which will give a reliable representation of the coal composition. About 1000 count was performed on each sample. The results are presented as mineral free volume percentage, DISKUS-MACERAL software that is equipped with digital cameras and automatic stage which is advancement over the “point counter” was used for this macerals analysis.

3.3.3.4 Materials for kerogen isolation

The materials used for the kerogen isolation and palynofacies studies are mortar and pestle, weighing balance, sample cups, pipettes, centrifuge, Fume cupboard and Branson sonifer. Others are test tubes, glass slide and cover slip, hydrochloric acid (HCl), hydrofluoric acid (HF), distilled water, filter paper, 250 ml polypropylene beakers, zinc bromide (ZnBr₂), Sigma Aldrich Canada balsam (a mounting medium), and personal protective wears such as safety gloves, glasses and coverall.

Note that:

Hydrochloric acid was used to remove/digest carbonates from the samples.

Hydrofluoric acid was used to remove/digest silicate minerals from the samples.

Distilled water was used to neutralize (pH of 7) the effect of the acids on the samples.

3.3.3.5 Kerogen isolation procedure

Kerogen isolation was carried out in conformity with the standard methods for palynological analysis (Kaiser and Ashraf, 1974; Traverse, 1988; Wood et al., 1996) see Figure 3.13. About 20 g of pulverized samples (~1 mm) placed in 250 ml polypropylene beakers was treated with 10 % hydrochloric acid (HCl) and left for at least 1-2 hours to remove any calcareous material. The content of the beaker was shaken gently for even distribution of the acid while avoiding splashing. After settling,

the acid was decanted and the residue was washed with distilled water and centrifuged five times in order to remove the calcium ions that can form unwanted CaF_2 crystals when hydrofluoric acid (HF) is added. Taking necessary precaution, hydrofluoric acid (HF) with a concentration of 65 % was carefully added to the beaker and left for 24 hours in a fume cupboard to ensure a complete removal of silicate minerals. Afterward, distilled water was repeatedly, but periodically, used to wash the sample until a pH of 7 was attained. The sample was poured into a 25-ml test tube and centrifuged for five minutes at 2000 r.p.m.

The heavy mineral particles were removed using a ZnBr_2 solution (specific gravity of 2.3). 20 ml of ZnBr_2 with five drops of concentrated HCl added to improve better heavy liquid separation that was added to the sample and agitated. The test tubes were placed in an ultrasonic bath for 10 seconds and subsequently centrifuged for 30 minutes at 1500 r.p.m. With the aid of pipette, suspended fraction (kerogen) was transferred into another test tube, while the remaining mineral fraction was discarded. The kerogen in the test tubes with distilled water was centrifuged for 5 minutes at 2000 r.p.m. The isolated kerogen was divided into two: a fraction for Py-GC and the second fraction for visual kerogen typing. All the steps were repeated for each sample to obtain the isolated kerogens.

3.3.3.6 Glass slide mount

Wet isolated kerogens were carefully arranged on the glass slide and allowed to dry at 30 °C. Thereafter, permanent slides were prepared (mounted) using Sigma Aldrich Canada balsam (a mounting medium) covered with 24 x 32 mm cover slip. The slide was allowed to dry for about 20 minutes with excess glycerine removed after two days from the edge of the cover slip. One slide was prepared for each sample and used for visual kerogen study using a LEICA CTR 6000 Orthoplan microscope under transmitted light (Figure 3.13).

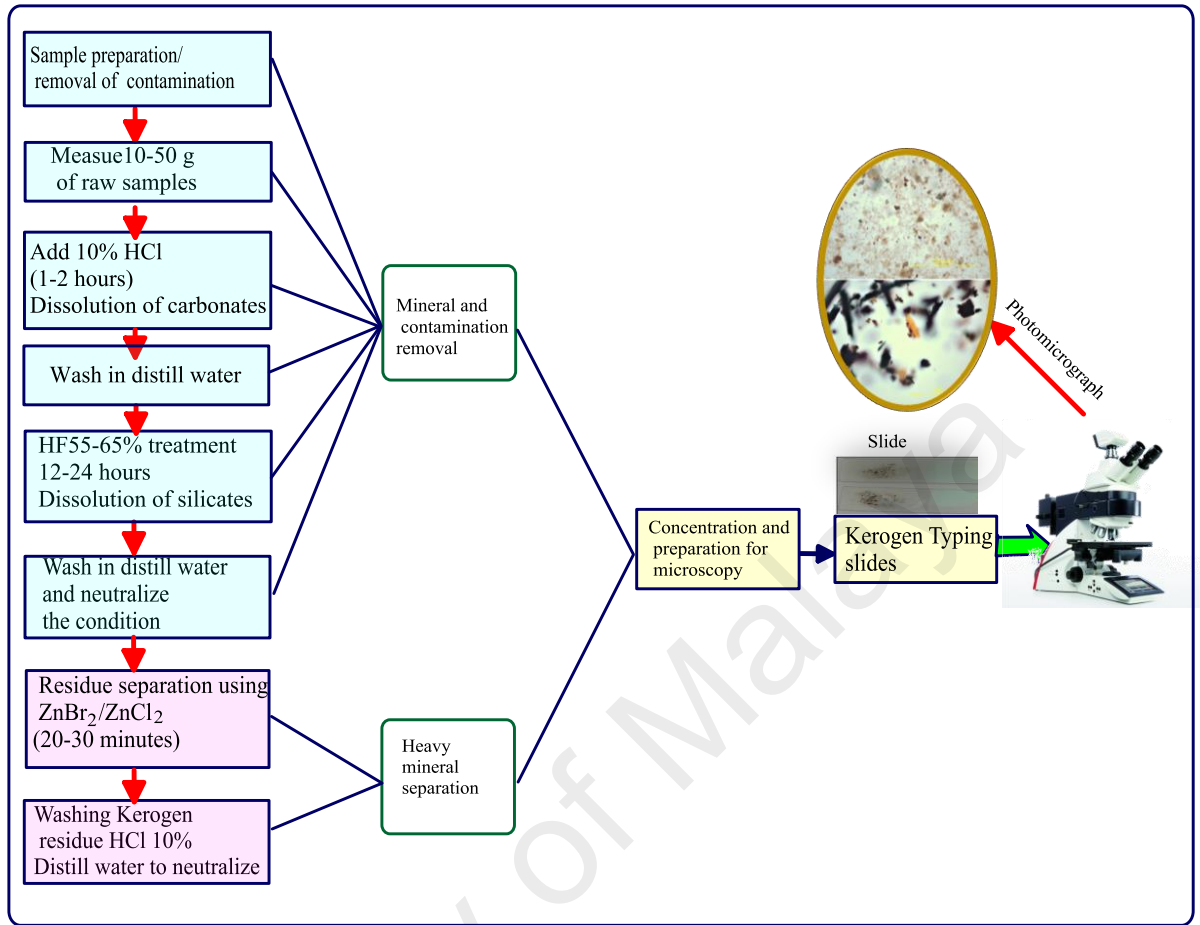


Figure 3.13: Flow chart of the kerogen isolation procedure for palynofacies studies.

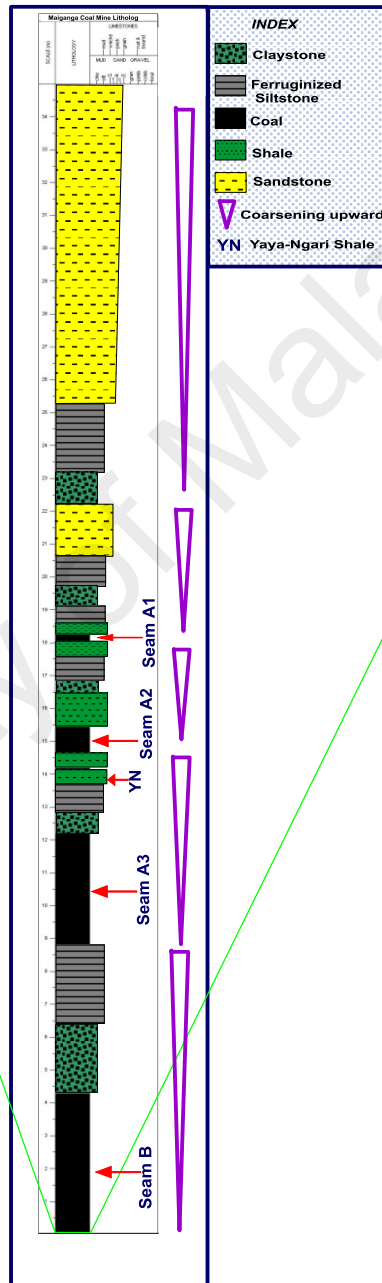
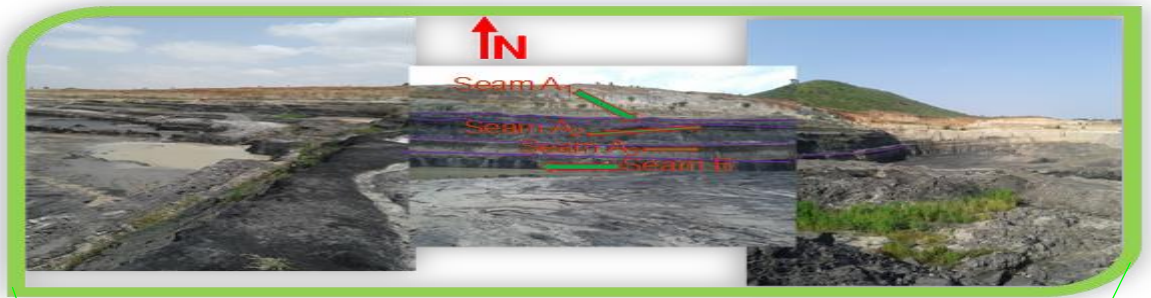
CHAPTER 4: RESULTS OF ANALYSES

4.1 General Statement

This chapter presents the results of organic/inorganic geochemical analyses and organic petrographic studies (see Chapter 3 for the methods) carried out to evaluate the source rock potential of the Gombe Formation. It covers the stratigraphic succession (lithostratigraphic description), bulk geochemical parameter, open system pyrolysis, organic petrographic data, molecular geochemical and bulk elemental data. Detail discussion and interpretation are presented in Chapter 5.

4.2 Stratigraphic succession

The stratigraphic succession of the studied Gombe Formation samples (Maiganga and Yaya-Ngari) is characterised by coarsening upward sequence of deltaic plain sedimentary facies (Figure 4.1). This comprises of coal seams interbedded with mudstones, and shales, while sandstones cap the sequence (Figure 4.1).



4.2.1 Coal

Based on the fieldwork conducted during this study, four coal seams (B, A₃, A₂ and A₁) were identified (Figure 4.1) and studied in detail. They are generally dark brown to brownish black predominantly lignite with some sub-bituminous coal especially in older seam B which is probably due to the associated fault in the area. These seams are thicker compared to the thin bed that was previously reported prior to exploration in the Maiganga coalfield (Figure 4.1). The laterally extensive seam B is hard and thicker (3.5-4.5 m) than A₃ (2.0-3.4 m), A₂ (0.8-2.0 m) and A₁ (0.4-0.6 m) which gradually thins out towards the south (Figure 4.2). The coal seams are dipping southwest due to series of tectonic activity followed by erosion which carve the area into present topography (Figure 4.1). Some peats (Figure 4.2b) observed were associated with the coal seam A₃, while the seams are interbedded with claystones, mudstones, shales and siltstones. These facies can be interpreted as low energy deltaic plain sediments with marine influence.

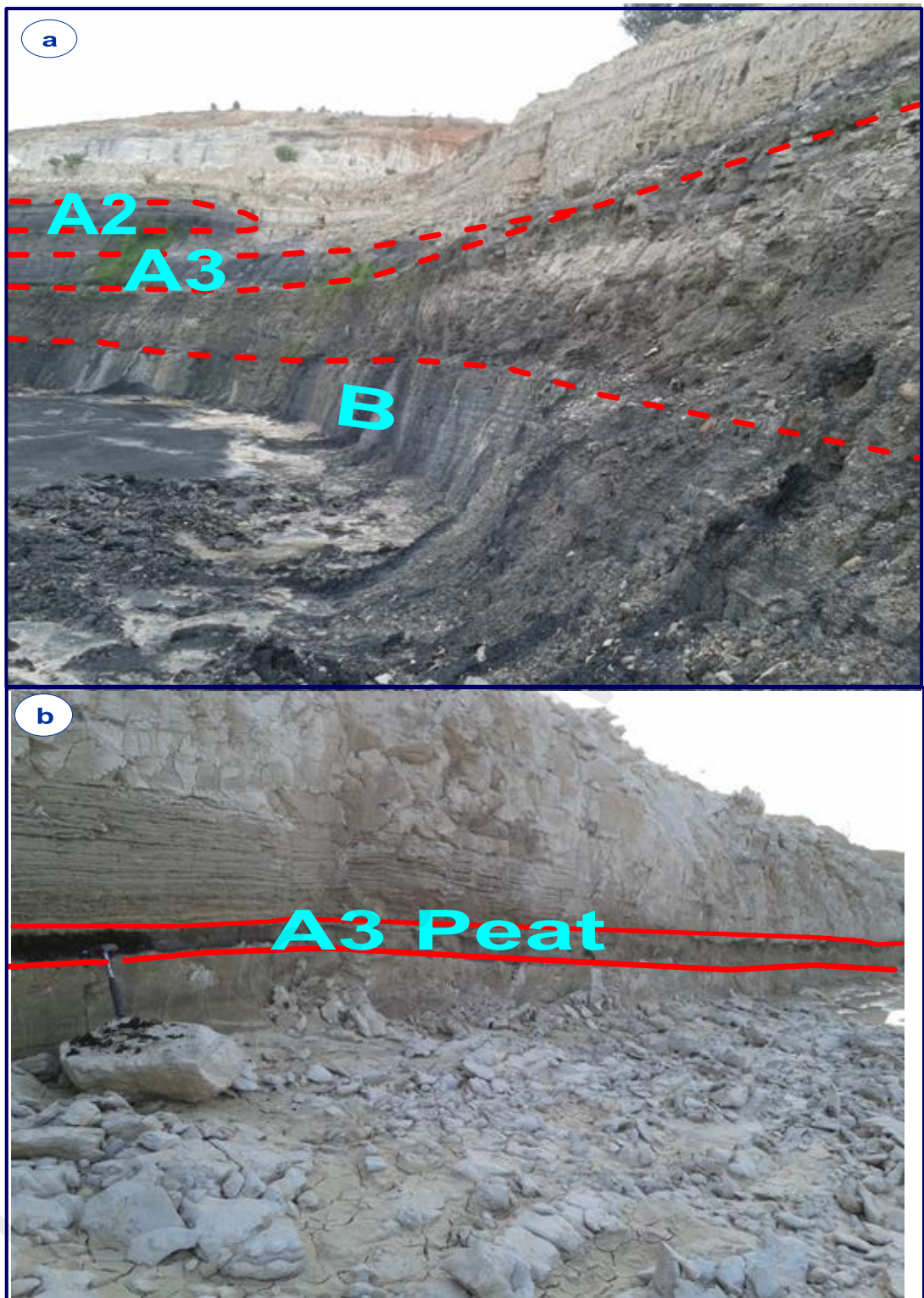


Figure 4.2: Illustration of: (a) the laterally extensive and thicker seams B compared with seam A₃ and A₂ which gradually thin out towards the south and (b) peats associated with seam A₃.

4.2.2 Mudstones (claystones and siltstones)

These are low energy facies comprising of graduation from claystones to siltstones with thickness ranging from 0.6 to 5.5 m (Figure 4.3 a-b). The mudstones are generally grey, well-sorted rocks with parallel lamination and evidence of rootlets which can be associated with terrigenous source input (Figure 4.3b). These facies are most often deposited on the coal facies especially at the basal part of the Gombe Formation (Figure 4.3a). However, in the upper part of this formation, their colour change to light grey/white with decreasing organic matter supply and becomes less laminated. Similarly, fine to medium-grained sandstones overlie the mudstones as the coal bed disappeared (Figure 4.1). This indicates a gradual increase in deposition energy in a delta plain setting

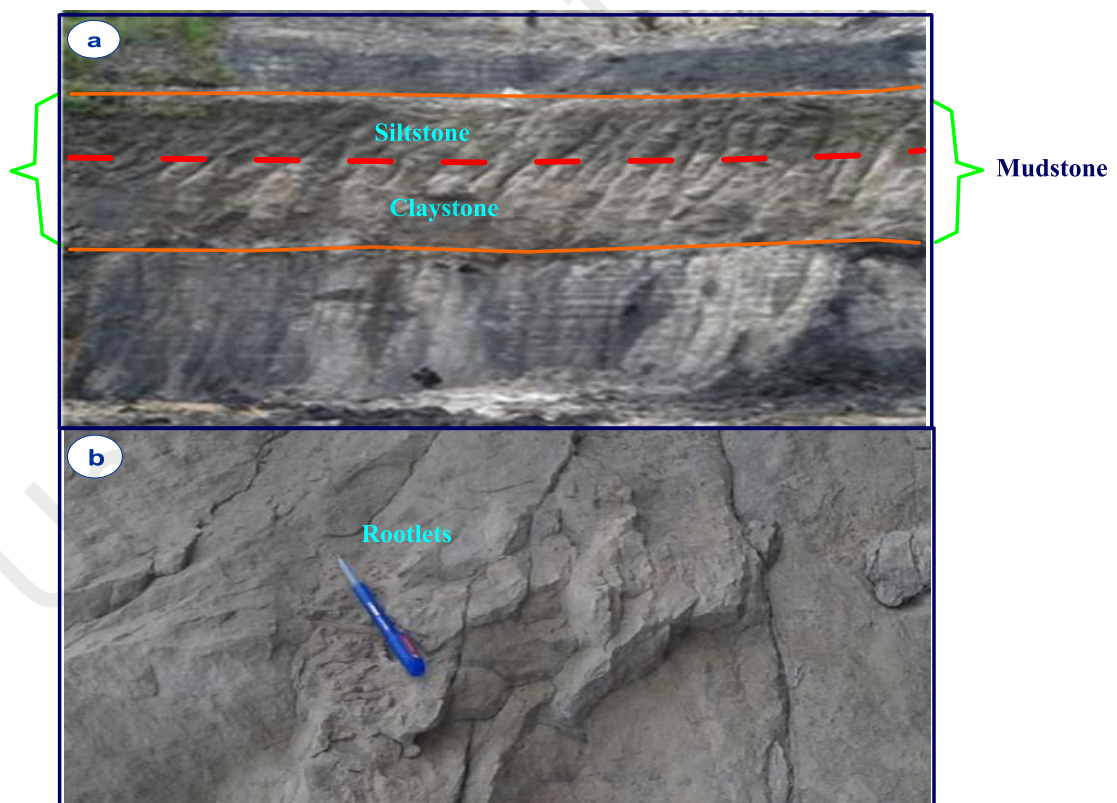


Figure 4.3: (a) Mudstone interbedded within coal seams (b) rootlets on mudstone as evidence of terrigenous source input.

4.2.3 Shales

4.2.3.1 Maiganga Shales

This represents organic rich brown-grey coloured, moderately sorted fine to medium-grained shales with thickness of 2.3 to 0.3 m (Figure 4.4 a-b). The shales are characterised by varying degree of fissility and often conformably deposited on the coal and mudstones facies (Figure 4.4a). They are occasionally interbedded with thin coal bed or associated with lenticular coal pods along faults plane. Evidence of land derived plant and rootlets were observed in some strata which suggest a reasonably high terrigenous source input in the area (Figure 4.4b).

4.2.3.2 Yaya-Ngari Shales

Yaya-Ngari shales are dark grey, moderately sorted medium-grained sedimentary facies with thickness of 2.2 to 0.5 m (Figure 4.4c). They show good organic matter richness compared to excellent organic matter content in Maiganga. The shales are characterised by varying degree of fissility and often associated with some sandy materials (Figure 4.4c). Just like Maiganga shales, Yaya-Ngari shales show evidence of land derived plant and rootlets in some strata, which is an indication of a reasonably high terrigenous source input in the area (Figure 4.4c).

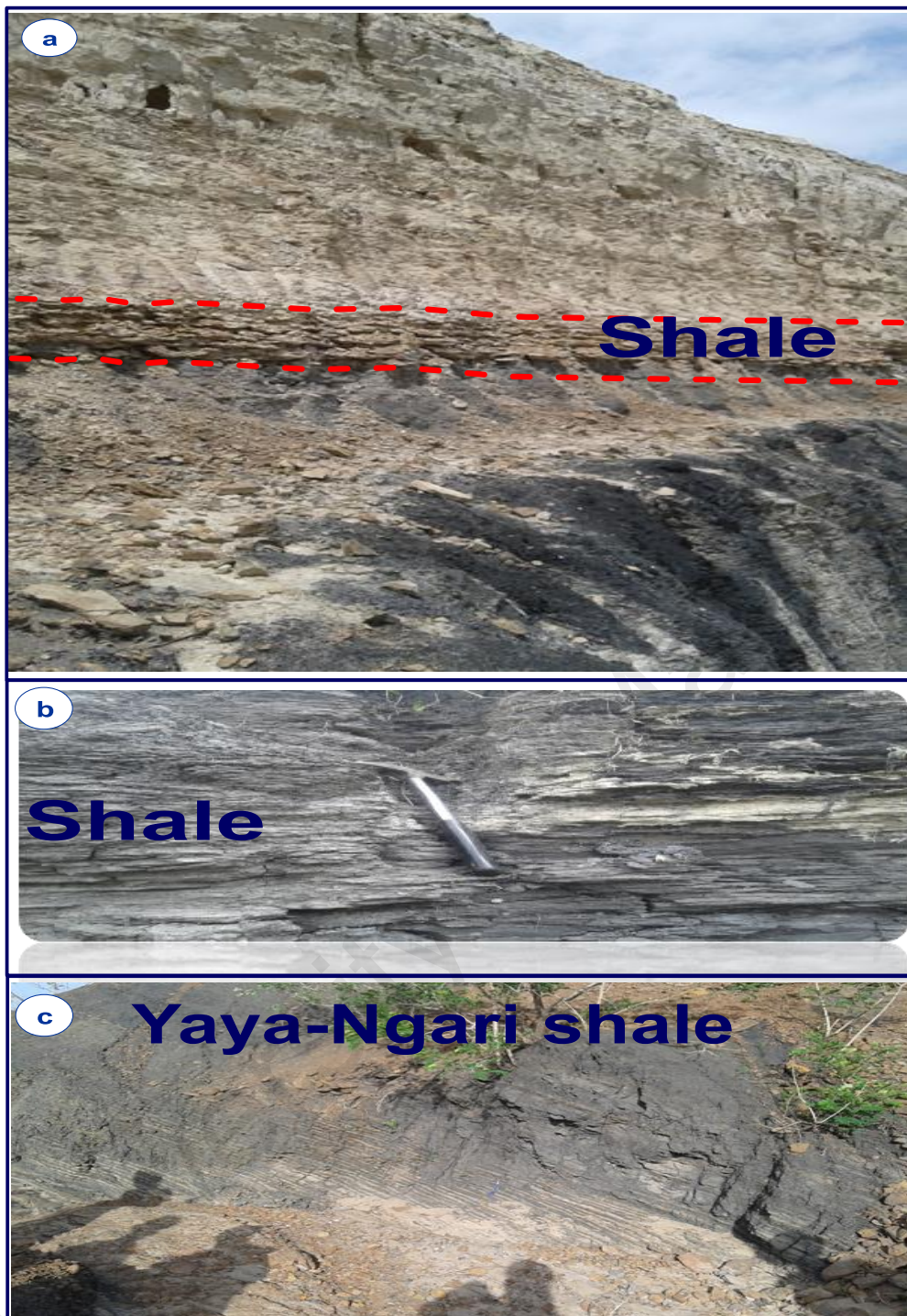


Figure 4.4: (a) Fine to medium-grained shales characterised by varying degree of fissility which overlie coal facies, (b) dark grey shales interbedded with coal showing rootlets which suggest terrigenous source input for the sediments, (c) Yaya-Ngari shale often associated with some sandy materials.

4.2.4 Sandstones

This can be divided into three lithofacies as shown below:

4.2.4.1 Poorly laminated sandstones

These facies consist of grey to light brown, poorly laminated, well-sorted, fine-grained sandstones (1.5-0.4 m). They are fairly indurated and show none or few biotubations (Figure 4.5a).

4.2.4.2 Laminated sandstones

This is made up of grey to light brown, parallel laminated, fine to medium-grained sandstones (3.9-0.6 m) interbedded with iron stones, clay and silty materials. They are marked by few biotubations, normal fault and joints filled with silty material (see Figure 4.5b).

4.2.4.3 Coarse sandstones

These sedimentary facies consist of medium to coarse-grained sandstones with thickness ranging from 10-2.6 m (Figure 4.5c). They are poorly laminated, white to brown quartz dominated by few trace fossils of horizontal burrowing organisms (*Thalassinoides*) with their molds filled with iron material (Figure 4.5d). They are faulted (normal fault) in some places. Pebbly coarse-grained sandstones cap this succession, showing evidence of abandoned distributaries of either a meandering fluvial system or deltaic channel.

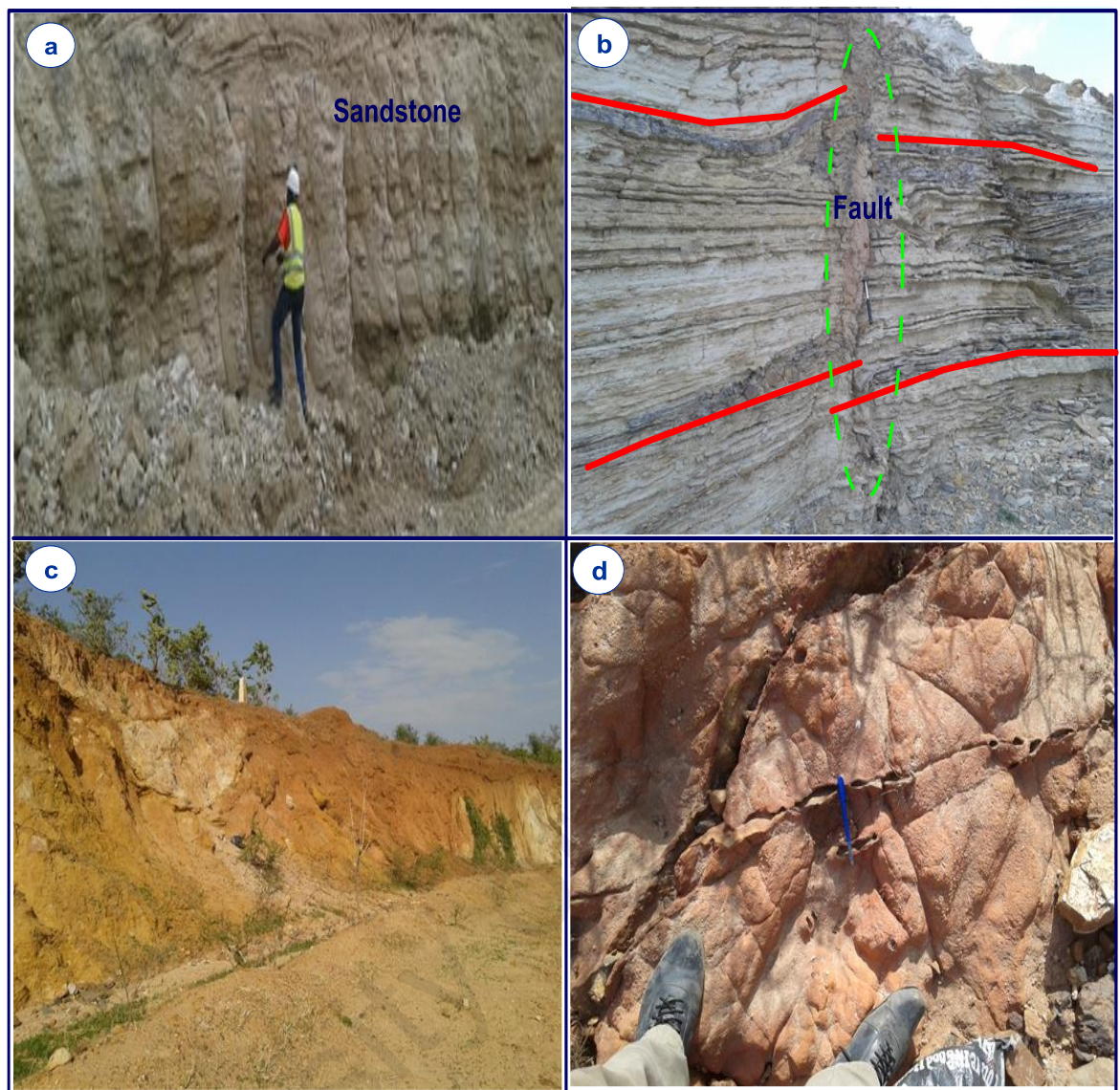


Figure 4.5: (a) poorly laminated fine-grained sandstone, (b) normal fault associated with parallel laminated, fine to medium-grained sandstones interbedded with iron stones, while clay and silty materials fill the fault plain, (c) medium to coarse-grained sandstones and (d) pebbly coarse-grained sandstones with trace fossils of horizontal burrowing organisms (*Thalassinoides*), with their molds filled with iron material.

4.3 Bulk organic geochemical data

The bulk organic geochemical data (Table 4.1) covers the results of the SRA pyrolysis and TOC carried out on the Cretaceous coals and organic rich sediments from the Gombe Formation in the Gongola Sub-basin. The results of the TOC analysis for the samples range from 0.8 to 80.0 wt. % (Table 4.1). The Maiganga coals, as expected, have relatively high TOC values ranging from 50.3 to 80.0 wt. % compared to the shale samples (3.8-24.3 wt. %) and mudstones (2.0-6.7 wt. %). Yaya-Ngari shales have fairly

moderate TOC ranging from 0.8 to 1.3 wt. %. Hydrocarbon yield (S₂) from pyrolysis varies from 0.22 to 158.84 mg HC/g rock. The S₂ trend was observed as follows: the Maiganga coal facies recorded relatively high S₂ (26.42-158.84 mg HC/g rock) compared to the shale (3.18-39.65 mg HC/g rock) and mudstones (0.69-5.07 mg HC/g rock), while a fairly moderate value is observed for the Yaya-Ngari shale (0.22-0.37 mg HC/g rock). T_{max} is generally < 435 °C, except the mudstone above seam A₂ with T_{max} of 436°C in Maiganga area. However, Yaya-Ngari shale samples have T_{max} ranging from 446 to 450 °C. Hydrogen Index (HI, mg HC/g TOC) is relatively high for Maiganga coal (41-234 mg HC/g TOC), moderate for shale (52-191 mg HC/g TOC) and mudstone (24-106 mg HC/g TOC), but low for Yaya-Ngari (23-35 mg HC/g TOC) (Table 4.1).

Table 4.1: TOC content, pyrolysis parameters and vitrinite reflectance data of the studied samples.

Period	Age	Sample	Lithology/Seam	TOC	Pyrolysis data (SRA)						R _o
		ID			S ₁	S ₂	T _{max}	HI	PI	PY	(%)
Upper Cretaceous	Maastrichtian	MGL1B	Coal/seam B	80.0	0.33	130.06	430	163	0.003	130.39	0.35
		MGL1B2	Coal/seam B	80.0	0.32	132.05	430	165	0.002	132.37	0.36
		MGL1C	Coal/seam B	78.4	0.27	158.84	420	203	0.002	159.11	0.32
		MGL1C2	Coal/seam B	69.7	0.35	157.91	421	227	0.002	158.26	0.35
		MGL2A	Coal/seam B	66.2	0.70	123.36	418	186	0.006	124.06	0.35
		MGL2A2	Coal/seam B	66.2	0.99	122.95	417	186	0.008	123.94	0.40
		MGL2B	Coal/seam B	69.4	0.63	59.17	422	85	0.011	59.8	0.28
		MGL2B2	Coal/seam B	62.0	0.59	60.25	421	97	0.010	60.84	0.36
		MGL2C	Coal/seam B	69.7	0.67	71.46	425	103	0.009	72.13	0.31
		MGL2C2	Coal/seam B	69.7	0.62	73.5	425	105	0.008	74.12	0.30
		MGL2D	Coal/seam B	60.0	0.71	56.88	424	95	0.012	57.59	0.26
		MGL2D2	Coal/seam B	60.5	0.85	57.02	423	94	0.015	57.87	0.26
		MGL3A	Coal/seam B	62.0	0.43	110.19	419	178	0.004	110.62	0.30
		MGL3B	Coal/seam B	78.5	0.33	85.25	421	109	0.004	85.58	0.36
		MGL3B2	Coal/seam B	62.0	0.29	84.62	421	136	0.003	84.91	0.36
		MGL2E	Mudstone	2.9	0.10	0.71	427	24	0.123	0.81	0.43
		MGL2E2	Mudstone	2.9	0.15	0.69	428	24	0.179	0.84	0.43
		MGL2F	Mudstone	2.0	0.07	1.98	434	99	0.034	2.05	0.42
		MGL2F2	Mudstone	2.0	0.06	1.85	434	93	0.031	1.91	0.41
		MGL2G	Siltstone	2.2	0.06	1.31	434	60	0.044	1.37	0.31
		MGL2G2	Siltstone	2.2	0.05	1.29	434	59	0.037	1.34	0.31
		MGL2H	Coal/seam A ₂	62.0	0.68	87.19	421	141	0.008	87.87	0.33
		MGL2H2	Coal/seam A ₃	67.3	0.88	109.22	420	162	0.008	110.1	0.33
		MGL2I	Coal/seam A ₃	67.3	0.47	152.27	429	226	0.003	152.74	0.32
		MGL2I2	Coal/seam A ₄	63.7	0.55	129.2	428	203	0.004	129.75	0.32
		MGL2J	Coal/seam A ₂	65.8	0.49	74.73	422	114	0.007	75.22	0.32
		MGL2J2	Coal/seam A ₃	64.9	0.45	82.25	422	127	0.005	82.7	0.32
		MGNS1	Coal/seam A ₃	65.2	0.24	26.42	421	41	0.009	26.66	0.34
		MGNS2	Coal/seam A ₃	76.7	0.34	36.97	417	48	0.009	37.31	0.33
		PSA38	Coal/seam A ₃	50.3	0.21	39.06	426	78	0.005	39.27	0.33

TOC: Total organic carbon (wt. %).

T_{max}: Temperature at maximum of S₂ peak(°C).

HI: Hydrogen Index = S₂ X 100 / TOC (mg HC/ g TOC).

PI: Production Index = S₁/(S₁+S₂).

S₁: Free hydrocarbon (HC) content (mg HC/ g rock).

S₂: Remaining HC generative potential (mg HC/ g rock).

R_o: Vitrinite reflectance (%).

PY: Production yield = S₁+S₂ (mg HC/g rock).

Table 4.1: TOC content, pyrolysis parameters and vitrinite reflectance data of the studied samples (continued).

Period	Age	Sample ID	Lithology/Seam	TOC	Pyrolysis data (SRA)					R _o (%)	
					S ₁	S ₂	T _{max}	HI	PI		PY
		MGL2K	Mudstone	4.8	0.10	5.07	431	106	0.019	5.17	0.37
		MGL2K2	Mudstone	4.7	0.11	4.95	431	105	0.022	5.06	0.37
		MGL2L	Shale	15.0	0.17	8.57	428	57	0.019	8.74	0.37
		MGL2L2	Shale	15.2	0.15	7.95	427	52	0.019	8.10	0.37
		MGL2N	Shale	9.6	0.24	14.18	427	148	0.017	14.42	0.34
		MGL2N2	Shale	9.7	0.35	13.89	427	143	0.025	14.24	0.34
		MGL2O	Coal/seam A ₁	65.4	0.56	98.53	423	151	0.006	99.09	0.30
		MGL2O2	Coal/seam A ₂	65.3	0.63	89.22	424	137	0.007	89.85	0.31
		MGL2P	Coal/seam A ₁	55.9	0.66	130.74	426	234	0.005	131.40	0.35
		MGL2P2	Coal/seam A ₂	55.8	0.68	129.82	427	233	0.005	130.50	0.35
		MGL2Q	Shale	24.3	0.42	32.56	427	134	0.013	32.98	0.30
		MGL2Q2	Shale	24.2	0.49	29.68	427	123	0.016	30.17	0.30
		MGL2R	Mudstone	6.6	0.12	3.63	436	55	0.032	3.75	0.35
		MGL2R2	Mudstone	6.7	0.11	3.95	436	59	0.027	4.06	0.38
		MGL2S	Shale	20.3	0.68	37.51	424	185	0.018	38.19	0.35
		MGL2S2	Shale	20.8	0.57	39.65	425	191	0.014	40.22	0.35
		MGL2T	Coal/seam A ₀	52.0	0.41	70.69	423	136	0.006	71.1	0.32
		MGL2T2	Coal/seam A ₁	51.6	0.45	65.72	423	127	0.007	66.17	0.31
		MGL2U	Shale	3.8	0.12	3.18	433	84	0.036	3.30	0.41
		MGL2U2	Shale	3.8	0.14	3.62	429	95	0.037	3.76	0.41
		YN1A	Shale	1.1	0.16	0.37	449	34	0.302	0.53	0.71
		YN1A2	Shale	1.0	0.14	0.35	448	35	0.286	0.49	0.71
		YN1B	Shale	1.0	0.15	0.24	447	24	0.385	0.39	0.71
		YN1B2	Shale	1.0	0.14	0.23	446	23	0.378	0.37	0.71
		YN1C	Shale	1.3	0.17	0.34	450	26	0.333	0.51	0.72
		YN1C2	Shale	1.2	0.16	0.33	450	28	0.327	0.49	0.72
		YN1D	Shale	0.8	0.16	0.25	447	31	0.390	0.41	0.90
		YN1D2	Shale	0.9	0.15	0.22	448	24	0.405	0.37	0.89

TOC: Total organic carbon (wt. %).

T_{max}: Temperature at maximum of S₂ peak(°C).

HI: Hydrogen Index = S₂ X 100 / TOC (mg HC/ g TOC).

PI: Production Index = S₁/(S₁+S₂).

S₁: Free hydrocarbon (HC) content (mg HC/ g rock).

S₂: Remaining HC generative potential (mg HC/ g rock).

R_o: Vitrinite reflectance (%).

PY: Production yield = S₁+S₂ (mg HC/g rock).

4.4 Extractable organic matter - EOM (or bitumen)

Extractable organic matter (EOM yield; Table 4.2) is a measure of the free hydrocarbon (gas or oil) that can be obtained without cracking the kerogen. This provides parameters such as bitumen and hydrocarbon in ppm which can be compared with the S1, S2 and TOC to determine organic matter richness (quantity) and hydrocarbon generation potential of the Gombe Formation. The classification is based on Peters and Cassa (1994) and Peters et al. (2005).

Table 4.2 shows a relatively high EOM value for the Maiganga samples (5031.2 to 76946.2 ppm), moderate for mudstones (602.6 to 9237.6 ppm) and shale (1910.4 to 6150.5 ppm), compared with low range from 206.6 to 1250.1 ppm for the Yaya-Ngari samples. Contents of aliphatic, aromatic, nitrogen-sulphur-oxygen (NSO) compound fractions and hydrocarbons (calculated as a sum of the aliphatic and aromatic fractions) are given in Table 4.2. As expected, the coal facies have relatively high concentrations of hydrocarbons (1836.8-13974.3 ppm) followed by the mudstones (258.2-4673.1 ppm) and shale (525.4-2229.6 ppm), while Yaya-Ngari has relatively low values ranging from 71.2 to 570.1 ppm (Table 4.2). Usually, EOM yield from coal is high, as observed in this study, thus caution should be applied in interpreting and comparing it with other parameters (Peters and Cassa, 1994). The aliphatic and aromatic fractions were further analysed by GCMS.

Table 4.2: Extractable organic matter and relative percentages of saturates, aromatics and nitrogen-sulfur-oxygen (NSO) compounds of EOM.

Samples ID	Lithology/Seam	Bitumen extraction and chromatographic fractions (ppm of whole rocks)						Chromatographic fractions of bitumen extraction (EOM wt%)			
		EOM (bitumen)	Saturated HCs	Aromatic HCs	NSO compounds	HCs	HCs/EOM	Saturated HCs	Aromatic HCs	NSO compounds	HCs
MGL1B	Coal/seam B	18014.5	1852.7	7159.1	9002.7	9011.8	0.50	10.3	39.7	50.0	50.0
MGL1C	Coal/seam B	17920.2	1741.9	8069.2	8109.1	9811.1	0.55	9.7	45.0	45.3	54.7
MGL1C2	Coal/seam B	15650.2	1449.0	6658.0	7543.2	8107.0	0.52	9.3	42.5	48.2	51.8
MGL2A	Coal/seam B	20242.7	1900.3	7518.7	10823.6	9419.0	0.47	9.4	37.1	53.5	46.5
MGL2A2	Coal/seam B	20169.1	2005.2	8088.7	10075.2	10093.9	0.50	9.9	40.1	50.0	50.0
MGL2B	Coal/seam B	5031.2	479.2	1357.6	3194.4	1836.8	0.37	9.5	27.0	63.5	36.5
MGL2C	Coal/seam B	18112.8	3820.2	7640.3	6652.3	11460.5	0.63	21.1	42.2	36.7	63.3
MGL2D	Coal/seam B	12816.8	2344.5	4220.2	6252.1	6564.7	0.51	18.3	32.9	48.8	51.2
MGL3A	Coal/seam B	46357.7	9037.2	4937.0	32383.4	13974.3	0.30	19.5	10.7	69.9	30.1
MGL3B	Coal/seam B	35507.0	4000.8	3750.7	27755.5	7751.5	0.22	11.3	10.6	78.2	21.8
MGL2E	Mudstone	1120.6	353.2	182.7	584.6	535.9	0.48	31.5	16.3	52.2	47.8
MGL2F	Mudstone	2307.2	456.5	937.7	913.0	1394.2	0.60	19.8	40.6	39.6	60.4
MGL2G	Siltstone	602.6	146.3	111.9	344.3	258.2	0.43	24.3	18.6	57.1	42.9
MGL2H	Coal/seam A3	17505.7	3501.1	3267.7	10736.8	6768.9	0.39	20.0	18.7	61.3	38.7
MGL2I	Coal/seam A3	10897.1	3912.7	2706.0	4278.4	6618.7	0.61	35.9	24.8	39.3	60.7
MGL2J	Coal/seam A3	15060.0	3869.6	3974.2	7216.3	7843.8	0.52	25.7	26.4	47.9	52.1
MGL2J2	Coal/seam A3	14150.9	3650.5	3149.9	7350.5	6800.4	0.48	25.8	22.3	51.9	48.1
MGNS1	Coal/seam A3	73941.8	1570.7	845.7	71525.4	2416.4	0.03	2.1	1.1	96.7	3.3
MGNS2	Coal/seam A3	25442.1	2650.1	9832.4	12959.7	12482.4	0.49	10.4	38.6	50.9	49.1
PSA3 -8	Coal/seam A3	76946.2	1832.1	3164.5	71949.7	4996.5	0.06	2.4	4.1	93.5	6.5
MGL2K	Mudstone	9237.6	1956.2	2716.9	4564.4	4673.1	0.51	21.2	29.4	49.4	50.6
MGL2L	Shale	2049.1	192.7	332.8	1523.7	525.4	0.26	9.4	16.2	74.4	25.6
MGL2N	Shale	5160.5	313.6	741.3	4105.6	1054.9	0.20	6.1	14.4	79.6	20.4
MGL2O	Coal/seam A2	6974.7	1367.6	1914.6	3692.5	3282.2	0.47	19.6	27.5	52.9	47.1
MGL2P	Coal/seam A2	19323.8	2504.9	5224.6	11594.3	7729.5	0.40	13.0	27.0	60.0	40.0
MGL2P2	Coal/seam A2	18500.1	2600.2	5200.1	10699.8	7800.3	0.42	14.1	28.1	57.8	42.2
MGL2Q	Shale	4344.4	757.7	1212.4	2374.3	1970.1	0.45	17.4	27.9	54.7	45.4

Table 4.2: Extractable organic matter and relative percentages of saturates, aromatics and nitrogen-sulfur-oxygen (NSO) compounds of EOM (continued).

MGL2R	Mudstone	1263.2	185.3	202.1	875.8	387.4	0.31	14.7	16.0	69.3	30.7
MGL2S	Shale	5866.1	807.7	1360.3	3698.2	2167.9	0.37	13.8	23.2	63.0	37.0
MGL2S2	Shale	6150.5	891.2	1338.4	3920.9	2229.6	0.36	14.5	21.8	63.7	36.3
MGL2T	Coal/seam A1	7171.4	765.0	4398.4	2008.0	5163.4	0.72	10.7	61.3	28.0	72.0
MGL2T2	Coal/seam A1	7075.9	801.0	4124.9	2150.0	4925.9	0.70	11.3	58.3	30.4	69.6
MGL2U	Shale	1910.4	366.4	366.4	1177.7	732.8	0.38	19.2	19.2	61.6	38.4
YN1A	Shale	1093.4	177.3	236.4	679.7	413.7	0.38	16.2	21.6	62.2	37.8
YN1A2	Shale	1100.1	189.1	251.8	659.2	440.8	0.40	17.2	22.9	59.9	40.1
YN1B	Shale	377.1	61.4	78.9	236.8	140.3	0.37	16.3	20.9	62.8	37.2
YN1B2	Shale	1050.5	120.0	270.5	660.0	390.5	0.37	11.4	25.7	62.8	37.2
YN1C	Shale	1101.5	213.2	284.3	604.1	497.5	0.45	19.4	25.8	54.8	45.2
YN1C2	Shale	1250.1	240.1	330.0	680.0	570.1	0.46	19.2	26.4	54.4	45.6
YN1D	Shale	206.6	21.4	49.9	135.3	71.2	0.34	10.3	24.1	65.5	34.5
YN1D2	Shale	809.1	122.2	151.6	535.2	273.8	0.34	15.1	18.7	66.2	33.8

EOM= Extractable organic matter (Bitumen extraction)

NSO= Nitrogen, Sulfur, Oxygen components.

HCS= Hydrocarbon fractions (Saturated + Aromatic HCs).

4.5 Molecular geochemical analysis

In this study, biomarkers such as *n*-alkanes, isoprenoids, terpanes and steranes are used for geochemical analysis. The GC-MS chromatographic patterns and distributions of *n*-alkanes, acyclic isoprenoids, tricyclic terpanes, hopanes and steranes were analysed using TIC/*m/z* 85, *m/z* 191 and *m/z* 217. The compounds (see Appendix B) were determined on the basis of their retention time and, in comparison with literature data (e.g. Kitson et al., 1996; Philp, 1985; Peters et al., 2005; Amijaya et al., 2006; El-Diasty and Moldowan, 2012; Makeen et al., 2015c; Ayinla et al., 2017a).

4.5.1 *n*-Alkanes and acyclic isoprenoids

The *n*-alkanes distribution of the studied coal and mudstone samples from the Gombe Formation comprise mainly from *n*-C₁₅ to *n*-C₃₃ (Figure 4.6). Alkanes within the range between *n*-C₂₃ and *n*-C₃₃ (higher molecular weight compounds) account for the significant fraction of the chromatographic distribution of the analysed samples. Odd *n*-alkanes predominate over even *n*-alkanes (Figures 4.6a-f) with significant relative abundance of *n*-C₂₇, *n*-C₂₉ and *n*-C₃₁ (higher plant molecular compounds) in Maiganga samples compared to Yaya-Ngari shale. This gives a relatively high carbon preference index (CPI >1.06; Table 4.3). Pristane to phytane ratio (Pr/Ph) (Figures 4.6a-f) for all the analysed Yaya-Ngari and Maiganga samples is above 1.00 (Table 4.3). The coal samples have Pr/Ph ratio ranging from 3.15 to 4.25 with an average of 3.66. The ratios of pristane to *n*-C₁₇ and phytane to *n*-C₁₈ (Pr/*n*-C₁₇ and Ph/*n*-C₁₈) were calculated (Table 4.3). All the analysed coal samples show a relatively low concentration of *n*-heptadecane (*n*-C₁₇) compared to pristane (except in seam A₂ where pristane is high), hence, Pr/*n*-C₁₇ ratio ranges from 0.39 to 7.40 with an average of 3.31. However, there is relatively more *n*-alkane (*n*-C₁₇) than pristane in the interbedded mudstone (from 0.45 to 0.68), shale (0.60-1.19) and Yaya-Ngari shale (0.33-0.46). Similarly, the analysed Gombe Formation samples are generally characterised by a relatively high abundance

of *n*-alkane (*n*-C₁₈) over the isoprenoid phytane (Ph). Thus, the Ph/*n*-C₁₈ ratio ranges from 0.13 to 1.40 with an average of 0.36 (Table 4.3).

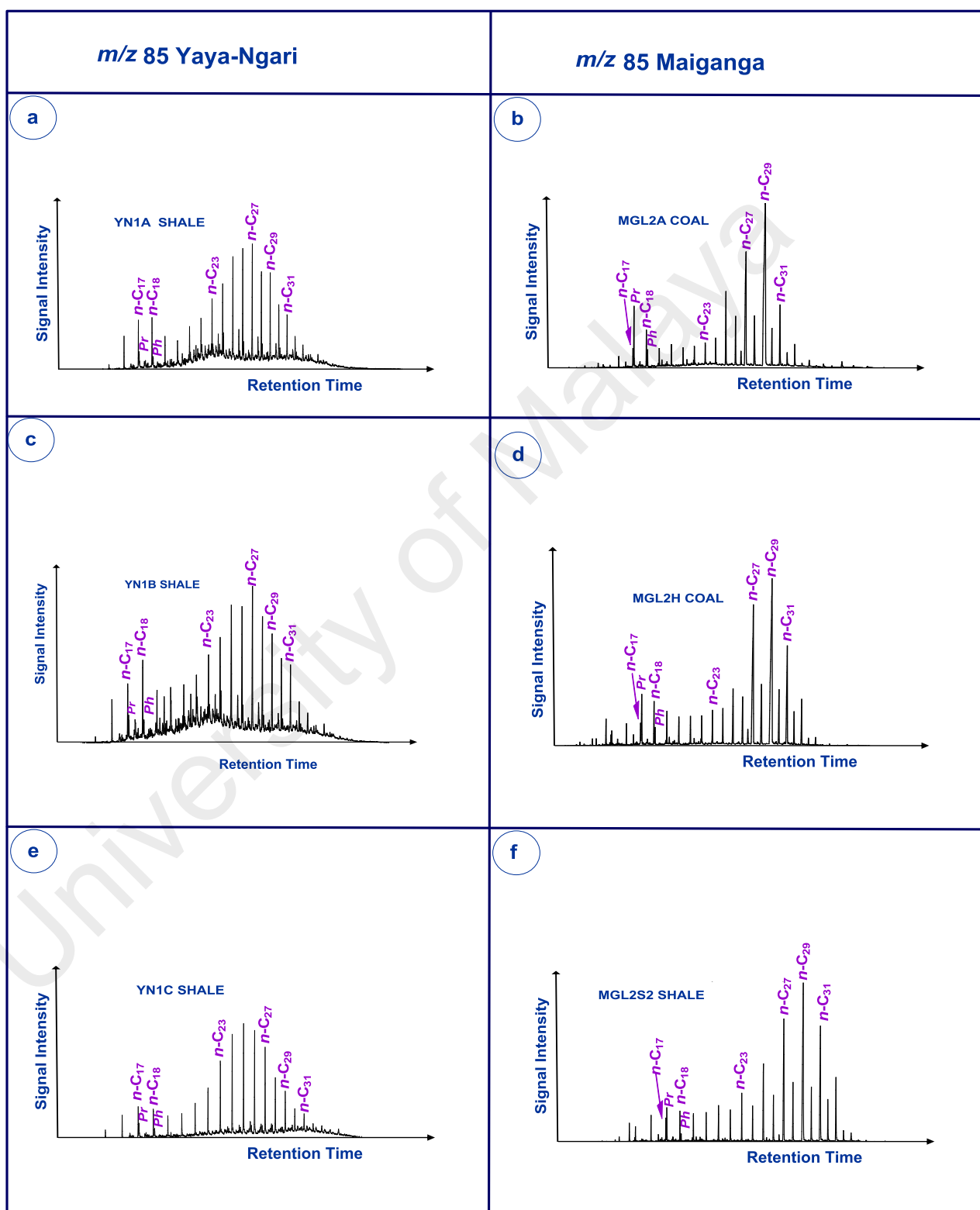


Figure 4.6: The mass fragmentograms of *m/z* 85 of saturated hydrocarbon fractions of representative samples from Maiganga and Yaya-Ngari.

Table 4.3: Biomarker ratios based on *m/z* 85 and 191 mass chromatograms for selected samples.

Sample ID	Lithology/ Seam	Normal alkanes and isoprenoids				<i>m/z</i> 191 (Hopane)								
		Pr/Ph	Pr/n C ₁₇	Ph/n C ₁₈	CPI	C ₂₃ /C ₂₄ TT	C ₂₄ Tetra/ C ₂₆ TT	C ₂₃ TT/ C ₃₀ H	C ₂₄ Tetr a/C ₃₀ H	Ts/(Ts+T m)	C ₂₉ / C ₃₀ H	C ₃₁ R/C ₃₀ H	C ₃₂ 22S/(22S+22R)	
MGL1C2	Coal/seam B	3.15	2.14	0.53	2.71	2.76	4.00	0.13	0.04	0.22	0.63	0.63	0.33	
MGL2A	Coal/seam B	3.50	3.27	0.48	2.27	1.40	4.00	0.06	0.06	0.25	0.58	0.53	0.11	
MGL2B	Coal/seam B	4.14	2.07	0.37	2.65	2.67	3.50	0.10	0.15	0.06	2.86	0.93	0.31	
MGL2C	Coal/seam B	3.50	4.38	1.00	3.44	2.35	2.67	0.07	0.08	0.27	1.07	0.65	0.34	
MGL2D	Coal/seam B	3.70	7.40	1.00	2.88	2.33	3.50	0.05	0.18	0.17	3.05	0.89	0.48	
MGL2E	Mudstone	2.50	0.63	0.22	1.89	2.00	2.00	0.02	0.07	0.10	1.63	0.91	0.50	
MGL2F	Mudstone	1.36	0.54	0.29	1.68	2.00	1.50	0.03	0.04	0.09	2.51	0.74	0.22	
MGL2G	Siltstone	1.83	0.45	0.23	1.25	2.00	2.50	0.07	0.17	0.12	4.67	1.33	0.50	
MGL2H	Coal/seam A ₃	3.15	2.28	0.37	2.16	2.00	2.50	0.09	0.16	0.05	1.61	1.42	0.23	
MGL2I	Coal/seam A ₃	3.90	6.83	1.40	2.74	2.00	2.38	0.07	0.08	0.25	0.83	0.57	0.32	
MGL2L	Shale	4.00	0.95	0.21	1.79	2.50	2.00	0.02	0.07	0.22	1.23	0.95	0.09	
MGL2N	Shale	3.00	0.60	0.14	2.36	2.00	3.00	0.01	0.03	0.30	1.42	0.88	0.06	
MGL2P	Coal/seam A ₂	3.67	0.39	0.13	1.81	2.22	1.00	0.02	0.03	0.22	1.30	1.30	0.05	
MGL2Q	Shale	2.78	0.63	0.24	1.80	2.00	1.50	0.04	0.12	0.13	1.19	0.96	0.12	

Table 4.3: Biomarker ratios based on m/z 85 and 191 mass chromatograms for selected samples (continued).

MGL2R	Mudstone	1.91	0.68	0.26	1.82	2.00	2.00	0.01	0.03	0.17	1.33	0.47	0.17
MGL2S	Shale	3.30	1.14	0.32	2.01	3.00	2.00	0.08	0.10	0.16	1.40	1.20	0.16
MGL2S2	Shale	2.91	1.19	0.34	2.02	1.50	2.50	0.00	0.16	0.06	2.09	2.11	0.47
MGL2T	Coal/seam A ₁	4.25	1.06	0.18	3.16	2.00	3.00	0.03	0.06	0.25	1.29	0.94	0.17
MGL2U	Shale	2.71	0.61	0.22	2.22	2.08	2.50	0.02	0.04	0.08	1.52	0.57	0.10
YN1A	Shale	1.67	0.33	0.19	1.14	1.78	1.14	0.27	0.14	0.50	0.92	0.43	0.52
YN1A2	Shale	1.43	0.34	0.22	1.14	1.55	1.18	0.29	0.13	0.48	0.90	0.43	0.58
YN1B	Shale	1.35	0.46	0.24	1.12	2.16	1.55	0.36	0.15	0.48	0.82	0.37	0.58
YN1B2	Shale	1.38	0.46	0.23	1.09	2.27	1.25	0.39	0.14	0.40	0.91	0.36	0.55
YN1C	Shale	1.50	0.33	0.25	1.06	2.67	1.04	0.33	0.04	0.44	0.75	0.46	0.52
YN1C2	Shale	1.50	0.38	0.22	1.09	2.14	1.31	0.36	0.12	0.44	0.88	0.45	0.53
YN1D	Shale	1.00	0.41	0.23	1.17	2.00	1.10	0.59	0.20	0.47	0.96	0.36	0.57
YN1D2	Shale	1.06	0.42	0.20	1.15	1.93	1.10	0.58	0.21	0.48	0.95	0.36	0.58

CPI: Carbon preference index (1): $\{2(C_{23} + C_{25} + C_{27} + C_{29}) / (C_{22} + 2[C_{24} + C_{26} + C_{28}] + C_{30})\}$. **Pr:** Pristane. **Ph:** Phytane. **C₂₉/C₃₀:** C₂₉ norhopane/C₃₀ hopane. **Ts:** (C₂₇ 18a(H))-22,29,30-trisnorhopane). **Tm:** (C₂₇ 17a(H))-22,29,30-trisnorhopane).

4.5.2 Terpanes and steranes

GC-MS can provide chromatograms of specific biomarker such as ion m/z 191 and 217 which represents terpane and sterane distributions respectively (see Appendix B for peak labels). The m/z 191 of the analysed samples from the Gombe Formation (Maiganga and Yaya-Ngari areas) shows predominance of the C_{30} -hopane, C_{29} -norhopane, 17α (H)-trisnorhopane (Tm), C_{31} homohopane and a reasonable amount of homohopanes (C_{32} – C_{35}), occurring in a stair-step pattern especially for Yaya-Ngari shale, with relatively low amounts of tricyclic and tetracyclic terpanes (Figures 4.7a, 4.7c, 4.7e and 4.7g). Yaya-Ngari samples have low abundance of C_{29} norhopane compared to that of C_{30} hopane while reverse order was obtained for Maiganga coal. Thus, $C_{29}/C_{30}17\alpha$ (H) hopane ratio is generally higher in Maiganga (from 0.58 to 4.67) than Yaya-Ngari (from 0.75 to 0.96) (Table 4.3). Calculated C_{31} homohopane/ C_{30} hopane ($C_{31}R/C_{30}H$) ratio ranges from 0.36 to 2.11 (Table 4.3). As expected for coal the $C_{31}R/C_{30}H$ ratio is high ranging from 0.53 to 1.42 as previously reported by Quirke et al. (1984). Following the same trend, the shale, mudstones and Yaya-Ngari samples also recorded high $C_{31}R/C_{30}H$ ratio > 0.25 which shows that the studied areas have these distinguishing characteristics (see Table 4.3). The abundance of Tm is slightly higher than that of Ts in the studied Yaya-Ngari samples (Figures 4.7a and 4.7c), while the reverse order was obtained for Maiganga. The $Ts/(Ts+Tm)$ ratio is shown in Table 4.3. Homohopane distribution is dominated by C_{31} homohopane and decreased in a cascading pattern from C_{31} to C_{35} homohopane especially in Yaya-Ngari samples (Figures 4.7a and 4.7c). The concentrations of tricyclic terpane and tetracyclic terpane in the analysed samples from Yaya-Ngari and Maiganga are low (Table 4.3). These samples also have a relatively low C_{24} tricyclic terpane compared with C_{23} tricyclic terpanes which give average C_{23}/C_{24} tricyclic terpane ratios of 2.15 for Maiganga and

1.21 for Yaya-Ngari (Table 4.3). Other computed biomarker ratios are shown in Table 4.3 which were integrated in deciphering the source rock characteristics.

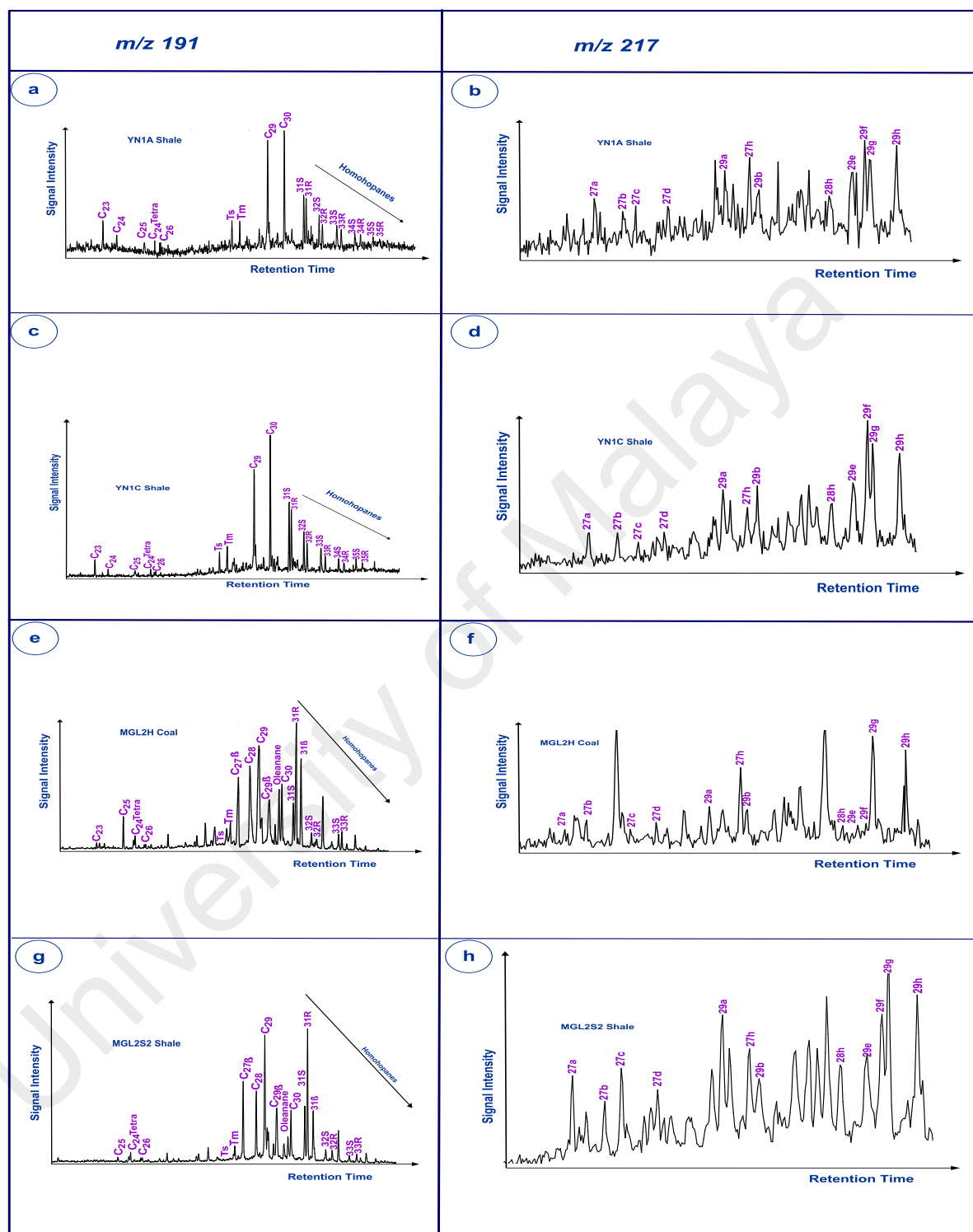


Figure 4.7: The mass fragmentograms of m/z 191 (left; a, c, e, g) and 217 (right; b, d, f, h) of saturated hydrocarbon fractions of the analysed Maiganga and Yaya-Ngari samples.

The GC-MS chromatograms, m/z 217 (Figures 4.7b, 4.7d, 4.7f and 4.7h), represent sterane distribution. Steranes originate from sterols in higher plants and algae (Huang and Meinschein, 1979; Tissot and Welte, 1984; Volkman, 1986; Peters et al., 2005; Farhaduzzaman et al., 2012). The studied coal, shale and mudstones from the Gombe Formation have high concentration of steranes and diasteranes (especially Yaya-Ngari samples). Values of the most common sterane parameters, such as relative percentages of C_{27} , C_{28} and $C_{29}\alpha\alpha\alpha(20R)$ regular steranes as well as the ratios of C_{27}/C_{29} regular sterane are listed in Table 4.4. Over all, the result reveals a higher concentration of $C_{29}\alpha\alpha\alpha(20R)$ sterane (34.29-68.21%) compared to $C_{28}\alpha\alpha\alpha(20R)$ (16.42-41.03%) and $C_{27}\alpha\alpha\alpha(20R)$ (10.60-37.76%) in the analysed samples. This means that both Maiganga and Yaya-Ngari received significantly more terrigenous input (C_{29} steranes) than marine and lacustrine biomarker signatures (C_{27} and C_{28} steranes).

The relative high percentages of C_{29} steranes over the C_{27} steranes give C_{27}/C_{29} regular sterane ratio which is generally <1 (Table 4.4). Sterane biomarker ratios used as thermal maturity indicators such as $C_{29}\beta\beta/(\beta\beta+\alpha\alpha)$ and $C_{29}20S/(20S+20R)$ were also presented as shown in Tables 4.4. It is noted that generally the concentration of hopanes (on m/z 191) are more than steranes (on m/z 217) as shown by low sterane/hopane ratio (<1) pointing to more bacterial influence in the area (see Table 4.4).

Similarly, the aromatic Dibenzothiophenes/phenanthrenes (DBT/P) ratio (m/z 184 and 178) is significantly low (<1), following the high concentration of phenanthrenes compared to low dibenzothiophenes in all the analysed samples (Figure 4.8; Table 4.4). This is not surprising as deltaic settings are usually characterised by DBT/P ratio of <1 (Hughes et al., 1985; Peters et al., 2005).

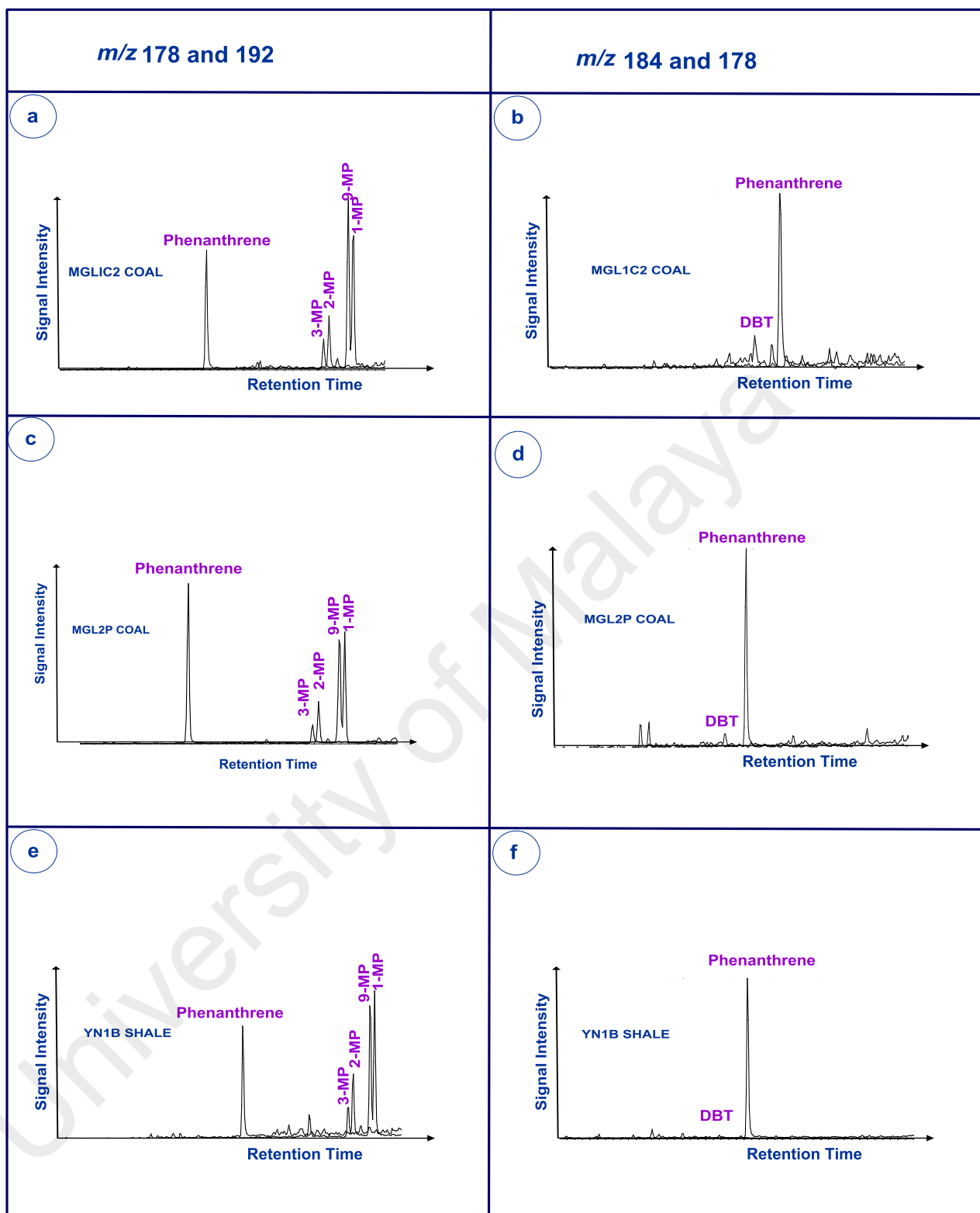


Figure 4.8: The mass fragmentograms of Phenanthrenes (m/z 178), Methylphenanthrenes isomers (m/z 192) and aromatic Dibenzothiophenes (m/z 184) for aromatic hydrocarbon fractions of the analysed Maiganga and Yaya-Ngari samples.

Table 4.4: Biomarker ratios based on m/z 191, 217, 184 and 178 mass chromatograms for selected samples.

Sample ID	Lithology/ Seam	m/z 217 (Steranes)						steranes/ Hopanes ratio	DBT/P
		Regular steranes (%)			C ₂₇ /C ₂₉	C ₂₉ 20S/(20S+20R)	C ₂₉ ββ/(ββ+αα)		
		C ₂₇	C ₂₈	C ₂₉					
MGL1C2	Coal/seam B	14.71	38.24	47.06	0.31	0.26	0.34	0.03	0.17
MGL2A	Coal/seam B	32.38	33.33	34.29	0.94	0.30	0.33	0.05	0.20
MGL2B	Coal/seam B	23.33	20.00	56.67	0.41	0.26	0.35	0.12	0.10
MGL2C	Coal/seam B	15.38	41.03	43.59	0.35	0.23	0.22	0.03	0.12
MGL2D	Coal/seam B	22.06	32.35	45.59	0.48	0.31	0.33	0.07	0.13
MGL2E	Mudstone	23.19	33.33	43.48	0.53	0.33	0.32	0.03	0.02
MGL2F	Mudstone	37.76	24.49	37.76	1.00	0.21	0.32	0.04	===
MGL2G	Siltstone	34.44	26.67	38.89	0.89	0.32	0.39	0.78	===
MGL2H	Coal/seam A3	35.03	19.77	45.20	0.78	0.15	0.14	0.08	0.35
MGL2I	Coal/seam A3	20.48	28.92	50.60	0.40	0.14	0.25	0.01	0.20
MGL2L	Shale	20.72	26.13	53.15	0.39	0.33	0.39	0.03	0.12
MGL2N	Shale	25.64	21.79	52.56	0.49	0.20	0.26	0.02	0.30
MGL2P	Coal/seam A2	10.60	21.19	68.21	0.16	0.24	0.33	0.01	0.07
MGL2Q	Shale	14.05	34.71	51.24	0.27	0.17	0.32	0.02	0.09
MGL2R	Mudstone	20.18	22.81	57.02	0.35	0.36	0.38	0.04	===
MGL2S	Shale	14.10	21.79	64.10	0.22	0.18	0.29	0.02	0.09
MGL2S2	Shale	15.07	21.92	63.01	0.24	0.36	0.38	0.03	0.09
MGL2T	Coal/seam A1	15.44	22.82	61.74	0.25	0.18	0.36	0.02	0.10
MGL2U	Shale	15.04	25.56	59.40	0.25	0.27	0.30	0.03	0.10
YN1A	Shale	37.42	17.79	44.79	0.84	0.43	0.55	0.17	0.30
YN1A2	Shale	37.31	16.42	46.27	0.81	0.44	0.54	0.17	===
YN1B	Shale	36.82	22.39	40.80	0.90	0.35	0.54	0.19	0.08
YN1B2	Shale	36.84	21.05	42.11	0.88	0.43	0.53	0.18	0.20
YN1C	Shale	32.06	21.53	46.41	0.69	0.40	0.55	0.24	0.40
YN1C2	Shale	31.96	21.65	46.39	0.69	0.50	0.55	0.25	===
YN1D	Shale	35.07	20.38	44.55	0.79	0.50	0.51	0.19	===
YN1D2	Shale	34.95	20.39	44.66	0.78	0.49	0.52	0.20	===

4.6 Kerogen pyrolysis (Py-GC)

The Py-GC of kerogen was used in characterising the remaining hydrocarbon generative potential of the Gombe Formation samples. Thus, chromatographic “fingerprints” and “type index” (ratio of *m(+p)*-xylene to *n*-octene) gives an idea of the kerogen type and expected hydrocarbons to be produced during maturation (Larter and Douglas, 1980; Larter, 1984; Hartwig et al., 2012). In this study, the pyrolysis gas chromatography (Py-GC) distribution (Figure 4.9) of the analysed Maiganga coal and mudstones is characterised by *n*-alkane/*n*-alkene peaks from *n*-C₁ to *n*-C₃₅ which shows notable high abundance of < C₁₂ compared to moderate amount of *n*-C₁₂₊ as well as prist-1-ene on the pyrograms. Similarly, aromatic compounds such as toluene, 2, 3 dimethylthiophene, *m(+p)*-xylene, phenol and cadalene were observed in the Py-GC pyrogram (Figure 4.9) with significant dominance of toluene in all of the analysed samples. On the other hand, the Yaya-Ngari shales are characterised by very little to absence of the *n*-alkane/*n*-alkene peaks from *n*-C₁ to *n*-C₃₃ (see YN1A2 in Figure 4.9). The type index which is a proxy for kerogen type was calculated as the abundance ratio of *m(+p)*-xylene to *n*-octene as well as cadalene/*m(+p)*-xylene (cd/xy) ratio (Table 4.5).

One of the characteristics of all the analysed samples (coal and mudstones) is the relatively moderate amount of *m(+p)*-xylene compared to cadalene which results in low cd/xy ratio (0.04-0.18). Similarly, a varied value (0.29-1.38) is recorded for the “kerogen type index”. The “kerogen type index” of the mudstones (0.29-0.80) is slightly lower than that of the coal facies (0.43-1.38). This is an indication of heterogenous organic matter and mixed kerogen type (III/II) for the analysed Gombe Formation samples.

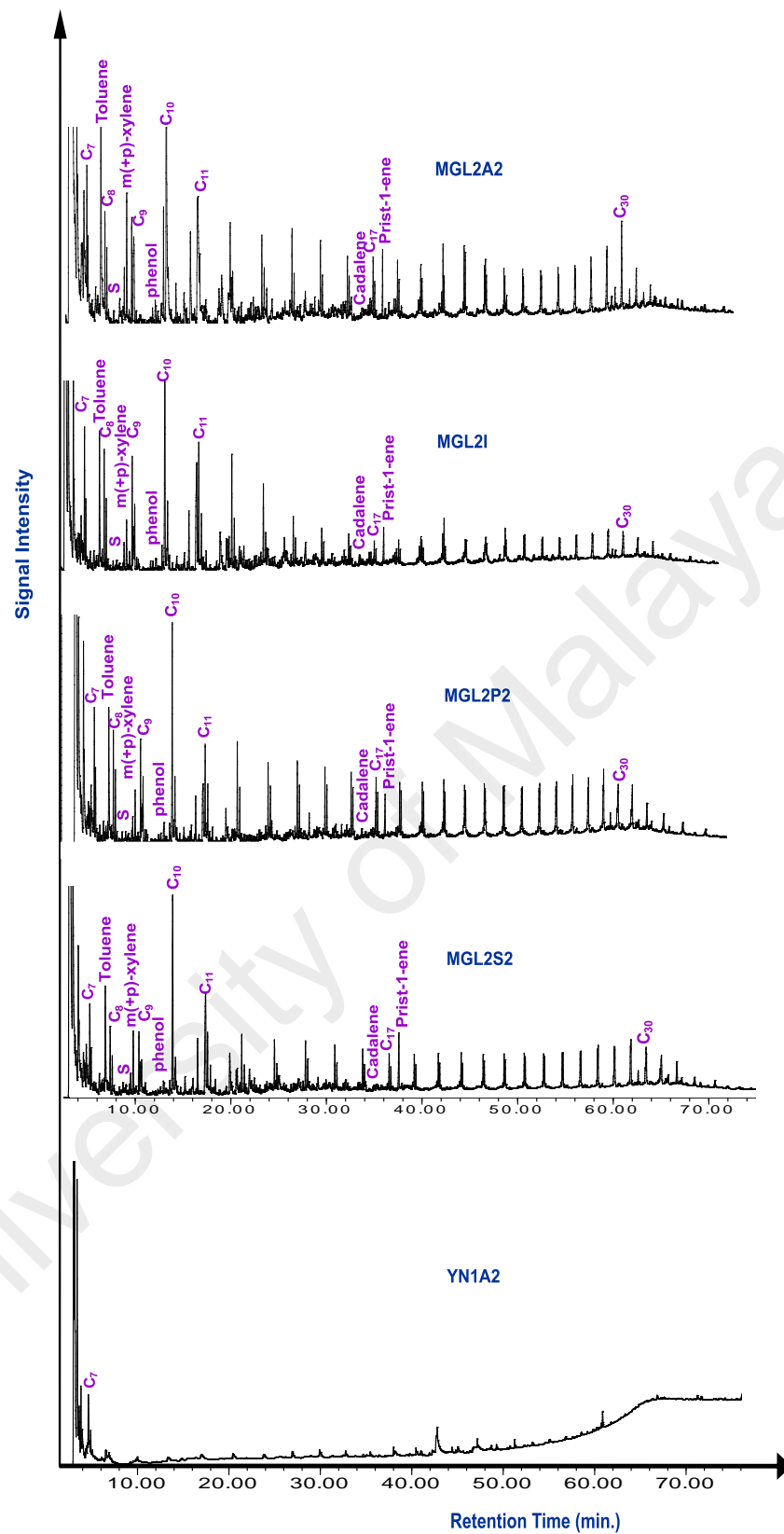


Figure 4.9: The Py-GC trace of the analysed samples.
S: 2,3 dimethylthiopene

Table 4.5: Py-GC parameters of the analysed samples.

Period	Age	Sample ID	Lithology/seam	n-Octene (C ₈) %	m+(p)-Xylenes %	Phenol %	cd/xy	Type index		
Upper Cretaceous	Maastrichtian	MGL1B2	Coal/seam B	37.21	51.16	11.63	0.18	1.38		
		MGL1C2	Coal/seam B	43.33	50.00	6.67	0.10	1.15		
		MGL2A2	Coal/seam B	44.12	47.06	8.82	0.16	1.07		
		MGL2B2	Coal/seam B	40.74	51.85	7.41	0.07	1.27		
		MGL2C2	Coal/seam B	42.86	48.57	8.57	0.12	1.13		
		MGL2D2	Coal/seam B	47.89	45.07	7.04	0.06	0.94		
		MGL3A	Coal/seam B	48.00	44.00	8.00	0.14	0.92		
		MGL3B2	Coal/seam B	40.00	48.00	12.00	0.08	1.20		
		MGL2E2	Mudstone	71.43	23.81	4.76	0.07	0.33		
		MGL2F2	Mudstone	72.34	21.28	6.38	0.10	0.29		
		MGL2G2	Siltstone	51.28	41.03	7.69	0.06	0.80		
		MGL2H2	Coal/seam A ₃	43.75	40.63	15.63	0.09	0.93		
		MGL2I	Coal/seam A ₃	66.67	28.57	4.76	0.17	0.43		
		MGL2J2	Coal/seam A ₃	66.67	29.63	3.70	0.13	0.44		
		MGL2K2	Mudstone	68.09	23.40	8.51	0.09	0.34		
		MGL2L2	Shale	65.45	27.27	7.27	0.13	0.42		
		MGL2O2	Coal/seam A ₂	46.15	46.15	7.69	0.08	1.00		
		MGL2P2	Coal/seam A ₂	62.50	29.17	8.33	0.14	0.47		
		MGL2Q	Shale	62.26	28.30	9.43	0.07	0.45		
		MGL2R2	Mudstone	68.75	20.83	10.42	0.05	0.30		
		MGL2S2	Shale	62.20	29.10	9.70	0.08	0.46		
		MGL2T2	Coal/seam A ₁	42.62	39.34	18.03	0.08	0.92		
		MGL2U	Shale	62.75	23.53	13.73	0.04	0.38		
		MGL2U2	Shale	66.67	20.51	12.82	0.06	0.31		
		Min. Value				37.21	20.51	3.70	0.04	0.29
		Max.value				72.34	51.85	18.03	0.18	1.38
		Average				54.85	36.05	9.10	0.10	0.73

m(+p)-xylenes, cd/xy: cadalene/m(+p)-xylenes, Type index: m(+p)-xylenes %/n-octene.

n-Octene (C₈) % - percent concentration of n-Octene (C₈) in relation to m+(p)-Xylenes and Phenol.

m+(p)-Xylenes (%) - percent concentration of m+(p)-Xylenes in relation to n-Octene (C₈) and Phenol.

Phenol (%) - percent concentration of Phenol in relation to n-Octene (C₈) and m+(p)-Xylenes.

n-Octene (C₈) % + m(+p)-xylenes% + Phenol % =100 (used for Figure 5.6).

4.7 Ultimate analysis

Table 4.6 shows the result of ultimate analysis obtained from coal samples of the Gombe Formation. This is used to complement the kerogen type determination and hydrocarbon product that can be generated. The ultimate analysis provides information about the relative percentage weight of carbon, hydrogen, oxygen, nitrogen and total sulfur content. However, the oxygen content (weight %) as well as the atomic H/C and O/C ratios were calculated from the result of elemental CHNS. The average, minimum, and maximum values of all the parameters for the analysed coals are as presented in Table 4.6.

Based on the ultimate analysis (Table 4.6), the analysed coals indicated a relatively high carbon content (68.9-80.5 wt.%) with an average of 73.2 wt.% (Table 4.6). The maximum carbon content of the analysed coals was recorded in seam B (MGL1B2; Table 4.6) close to a fault plain. Calculated oxygen concentration is high (12.2-24.1 wt.%) in comparison to hydrogen, nitrogen and sulfur contents. Hydrogen concentration in the samples ranges from 5.20 to 5.90 wt.% with average of 5.68 wt.%. Although, the nitrogen concentration (1.15-1.50 wt.%) is relatively lower than the hydrogen content, it is higher than sulfur contents (0.18-0.46 wt.%; Table 4.6).

Table 4.6: Ultimate Analysis showing CHNSO concentration of the analysed coal samples.

Period	Age	Sample ID	Lithology/seam	Ultimate Analysis					Atomic Ratio			
				C (wt.%)	H (wt.%)	N (wt.%)	TS (wt.%)	O (wt.%)	H/C	O/C		
Upper Cretaceous	Maastrichtian	MGL1B2	Coal/seam B	80.50	5.48	1.50	0.38	12.20	0.81	0.11		
		MGL1C2	Coal/seam B	78.90	5.80	1.35	0.46	13.49	0.88	0.13		
		MGL2A2	Coal/seam B	71.22	5.90	1.19	0.29	21.40	0.99	0.23		
		MGL2B2	Coal/seam B	75.00	5.60	1.29	0.22	17.89	0.90	0.18		
		MGL2C2	Coal/seam B	73.64	5.86	1.25	0.25	19.00	0.95	0.19		
		MGL2D2	Coal/seam B	74.00	5.68	1.20	0.24	18.88	0.92	0.19		
		MGL3A2	Coal/seam B	69.80	5.77	1.22	0.22	22.99	0.99	0.25		
		MGL3B2	Coal/seam B	80.00	5.86	1.20	0.24	12.71	0.88	0.12		
		MGL2H2	Coal/seam A ₃	71.00	5.20	1.25	0.28	22.27	0.88	0.24		
		MGL2I	Coal/seam A ₃	71.30	5.50	1.23	0.18	21.79	0.93	0.23		
		MGL2J2	Coal/seam A ₃	70.00	5.50	1.15	0.42	22.93	0.94	0.25		
		MGL2O2	Coal/seam A ₂	72.60	5.80	1.27	0.30	20.00	0.96	0.21		
		MGL2P2	Coal/seam A ₂	68.90	5.50	1.20	0.31	24.09	0.96	0.26		
		MGL2T	Coal/seam A ₁	70.00	5.85	1.22	0.29	22.64	1.00	0.24		
		MGL2T2	Coal/seam A ₁	71.60	5.90	1.20	0.27	21.00	0.99	0.22		
		Min. value				68.90	5.20	1.15	0.18	12.20	0.81	0.11
		Max. value				80.50	5.90	1.50	0.46	24.09	1.00	0.26
Average				73.23	5.68	1.25	0.29	19.55	0.92	0.20		

C: Carbon.

H: Hydrogen.

N: Nitrogen.

TS: Total sulfur content.

O: Calculated oxygen content = 100 - (C + H + N + TS).

4.8 Organic petrographic analysis

Liptinite, vitrinite/huminite and inertinite are the three basic maceral groups in coal and sedimentary rocks. They display distinguishing characteristics under microscope in terms of colour, relief of polished surface, morphology (shape and structure) reflectance and fluorescence (Teichmuller, 1989; ICCP, 2001; Abdullah, 2003; Sykorova et al., 2005; Hakimi and Abdullah, 2014; Pickel et al., 2017). Thus, they are employed in this study as vital tool for the determination of thermal maturity, kerogen typing, organic matter source input, paleodepositional condition and evaluation of source rock hydrocarbon generation potential.

4.8.1 Vitrinite/ulminite reflectance measurements

Table 4.1 shows the results of reflectance measurements of ulminite (low ranks equivalence of vitrinite) for Maiganga samples (coals and mudstones) and vitrinite reflectance measurements for the Yaya-Ngari samples respectively. About 50 to 100 measurements were made on each sample. Ulminite mean reflectance for Maiganga coals ranges from 0.26 to 0.40% with an average of 0.33% which is slightly low compared to that of the mudstone (0.31-0.43%) and the shale (0.30-0.41%). However, Yaya-Ngari shales recorded notably higher values ranging from 0.71 to 0.90% (Table 4.1).

4.8.2 Maceral analysis

Based on point counting analysis of about 1000 points per sample performed on the Gombe Formation samples, Table 4.7 shows the maceral composition (vol. %), tissue preservation index (TPI) and gelification index (GI) (Diessel, 1986) of the analysed coals. The huminite macerals account for significant part of the maceral composition ranging from 45 to 73% with an average of 58.33%. However, there is a relatively moderate amount of inertinites (8-35% with average of 20.17%) and liptinite

(14-29% with average of 21.50%) maceral content in the analysed Gombe Formation coal. The observed huminite maceral in the studied samples are telohuminite (textinite and ulminite), detrohuminite (attrinite and densinite), gelohuminite (corpohuminite and gellinite i.e. porigelinite). There is a relatively high percentage of the detrohuminite (5-41% with average of 17.33%) and porigelinites (2-24% with average of 15.25%) compared to moderate corpohuminite (3-16%), ulminite (2-16%) and textinite (3-14%) in the coals.

Following Pickel et al., (2017)'s classification of liptinite, the studied coals from the Gombe Formation (Table 4.7) as observed under UV-light comprises of resinite, liptodetrinite, sporinite, cutinite, structureless exsudatinites, bituminite and suberinite with decreasing order (Figures 4.10a-h). The resinite occurs mainly as oval to semi-rounded shapes (Figure 4.10a). They display varied colour under the UV-light ranging from yellow to orange (brown with some patches in reflected light) with varied percentage concentration from 2 to 12%. Oil stains are associated with some of the observed resinites (Figure 4.10a). The liptodetrinites vary from 1 to 10%. Sporinites are characterised by yellow to light yellow colour, different shapes (oval to rounded) with some showing evidence of shrinkage, which might indicate bedding planes. Some of the sporinites appear in isolation while others occur in cluster "bilobe" or "trilobe". It has fairly moderate concentration (1-8%). The percentage concentration of exsudatinites and bituminite in the studied coals ranges from 0 to 4%, while suberinite is generally low in concentration (average < 1%).

Inertinite group constitutes 20.17% of total maceral composition (Table 4.7). Inertinite in the studied Gombe Formation coals consist predominantly of fusinite, semi-fusinite, micrinite and inertodetrinites that are widely dispersed in all the studied samples. Apart from these macerals, other identified inertinite macerals are macrinite and funginite (Figure 4.10n). The studied coals are characterised by fusinite (2-16%),

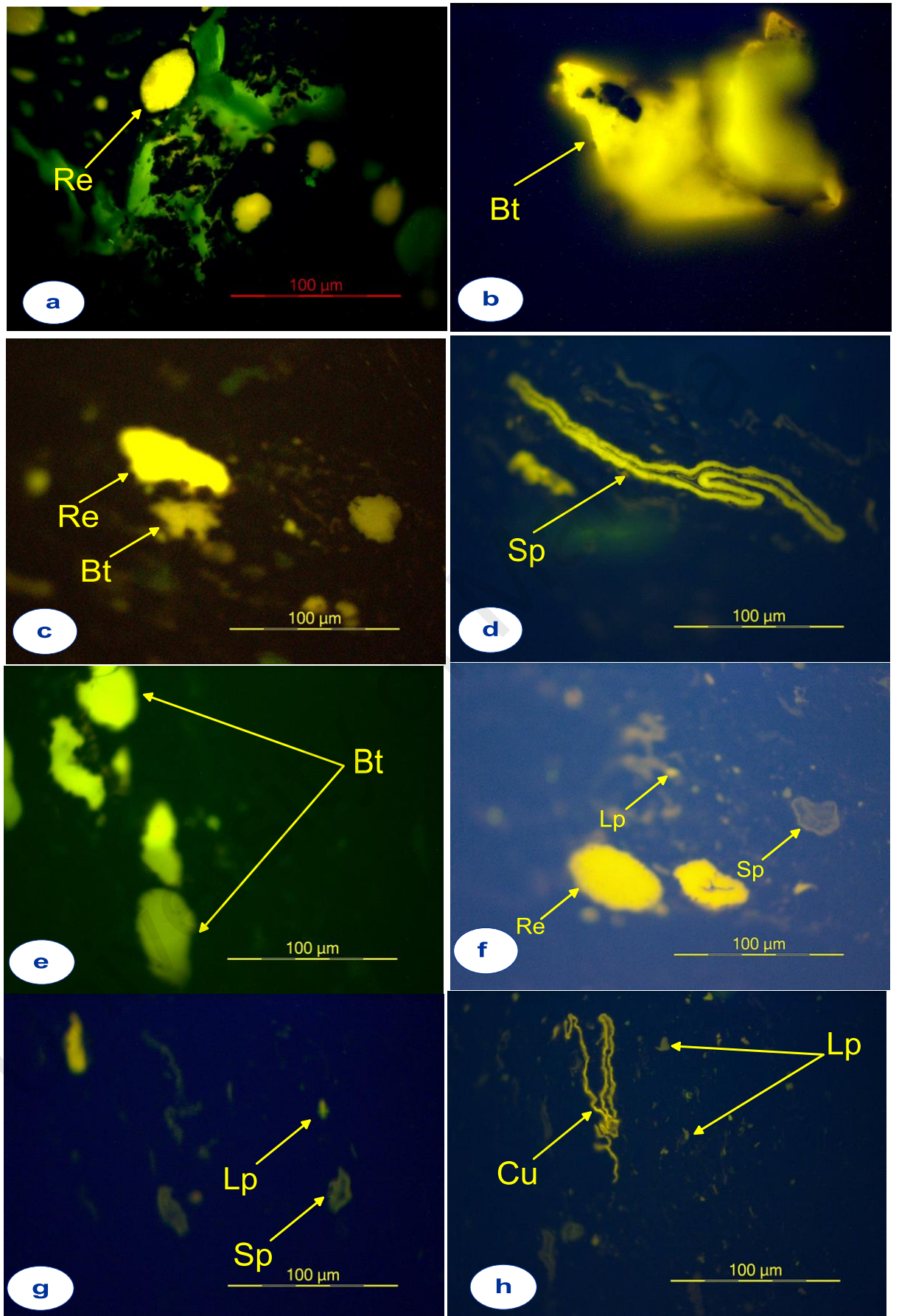
semi-fusinite (1-15%) and micrinite (0-18%) as well as inertodetrinite (2-9%). Macrinite and funginite occur in minor quantity with an average of < 1% of total maceral composition. Some of the telohuminites are associated with fusinite, semi-fusinite and inertodetrinites. Based on these percentages, the calculated TPI and GI (Table 4.7) show relatively moderate values for all of the analysed samples ranging from 0.33 to 5.14 and 1.32 to 8.13 respectively.

University of Malaya

Table 4.7: Maceral composition of the analysed coal samples.

Sample ID	Lithology/seam	Huminite						Inertinites							Liptinite								TPI	GI	Ro (%)
		Tx	U	Dh	Ch	Pg	TH	Fg	Idt	F	Sf	Mi	Ma	TI	SP	Cu	Rs	Lp	Sub	Ex	Bt	TL			
MGL1C2	Coal/seam B	5	6	16	14	17	58	0	4	7	12	3	0	26	1	4	2	1	0	4	4	16	1.15	2.23	0.35
MGL2A2	Coal/seam B	9	14	8	4	10	45	1	9	4	1	18	1	34	1	1	6	7	2	3	1	21	1.33	1.32	0.40
MGL2B2	Coal/seam B	6	6	41	7	13	73	0	4	3	5	1	0	13	1	2	2	6	0	2	1	14	0.38	5.62	0.36
MGL2D2	Coal/seam B	4	5	34	3	17	63	0	4	2	8	0	0	14	1	2	8	9	0	2	1	23	0.45	4.50	0.34
MGL3B2	Coal/seam B	9	12	5	7	18	51	1	2	16	15	1	0	35	2	2	3	6	0	0	1	14	5.14	1.46	0.40
MGL2H2	Coal/seam A ₃	11	10	7	16	24	68	1	2	4	2	4	1	14	2	4	6	4	0	1	1	18	2.30	4.86	0.33
MGL2I2	Coal/seam A ₃	14	16	5	7	23	65	1	2	4	1	0	0	8	2	2	12	3	0	4	4	27	4.43	8.13	0.32
MGL2J2	Coal/seam A ₃	7	10	13	9	16	55	1	7	7	4	0	0	19	7	3	3	8	2	3	0	26	1.05	2.89	0.32
MGL2O2	Coal/seam A ₂	5	8	14	8	16	51	2	2	4	11	1	0	20	8	7	4	6	0	1	3	29	1.50	2.55	0.31
MGL2P2	Coal/seam A ₂	3	2	35	9	2	51	1	4	7	8	3	1	24	7	4	3	9	0	1	1	25	0.33	2.13	0.35
MGL2T1	Coal/seam A ₁	9	14	15	8	14	60	1	5	4	4	2	1	17	6	1	5	9	0	1	1	23	1.29	3.53	0.32
MGL2T2	Coal/seam A ₁	10	11	15	11	13	60	2	5	5	3	2	1	18	4	2	4	10	0	1	1	22	1.14	3.33	0.31
Min value		3	2	5	3	2	45	0	2	2	1	0	0	8	1	1	2	1	0	0	0	14	0.33	1.32	0.31
Max. value		14	16	41	16	24	73	2	9	16	15	18	1	35	8	7	12	10	2	4	4	29	5.14	8.13	0.40
Average		7.67	9.5	17.33	8.58	15.25	58.33	0.92	4.17	5.58	6.17	2.92	0.42	20.17	3.50	2.83	4.83	6.50	0.33	1.92	1.58	21.50	1.71	3.55	0.34

Tx Textinite Sp Sporinite TL Total liptinite TI Total Inertinite
 U Ulminite Cu Cutinite Fg Funginite
 Dh Detrohuminite Rs Resinite Idt Inertodetrinite
 Ch Corpohuminite Lp Liptodetrinite F Fusinite
 Pg Porigelinite Sub Suberinite Sf Semifusinite
 TH Total huminite Ex Exsudatinite Ma Macrinite
 TPI Tissue Preservation Index = (Telohuminite+Semifusinite)/(Detrohuminite+Macrinite+Inertodetrinite)
 GI Gelification Index = Huminite/Inertinite



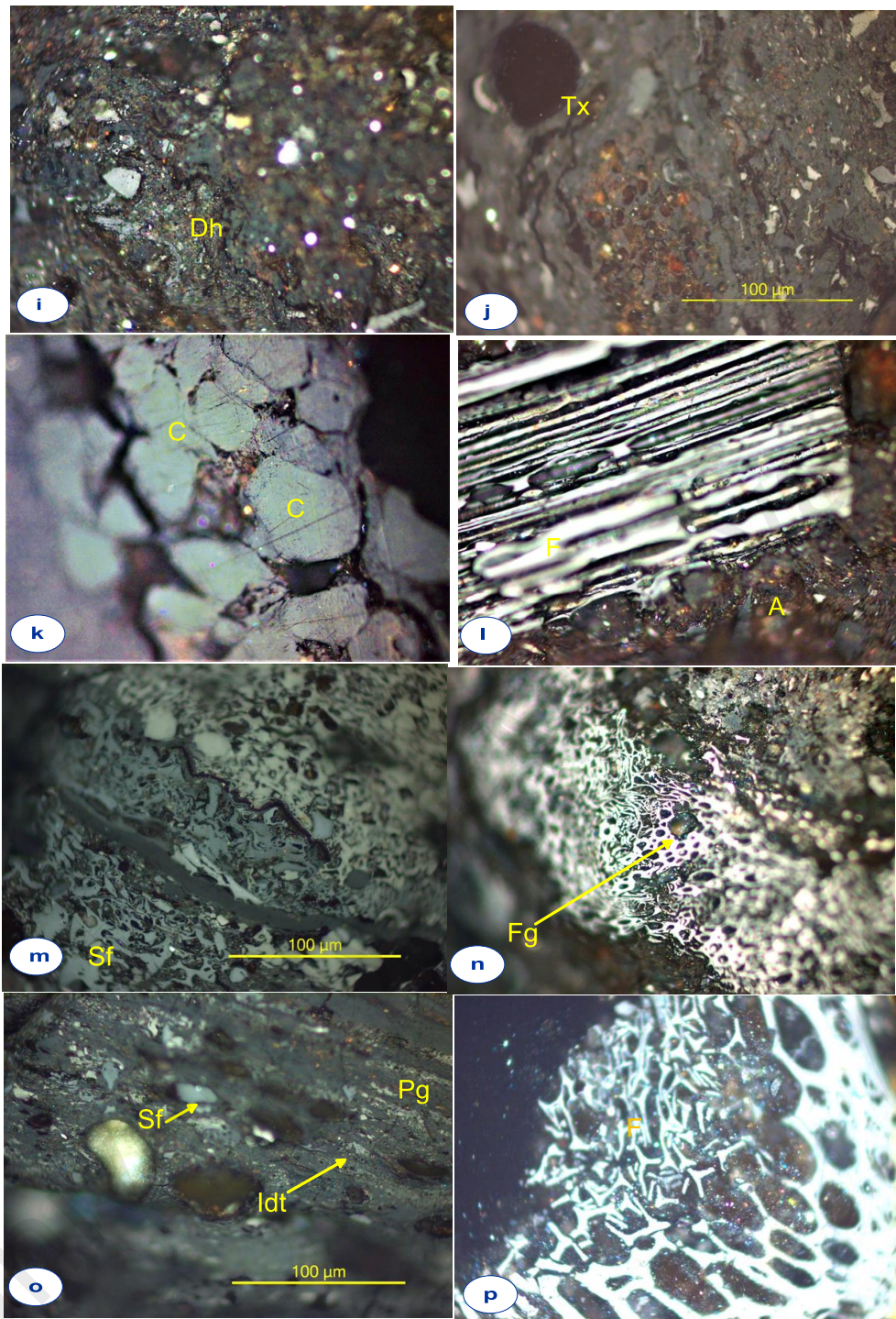


Figure 4.10: Photomicrographs of identified liptinites (a-j), huminites and inertinites macerals (k-r) in Maiganga coal showing cutinite maceral (Cu), resinite maceral (Re), liptodetrinite macerals (Lp), sporinite maceral (Sp), bituminite (Bt), textinite maceral (Tx), corphuminite maceral (C), porigelinite (Pg) detrohuminite maceral (Dh) attrinite maceral (A), fusinite (F), funginite (Fg), semifusinite (Sf) and inertrodetrinite (Idt).

4.8.3 Palynofacies

This is a useful tool for kerogen typing, paleoenvironment indicator, determination of thermal maturity and hydrocarbon generation potential of source rock (Tissot and Welte, 1984). It relies on the relative abundance of the three kerogen groups (AMO, Phytoclast and palynomorphs (Tyson, 1995; Mendonça Filho et al., 2012; Mustapha et al., 2017). Figure 4.11 shows the photomicrographs of identified palynomorphs (P), phytoclast (Ph) and amorphous organic matter (AOM) for the studied Yaya-Ngari shale (a and b) and Maiganga mudstones (b-h). Yaya-Ngari samples show significant amount of dark-brown to orange colour phytoclast compared to brown heterogenous AOM and brown to orange palynomorphs. The palynomorphs are often <math><10\ \mu\text{m}</math>, although few ones are up to 80 μm sizes (Figure 4.11a and b). In the case of Maiganga facies, they are characterised by mainly terrestrial kerogen group. Figure 4.11c-h shows photomicrographs of highly oxidized black, opaque tissues of higher plants often associated with some brown degraded tissue of higher plants, light brown AOM (probably resin and algae material) and trilate spore and pollens of plants. This is an indication of a more gas-prone Type III kerogen than the associated liptinitic materials of oil-prone Type II kerogen as observed under the UV-light.

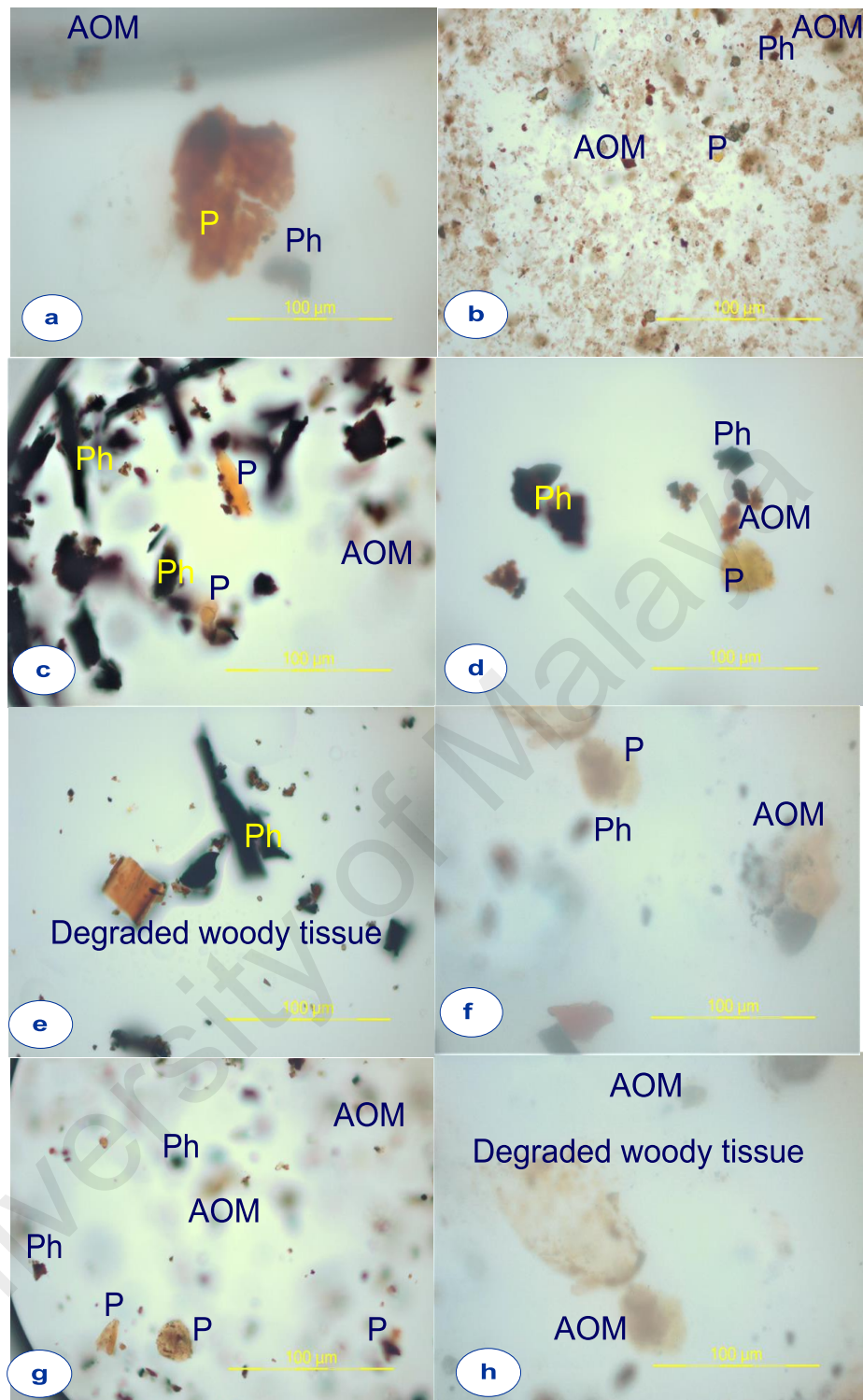


Figure 4.11: Photomicrographs of identified palynomorphs (P), phytoclast (Ph) and amorphous organic matter (AOM) in the studied Yaya-Ngari shale (a and b) and Maiganga mudstones (c-h).

4.9 Bulk kinetics for hydrocarbon generation

Representative coal samples were subjected to open system pyrolysis analysis to determine its bulk kinetic for petroleum generation. This is a function of the frequency factor and distribution of activation energy (Table 4.8) which in turn depends on composition of organic matter (Dieckmann, 2005). Analysed samples have overall activation energy distributions ranging from 40–70 kcal/mol, with related frequency factors ranging from 1.9953E+13/s to 3.6010E+15/s (Table 4.8). This range indicates non-homogenous organic matter (Schenk et al., 1997; Petersen and Rosenberg, 2000; Hakimi et al., 2015; Abbassi et al. 2016). Calculated results were based on a constant geological heating rate of 3.3 °C/My used while determining the bulk petroleum generation temperature and their corresponding transformation ratio (TR). The onset of bulk petroleum generation is expected at a lower temperature from 116-134 °C (about 0.68-0.79 Ro%), while the peak of the generation is around 139 to 155. °C (about 0.84-1.04Ro%) as shown in Table 4.8.

Table 4.8: Bulk kinetic parameters for hydrocarbon generation of the selected samples.

Sample ID	Activation energy	A[1/S]	Onset Temp. (°C)	Peak Temp. (°C)	Onset (Ro %)	Peak (Ro %)	Peak (TR%)
MGL1C	43-67	4.3552E+14/s	125	151	0.73	0.99	50
MGL2A	40-64	1.9953E+13/s	118	139	0.68	0.84	48
MGL2B	42-66	8.3145E+13/s	134	154	0.79	1.08	52
MGL2D	43-67	6.2883E+13/s	116	144	0.68	0.89	45
MGL3B	46-70	1.0431E+15/s	126	155	0.73	1.07	50
MGL2H	42-66	1.3754E+14/s	121	147	0.70	0.93	45
MGL2I	42-66	2.4659E+14/s	131	152	0.77	1.01	52
MGL2O	43-67	2.8902E+14/s	127	151	0.74	0.99	51
MGL2P	42-66	2.3367E+14/s	133	151	0.78	1.00	50
MGL2T	44-68	3.6010E+15/s	120	150	0.69	0.98	52

A: pre-exponential factors. Onset Temp. (°C): onset (TR 10%) temperature.

Peak Temp. (°C): peak generation (geological T_{max}) temperature.

Onset (Ro %): computed Onset % Ro. Peak (Ro %): computed Peak % Ro.

4.10 Bulk elemental analysis

Elemental analysis (ICPMS) provides information about the major and trace element composition. This can be used to infer the source of organic matter, paleodepositional condition, tectonic setting and paleoclimate in basins. In this study, the result of the ICP-MS analysis (Table 4.9 and 4.10) shows that oxides of major elements in the analysed coals, mudstones and shale from Gongola sub-basin are SiO₂, Al₂O₃, TiO₂, Fe₂O₃, CaO, MgO, Na₂O, K₂O, P₂O₅ and MnO. On the other hand, the trace elements detected are V, Ni, Sr, Ba, Cr, U, Rb, Ga and Ce. The ratios of Sr/Ba, V/Ni, Ga/Rb, V/Cr, V/(V+Ni), K/Al, Al/ Si and Ti/ Al were calculated accordingly (Table 4.9).

4.10.1 Geochemistry of major oxides

The concentration of major oxides in the mudstones and shale facies (Maiganga and Yaya-Ngari) is predominated by SiO₂ (46.7-78.1%), Al₂O₃ (9.59-24.3%), Fe₂O₃ (1.57-4.19%), TiO₂ (1.25-1.75%) and K₂O (0.71-2.11%). This is similar to the observed trend for the coal facies which are characterised by relatively moderate concentrations of SiO₂ (1.13-16.7%), Al₂O₃ (0.34-5.37%), Fe₂O₃ (0.38-2.3%), and CaO (0.58-1.2%). However, the concentration of other major oxides is < 1%. Seam A₂ and A₃ recorded the maximum values of SiO₂, Al₂O₃, and TiO₂ (see Table 4.9). This is probably associated with deposition of more sandstone characterised by high energy of deposition as the seams become younger upwardly (see Figure 4.1). The Si, Al and Ti are important elements associated with SiO₂, Al₂O₃ and TiO₂ respectively, (Ross and Bustin, 2009).

Concentration of Al₂O₃ is associated with SiO₂ (see Table 4.9) as a major oxide in the Gombe Formation coals and mudstones. Generally, all the mudstones recorded a significant high concentration of Al compared to the coals. High Al in Maiganga coals and mudstones is a reflection of amount of clay minerals such as kaolinite and illite in the area. Kaolinite are usually characterised by high aluminum (Al) contents, whereas

illite generally has high potassium (K) contents (Hieronymus et al., 2001, Ratcliffe et al., 2004; and Beckmann et al., 2005). High kaolinite in contrast to illite can be read from the general trend of high “Al” compared to” K” (see Table 4.9). This gives average K/Al ratios of 0.02 and 0.10 for the coals and mudstones respectively. The observation is consistent with the observed trend in the Yola sub-basin, within the same Northern Benue Trough by Sarki Yandoka et al. (2015a).

University of Malaya

Table 4.9: Major oxides composition of the analysed samples.

Sample ID	Lithology/ Seam	TOC	TS	Major Oxides (wt.%)												
				SiO ₂	Al ₂ O ₃	TiO ₂	Fe ₂ O ₃	CaO	MgO	Na ₂ O	K ₂ O	P ₂ O ₅	K/Na	K/Al	Fe/Al	Al + K + Na
MGL1B2	Coal/seam B	80.00	0.38	2.34	0.93	0.07	0.55	0.58	0.18	0.04	0.05	0.19	1.25	0.05	0.59	1.02
MGL2A2	Coal/seam B	66.20	0.29	1.23	0.34	0.04	0.38	1.20	0.39	0.01	0.01	0.04	1.00	0.03	1.12	0.36
MGL2C2	Coal/seam B	69.70	0.25	2.39	1.09	0.07	2.30	1.15	0.39	0.01	0.01	0.01	1.00	0.01	2.11	1.11
MGL3B2	Coal/seam B	62.00	0.22	1.61	0.99	0.04	0.39	1.08	0.39	0.01	0.01	0.01	1.00	0.01	0.39	1.01
MGL2H2	Coal/seam A ₃	67.30	0.28	1.13	0.58	0.03	0.57	0.85	0.28	0.01	0.01	0.01	1.00	0.02	0.98	0.60
MGL2I2	Coal/seam A ₃	63.66	0.18	3.09	0.47	0.08	0.49	1.01	0.33	0.01	0.01	0.01	1.00	0.02	1.04	0.49
MGL2O2	Coal/seam A ₂	65.40	0.30	5.52	1.65	0.17	0.62	0.97	0.33	0.01	0.02	0.01	2.00	0.01	0.38	1.68
MGL2P2	Coal/seam A ₂	55.90	0.31	16.71	5.37	0.40	0.93	1.11	0.41	0.01	0.12	0.01	12.00	0.02	0.17	5.50
MGL2T1	Coal/seam A ₁	51.60	0.29	13.67	4.84	0.35	1.54	0.87	0.36	0.02	0.10	0.01	5.00	0.02	0.32	4.96
Min. Value		51.60	0.18	1.13	0.34	0.03	0.38	0.58	0.18	0.01	0.01	0.01	1.00	0.01	0.17	0.36
Max. Value		80.00	0.38	16.71	5.37	0.40	2.30	1.20	0.41	0.04	0.12	0.19	12.00	0.05	2.11	5.50
Average		64.64	0.28	5.30	1.81	0.14	0.86	0.98	0.34	0.01	0.04	0.03	2.81	0.02	0.79	1.86
MGL2E2	Mudstone	2.90	0.95	71.00	10.50	1.51	4.00	0.15	0.21	0.12	1.91	0.08	15.80	0.18	0.38	12.53
MGL2F2	Mudstone	2.00	0.10	72.89	10.93	1.61	4.19	0.16	0.21	0.09	1.66	0.08	18.44	0.15	0.38	12.68
MGL2G2	Siltstone	2.20	0.01	78.10	9.59	1.25	2.55	0.08	0.12	0.09	2.11	0.04	23.44	0.22	0.27	11.79
MGL2k2	Mudstone	4.80	0.05	47.00	24.35	1.50	2.90	0.26	0.34	0.05	0.98	0.07	19.60	0.04	0.12	25.38
MGL2L2	Shale	15.00	0.13	47.51	24.24	1.69	3.00	0.24	0.34	0.05	1.01	0.07	20.20	0.04	0.12	25.30
MGL2N2	Shale	9.60	0.07	46.79	24.27	1.36	1.86	0.28	0.34	0.05	0.71	0.04	14.20	0.03	0.08	25.03
MGL2Q2	Shale	24.30	0.23	47.00	16.61	1.38	1.57	0.39	0.34	0.05	0.79	0.06	15.80	0.05	0.09	17.45
MGL2R2	Mudstone	6.60	0.08	47.50	16.20	1.36	1.59	0.37	0.34	0.05	0.79	0.06	15.80	0.05	0.10	17.04
MGL2S2	Shale	20.30	0.21	48.36	17.00	1.40	1.61	0.35	0.33	0.05	0.81	0.05	16.20	0.05	0.09	17.86
MGL2U2	Shale	3.80	0.04	56.57	24.17	1.75	1.63	0.12	0.30	0.06	1.16	0.06	19.33	0.05	0.07	25.39
Min. Value		2.00	0.01	46.79	9.59	1.25	1.57	0.08	0.12	0.05	0.71	0.04	14.20	0.03	0.07	11.79
Max. Value		24.30	0.95	78.10	24.35	1.75	4.19	0.39	0.34	0.12	2.11	0.08	23.44	0.22	0.38	25.39
Average		9.15	0.19	56.27	17.79	1.48	2.49	0.24	0.29	0.07	1.19	0.06	17.88	0.09	0.17	19.05

Table 4.9: Major oxides composition of the analysed samples (continued)

YN1A	Shale	1.10	0.02	59.78	20.59	1.63	3.79	0.51	0.57	0.09	1.71	0.05	19.00	0.08	0.18	0.02
YN1B	Shale	1.00	0.02	60.59	20.49	1.71	2.99	0.36	0.47	0.09	1.63	0.05	18.11	0.08	0.15	0.02
YN1C	Shale	1.30	0.02	60.33	21.06	1.67	2.52	0.39	0.50	0.09	1.57	0.04	17.44	0.07	0.12	0.02
YN1D	Shale	0.80	0.02	63.91	19.03	1.59	2.89	0.44	0.25	0.12	1.49	0.09	12.42	0.08	0.15	0.03
Min. Value		0.80	0.02	59.78	19.03	1.59	2.52	0.36	0.25	0.09	1.49	0.04	12.42	0.07	0.12	0.02
Max. Value		1.30	0.02	63.91	21.06	1.71	3.79	0.51	0.57	0.12	1.71	0.09	19.00	0.08	0.18	0.03
Average		1.05	0.02	61.15	20.29	1.65	3.05	0.43	0.45	0.10	1.60	0.06	16.74	0.08	0.15	0.02

University of Malaya

4.10.2 Geochemistry of trace elements

Geochemical studies of trace elements have many applications in Geoscience. Previous works have shown that certain trace elements such as V, Ni, Cu, Cr and Mn are redox-sensitive elements. These can be used to infer the paleodepositional condition during sedimentation (Akinlua et al., 2010; Mohialdeen and Raza, 2013; Armstrong-Altrin and Machain-Castillo, 2016). Similarly, concentrations of Ba, Sr, Rb and V are important for discriminating seawater from freshwater (Reimann and De Caritat, 1998; Makeen et al., 2015a).

University of Malaya

Table 4.10: Trace elements composition of the analysed samples. (continued)

Sample ID	Lithology/ seam	Trace elements (ppm)																						
		Mn	V	Ni	Sr	Ba	Ce	Co	Cr	Cu	Rb	Ga	Sc	U	Th	As	Mo	Pb	Ni/Co	Sr/Ba	U/Th	Ga/Rb	V/Ni	V/(V+Ni)
MGL1B2	Coal/seam B	0.01	5.00	1.50	296.10	768.00	7.30	1.20	20.00	4.00	1.70	1.70	0.80	0.20	0.90	0.60	1.10	1.50	1.25	0.39	0.22	1.00	3.33	0.77
MGL2A2	Coal/seam B	0.01	4.00	1.30	131.60	121.00	4.00	0.60	20.00	2.40	0.40	1.30	0.90	0.10	0.30	0.40	0.10	1.10	2.17	1.09	0.33	3.25	3.08	0.75
MGL2C2	Coal/seam B	0.07	7.00	3.40	71.60	72.00	6.40	3.50	20.00	3.50	0.30	1.40	0.70	0.10	1.00	0.40	0.10	2.10	0.97	0.99	0.10	4.67	2.06	0.67
MGL3B2	Coal/seam B	0.01	4.00	1.30	74.00	155.00	3.40	0.60	20.00	3.20	0.70	1.50	0.80	0.10	0.50	0.40	0.40	2.80	2.17	0.48	0.20	2.14	3.08	0.75
MGL2H2	Coal/seam A ₃	0.01	7.00	12.40	49.10	51.00	2.90	6.30	20.00	4.30	0.40	1.20	0.80	0.10	0.30	0.40	0.10	1.60	1.97	0.96	0.33	3.00	0.56	0.36
MGL2I2	Coal/seam A ₃	0.01	7.00	8.80	55.70	99.00	4.30	2.10	20.00	3.40	0.30	0.50	0.90	0.10	0.60	0.40	0.20	2.40	4.19	0.56	0.17	1.67	0.80	0.44
MGL2O2	Coal/seam A ₂	0.02	13.00	14.80	60.80	91.00	9.70	5.30	20.00	10.10	0.70	4.30	2.00	0.30	2.30	0.40	0.30	4.40	2.79	0.67	0.13	6.14	0.88	0.47
MGL2P2	Coal/seam A ₂	0.02	22.00	20.30	77.20	115.00	25.10	12.40	40.00	20.40	7.60	8.90	5.00	1.10	5.10	0.40	0.20	8.90	1.64	0.67	0.22	1.17	1.08	0.52
MGL2T1	Coal/seam A ₁	0.04	37.00	11.10	62.90	100.00	16.80	6.30	40.00	17.40	6.20	14.20	5.00	1.10	3.80	0.40	0.30	6.10	1.76	0.63	0.29	2.29	3.33	0.77
Min. Value		0.01	4.00	1.30	49.10	51.00	2.90	0.60	20.00	2.40	0.30	0.50	0.70	0.10	0.30	0.40	0.10	1.10	0.97	0.39	0.10	1.00	0.56	0.36
Max. Value		0.07	37.00	20.30	296.10	768.00	25.10	12.40	40.00	20.40	7.60	14.20	5.00	1.10	5.10	0.60	1.10	8.90	4.19	1.09	0.33	6.14	3.33	0.77
Average		0.02	11.78	8.32	97.67	174.67	8.88	4.26	24.44	7.63	2.03	3.89	1.88	0.36	1.64	0.42	0.31	3.43	2.10	0.72	0.22	2.81	2.02	0.61
MGL2E2	Mudstone	0.06	82.00	26.00	76.00	549.00	120.00	26.00	90.00	11.00	50.00	13.40	12.00	6.90	25.00	0.73	0.62	13.70	1.00	0.14	0.28	0.27	3.15	0.76
MGL2F2	Mudstone	0.07	89.00	26.00	75.30	555.00	125.60	27.30	100.00	10.20	44.10	13.30	11.00	7.50	24.20	0.70	0.60	14.40	0.95	0.14	0.31	0.30	3.42	0.77
MGL2G2	Siltstone	0.06	50.00	20.00	93.70	712.00	88.30	6.20	60.00	6.60	52.10	11.30	7.00	5.40	24.30	0.50	0.10	6.50	3.23	0.13	0.22	0.22	2.50	0.71
MGL2k2	Mudstone	0.06	139.00	42.00	79.00	390.00	151.00	22.90	160.00	31.00	53.20	29.00	19.00	6.00	21.90	0.05	0.30	20.00	1.83	0.20	0.27	0.55	3.31	0.77
MGL2L2	Shale	0.05	140.00	43.00	81.80	394.00	150.60	23.70	160.00	30.90	53.20	30.70	19.00	6.00	21.90	0.05	0.30	21.70	1.81	0.21	0.27	0.58	3.26	0.77
MGL2N2	Shale	0.01	121.00	26.00	66.60	298.00	115.10	6.90	140.00	38.80	54.50	27.10	17.00	5.00	17.20	0.50	0.20	13.10	3.77	0.22	0.29	0.50	4.65	0.82
MGL2Q2	Shale	0.02	100.00	28.00	75.40	299.00	134.00	15.50	120.00	35.80	47.60	19.60	15.00	6.40	19.80	0.50	0.30	20.00	1.81	0.25	0.32	0.41	3.57	0.78
MGL2R2	Mudstone	0.02	103.00	28.00	74.90	297.00	134.00	17.00	140.00	34.00	48.00	19.60	16.00	7.40	19.20	0.49	0.30	19.00	1.65	0.25	0.39	0.41	3.68	0.79
MGL2S2	Shale	0.02	104.00	29.00	73.00	299.00	140.00	20.00	120.00	32.00	52.00	25.00	16.50	8.40	20.00	0.50	0.29	20.00	1.45	0.24	0.42	0.48	3.59	0.78

Table 4.10: Trace elements composition of the analysed samples. (continued)

MGL2U1	Shale	0.01	138.00	36.00	69.20	411.00	160.00	22.10	150.00	30.30	51.60	31.80	20.00	6.80	21.40	0.50	0.30	21.80	1.63	0.17	0.32	0.62	3.83	0.79
Min. Value		0.01	50.00	20.00	66.60	297.00	88.30	6.20	60.00	6.60	44.10	11.30	7.00	5.00	17.20	0.05	0.10	6.50	0.95	0.13	0.22	0.22	2.50	0.71
Max. Value		0.07	140.00	43.00	93.70	712.00	160.00	27.30	160.00	38.80	54.50	31.80	20.00	8.40	25.00	0.73	0.62	21.80	3.77	0.25	0.42	0.62	4.65	0.82
Average		0.04	106.60	30.40	76.49	420.40	131.86	18.76	124.00	26.06	50.63	22.08	15.25	6.58	21.49	0.45	0.33	17.02	1.91	0.20	0.31	0.43	3.50	0.77
YN1A	Shale	0.02	125.00	37.00	94.20	575.00	151.50	15.00	130.00	19.70	84.50	25.50	17.00	7.70	22.50	0.50	0.50	14.90	2.47	0.16	0.34	0.30	3.38	0.77
YN1B	Shale	0.02	116.00	35.00	98.00	600.00	175.80	13.10	130.00	21.40	72.40	25.40	17.00	7.20	24.10	0.50	0.20	8.20	2.67	0.16	0.30	0.35	3.31	0.77
YN1C	Shale	0.07	118.00	33.00	85.70	660.00	177.70	10.80	130.00	19.50	67.50	27.60	17.00	6.10	23.70	0.50	0.10	12.50	3.06	0.13	0.26	0.41	3.58	0.78
YN1D	Shale	0.03	94.00	29.00	90.60	676.00	160.00	16.90	110.00	5.90	54.40	22.00	14.00	7.20	24.30	0.50	3.00	15.90	1.72	0.13	0.30	0.40	3.24	0.76
Min. Value		0.02	94.00	29.00	85.70	575.00	151.50	10.80	110.00	5.90	54.40	22.00	14.00	6.10	22.50	0.50	0.10	8.20	1.72	0.13	0.26	0.30	3.24	0.76
Max. Value		0.07	125.00	37.00	98.00	676.00	177.70	16.90	130.00	21.40	84.50	27.60	17.00	7.70	24.30	0.50	3.00	15.90	3.06	0.16	0.34	0.41	3.58	0.78
Average		0.04	113.25	33.50	92.13	627.75	166.25	13.95	125.00	16.63	69.70	25.13	16.25	7.05	23.65	0.50	0.95	12.88	2.48	0.15	0.30	0.37	3.38	0.77

Table 4.10 shows the trace element distribution of the studied coal and mudstones from Gombe Formation in the Gongola sub-basin. The distribution is dominated by Ba, Ce, Cr, V and Sr with moderate concentration of Ni, Ga, Rb, while other trace elements are less. These trace elements show a relatively high concentration in the mudstones compared to the coal facies. This relationship is consistent with the Clarkes' world trace element contents in coals and carbonaceous shale (Swaine, 1990; Ketris and Yudovich, 2009). The mudstones and shale are characterised by varied concentration of Ba (297-712 ppm compared to Ce (88-178 ppm), Cr (60-160 ppm), V (50-140 ppm), and Sr (67-98). On the other hand, the coal facies have relatively moderate amount of Ba (51-768 ppm), Ce (3-25 ppm), Cr (20-40 ppm), V (4-37 ppm) and Sr (49-296 ppm) (Table 4.10). The relatively high concentration of vanadium, an important biophile trace element, compared to Ni and Co in the studied samples is worth noting. This is similar to the trend in the Yola sub-basin but in contrast to the trend in Niger-Delta where the biophile elements were predominated by Ni, followed by V and Co (Akinlua et al., 2007; Sarki Yandoka et al., 2015a).

4.10.3 Geochemistry of clay minerals

Whole rock powder and <2-micron clay fraction approaches were used for the XRD (X-ray diffraction) analysis. This is employed in this study to provide rapid identification of minerals especially the clay minerals in order to gain more insight to the inorganic geochemical composition of the Gombe Formation samples. It is useful in distinguishing the mineralogy of the fine grained sedimentary facies which are difficult to identify under the microscope (Makeen et al., 2016). Identified clay minerals on the diffractogram are predominated by kaolinite and chlorite often associated with montmorillonite with minor occurrence of illite, and corrensite (Figure 4.12). Other associated minerals are quartz, calcite, feldspars (Figure 4.12). This is an indication that the elements Si, Al, Ti and K observed from the major oxide originate from mixed clay

assemblages in the Gombe Formation (Maiganga and Yaya-Ngari). Similarly, the contrasting relationship between the predominating kaolinite clay mineral and the illite is typical of semi-arid to slightly humid-warm climatic conditions.

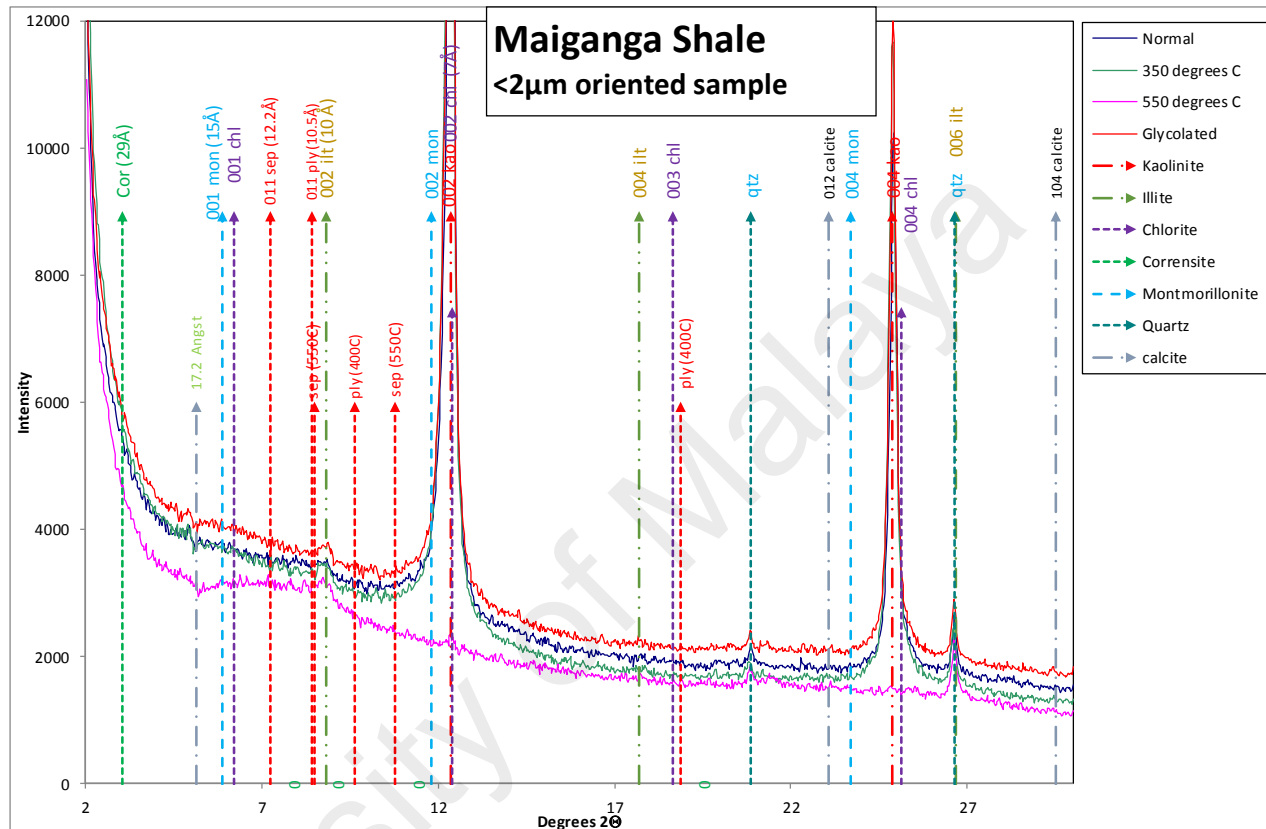


Figure 4.12a: Identified clay minerals on the diffractogram of Maiganga shale are kaolinite, chlorite, montmorillonite, illite, and corrensite often associated with calcite and quartz.

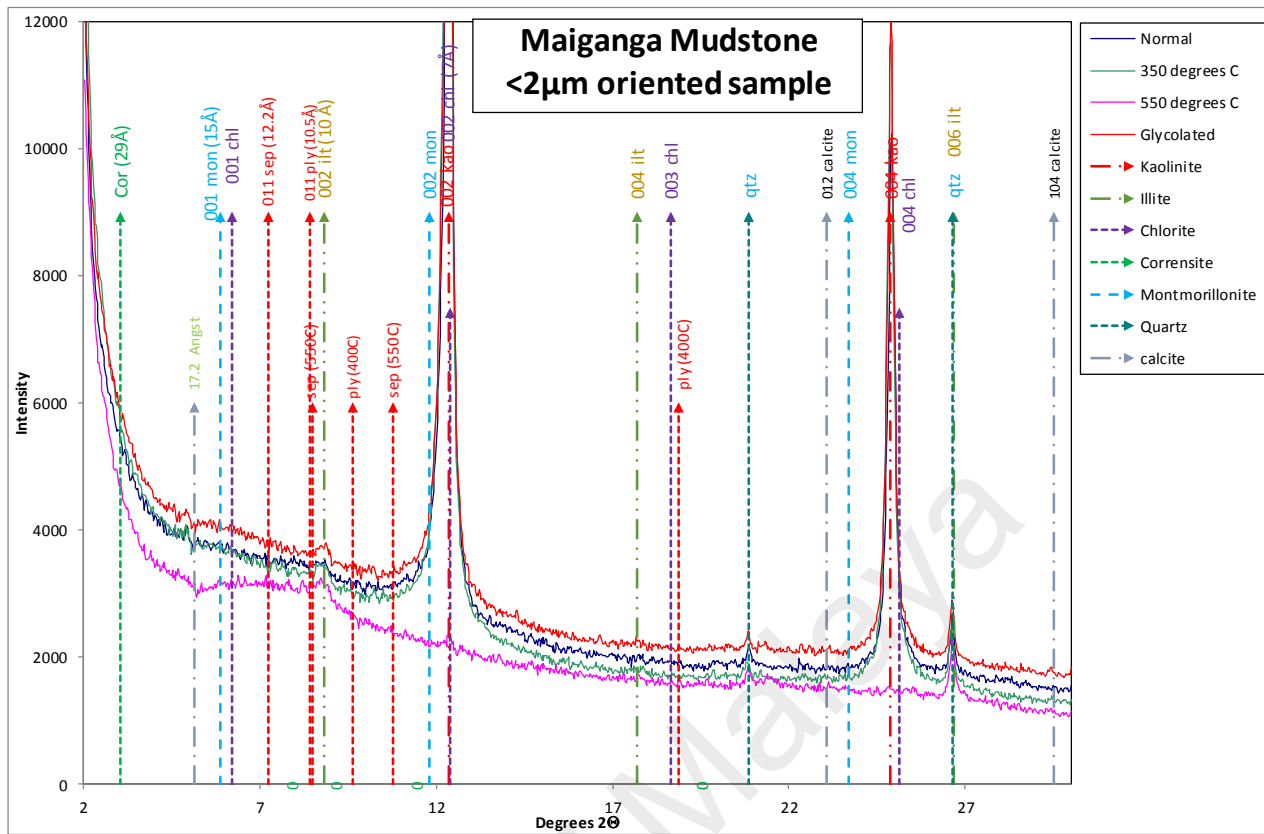


Figure 4.12b: Identified clay minerals on the diffractogram of Maiganga mudstone are kaolinite, chlorite, montmorillonite, illite, and corrensite often associated with calcite and quartz.

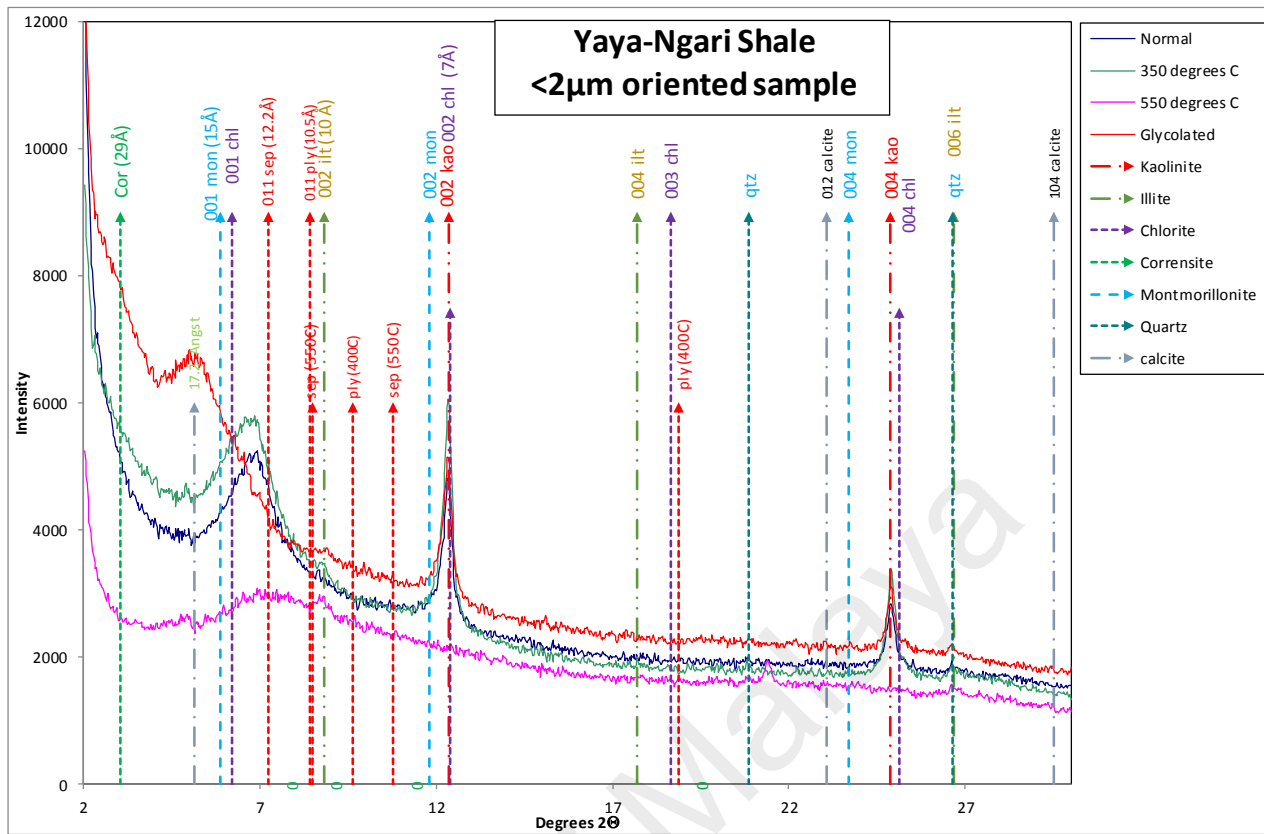


Figure 4.12c: Identified clay minerals on the diffractogram of Yaya-Ngari shale are kaolinite, chlorite, montmorillonite, illite, and corrensite often associated with calcite and quartz.

CHAPTER 5: DISCUSSION

5.1 Source rock characterisation

This chapter focuses on source rock characterisation of the analysed Gombe Formation samples based on the results of the analyses carried out as presented in Chapter 4. It covers the organic matter quantity (richness), quality, origin, paleoenvironment, vertical and lateral extents as related to hydrocarbon generation potential and thermal maturity. The chapter ends with discussion on the tectonic setting and paleoclimatic conditions which are also crucial in determining petroleum source rock potential in relation to the depositional environment. These were assessed using parameters and ratios based on the performed organic and inorganic geochemical analyses (see Chapter 3).

5.2 Stratigraphic succession

Based on the stratigraphic succession of the studied Gombe Formation and sedimentary structures, a delta plain setting characterised by at least four (4) depositional cycles of coarsening upward in a progradational wave dominated sequence can be inferred (Figure 4.1). This is evident from gradual transition from reasonably thick coal facies through the interbedded mudstones and shales up to the sandstone facies (Ayinla et al., 2017a). The presence of parallel laminated sandstones within the coarsening upward sequence as well as rootlets on mudstones are evidences of more terrigenous source input in the deltaic setting. Series of faults observed in the area are manifestation of tectonic activity which characterise the entire Benue trough especially the pre-Palaeogene sediments in the Northern Benue Trough (Ayinla et al., 2017b; Abubakar, 2014).

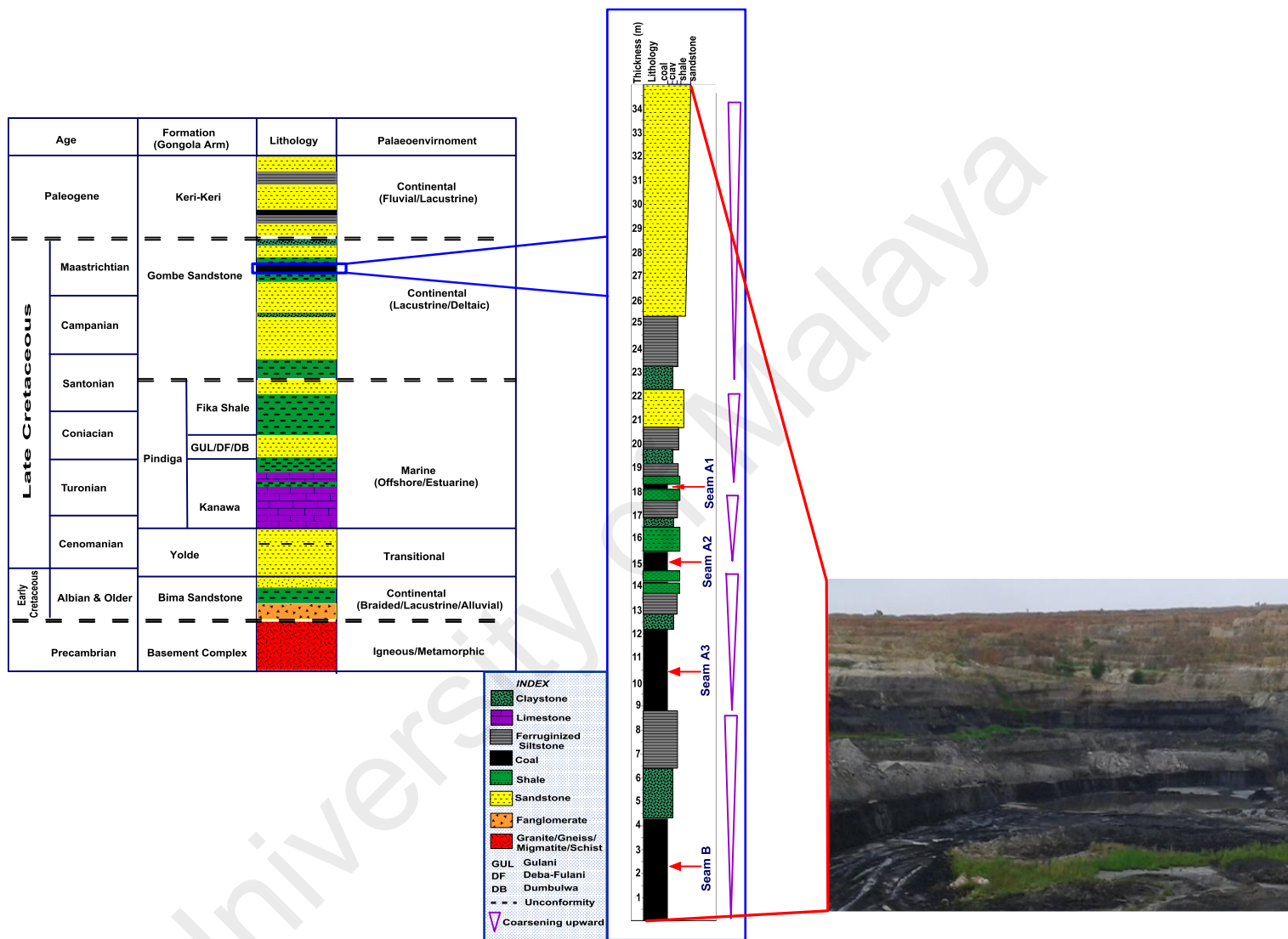


Figure 5.1: Stratigraphy of the studied coal bearing formation in the Northern Benue Trough as exposed at the Maiganga coalfield.

5.3 Total organic matter (richness)

Organic matter richness and generative potential of coals and mudstones from Maiganga and Yaya-Ngari areas were evaluated using pyrolysis parameter (e.g. S₂ yield), TOC content and bitumen extraction data (e.g. extractable organic matter, EOM and hydrocarbon yields), (see Table 4.2). The first and one of the most important factors for oil and gas generation in a sedimentary basin is presence of sufficient organic matter upto certain threshold as suggested by Tissot and Welte (1984) as well as Peters and Cassa (1994). Thus, total organic carbon content determination (TOC) in Gombe Formation gives a measure of the source rock richness for hydrocarbon generation (see Table 4.1). Research has shown that the lowest acceptable TOC for potential source rock is 0.5%, although, it is a known fact that coal usually shows a high value (Peter and Cassa, 1994). This made it necessary to integrate other parameters such as pyrolysis S₂ and maceral analysis of coal while assessing the source rock hydrocarbon generation potential.

As expected of coals, the TOC results indicate an excellent potential for Maiganga coals (>50.3 wt.%) compared to very good to excellent for shale (> 3.7wt.%) and mudstones (from 2.0 to 6.7 wt.%), while Yaya-Ngari shale has fair to good quantity (from 0.8 to 1.3 wt.%). Hydrocarbon yield (S₂) from pyrolysis of the Gombe Formation samples varies from 0.24 to 158.84 mg HC/g rock with Maiganga coal facies ranging from 26.42 to 158.84 mg HC/g rock and other sediments with a fairly moderate value. The hydrocarbon yields (S₂) are in agreement with TOC contents indicating fair-good source rock richness for Yaya-Ngari and very good to excellent for Maiganga based on Peters and Cassa (1994) (Figure 5.2). It is important to note that, the high TOC and S₂ values for the coal samples does not necessarily mean excellent source rock potential. Available evidence from organic petrography and Py-GC indicate gas prone and poor oil source rock for the coal.

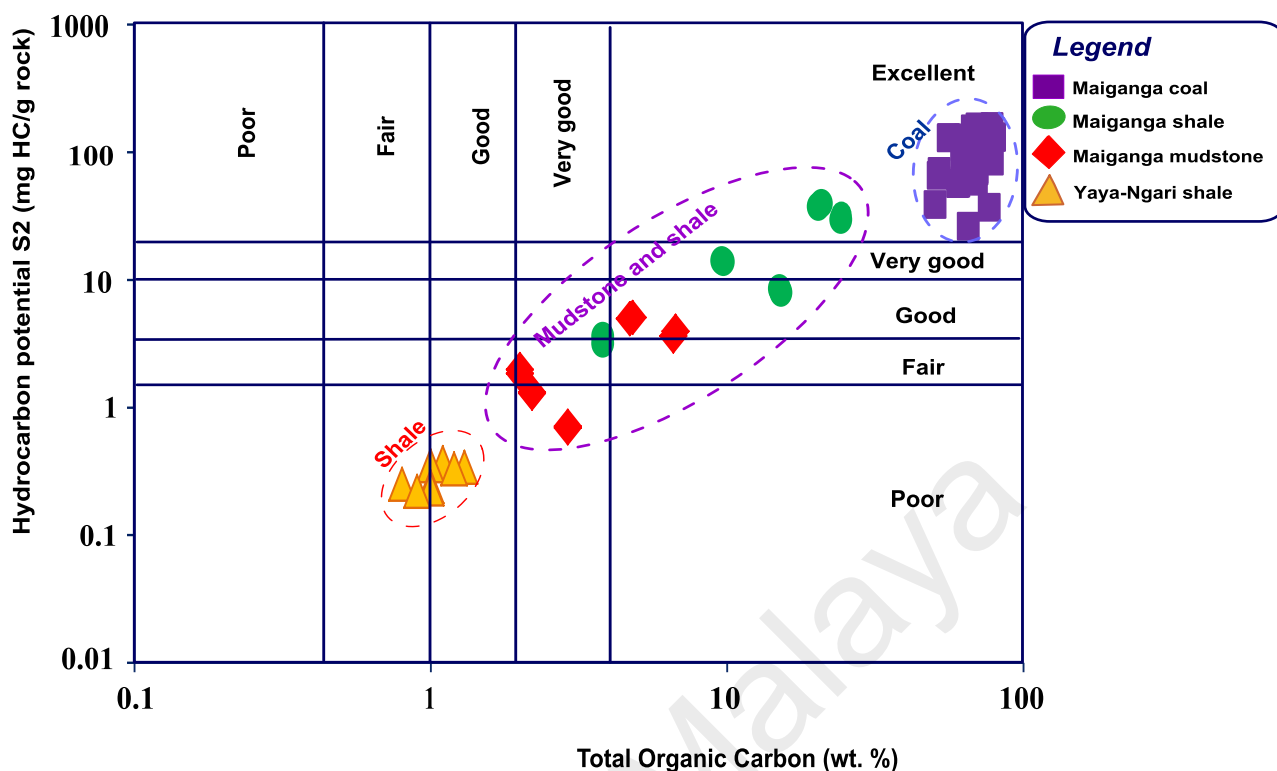


Figure 5.2: The cross plot of S2 (mg HC/g rock) versus TOC (wt.%) showing the hydrocarbon potential for the analysed Maiganga and Yaya-Ngari samples.

The contents of EOM (bitumen) and hydrocarbons (saturates + aromatics) can be compared with the S1, S2 and TOC in determining the source richness and hydrocarbon generation potential (Peters and Cassa, 1994; Peters et al., 2005). The EOM contents (Table 4.2) recorded relatively high values for the Maiganga coal, moderate for the mudstones and shale compared to the low values for Yaya-Ngari samples. Hydrocarbons contents (Table 4.2) showed that the coal facies have relatively high concentration (1836.8-13974.3 ppm), followed by the mudstones and shale, while Yaya-Ngari displayed relatively low values (71.2-570.1 ppm). These values indicate fair-good to excellent organic source richness and generative potential as demonstrated by the cross plot of EOM versus TOC (Figure 5.3) as well as the bar plot of the hydrocarbon fractions (saturated+aromatic HC) of the EOM (Figure 5.4).

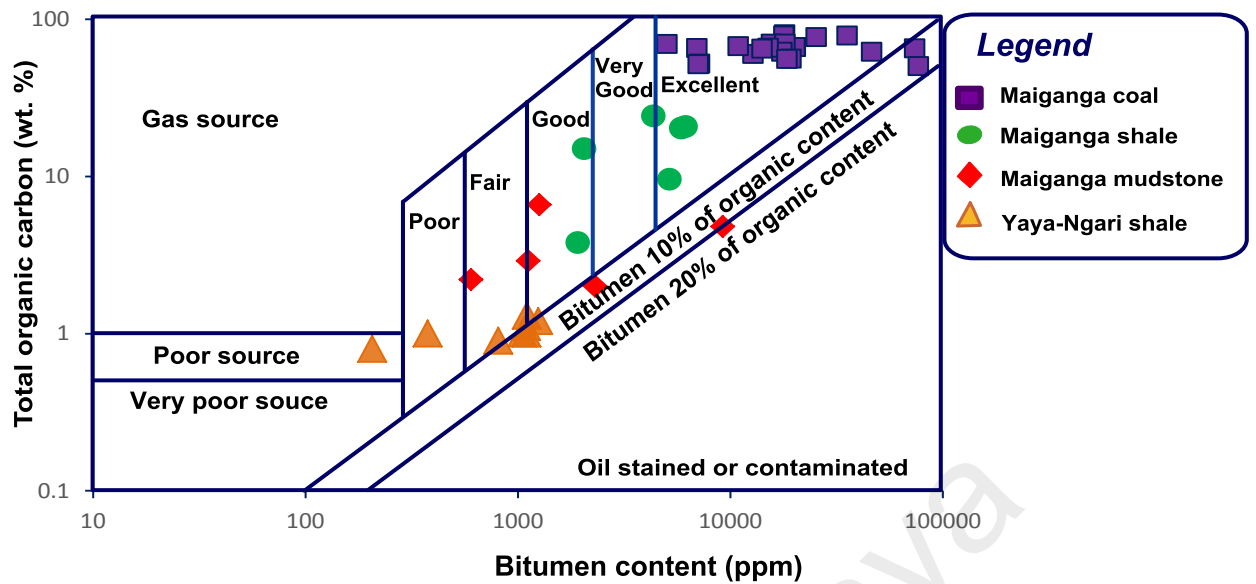
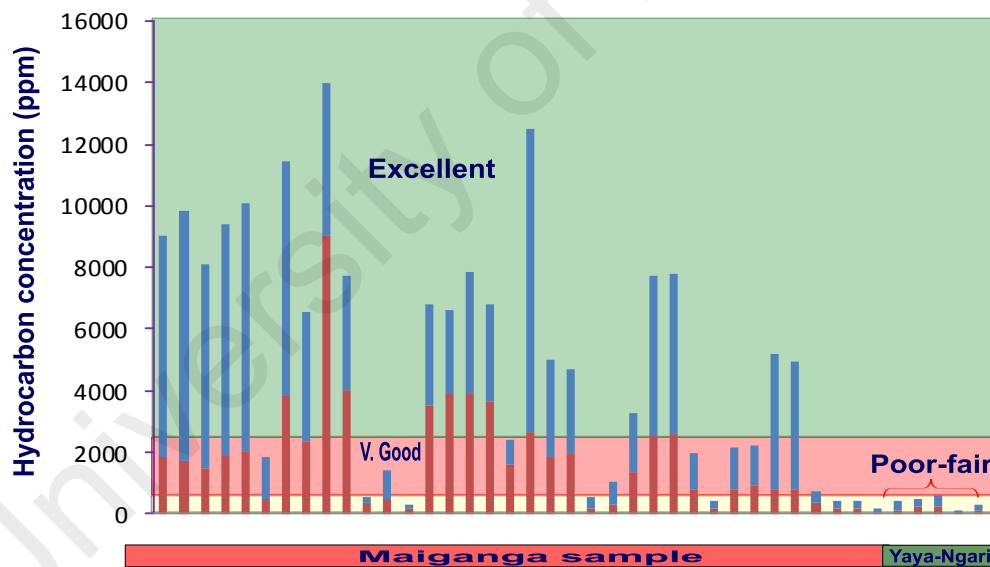


Figure 5.3: The cross plot of Total organic carbon content (TOC, wt. %) versus Bitumen content (ppm) showing the hydrocarbon potential for the analysed Maiganga and Yaya-Ngari samples.



Legend

- Aliphatic fraction concentration (ppm)
- Aromatic fraction concentration (ppm)

Figure 5.4: The bar plot of hydrocarbons concentration (aliphatic+aromatic fraction) of the extractable organic matter (ppm) showing the hydrocarbon potential of analysed Maiganga and Yaya-Ngari samples.

5.4 Type of organic matter (quality)

Kerogen pyrolysis data (HI and Py-GC) supported by organic petrography can provide information on the organic matter type (quality) of potential source rocks (e.g. Giraud (1970); Tissot and Welte, 1984; Korkmaz and Kara, 2007; Dembicki, 2009; Sarki Yandoka et al., 2016). Type I and II kerogen, which is commonly derived from lacustrine and marine organic matter and corresponding source rocks, are capable of generating liquid hydrocarbons. Primary biogenic organic matter which forms Type III kerogen is mainly composed of woody materials and more susceptible to generating gas. Type IV kerogen is composed of inert materials with no potential of generating hydrocarbons (Peters and Cassa, 1994; Hakimi et al., 2011).

5.4.1 Type of organic matter based on SRA

In this study, kerogen classification diagrams were constructed using HI vs. T_{max} based on earlier works given by Mukhopadhyay et al., (1995) and adapted after Hakimi et al., (2011). The pyrolysis data (HI vs. T_{max}) (Figure 5.5) indicated that the analysed samples are generally plotted in the early to relatively mature zone of mixed Type III-II and predominantly Type III kerogen as indicated by the HI values in the range of 23 to 234 mg HC/g TOC (Table 4.1), Singh et al., (2016) suggested that predominance of Type-III kerogen with a little bit of Type-II kerogen as shown in Figure 5.5 is a good indicator of high terrestrial source for the samples. Therefore, these HI values as shown in Figure 5.5 suggest that the sediments may be expected to generate mainly gas and limited amount of liquid hydrocarbons. Moreso, Maiganga samples with hydrogen index <200 mg HC/g TOC that contains a Type III vitrinitic kerogen would be expected to generate gas, while samples with HI values higher than 200 mg HC/g TOC can generate some oil and perhaps, their main generation products are gas and condensate (Hunt, 1996). The presence of liptinitic macerals (14-29%) is most apparent to the oil and gas prone nature of the analysed Maiganga

samples of mainly Type III-II and Type III kerogens (see Figure 4.10) as well as palynofacies analysis (Figure 4.11). On the other hand, Yaya-Ngari shales contain mainly Type IV kerogen with no potential for hydrocarbon generation based on very low HI (<50 mg HC/g TOC; Table 4.1).

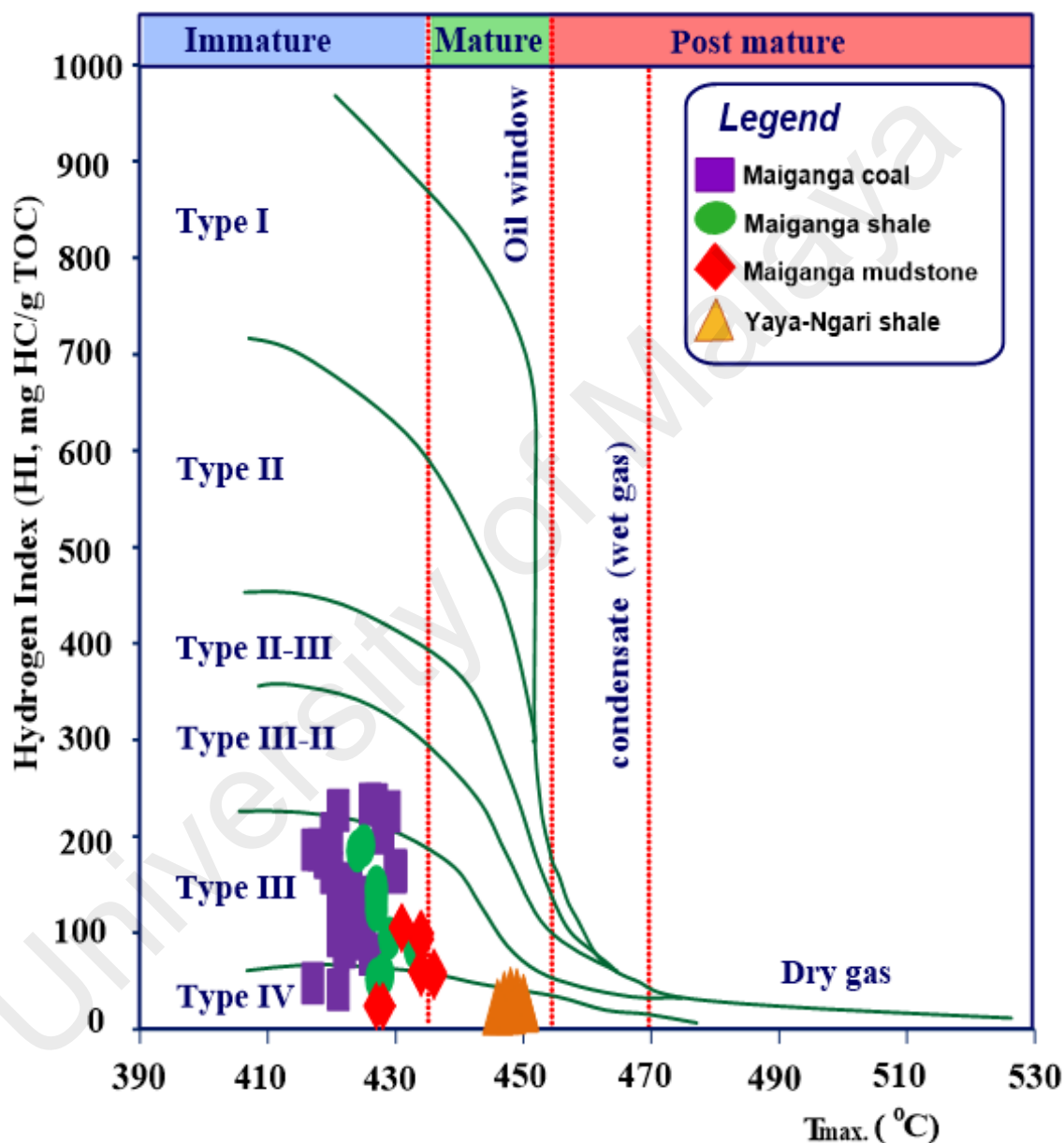


Figure 5.5: The plot of the Hydrogen Index (HI, mg HC/gTOC) versus pyrolysis T_{max} (°C) showing the kerogen type of the analysed Maiganga and Yaya-Ngari samples.

5.4.2 Type of organic matter based on Py-GC

It is worth noting that integration of supplementary method such as Py-GC has been pointed out as a way of reducing likely fallacies that may result from SRA/Rck-Eval pyrolysis in order to ensure accurate evaluation of organic matter type (Dembicki, 2009). This current study uses Py-GC for qualitative evaluation of the remaining hydrocarbon which can be generated during maturation or by the cracking of the kerogen in a sedimentary formation. Based on the predominating number of *n*-alkane/*n*-alkene carbon displayed on the Py-GC pyrogram, Dembicki (2009) distinguished kerogen into four types. These are Type I kerogen (dominated by $<n\text{-C}_{10}$ and $>n\text{-C}_{15}$), an intermediate Type II kerogen (dominated by $<n\text{-C}_{10}$ with average concentration of $>n\text{-C}_{15}$), Type III (dominated by $<n\text{-C}_{10}$) and Type IV kerogen (little or no pyrogram signal). Similarly, Larter and Douglas (1980) suggested that “type index” values can be used as proxy for classifying kerogen into type Type I kerogen (< 0.4), Type II kerogen (from 0.4 to 1.3) and Type III kerogen (from 1.3 to more than 20).

In this study, the Py-GC trace of the analysed Maiganga coals (see Figure 4.9) display an intermediate concentration of $n\text{-C}_1$ to $n\text{-C}_{35}$ with relatively high abundance of $<n\text{-C}_{12}$ especially $n\text{-C}_{10}$ which is a reflection of gas/oil- prone Type III/II kerogen. Also, the *n*-alkane/*n*-alkene carbon on the pyrogram extends up to the higher molecular weight compounds between the range of $n\text{-C}_{30}$ and $n\text{-C}_{35}$. This further supports presence of oil-prone Type II kerogen within the area. Table 4.5 shows the “type index” ranging from 0.43 to 1.38 for the analysed coal. About 43% of the “type index” values is > 1 , while around 36% of the values falls between > 0.9 and 1 while only about 21% have values close to the upper boundary of Type II kerogen (0.43- 0.47). This means that almost 80% of the “Type index value” falls in the boundary between Type II and Type III kerogen with more proximity towards the Type III than Type II kerogen as suggested by Dembicki (2009). However, the Maiganga mudstones are predominated by Type II.

Thus, based on the “Type index” values it can be concluded that Gombe Formation contains Type III/II kerogen at the Miaganga area.

In the same way, the Py-GC pyrograms of the analysed Miaganga samples (Figure 4.9) also show *n*-alkane/*n*-alkene doublets in the low molecular weight (<*n*-C₁₂) associated reasonably with high concentration of organic aromatic compounds such as toluene and *m*(+*p*)-xylene while 2,3 dimethylthiophene and phenol occur in low concentration. All these, give an indication of a mixture of oil and gas with predominance of gas generation potential owing to richness in aromatics with reasonable aliphatic concentration for the Gombe Formation samples.

The Ternary plots (Figure 5.6) that are used to distinguish the kerogen type based on compounds *m*(+*p*)-xylene, *n*-octene and phenol indicates dominance of Type III/II interface with some Type II kerogen. This is in line with the inferred gas prone Type III kerogen with some Type II/III kerogen capable of generating oil for the Gombe Formation coal based on the hydrogen index of more than 200 mg HC/g TOC (Ayinla et al., 2017a). This inference is also supported by the cross plot of the atomic H/C against O/C (Figure 5.7) which can be interpreted as type III/II kerogen with mainly gas generation potential. This plot shows that the analysed coals have not fully entered the catagenesis stage of oil generation window which supports the immature nature of the analysed coal. The observation is consistent with the huminite reflectance measurements of < 0.5% R_o (see Table 4.1) as well as biomarker analysis reported by Ayinla et al. (2017a). In contrast, the Yaya-Ngari shales show a typical Type IV kerogen with very little to absence of pyrogram signal of the *n*-alkane/*n*-alkene peaks from *n*-C₁ to *n*-C₃₃ (see YN1A2 in Figure 4.9).

The ratio of cadalene/*m*(+*p*) xylenes (cd/xy) calculated as shown in Table 4.5 can serve as semi quantitative and qualitative measure of kerogen hydrocarbon generation potential as well as relative concentration of aliphatic and aromatic contents

(Van Aarssen et al., 1992; Adegoke et al., 2015). The analysed Gombe Formation samples are characterised by low ratio of polycyclic aromatic hydrocarbon compound (cadalene) compared to aromatic xylene (cd/xy) which ranges from 0.04 to 0.18. This is an indication of high plants terrigenous source input as was previously reported by Solli et al. (1984). The observation is consistent with the predominance of C₂₉ααα(20R) sterane over other steranes that was reported by Ayinla et al. (2017a).

5.4.3 Type of organic matter based on organic petrography

Organic petrographic studies can provide an insight into kerogen type as suggested by many authors (e.g. Giraud, 1970; Mendonça Filho et al., 2012; Mustapha et al., 2017). Type I kerogens are characterised by algal lipid/liptinite maceral from marine setting producing more “aliphatic” pyrolysates compared to terrigenous Type III kerogens from higher plants which produce “aromatic” pyrolysates. In this study, there is predominance of huminite maceral (average 58%) compared to liptinite and inertinite. This is a reflection of more of terrigenous Type III kerogens compared to moderate amount of liptinite macerals (Type I/II kerogen macerals). Based on maceral analysis, it can be inferred that gas prone Type III kerogen is more than the average amount of other oil prone liptinite maceral groups. Similarly, the palynofacies analysis shows abundance of phytoclast with some palynomorph and AOM. All these are indications supporting gas prone nature of the Maiganga coals with minimum amount of oil.

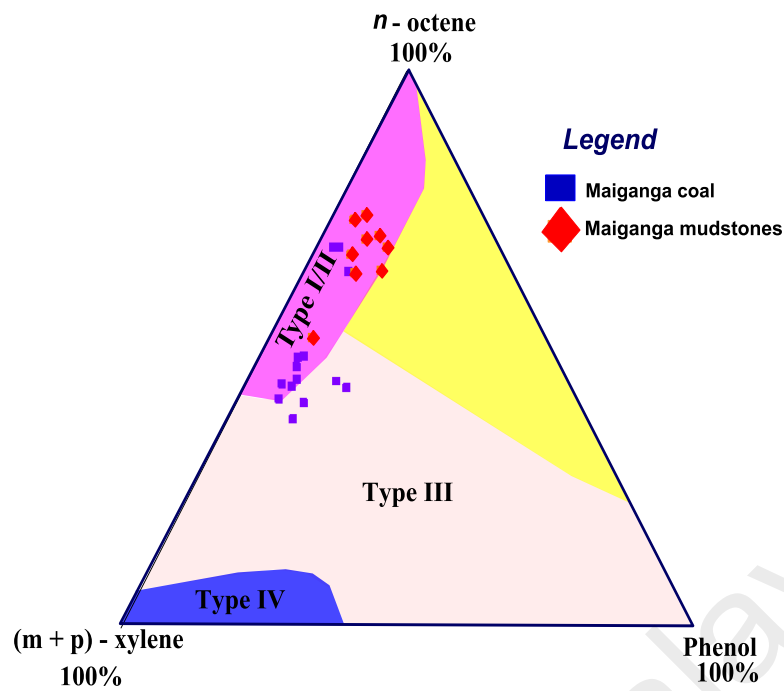


Figure 5.6: The Ternary plot based on compounds, m(+p)-xylene, *n*-octene (*n*-C₉) and phenol, showing the kerogen type of the analysed Maiganga coal (modified after Larter, 1984).

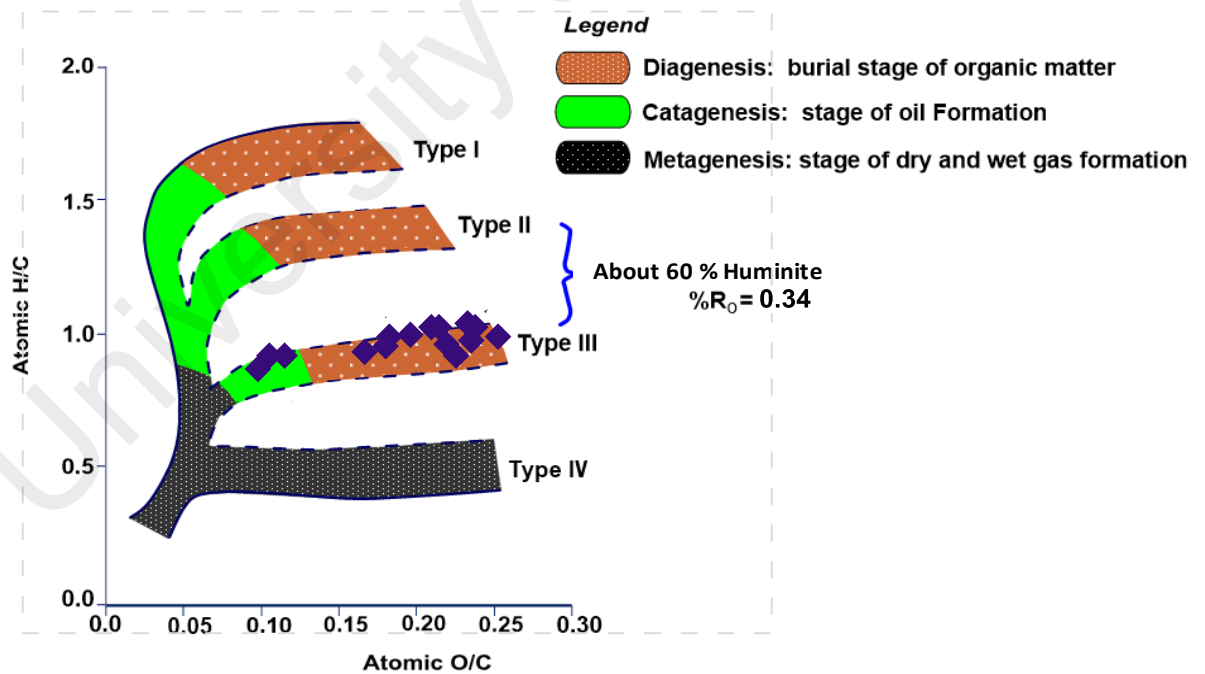


Figure 5.7: The cross plot of atomic H/C versus atomic O/C on the Van Krevelen diagram showing the kerogen type of the analysed coal samples (adapted after Peters and Cassa, 1994).

5.5 Origin of organic matter

Organic matter source inputs were determined based on molecular geochemistry and organic petrography. Analytical results of both biomarker and non-biomarker can complement each other to provide more reliable interpretation of the organic matter origin either terrestrial, marine or mixed source (Peters and Moldowan, 1993; Peters et al., 2005; Hakimi et al., 2011; Hakimi and Abdullah, 2013; El Diasty and Moldowan, 2013; Makeen et al., 2015c; Zulkefley et al., 2015).

In this study, observation from m/z 85 distribution (Figure 4.6a-f), shows terrestrial source for the organic matter (Peters et al., 2005; Zulkefley et al., 2015). This is evident as significant fractions of the normal alkane chromatographic distribution are mainly within the range of n -C₂₃ and n -C₃₃ of the GCMS ion m/z 85 chromatograms. The preponderance of high molecular weight compounds from n -C₂₃ upward and high concentration of odd n -alkane compared to even n -alkane (Figure 4.6a-f), especially significant relative abundance of n -C₂₇, n -C₂₉ and n -C₃₁ (higher plant molecular compounds) for Maiganga samples (Figure 4.6b, 4.6d and 4.6f), indicates terrestrial source for the organic matter (Tissot and Welte, 1984). This is in line with the CPI value that is generally >1.06 for both Maiganga and Yaya-Ngari (see Table 4.3) indicating land plant origin for the analysed Gombe Formation sediments.

Pristane (Pr) and phytane (Ph) derived from phytol side chain of chlorophyll usually display the most abundant concentration among the acyclic isoprenoid in hydrocarbon as well as sediments. Pr and Ph are often associated with normal alkanes n -C₁₇ and n -C₁₈ respectively (Powell and McKirdy, 1973; Peters et al., 2005). Their relative concentrations as shown in the cross plot of Pr/ n -C₁₇ vs. Ph/ n -C₁₈ (Figure 5.8) can be used to infer the source of the organic matter as well as paleodepositional conditions of a sedimentary basin (Peters et al., 2005; Makeen et al., 2015c). The plot shows that Maiganga coals, mudstones and shales contain a dominant terrestrial source

input of Type III kerogen, while Yaya-Ngari samples are characterised by mixed organic matter deposited in transitional environment. This indicates a progressive movement towards marine source input.

Terpane and sterane biomarkers distribution on the m/z 191 and 217 chromatogram respectively were also indicative of more terrigenous origin for Gombe Formation samples. A common feature of the m/z 191 chromatograms of saturated hydrocarbon fraction of all the analysed samples (Figure 4.7) is high concentration of the hopanes relative to tricyclic and tetracyclic terpanes as well as steranes (on m/z 217). Thus, a low sterane/hopane ratio generally <1 suggests more terrigenous and/or microbially reworked organic matter source for the Gombe Formation samples (Tissot and Welte, 1984; El-Diasty and Moldowan, 2012). The computed ratios of concentration C_{23}/C_{24} tricyclic terpane (average 2.12) and C_{24} tetracyclic/ C_{26} tricyclic terpane (average 2.14) is high and fall within the range reported for Jurassic to Early Cretaceous non-marine shale described by El-Diasty and Moldowan (2012). Similarly, the cross plot of C_{23}/C_{24} tricyclic terpane versus C_{24} tetracyclic/ C_{26} tricyclic (Figure 5.9) indicate a significant terrigenous source with more marine contribution in Yaya-Ngari compared to Maiganga facies.

Furthermore, chromatogram of m/z 191 reveals presence of oleanane in some of the studied samples from Maiganga (Figure 4.7e and 4.7g). Angiosperms, which are the precursor of oleanane, gained recognition in Late Cretaceous (Grantham et al., 1983; Brooks 1986; Ekweozor and Telnaes, 1990; Peters et al., 2005; Jauro et al., 2007). The presence of oleanane in the studied samples suggests source input of angiosperms of Cretaceous or younger age as reported by Sarki Yandoka et al. (2015a) for the Lamja coals in Yola sub-basin. Murray et al. (1994) suggested that oleanane is best preserved in deltaic rocks influenced by marine waters during early diagenesis, which supports the depositional setting of the studied samples. The high C_{29} norhopane also supports

terrestrial organic matter source whereby the bacterial influence is apparent from the cross plot of Pr/n-C₁₇ vs. Ph/n-C₁₈ (Figure 5.8).

Steranes derived from sterol in higher plant and algae are the second most important group of biomarkers and their concentrations have proved useful in discriminating source input of organic facies (El Diasty and Moldowan, 2012, 2013; Makeen et al., 2015c; Han et al., 2017). The dominating percentages of C₂₇, C₂₈ and C₂₉ steranes on *m/z* 217 would suggest marine, lacustrine and terrestrial sources respectively (Waple and Machilhara, 1991; Peters et al., 2005). Higher amount of C₂₉ααα(20R) steranes, in the studied samples compared to other steranes, in the range of 34.29% to 68.21% (Table 4.4) also supports dominance of terrestrial source with varying marine and lacustrine influences.

The ternary diagram ((Figure 5.10) based on the relative percentages of C₂₇, C₂₈ and C₂₉ ααα(20R) steranes of the analysed samples indicate dominance of terrestrial high plant with planktonic and bacterial influence. This is consistent with cadalene/m(+p) xylenes (cd/xy) concentration ratio in Section 5.4 above and Pr/n-C₁₇ vs. Ph/n-C₁₈ plot (Figure 5.8) which indicates terrestrial type III kerogen for Maiganga, trending to transitional mixed organic matter source input in Yaya-Ngari. The interpretation of organic matter source based on the clustered plot of C₂₇/C₂₉ regular sterane versus pristane/phytane ratio (Figure 5.11) shows a gradual transition from mainly terrigenous source input for Maiganga in the southern area to mixed organic matter for Yaya-Ngari in the northern part of the study location (see Figure 1.1). This is a clear indication of predominance of terrigenous source input in the studied Gombe Formation samples.

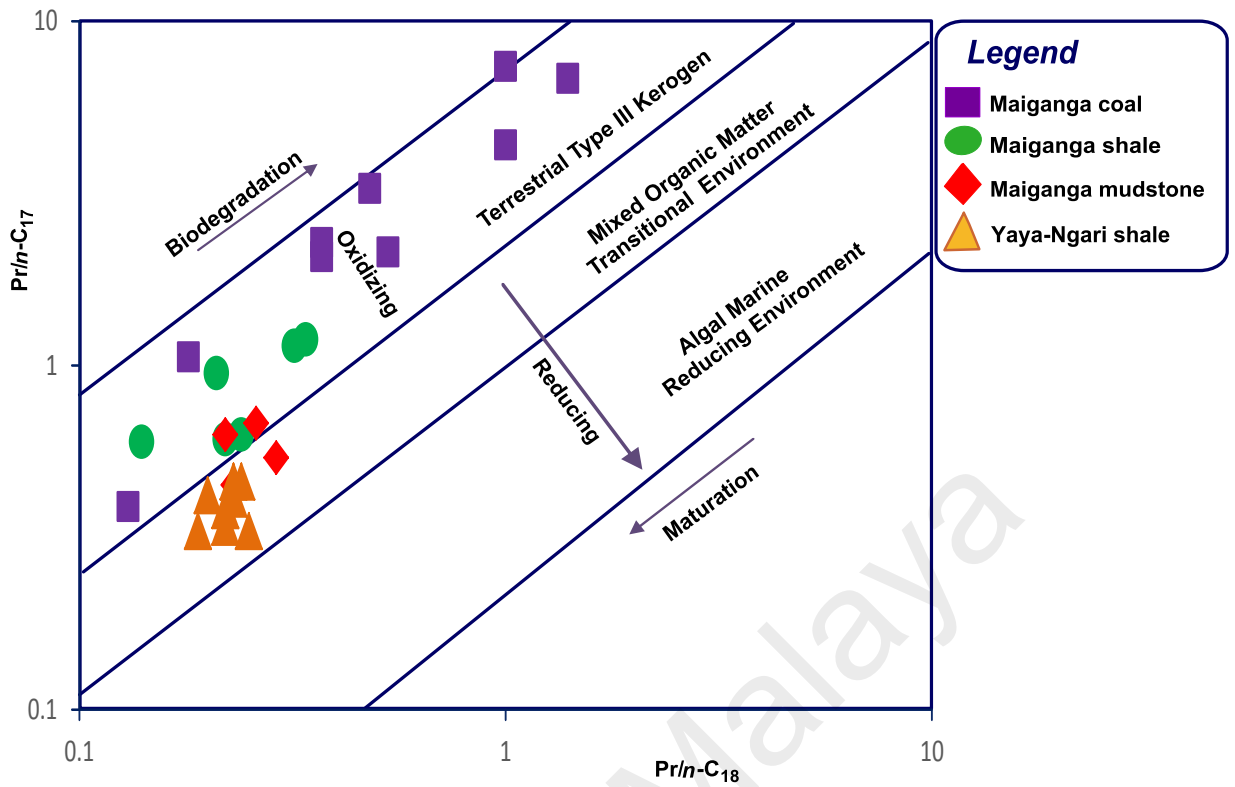


Figure 5.8: The cross plot of $Pr/n-C_{17}$ versus $Pr/n-C_{18}$ showing the organic matter source input for the analysed Maiganga and Yaya-Ngari samples.

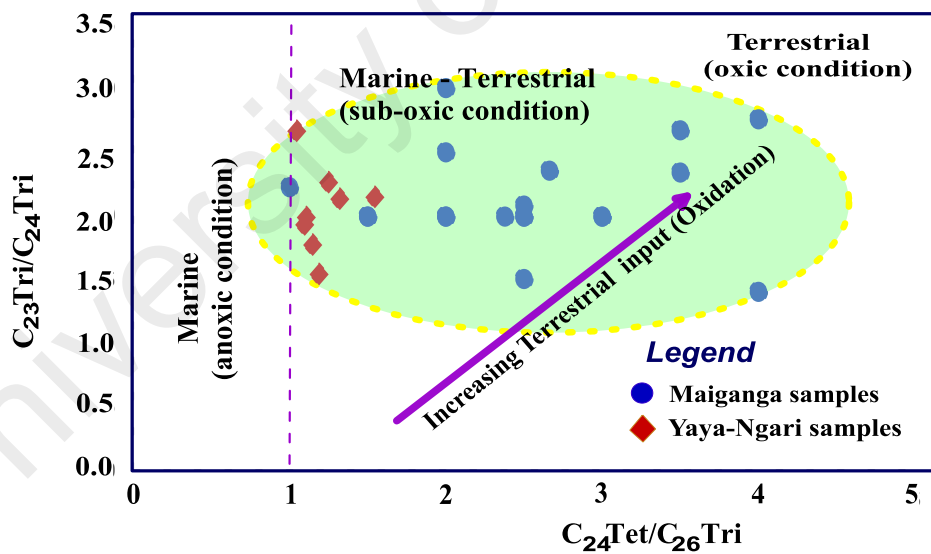


Figure 5.9: The cross plot of C_{23}/C_{24} tricyclic terpane versus C_{24} tetracyclic/ C_{26} tricyclic indicating significant terrigenous source input with more marine contribution in Yaya-Ngari compared to Maiganga facies.

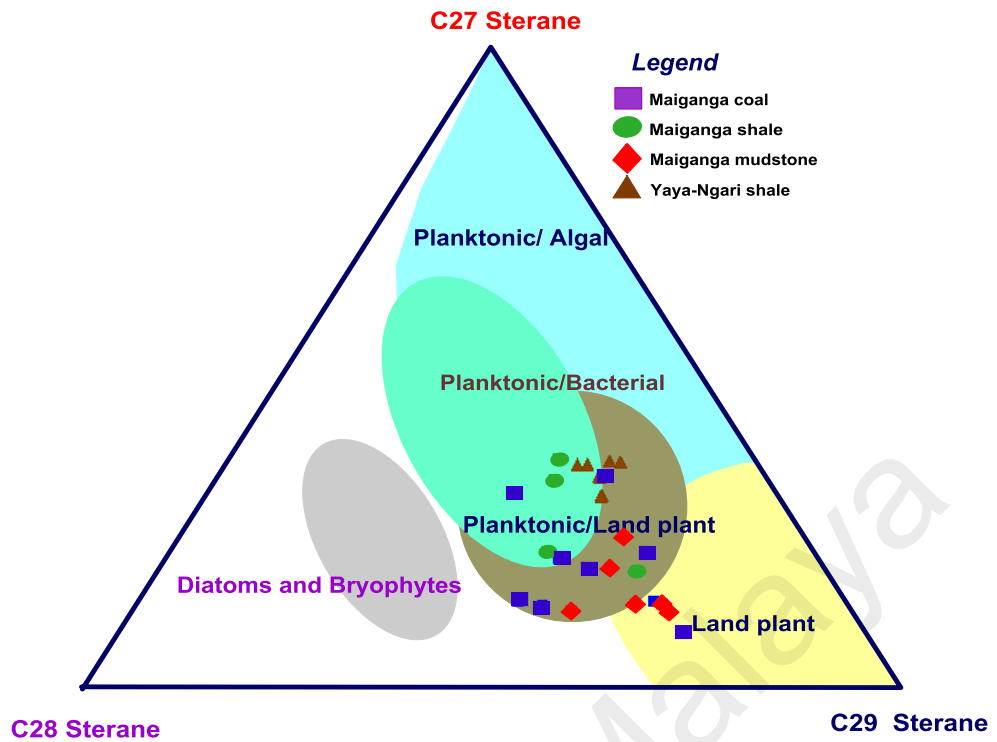


Figure 5.10: Ternary plot of C₂₇, C₂₈ and C₂₉ $\alpha\alpha\alpha(20R)$ regular steranes indicating organic matter source input for the analysed Maiganga and Yaya-Ngari samples.

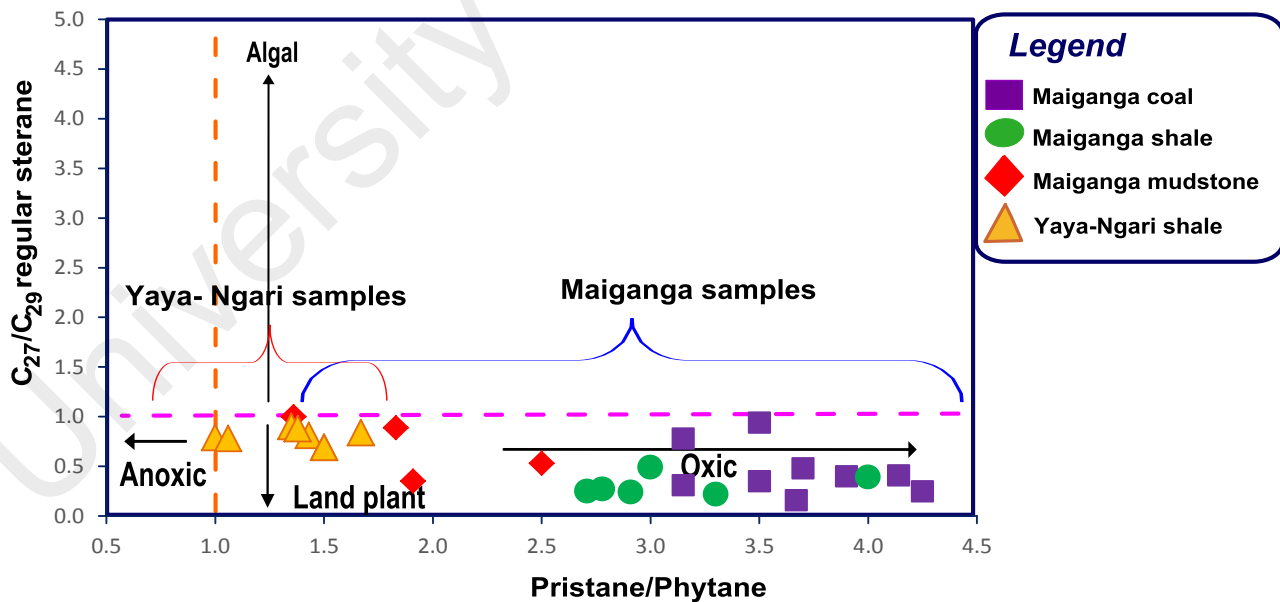


Figure 5.11: The cross plot of C₂₇/C₂₉ regular sterane versus pristane/phytane showing the redox condition during deposition of Maiganga and Yaya-Ngari sediments.

Petrographic studies under reflected white light showed dominance of huminite/vitrinite macerals composed of both gelified (corpohuminite/porigelinite) and ungelified (textinite, ulminite and attrinite) cell walls of higher plant origin. Some of the coals have a lot of ungelified humic groundmass of attrinite, which are occasionally densely packed together as densinite (Figures 4.10a-j). Similarly, the angular, “strand” shapes and high reflecting nature of fusinite, semifusinite, inertodetrinite and funginite are likely remains of forest fire (burnt wood, leaves and roots) that give an indication of a relatively high terrestrial (land plant) source input. This inference is in line with the observation under the UV light showing moderate amount of sporinite, cutinite, resinite, liptodetrinite (Figure 4.10) resulting in the prevalence of C₂₃₊ normal alkane suggesting a higher molecular plant source.

5.6 Paleodepositional environment and preservation condition during sedimentation

Paleodepositional setting and condition of deposition of the analysed Gombe Formation samples were evaluated based on the calculated tissue preservation index (TPI), gelification index (GI) as well as the major and trace elements composition (ICPMS) and GC-MS distributions (e.g. pristane to phytane ratio) of sedimentary facies (e.g. Diessel, 1992, Peters et al., 2005; Singh et al., 2012; Sia and Abdullah, 2012).

Maceral analysis is useful to predict the paleodepositional setting of coal facies. Higher amount of huminite (Table 4.7) especially detrohuminite and textinite in the sample is considered as evidence of plant abundance. On the other hand, moderate amount of inertinite suggests oxidation of the materials. Sia and Abdullah (2012) suggested that the cross plot of TPI versus GI does not in all cases depict the paleodepositional environment. Nevertheless, the studied samples plot in the upper deltaic plain (Figure 5.12) of the Diessel’s diagram. Thus, the analysed Gombe

Formation samples were interpreted to have been sourced from the proximal terrestrial environment characterised by high forest plant materials due to presence of a reasonable amount of detrohuminite and textinite with a sizeable amount of inertodetrinite, fusinite and semi fusinite. These materials are characterised by high degree of gelification of plant tissues in a persistent wet raised bog as evident by the relatively high GI > 1 for all the samples (Diessel, 1992). Moreover, the studied coals show a reasonable percentage of ulminite (2-16%) and porigelinites (2-24%). This indicates a preservation of more plant tissues which are compressed and gelified under wet conditions (Diessel, 1992; Sýkorová et al., 2005). The biochemical gelification process is accelerated by the supply of Ca in the paleomire (see Table 4) based on the positive correlation between the TOC and CaO ($r^2 = 0.81$). Most of the samples are characterised by relatively high tissue preservation index (TPI > 1; Table 4.7) which suggests mild humification of the organic matter within the Gombe Formation. Sia and Abdullah (2012) suggested that moderate humification, as obtainable in the Gombe Formation, is often associated with rapidly subsiding forested raised bog.

According to Pickel et al. (2017) classification of liptinite, 65-75% of yearly forest litter is leaves which are the main precursor of cuticles. Following this observation, the reasonably moderate amount of liptinite macerals such as cutinite, sporinite and resinite in the Gombe Formation sample is consistent with the forested raised bog. Resinite is believed to contribute to early liquid hydrocarbon generation especially at diagenetic stage (Powell et al., 1978). In actual sense, the studied samples have varied amount of resinite (2-12%). It is good to note that the maximum values were recorded within seam A₃ (12%) and seam B (8%). This suggests the possibility of early hydrocarbon generation in the two seams. Therefore, based on the moderately varied range of TPI (0.33-5.14), a gradual change in the vegetation type together with subsidence rate in the Gombe Formation paleomire can be inferred. On the other hand,

the low to moderate values of GI (1.32-8.13) suggests a moderate stratified water table during the deposition of the coals which enhances gelification of plant tissues.

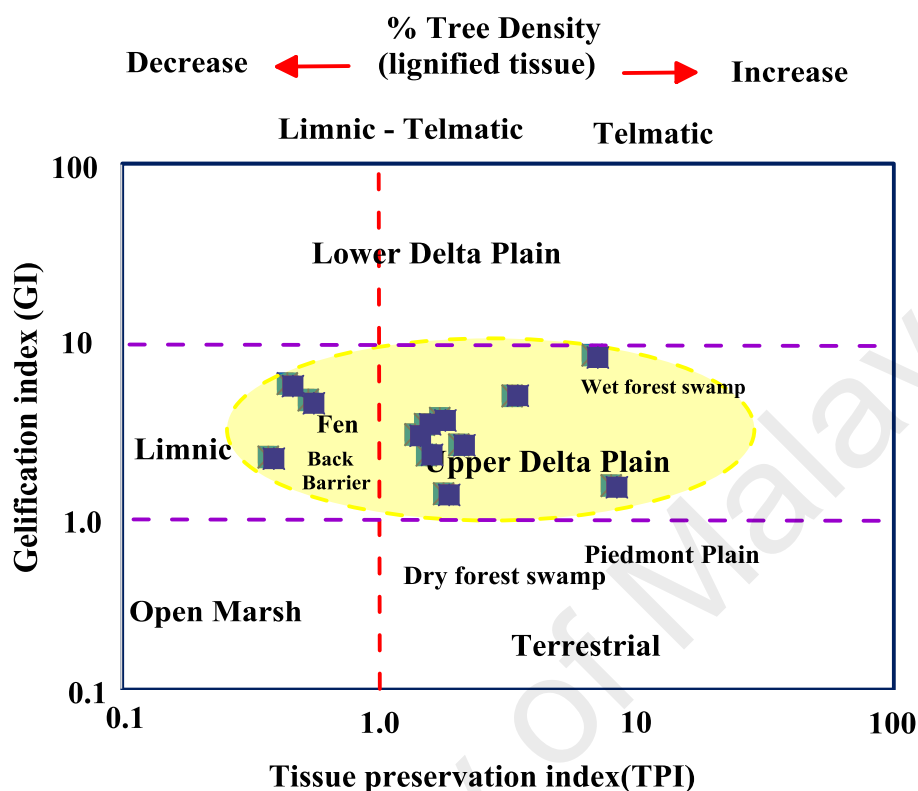


Figure 5.12: Bivariate plot of GI versus TPI showing the paleodepositional condition of Gombe Formation (modified after Diessel, 1986; Kalkreuth and Leckie, 1989; Wan Hasiyah, 2002).

Paleodepositional (redox) condition of an area can be evaluated based on pristane to phytane ratio from m/z 85 chromatograms and homohopanes distribution from m/z 191 as well as trace element composition (Peters et al., 2005). Anoxic depositional conditions are indicated by low Pr/Ph ratio of < 0.6 , from 0.6 to 3 is typical for sub-oxic and greater than 3 for oxic environments (Peters and Moldowan, 1993). The studied coal samples show a relatively high concentration of pristane compared to phytane (Figure 4.6b, 4.6d and 4.6f) resulting in the Pr/Ph > 3.00 (Table 4.3) which supports deposition under oxic depositional condition in a terrestrial and mixed (transitional) environment. The values of Pr/Ph ratio of the mudstones and shale indicate sub-oxic to oxic conditions. The moderate pristane to phytane ratio (from 1.0 to

1.67) (Table 4.3) suggests suboxic depositional setting for Yaya-Ngari samples. This is in accordance with the cluster plot of C_{27}/C_{29} regular sterane versus Pr/Ph (Figure 5.11) and m/z 191 GC-MS distributions of the C_{31} to C_{35} homohopanes (Figure 4.7a and 4.7c), which showed a stair-step pattern. This homohopane pattern, associated with suboxic depositional setting, was also observed in Yola sub-basin which is the second bifurcated arm of the Gongola sub-basin (Peters et al., 2005; Sarki Yandoka et al., 2015a; Makeen et al., 2015c).

In support, the cross plot of Pr/ n - C_{17} vs. Ph/ n - C_{18} (Figure 5.8) indicates a deposition of Type III kerogen within an oxidizing environment in Maiganga and mixed organic matter source input in Yaya-Ngari area within a suboxic conditions. The high ratios of C_{23}/C_{24} tricyclic terpane (1.4-3) and C_{24} tetracyclic/ C_{26} tricyclic terpane (1-4) observed in this study favours gradual transition from mainly terrestrial sourced organic matter deposited under oxic to suboxic conditions in Maiganga to basically suboxic depositional conditions in Yaya-Ngari (Table 4.3). This is illustrated based on the plot C_{23}/C_{24} tricyclic terpane versus C_{24} tetracyclic/ C_{26} tricyclic (Figure 5.9) as described by El-Diasty and Moldowan (2012) showing predominately terrestrial organic facies with varying bacterial and algal contributions.

The $C_{31}R/C_{30}$ hopane ratio is a good molecular tool to differentiate marine from lacustrine environmental influence in the source input of shales and mudstones (since low rank coals are known to show high values). Marine depositional setting is characterised by $C_{31}R/C_{30}$ hopane ratio above 0.25 while lacustrine environment is known to have value below 0.25 (Peters et al., 2005). In this study, a range between 0.36 and 2.11 (Table 4.3) was obtained which suggests a marginal marine (delta) environment. It can thus be inferred that the area under study has marine influence. This observation is consistent with the depositional setting of the lateral equivalence of Gombe Formation in the Chad (Bornu) basin as reported by Ayinla et al., 2013.

The GC-MS result of saturated hydrocarbon is corroborated by the aromatic hydrocarbon fraction. Observed low concentration of dibenzothiophenes compared to aromatic phenanthrenes (m/z 184 and 178) resulted in DBT/P ratio of <1 (Figure 4.8 and Table 4.4). Thus, Hughes et al., (1995) suggest that the cross plot of DBT/P versus Pr/Ph ratio is a powerful way of discriminating source rock depositional environment. This plot indicates a marginal marine environment mainly deltaic setting (Maiganga) associated marine shale at Yaya-Ngari (Figure 5.13) for the analysed sediments. Similarly, Holba, et al. (2003) observed that deltaic settings are usually characterised by high concentration of hopane compared to sterane resulting in hopane/(hopane+sterane) ratio > 0.7 . Such a relationship exists between hopane and steranes in the studied sample is consistent with deltaic depositional environment.

Moreover, the geochemistry of major oxides and trace elements in the analysed sediments are used to interpret the paleodepositional environment and condition during sedimentation of the Gombe Formation. Table 4.9 shows a relatively high abundance of SiO_2 and TiO_2 in relation to other major oxides which also establishes a terrestrial source for the upper deltaic plain sediments in the Gombe Formation. CaO concentration shows a positive correlation ($r^2 = 0.81$) to TOC contents (see Appendix C1) suggesting a gradual increase in supply from calcium-rich environment (e.g. marine) with increase in organic matter. Considering this fact, together with low concentration of CaO (0.08–1.20), a delta plain characterised with some marine influence is deduced for the Gongola sub-basin. This amount of CaO in the samples can be attributed to the occurrence of detrital carbonates derived from either geogenic, biogenic or pedogenic carbonates of the Gongola sub-basin. The positive correlation between TOC and CaO points to possibility of biogenic carbonates within the deltaic setting.

The concentrations of trace elements such as V, Ni, U, Th, Mo, Co, Sr and Ba have also proved useful in determining the redox condition during sedimentation (Peters

et al., 2005; Adegoke et al., 2014; Makeen et al., 2015a). Vanadium (V) and nickel (Ni) are important metals usually incorporated with organic matter during early diagenesis stage and are useful indicators of redox conditions during sedimentation (Peters et al., 2005; Galarraga et al., 2008). Based on the V/Ni ratio, Galarraga et al., (2008), distinguish depositional environment into reducing ($V/Ni > 3$) and suboxic environment (V/Ni from 1.9 to 3). In this study, the V/Ni ratios is relatively high for the analysed Yaya-Ngari shale (from 3.24 to 3.58; average 3.38) and Maiganga mudstones (from 2.50 to 4.65; average of 3.46) compared to the coal facies (from 0.56 to 3.33; average of 2.02). This is an indication of terrestrial source organic matter deposited under suboxic to oxic condition in a deltaic setting as shown by the bivariate plot of vanadium (V) versus nickel (Ni) (Figure 5.14). Similarly, the low $V/(V + Ni)$ ratio ranging from 0.36 to 0.82 with average of 0.69 observed for these samples fall within the range reported for the dysoxic Chad (Bornu) basin by Adegoke et al. (2014).

The relatively low total sulfur content coupled with moderate $V/(V + Ni)$ ratio as shown on the bivariate plot (Figure 5.15) further supports suboxic to oxic condition during the sedimentation of the organic matter. Drawing inference from the works of Hakimi et al. (2017), the ratio of major elements Fe/Al which is generally < 0.5 (especially for the Gombe mudstones and shales; 0.07-0.38) further supports the suboxic to oxic conditions for the sediment. This observation is consistent with the earlier report based on biomarker studies for the area (Ayinla et al., 2017a).

Uranium (U) and thorium (Th) form another set of redox-sensitive elements, which are important in interpreting paleodepositional conditions during sedimentation (Calvert and Pedersen, 1993; Tribovillard et al., 2005). Based on the concentration of U, Pattan and Pearce (2009), differentiate reducing conditions ($U > 10$ ppm) from oxic conditions ($U > 4$ ppm or less). The studied Gombe Formation samples (coal and

mudstones) have low to moderate U concentration (0.10-8.40 ppm) which is an indication of suboxic to oxic conditions during sedimentation (Table 4.10).

The total organic matter content and U concentration in the Gombe Formation show a negative correlation ($r^2 = 0.89$; Figure 5.16), indicating the removal of the U by the organic matter (see Appendix C2) (Mangini, 1978; Pattan and Pearce, 2009). Authigenic U enrichment (5-8 ppm) in Atlantic sediments during the last glacial stage (12-24 ka) is associated with a process caused by changes in sediment accumulation rate and maxima sediments. Observed U concentration in both organic matter rich and poor sediment ranging from 1-7ppm indicates that there is major change in sediment accumulation rate. Thus, the possibility of post depositional diagenesis causing U enrichment is possible. Since, there is usually a contrasting relationship between U and Th, the U/Th ratio is useful in evaluating paleo-redox conditions. High U/Th ratio suggests deposition under anoxic conditions, while low ratio points to suboxic and oxic conditions (Pattan and Pearce, 2009, Wang et al., 2016). The analysed samples are characterised by a relatively low U/Th ratio (0.10-0.42). Thus, it suggests deposition under moderate oxygen conditions.

Wang et al. (2016) observed that Ce concentration and TOC content usually show negative correlation in oxidizing environment (suboxic to oxic) and positive correlation in reducing environment (anoxic). Therefore, suboxic to oxic paleodepositional conditions is inferred for the studied Gombe Formation coals and mudstones based on the negative correlation between TOC contents and Ce concentration ($r^2 = 0.89$; Appendix C2).

Molybdenum (Mo) concentration is one of the key drivers controlling the paleoredox conditions of ocean and sediments. Thus, it has the potential to serve as a proxy for depositional conditions (Ruebsam et al., 2017). Gradual weathering and erosion of terrigenous materials account for about 90% of Mo in the oceans, while other

sources such as low temperature hydrothermal source contribute < 10% (McManus et al., 2002 and 2006). Research has shown that there exists a direct relationship between high Mo concentration and increasing anoxic conditions (Alberdi-Genolet and Tocco, 1999). Concentrations of trace element Mo from 5 to 40 ppm was reported to indicate an anoxic condition (Piper, 1994; Crusius et al., 1996), while below 5 has been reported to indicate condition of suboxic to oxic settings (Adegoke et al., 2014). The analysed Gombe Formation samples have relatively low Mo concentration (<5 ppm) which indicates prevalence of oxic conditions in the area.

Cobalt (Co) concentration is a complementary paleo-redox indicator which is preferentially enriched under oxic conditions compared to Ni (Jones and Manning, 1994). Oxic conditions have Ni/Co ratio of < 5, while > 5 suggests suboxic conditions (Jones and Manning, 1994; Adegoke et al., 2014). In this case, based on the relatively low Ni/Co ratio (0.95-4.19) (Table 4.10), the analysed sediments were interpreted to have been deposited under oxic to slightly suboxic conditions of deposition.

The concentration of chromium (Cr) and vanadium (V) can be used as indicators of the paleoredox condition during deposition of sediments (Jones and Manning, 1994). Oxic conditions are higher in concentration of Cr compared to V. Thus, Jones and Manning, (1994) suggested that the V/Cr ratio above 2 is an indication of suboxic conditions which was not recorded for studied sample (V/Cr ratio < 1, Table 4.10). Therefore, the general low V/Cr ratio for the sample further supports predominance of oxic conditions for the sediments during sedimentation. According to Table 4.9 and 4.10 (see Appendix C2 for correlation Table), the Cr in the analysed samples shows a strong positive correlation to Al₂O₃ ($r^2 = 0.96$) and TiO₂ ($r^2 = 0.86$) but negative correlation to the organic matter content ($r^2 = 0.75$). This suggests inorganic source

associated with clay mineral rather than organic source for Cr in the Gombe Formation coals.

Although, series of physical and chemical process determine organic matter preservation in nature, it is also known to be controlled by the rate of sedimentation, clay mineral contents, and water column oxygenation levels (Zonneveld et al., 2010). Concentration of Strontium (Sr) and Barium (Ba) are key indicators of paleo-salinity (Wang, 1996; Makeen et al., 2015a). High Sr/Ba ratio corresponds to high salinity, whereas a low ratio suggests a low salinity (Deng and Qian, 1993; Makeen et al., 2015a). The studied samples have a relatively low Sr/Ba ratio indicating a relatively low saline water influence during deposition of the Gongola sub-basin (Maiganga and Yaya-Ngari) sediment. This is supported by the cross plot of Sr/Ba versus V/Ni ratios (Figure 5.17).

Additionally, the depositional environment of sediments dictates the quality and quantity of organic matter preservation. The studied sediments were deposited in a deltaic environment, (Figure 5.12 and Figure 5.13), under suboxic-oxic conditions. The high terrestrial source input of forest material with some marine and lacustrine influence occurs at a high rate, thus promoting higher input of land plants with reasonable marine and lacustrine inputs. This is supported by maceral analysis indicating predominance of huminite (average 58%) and significant contributions from liptinites (21%) and inertinites (20%) maceral during deposition of the Gombe Formation sedimentary facies (Ayinla et al., 2017b).

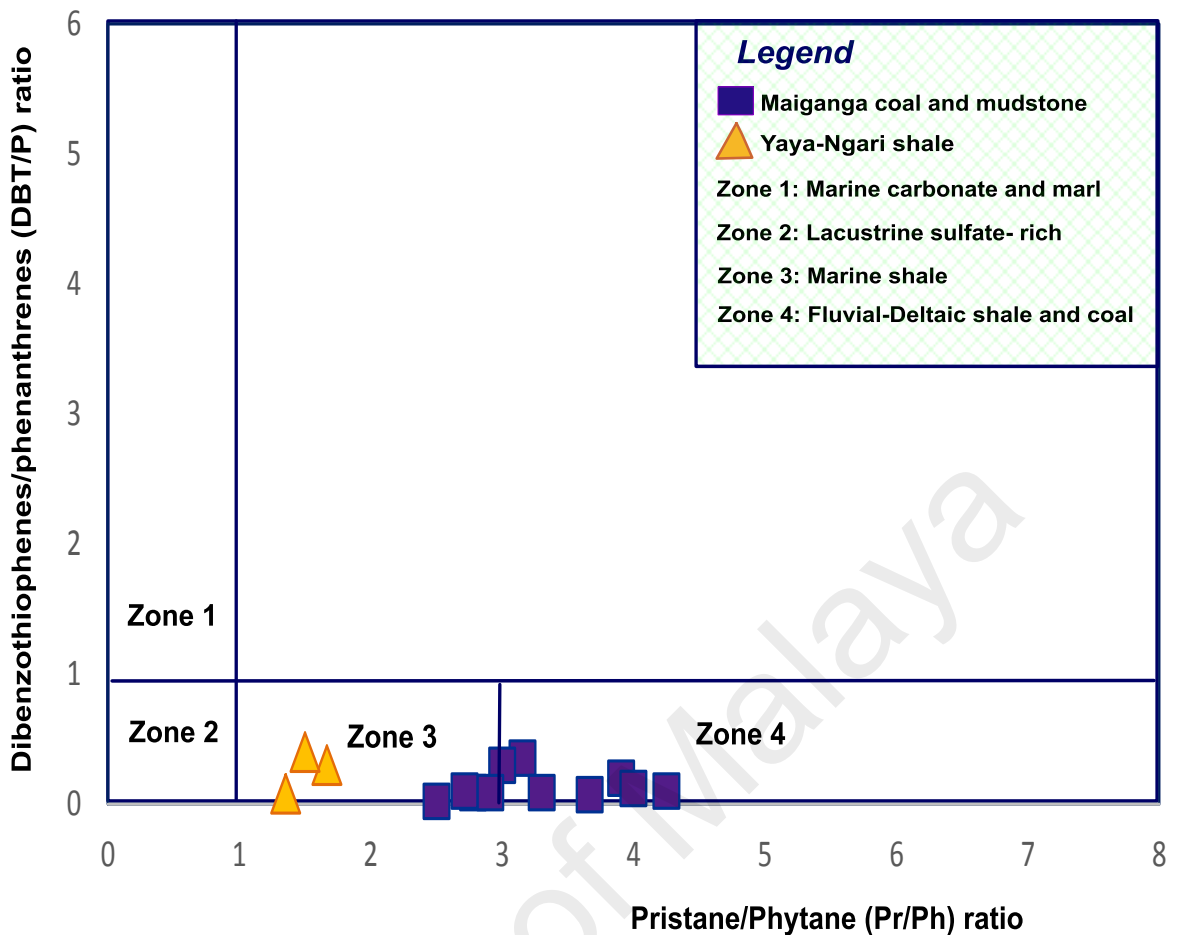


Figure 5.13: Cross plot of aromatic Dibenzo thiophenes/phenanthrenes (DBT/P) ratio (m/z 184 and 178) versus Pr/Ph ratio for discriminating the source rock depositional environment (after Hughes et al., 1995).

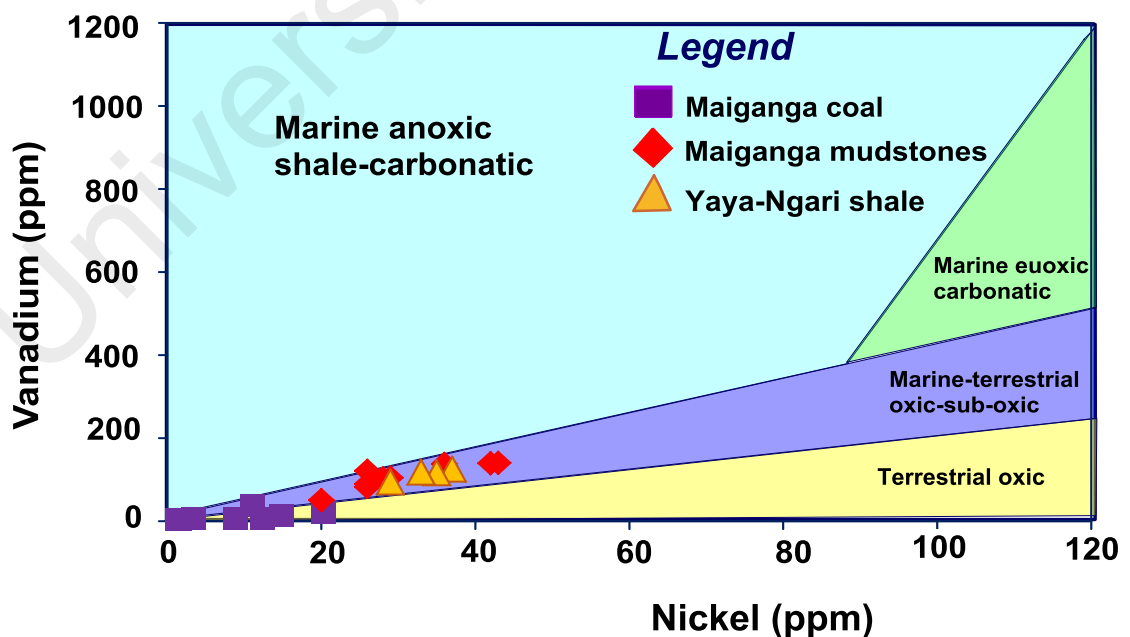


Figure 5.14: Bivariate plot of vanadium versus nickel showing the suboxic to oxic depositional condition for the analysed samples (adapted after Galarraga et al., 2008).

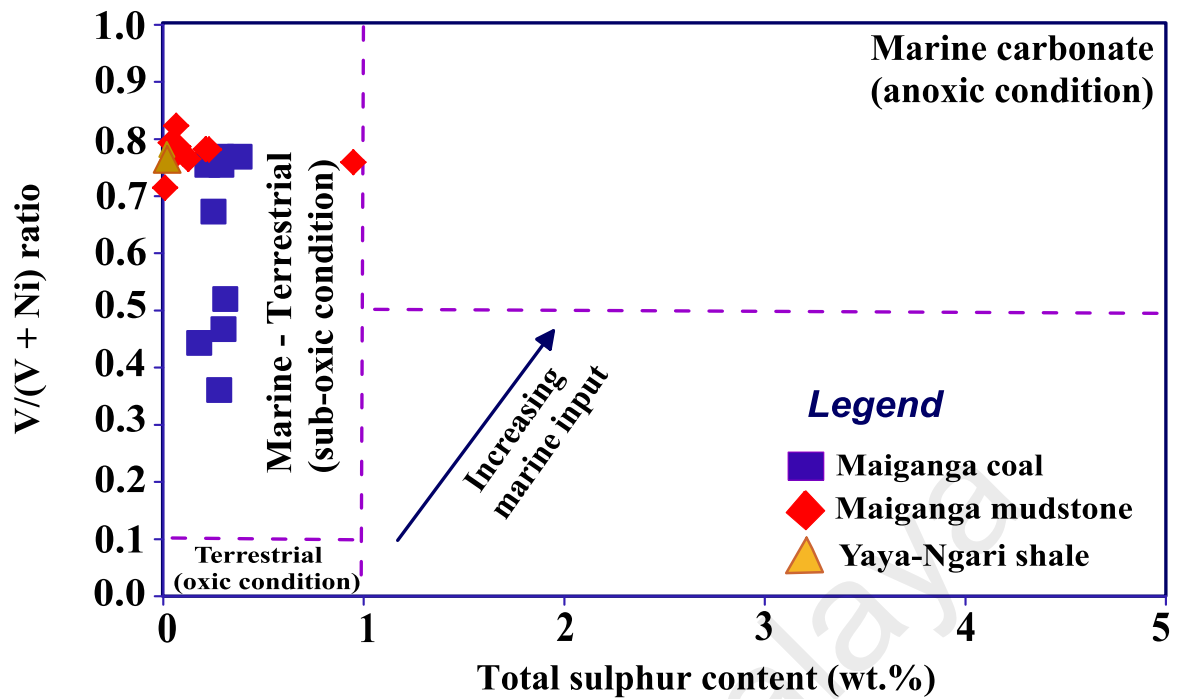


Figure 5.15: Trace element ratios of V/(V + Ni) versus total sulfur content (wt.%) of the analysed samples (adapted after Hakimi et al., 2017).

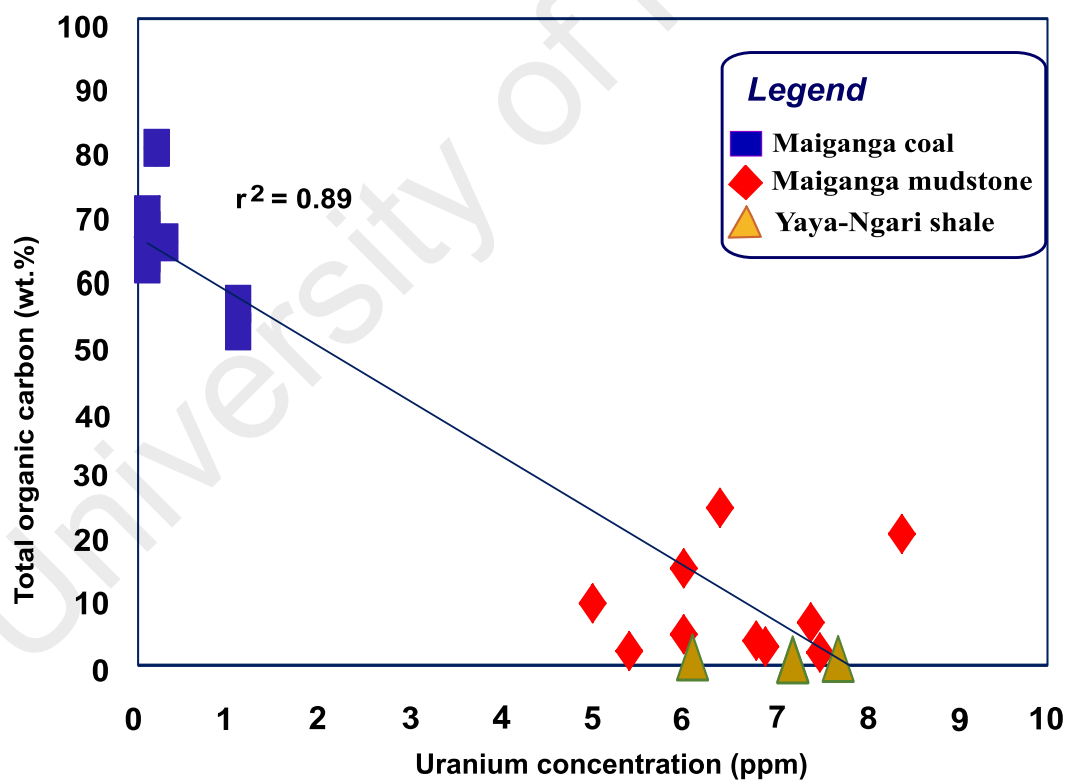


Figure 5.16: Bivariate plot showing the negative correlation between the total organic carbon content and uranium concentration during sedimentation of the analysed samples.

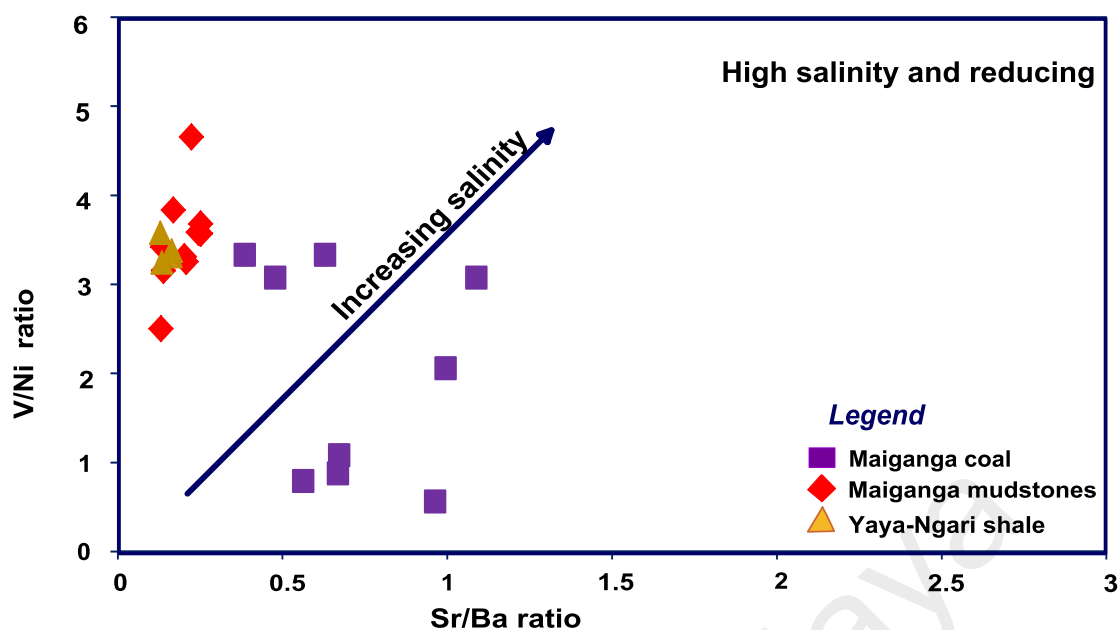


Figure 5.17: Bivariate plot of V/Ni ratio versus Sr/Ba ratio for the analysed sediments of the Gombe Formation (adapted after Jia et al., 2013).

5.7 Thermal maturity

Integration of organic petrography results, T_{max} ($^{\circ}C$), the production index (PI) and biomarker parameters such as plot of Pr/n-C₁₇ versus Ph/n-C₁₈, C₃₂ homohopane ratio (22S/22S+22R) and sterane ratio C₂₉ $\beta\beta/(\beta\beta+\alpha\alpha)$ can be used to infer, reliably, the source rock maturity (Tissot and Welte, 1984; Bordenave et al., 1993; Peters et al., 2005). The vitrinite/huminite reflectance (%Ro) obtained using oil immersion is relatively low for Maiganga (an average of 0.35 %Ro) compared to Yaya-Ngari (an average of 0.76 %Ro) (Table 4.1). The general distribution of the vitrinite reflectance in the study area as shown in Figure 5.18 indicates a relatively high thermal maturity corresponding to the oil generation window for the Yaya-Ngari shales but immature or pre-oil generation window for Maiganga (coals, shale and mudstones) (Table 4.1). Analysed sedimentary facies tends to show gradual increase in thermal maturity from Maiganga to Yaya-Ngari in the northeastern direction (Figure 5.18) Observed thermal maturity difference in this area can be related to series of folding and faulting due to igneous activity which affected the Cretaceous Gombe Formation (Ayinla et al., 2017a,

2017b). This interpretation is supported by the T_{max} , ($^{\circ}C$) results which is $>435^{\circ}C$ for Yaya-Ngari and generally $<435^{\circ}C$ in Maiganga, whilst the mudstone above seam A₂ with T_{max} , of $436^{\circ}C$ and huminite reflectance of 0.38 % R_o (Figure 5.5).

The cross plot of Pr/n-C₁₇ vs. Ph/n-C₁₈ (Figure 5.8) reveals that the analysed coal samples are of low thermal maturity typical of immature Type III kerogen while the non-coaly samples show a fairly high degree of thermal maturity especially at Yaya-Ngari. Table 4.1 shows the stage of oil generation based on the ratio of S1 to S1+S2 which is referred to as Production Index (PI). It is generally low in Maiganga (<0.13) compared to moderate values in Yaya-Ngari (0.29-0.41) pointing to mature organic matter as suggested by Peters and Cassa (1994). The EOM results also revealed that NSO compounds account for significant percentage of the bitumen (28.0-96.7 wt. %, of EOM) compared to the aliphatic and aromatic hydrocarbon which is consistent with low thermal maturity of the samples especially for the Maiganga coal (Figure 5.19; Table 4.2).

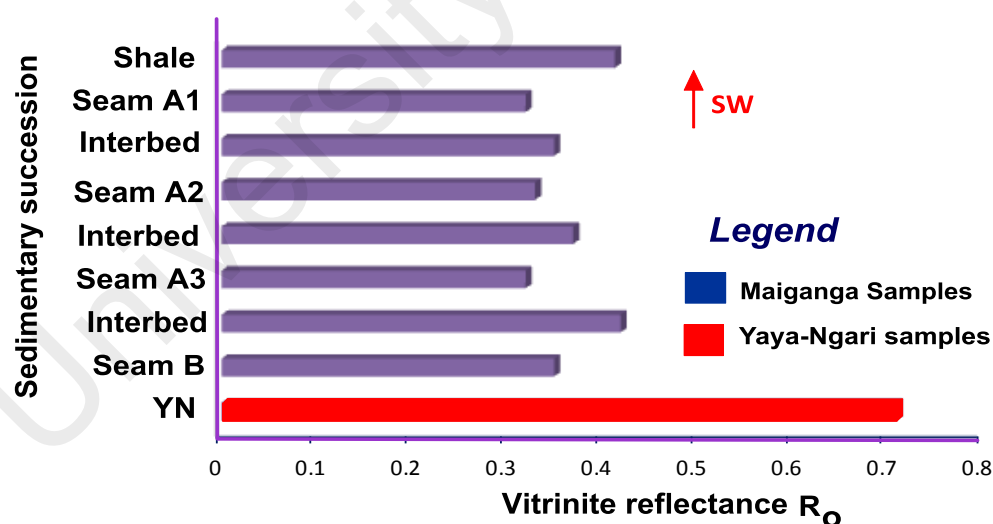


Figure 5.18: The bar plot of the analysed sedimentary succession versus average vitrinite reflectance showing the thermal maturity and maturation direction of organic matter in Maiganga and Yaya-Ngari areas.

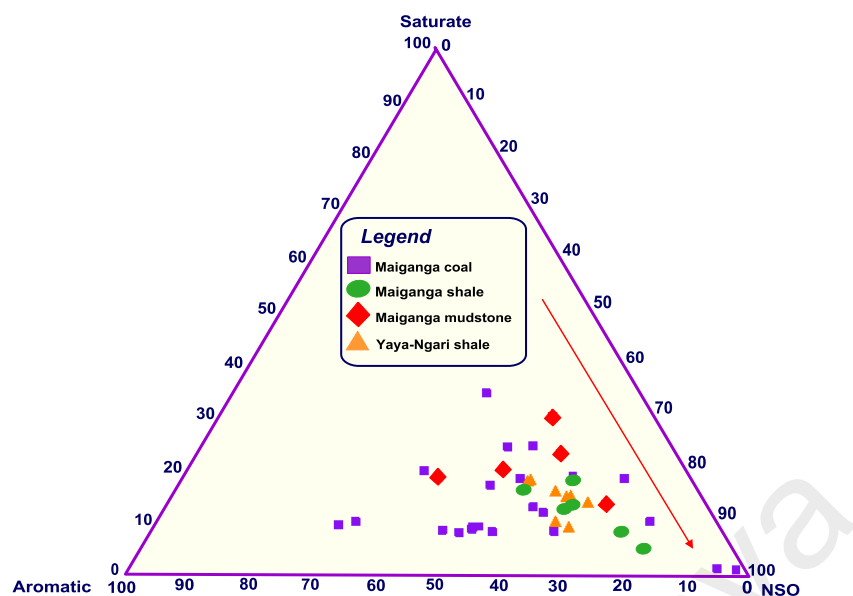


Figure 5.19: Ternary plot of saturated, aromatic and nitrogen-sulphur-oxygen compounds showing their relative concentration in the analysed Maiganga and Yaya-Ngari samples.

Apart from terpanes and steranes parameters, other biomarker signatures can be analysed to receive additional and dependable information about the thermal maturity of sedimentary basins. An example being carbon preference index (CPI) which is a measure of odd to even *n*-paraffin in the range of *n*-C₂₄ to *n*-C₃₄ (after Bray and Evans, 1961). Values of CPI significantly above one reflect immaturity. In this case, CPI > 1.25 characterised immature Maiganga samples (Table 4.3) whereas Yaya-Ngari samples have CPI of approximately 1 suggesting more mature organic matters (Peters and Moldowan, 1993).

A high degree of specificity of C₃₂ 22S/(22S + 22R) homohopane ratio in establishing thermal maturity, especially for immature to early oil generation window, has gained prominence among geochemist over the years (e.g. Peters et al., 2005; Hakimi and Abdullah, 2013). At low thermal maturity, chromatogram of *m/z* 191 displays predominance of 22R over the 22S epimers of the C₃₂ to C₃₅ homohopanes (Peters et al., 2005; Ayinla et al., 2017a). Maiganga facies show this characteristic (Figure 4.6e and 4.6g) which supports the immature state of the analysed coal samples.

On the other hand, the samples from Yaya-Ngari show a cascading pattern of the homohopanes displaying a relative dominance of the “S” over the “R” epimers. This indicates a moderate degree of thermal maturity.

The C_{32} 22S/(22S + 22R) homohopane ratio has values between 0.0 to 0.6 with increasing thermal maturity; below 0.50 to 0.54. This corresponds to just the beginning of “oil window”, while 0.57 to 0.62 implies “oil window”. In this study, the value of C_{32} 22S/(22S + 22R) homohopane ratio is generally <0.51 for Maiganga samples (Table 4.3, Figure 5.20) indicating pre-oil generation window, which trends to oil window in Yaya-Ngari (0.52-0.58) as suggested by Seifert and Moldowan (1986).

The C_{29} sterane ratio that is expressed as 20S/(20S+20R) can provide a complementary parameter to determine maturity, which can be used alongside C_{32} 22S/(C_{32} 22S + C_{32} 22R) homohopane ratio for better accuracy. It starts from zero and attains 0.52-0.55 (Seifert and Moldowan, 1986; Peters and Moldowan, 1993). In the studied Maiganga samples, 20S/(20S+20R) ratio is <0.50 which is a pointer to low thermal maturity. In the case of Yaya-Ngari, the samples show trends of early maturity reaching a maximum value of 0.50. This inference is supported by the C_{29} $\beta\beta/(\beta\beta+\alpha\alpha)$ sterane ratio (Table 4.3) as well as cross plot of 20S/(20S+20R) steranes versus C_{32} 22S/(22S+22R) homohopanes (Figure 5.20) that indicates immature source rock extract and early oil window for Maiganga and Yaya-Ngari respectively confirming former results.

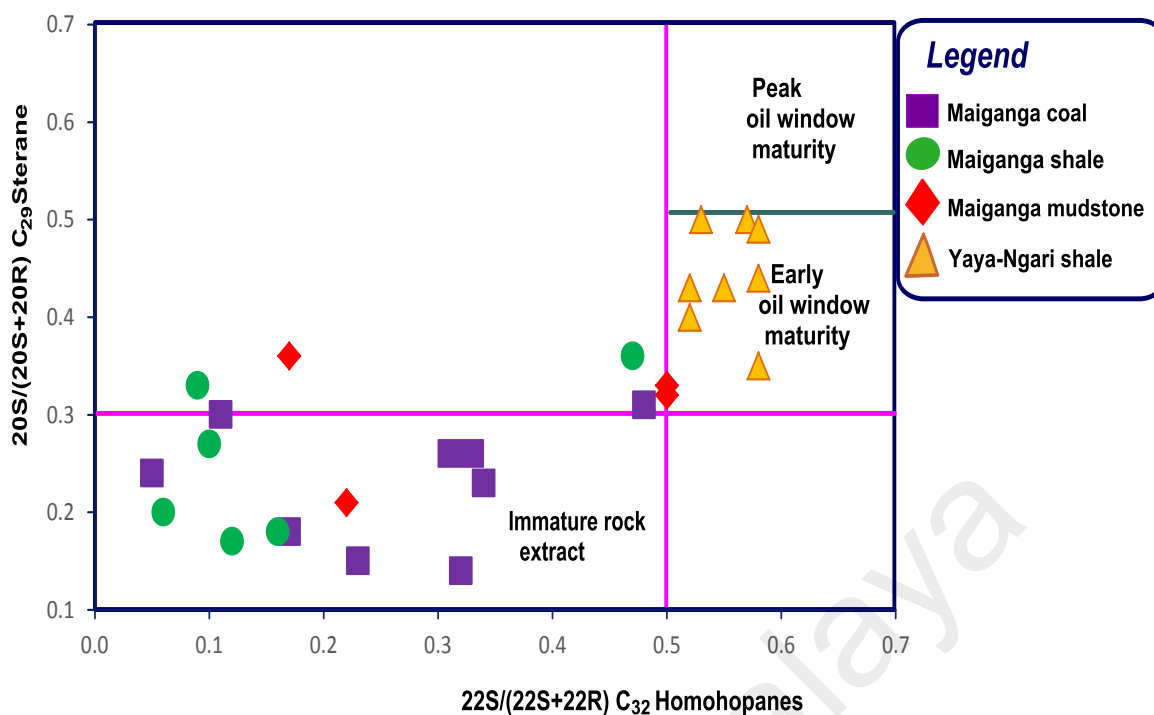


Figure 5.20: The cross plot of 20S/(20S+20R) C₂₉ steranes versus 22S/(22S+22R) C₃₂ homohopanes showing the thermal maturity of the organic matter in the analysed Maiganga and Yaya-Ngari samples.

5.8 Hydrocarbons generation potential

Quantity, quality, vertical and lateral extents of organic matter (OM) as well as thermal maturity are the crucial factors in determining a petroleum source rock potential. The hydrocarbon potential of the organic matter in Maiganga and Yaya-Ngari was assessed on the basis of pyrolysis (Py-GC and SRA), bitumen extraction and petrographic analysis.

Evaluation of total organic carbon content (TOC in wt.%) gives a measure of the sedimentary source bed richness for hydrocarbon generation (Peters and Cassa, 1994; Peters et al., 2005; Ayinla et al., 2017a). TOC values (wt. %) are categorized as excellent (>4), very good (2-4), good (1-2), fair (0.5-1) and poor (< 0.5) for hydrocarbon generation (Peters and Cassa, 1994). As expected for coals, the TOC results indicate excellent for Maiganga coals (>50.3 wt.%) compared to very good to excellent for shale (> 3.7wt.%) and mudstones (from 2.0 to 6.7 wt.%), while Yaya-Ngari shale has fair to good quantity (from 0.8 to 1.3 wt.%). High TOC values for coal

is in correlation with the high organic matter content usually associated with coal, especially seam B which is deeper, thicker and laterally continuous compared to other three seams (A₁, A₂ and A₃). Thus, seam B is expected to be more commercially viable for hydrocarbon generation compared to A₁ and A₂. The high TOC is corroborated by the hydrocarbon yield (S₂) indicating excellent source rock generative potential for the coal samples, fair to excellent for shale, poor to good for mudstones and poor for Yaya-Ngari shales shown on the cross plots of S₂ versus TOC (Figure 5.2).

The content of bitumen and hydrocarbons indicate excellent hydrocarbon potential for Maiganga coal (>4000 ppm), good to excellent for mudstones and shale with >1000 ppm EOM), However, Yaya-Ngari samples showed a poor to fair potential (Table 4.2). This is confirmed by the hydrocarbon contents which reveal an excellent potential for the coal (>2400 ppm), fair to excellent for Maiganga shale and mudstones (>300 ppm) but poor to fair for the Maiganga siltstone and Yaya-Ngari samples (<500 ppm). Data from Table 4.2 along with ternary plot (Figure 5.19) indicate predominance of aromatic over aliphatic hydrocarbons which are consistent with kerogen type.

Based on HI, the Maiganga coal can be classified as being capable of generating gas/oil (> 200 mg HC/g TOC) at higher maturity (Figure 5.5). The Maiganga mudstone and shale showed gas generation potential (< 200 mg HC/g TOC), whereas Yaya-Ngari shales do not possess hydrocarbons generation potential (Figure 5.5). This is evident and consistent with the observed Type III to Type III/II kerogen for Maiganga and Type IV for Yaya-Ngari from the Py-GC analysis (see section 5.4.2 above).

Wilkins and George (2002) suggested that presence of liptinitic macerals such as cutinite, sporite and resinite are indication of oil-prone Type II kerogen associated with hydrocarbon generation. This is moreso, when the liptinite maceral composition attains a threshold of 20% while oil stains are associated with some of the observed macerals such as resinites (Figure 4.10a; Appendix A2). All these are in favour of mixed gas and

oil potential with predominance of gas and limited amount of liquid hydrocarbon within Gongola sub-basin.

5.9 Bulk kinetics and predictions for hydrocarbon generation

The bulk kinetic of petroleum generation of a sample as reflected by the frequency factor and distribution of activation energy gives a picture of the OM composition (Dieckmann, 2005; Hakimi et al., 2015). In this case, observed overall activation energy distributions ranging from 40–70 kcal/mol, with related frequency factors of $1.9953\text{E}+13/\text{s}$ to $3.6010\text{E}+15/\text{s}$ (Figure 5.21, Table 4.8) is a clear indication of heterogeneous organic matter constituents often associated with terrigenous source input of the analysed facies (Schenk et al., 1997; Petersen and Rosenberg, 2000; Abbasi et al. 2016). Furthermore, the petroleum generation temperature and timing predictions were made based on the derived kinetic parameters. Computed results were based on a constant geological heating rate of $3.3\text{ }^{\circ}\text{C}/\text{My}$ while determining the bulk petroleum generation temperature and their corresponding transformation ratio (TR). This is in line with the work of Hakimi et al. (2015) as well as Dieckmann (2005) giving an average geological heating rate of $3\text{--}5\text{ }^{\circ}\text{C}/\text{My}$ for a typical sedimentary basin.

The relationship between temperature and transformation ratio of the organic facies in the analysed samples as well as the onset and peak generation (geol. T_{max}) temperatures is as presented in Table 4.8. This is used in predicting petroleum generation temperature of the analysed Upper Cretaceous coal in terms of onset (10% TR) and peak generation temperatures (Table 4.8) which reflect the temperatures at which kerogen conversion occurs. Based on this study, the onset of bulk petroleum generation is expected at a lower temperature from $116\text{--}134\text{ }^{\circ}\text{C}$ corresponding to $0.68\text{--}0.79\text{Ro}\%$, while the main phase of the generation would occur around $139\text{ to }155\text{ }^{\circ}\text{C}$ ($0.84\text{--}1.04\text{Ro}\%$). Hence, the studied coal samples have not entered the predicted oil

generation window for the expulsion of its hydrocarbon. Varied range in the generation temperature observed in this study (see Table 4.8) typify heterogeneous gas/oil prone Type III/II kerogen in Maiganga as indicated by pyrolysis HI as well as Py-GC reported by previous researchers (e.g. Onoduku et al., 2013; Ayinla et al., 2017a, 2017b). Thus, it can be inferred from the Table 4.8 that the analysed samples attain a reasonable transformation ratio at about 50 %.

University of Malaya

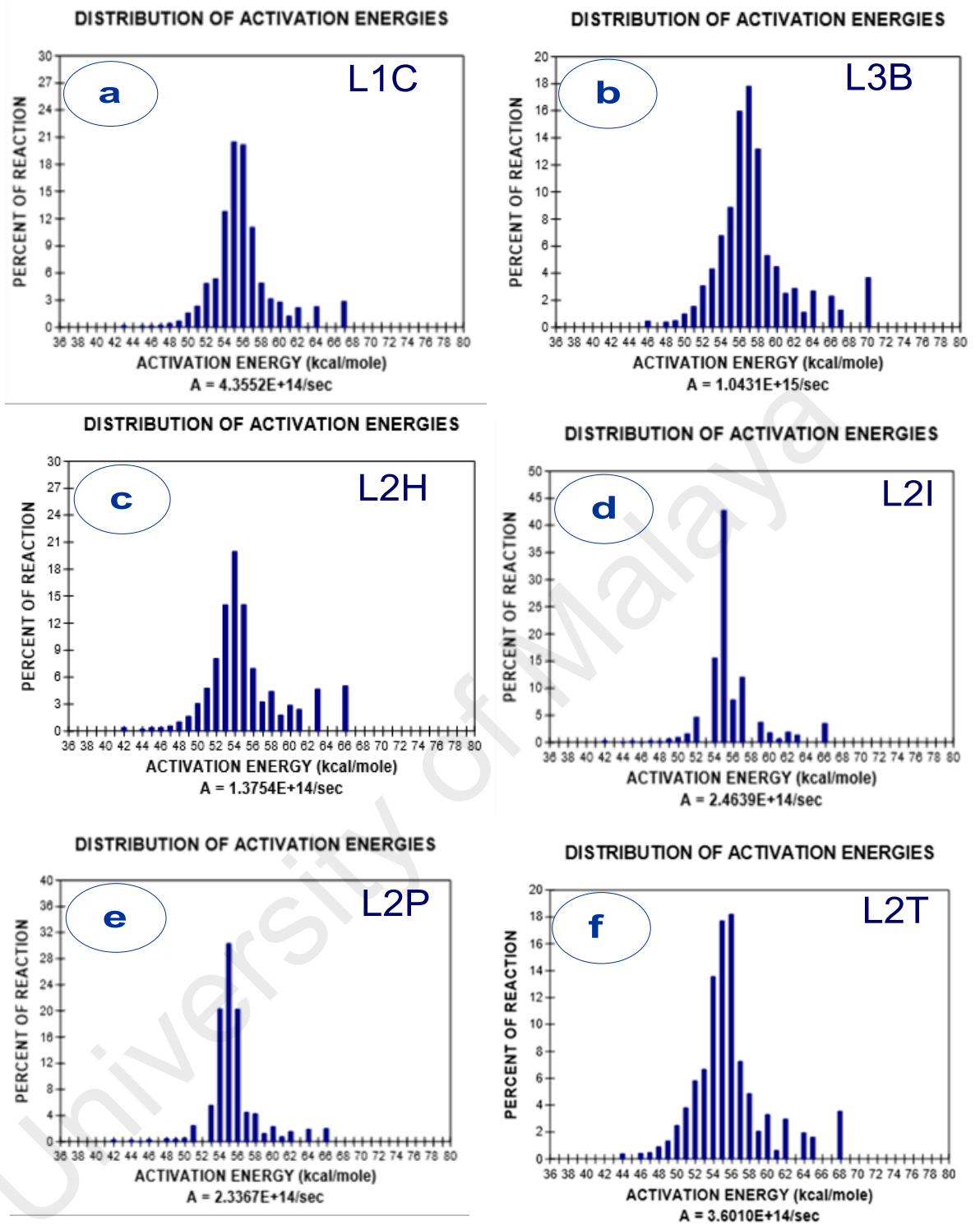


Figure 5.21: Activation energy distributions of selected coal samples from Gombe Formation.

5.10 Tectonic setting

Tectonic settings of sedimentary rocks can be inferred from the relative concentrations of major, trace and rare earth elements as well as bivariate plot of the major oxides as suggested by earlier researchers (Tao et al., 2013). This is due to the great effect of plate tectonic settings on the chemical compositions of rocks in a sedimentary basin (Peters et al., 2005; Makeen et al., 2015a). Thus, based on bulk geochemical analysis, three or four sedimentary origins and tectonic settings have been suggested i.e. oceanic island arc, continental island arc, active continental margin and passive margin (Maynard et al., 1982, Bhatia, 1983, Bhatia and Crook, 1986 and Roser and Korsch, 1986, Tao et al., 2013).

In this study, bivariate plot of $\log(K_2O/Na_2O)$ versus SiO_2 as was proposed by Roser and Korsch (1986) being applied to discriminate tectonic settings. These authors reported increase of K_2O/Na_2O and SiO_2 from volcanic arc through active continental margin to passive margin settings. In this study, such plots for the mudstones and shale facies from Gombe Formation were used to determine the tectonic setting of the studied area. The analysed shales and mudstones plot in the passive continental margin area (see Figure 5.21). This is consistent with Cretaceous tectonic events of West and Central Africa which is associated with the opening of the South American plate (Genik, 1992). The predominant force controlling the separation of the West African plates is the opening of the Atlantic Ocean in the Early Cretaceous (Guiraud and Maurin, 1992).

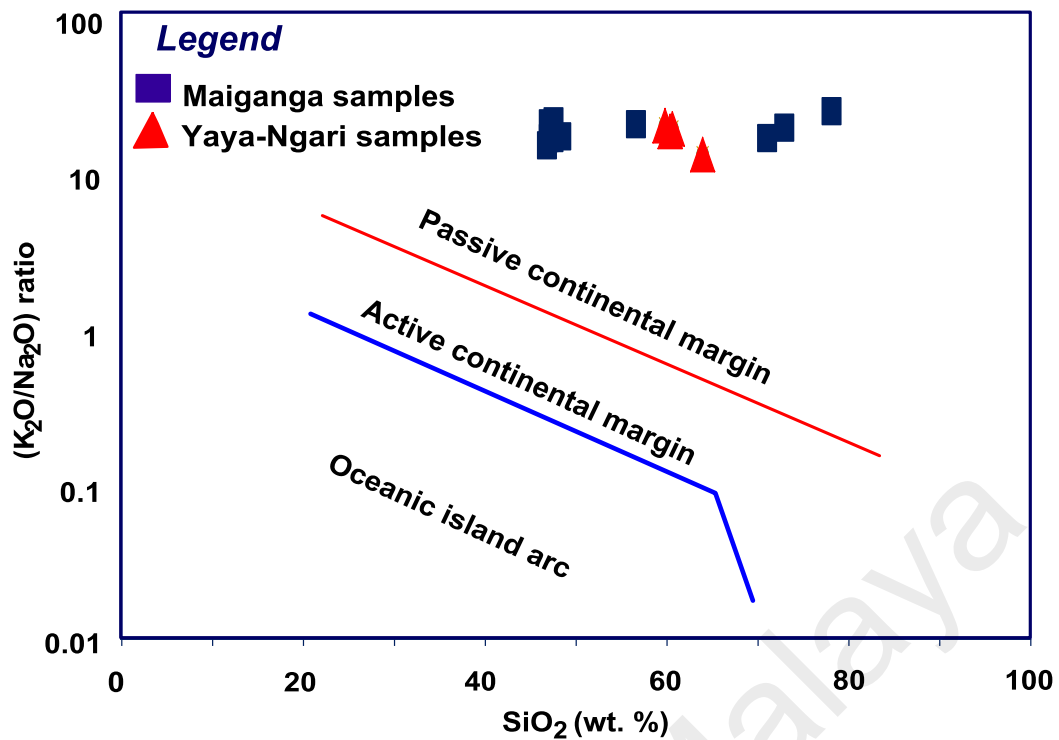


Figure 5.22: Bivariate plots of K₂O/Na₂O versus SiO₂ showing the tectonic setting of Gombe Formation based on analysed samples (adapted after Roser and Korsch, 1986).

5.11 Paleoclimatic conditions

Climatic conditions of a sedimentary basin play a significant role in organic matter input, mineralogy and geochemistry of sediments, hence, paleoclimatic conditions can be inferred from the major and trace element of its sedimentary facies (Suttner and Dutta, 1986; Hieronymus et al., 2001; Beckmann et al., 2005; Ratcliffe et al., 2004; Roy and Roser, 2013; Makeen et al., 2015a). Prior to this work, Abubakar et al. (2006) and Sarki Yandoka et al. (2015a) suggested predominance of semi-arid paleoclimate for the adjacent Yola sub-basin based on palynological constituents as well as major element composition. In this study, the distribution of the major oxides (Table 4.9) and trace elements (Table 4.10) in shales and mudstones as well as maceral composition (Table 4.7) were used in evaluating the paleoclimatic condition of the Gombe Formation. Similarly, the cross plot of SiO₂ versus (Al₂O₃ + K₂O + Na₂O) and Ga/Rb versus (K₂O/Al₂O₃) that have proved useful in determining the paleoclimatic conditions at the time of deposition of sandstones and mudstones were also employed

(Suttner and Dutta, 1986; Roy and Roser, 2013). Figures 5.22 and 5.23 show that the Maiganga mudstones and Yaya-Ngari shales analysed in this study were mainly deposited under semi-arid to slightly humid-warm climatic conditions. The predominant semi-arid paleoclimatic conditions are consistent with the relatively low Sr/Ba ratios for the mudstones and shales (average: 0.18; Table 4.10). This suggests a low saline water condition during sedimentation in Maiganga and Yaya-Ngari area. (Figure 5.17).

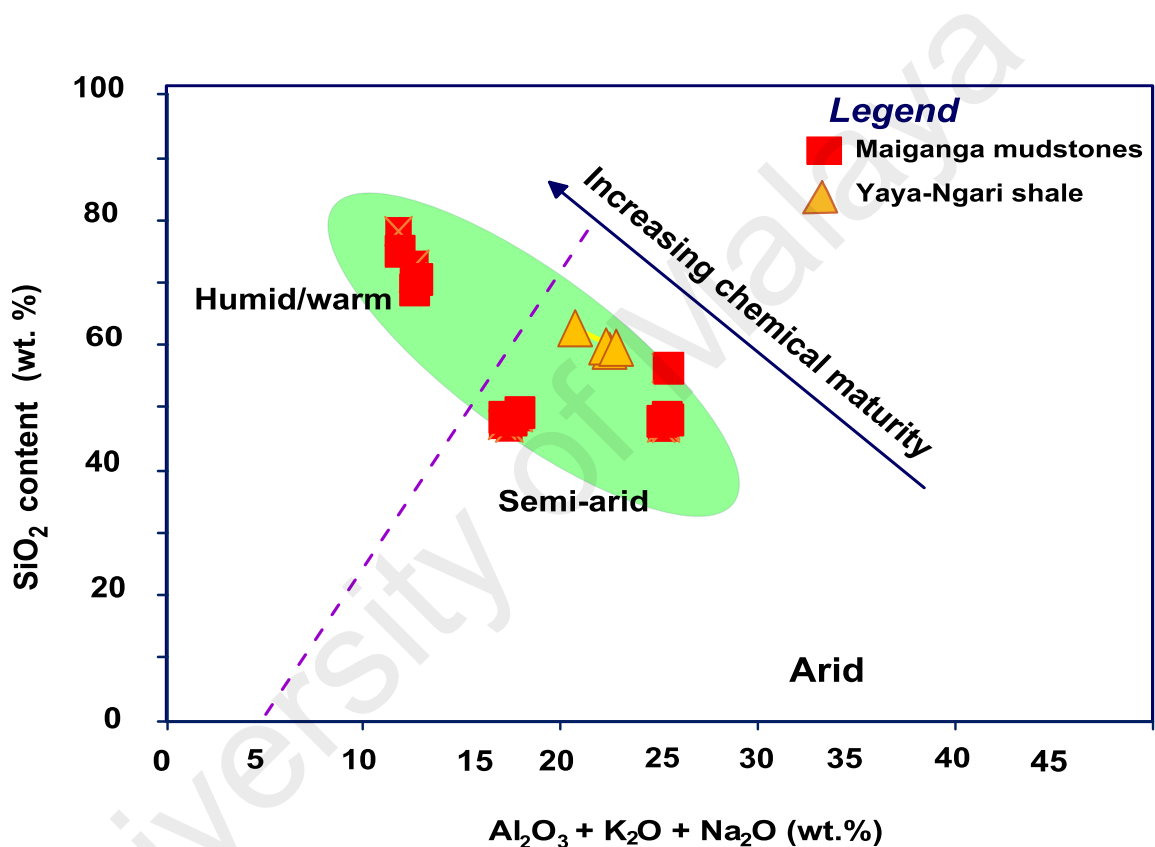


Figure 5.23: Binary SiO_2 versus $(Al_2O_3 + K_2O + Na_2O)$ showing the paleoclimatic condition during sedimentation of the analysed samples (adapted after Suttner and Dutta, 1986).

A warm and humid climate is usually known to be associated with aluminium (Al) and Gallium (Ga) which are always present in kaolinite (Hieronymus et al., 2001, Ratcliffe et al., 2004; Beckmann et al., 2005). On the other hand, potassium (K) and rubidium (Rb) are important constituents of illite, associated with cold and dry climate (Ratcliffe et al., 2004). These authors reported that rocks with high concentration of

illite have high K_2O/Al_2O_3 with low Ga/Rb ratios, but the reverse is the case in kaolinite rich rocks. The studied mudstones from the Gombe Formation are characterised by relatively high Ga/Rb (Table 4.10) and low K_2O/Al_2O_3 ratios (Table 4.9). This is an indication of high kaolinite clay mineral compared to illite clay mineral which was later found to be true based on XRD analysis (Figure 4.12). The bivariate plot of Ga/Rb versus K_2O/Al_2O_3 further supports this, and points to the semi-arid to humid-warm climatic conditions of the studied region (Figures 5.22 and 5.23). It also conforms with the observed trend for the Yola sub-basin which is the second bifurcated arm of Gongola sub-basin (Sarki Yandoka et al., 2015a). Semi-arid climate is often associated with increase in nutrient supply leading to high bioproductivity in the photic zone of water column as observed in Gombe Formation. Similarly, the recently discovered coal and other organic rich sediments in the Gombe Formation (see Table 4.1 for TOC) can also be related to the observed warm-humid climate (Figure 5.22 and 5.23) which is known to enhance mineral nutrient supply and phytoplankton growth (Talbot, 1988; Makeen et al., 2015a).

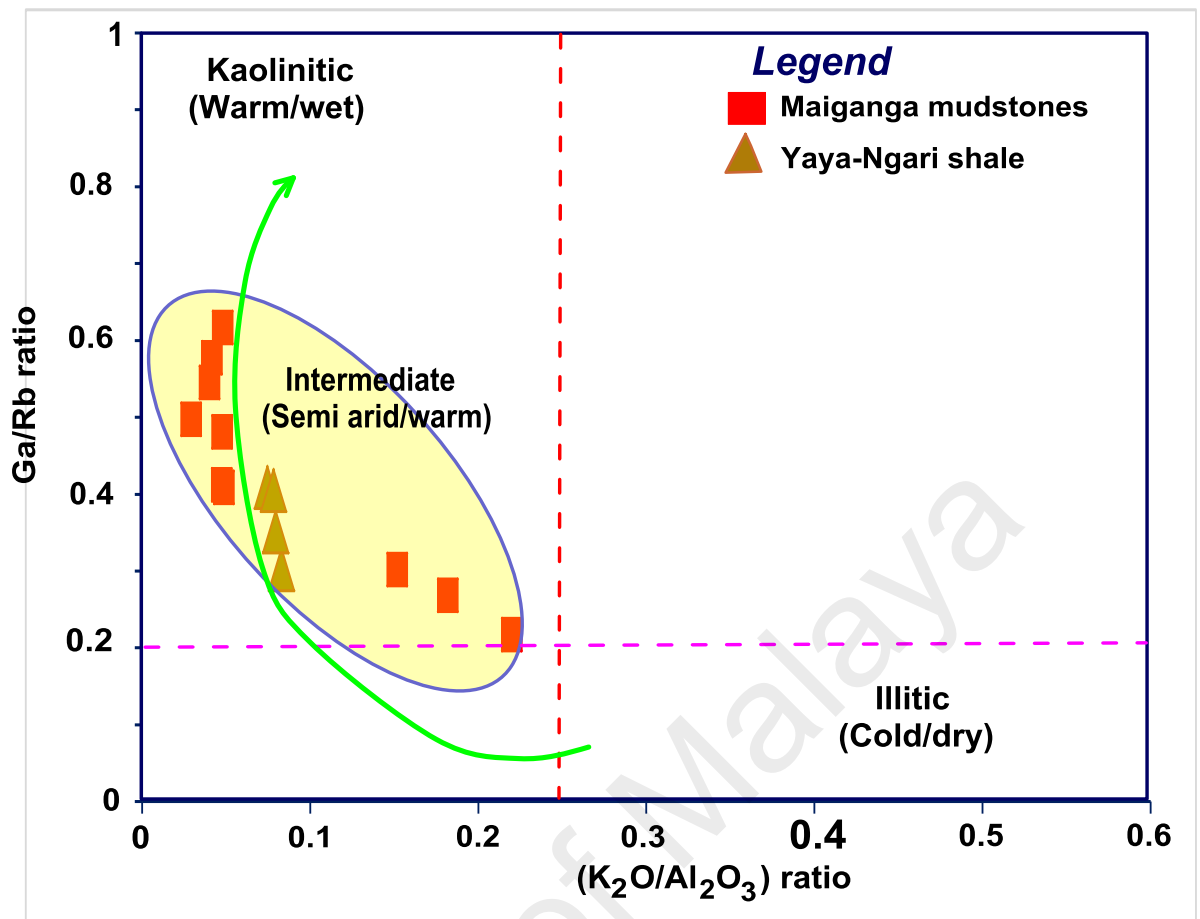


Figure 5.24: Ga/Rb ratio versus K₂O/ Al₂O₃ plot showing the paleoclimatic condition during sedimentation of the analysed samples (adapted after Roy and Roser, 2013).

CHAPTER 6: CONCLUSION AND RECOMMENDATION

6.1 Conclusion

Under-exploration of the Upper Cretaceous petroleum systems in the Northern Benue Trough Nigeria has been attributed largely to lack of subsurface samples and relevant studies. The focus of this study is an integration of field and geochemical (organic and inorganic) methods. The discovery of about 4.5 million tone of proven coal reserve and another 2 million ton of estimated reserve uncover a missing gap in the stratigraphy of the area. Recent access to samples from Maiganga coalfield revealed a need for detailed evaluation of the sedimentary facies types for better understanding of the hydrocarbon potential of the area. Organic/inorganic geochemical and petrographic characterisation of the Upper Cretaceous coals and organic rich mudstones from the Gombe Formation in the Gongola Sub-Basin were carried out to determine their quantity, quality, organic matter source input, paleodepositional condition, thermal maturity, hydrocarbons generation potential, tectonic setting and paleoclimatic conditions of the area.

Field observations in association with preliminary sedimentary facies studies showed at least four (4) depositional cycles with a coarsening upward trend of a delta plain depositional system. This comprises of four coal seams (B, A₃, A₂ and A₁) interbedded with moderately laminated and bioturbated claystones, siltstones, mudstones and shales which are well bedded. The succession is capped with thick beds of coarse to pebbly sandstone indicating increasing energy of deposition upwardly. Although lignite is the dominant coal rank observed on the field, it co-exists with peat (especially in seam A₃), and sub-bituminous coal (especially in seam B). This is an indication of increasing thermal maturity with increasing depth from younger seam A₃ to older seam B. The Gombe Formation is characterised by series of tectonic episodes (foldings and faulting) which perhaps contributed to the observed thermal maturity

difference between the analysed Yaya-Ngari shale and Maiganga samples. This is a known feature of the Northern Benue Trough especially at the end of Maastrichtian when there were several folding and faulting of pre-Paleogene sediments. Thus, seam A₁ and A₂ gradually thin out towards the southern part of the field due to erosion, while seam B is relatively continuous.

Evaluation of the organic matter richness on the basis of TOC indicates excellent for coal, very good to excellent for shale and mudstones. The result of the shale from Yaya-Ngari shows fair to good quantity. This is supported by the hydrocarbon yield (S₂) and EOM content showing similar trends for the organic facies in the Gombe Formation as illustrated by the cross relationship between TOC and S₂.

Biomarker assemblages and source rock analyses (SRA) reveal that Maiganga coals, mudstones and shales contain predominantly terrestrial source inputs/origin of mainly Type III/II and Type III kerogens with some lacustrine and marine influences which grades into mixed organic matter input within a transitional environment in the Yaya-Ngari area. This marine influence and bacterial input indicates a progressive marine influence and source input from southern to northern region of the study area. Maceral analysis and Py-GC studies reveal that the sedimentary facies in Maiganga area of the Gombe Formation have potential to generate liquid hydrocarbon, though still immature ($< 0.5\% R_o$). This is evident from average of more than 20% liptinite content and Type II/III kerogen, (Py-GC and HI > 200 mg HC/g TOC) suggesting that the Gombe Formation has a mixed oil and gas generation potential.

Paleodepositional (redox) condition of the Gombe Formation was evaluated based on calculated TPI versus GI, the major and trace elements composition as well as their ratios. All these parameters were supported by the GC-MS distributions such as pristane to phytane ratio, C₂₇/C₂₉ regular sterane versus Pr/Ph, C₃₁ to C₃₅ homohopanes pattern, cross plot of Pr/n-C₁₇ versus Ph/n-C₁₈, C₂₃/C₂₄ tricyclic terpane and C₂₄

tetracyclic/C₂₆ tricyclic terpane. Generally, biomarker studies suggest deposition of Type III/II kerogen within suboxic to oxic environment for the Maiganga, while Yaya-Ngari samples are characterised by mixed organic matter deposited in a suboxic conditions. Trace elements compositions further established suboxic to oxic depositional conditions for the studied Gombe Formation sample. TPI and GI (>1) as well as trace element composition suggest that terrigenous organic matter in the Gombe Formation is deposited in a delta plain setting characterised by moderate stratified water column and salinity.

Thermal maturity of the Formation was determined using vitrinite reflectance, T_{max}, bitumen extraction and biomarker parameters (e.g. Pr/n-C₁₇ vs. Ph/n-C₁₈, C₃₂ homohopane ratio (22S/22S+22R) and sterane ratio C₂₉ ββ/(ββ+αα). The results indicate immature pre-oil generation window stage for Maiganga coals, mudstones and shale. The maturity of Yaya-Ngari shale corresponds to an early oil generation window. In effect, the Gombe Formation thermal maturity ranges from pre-oil generation window to early oil generation window.

Based on the XRD and ICP-MS analysis, the Gombe Formation has a predominantly semi-arid to humid-warm paleoclimate. This is consistent with the relatively high Ga/Rb and low K₂O/Al₂O₃ ratios which are indications of high kaolinite clay mineral compared to illite clay mineral as confirmed by the XRD analysis of clay mineral. This is further strengthened by the cross plot of SiO₂ versus (Al₂O₃ + K₂O + Na₂O) and Ga/Rb versus (K₂O/Al₂O₃). Thus, the recently discovered coal and other organic rich sediments in the area can be related to the warm-humid climate which is known to enhance mineral nutrient supply and phytoplankton growth. The bivariate relationship of major oxides indicates a passive continental margin which was affected by the tectonic events of West and Central Africa in the Cretaceous period during the deposition of the Gombe Formation.

This study therefore, suggests that the Upper Cretaceous petroleum system of the Gongola Sub-basin consists of source rocks with good potential (thick coals beds, mudstones and shales) of mainly “gas-prone” and to a less extent “oil-prone”. Moreover, this data could be used as a guide for future exploration campaigns in the Northern Benue Trough and other similar basins around the world.

6.2 Recommendation

This work as well as the ongoing mining activities in the Maiganga coalfield has revealed that the Gongola sub-basin has been greatly under-explored. Consequent upon this development, I will like to recommend a detailed basin modeling based on geophysical data to identify important hydrocarbon related structural features for better understanding and exploration of the petroleum system in the basin. Similarly, it is necessary to carry out a detailed palynological biozonation and high-resolution biostratigraphy, which will enhance paleoenvironmental reconstruction of the entire basin. This, undoubtedly, when integrated with this work, will give more insight on the petroleum play system in the area.

REFERENCES

- Abbassi, S., Edwards, D.S., George, S.C., Volk, H., Mahlstedt, N., Di Primio, R., & Horsfield, B. (2016). Petroleum potential and kinetic models for hydrocarbon generation from the Upper Cretaceous to Paleogene Latrobe Group coals and shales in the Gippsland Basin, Australia. *Organic Geochemistry*, 91, 54-67.
- Abdullah W.H., & Abolins, P. (1999). Petrological and organic geochemical characterisation of the Tertiary coal-bearing sequence of Batu Arang, Selangor, Malaysia. *Journal of Asian Earth Sciences*, 16, 351-367.
- Abdullah, W.H. (2003). Coaly source rocks of NW Borneo: role of suberinite and bituminite in generation and expulsion. *Geological Society of the Malaysia, Bulletin*, 47, 119-129.
- Abubakar, M.B. (2014). Petroleum potentials of the Nigerian Benue Trough and Anambra Basin: A regional synthesis. *Natural Resources*. 5, 25–58.
- Abubakar, M.B., Dike, E.F.C., Obaje, N.G., Wehner, H., & Jauro, A. (2008). Petroleum prospectivity of Cretaceous Formations of Gongola Basin, Upper Benue Trough, Nigeria: An organic geochemical perspective on a migrated oil controversy. *Journal of Petroleum Geology*, 31, 387–408.
- Abubakar, M.B., & Obaje, N.G. (2001). Preliminary Biostratigraphic evaluation of the hydrocarbon potentials of the Cenomanian-Turonian horizon in the Gongola Formation, Upper Benue Trough, Nigeria. *Journal of Mining Geology*, 37, 121-128.
- Abubakar, M.B., Obaje, N.G., Luterbacher, H.P., Dike, E.F.C., & Ashraf A.R. (2006). A report on the occurrence of Albian–Cenomanian elater-bearing pollen in Nasara-1 well, Upper Benue Trough, Nigeria: Biostratigraphic and palaeoclimatological implications. *Journal of African Earth Sciences*, 45, 347-354.
- Adedosu, T.A. (2009). *Aspects of organic geochemistry of Nigerian coal as a potential source-rock of petroleum*. PhD thesis, University of Ibadan.
- Adegoke, A.K., Abdullah, W.H., Hakimi, M.H., Sarki Yandoka, B.M., & Abubakar, M.B., (2015). Kerogen characterization and petroleum potential of the Late Cretaceous sediments, Chad (Bornu) Basin, northeastern Nigeria. *Bulletin of the Geological Society of Malaysia*, 61, 29-42.
- Adegoke, A.K., Abdullah, W.H., Hakimi, M.H., Sarki Yandoka, B.M., Mustapha, K.A., & Aturamub, A.O. (2014). Trace elements geochemistry of kerogen in Upper Cretaceous sediments, Chad (Bornu) Basin, northeastern Nigeria: Origin and paleo-redox conditions. *Journal of African Earth Sciences*, 100, 675-683.
- Adegoke, O.S., Agumanu, A.E., Benkhelil M.J., & Ajayi, P.O. (1986). “New stratigraphic, sedimentologic and structural data on the Kerri-Kerri Formation,

Bauchi and Borno States, Nigeria". *Journal of African Earth Sciences*, 5, 249-277.

- Akande, S.O., Ojo, O.J., Erdtmann, B.D., & Hetenyi, M. (1998). Paleoenvironments, source rock potential and thermal maturity of the Upper Benue rift basins, Nigeria: Implications for hydrocarbon exploration. *Organic Geochemistry*, 29, 531-542.
- Akinlua, A., Adekola, S.A., Swakamisa, O., Fadipe, O.A., & Akinyemi, S.A. (2010). Trace element characterization of Cretaceous Orange Basin hydrocarbon source rocks. *Applied Geochemistry*, 25, 1587-1595.
- Akinlua, A., Ajayi, T.R., & Adeleke, B.B. (2007). Organic and inorganic geochemistry of Northwestern Niger Delta. *Geochemical Journal*, 41, 271-281.
- Alberdi-Genolet, M., & Tocco, R. (1999). Trace metals and organic geochemistry of the Machiques Member (Aptian-Albian) and La Luna Formation (Cenomanian-Campanian). *Venezuela. Chemical Geology*, 160, 19-38.
- Algeo T.J., & Maynard J.B. (2004). Trace element behavior and redox facies in core shales of Upper Pennsylvanian Kansas-type cyclothems. *Chemical Geology, Amsterdam*, 206, 289-318.
- Aliyu, A.H., Mamman, Y.D., Abubakar, M.B., Sarki Yandoka, B.M., & Shettima, B. (2017). Paleodepositional environment and age of Kanawa Member of Pindiga Formation, Gongola Sub-basin, Northern Benue Trough, NE Nigeria: Sedimentological and palynological approach. *Journal of African Earth Sciences*, 134, 345-351.
- Amijaya, H., Schwarzbauer, J., & Littke, R. (2006). Organic Geochemistry of the Lower Suban coal seam, South Sumatra Basin, Indonesia: palaeoecological and thermal metamorphism implications. *Organic Geochemistry*, 37, 261-279.
- Aquino Neto, F. R., Trendel, J. M., Restle, A., Connan, J., & Albrecht, P. A. (1983). Occurrence and formation of tricyclic and tetracyclic terpanes in sediments and petroleum. In: M. Bjorøy, C. Albrecht, C. Cornford, et al. (Eds.), *Advances in Organic Geochemistry 1981*, New York: John Wiley & Sons.
- Armstrong-Altrin, J.S., & Machain-Castillo, M.L. (2016). Mineralogy, geochemistry, and radiocarbon ages of deep sea sediments from the Gulf of Mexico, Mexico. *Journal of South American Earth Sciences*, 71, 182-200.
- Avbovbo, A.A., Ayoola, E.O., & Osabon, G.S.A. (1986). Depositional and structural style in Chad Basin northeastern Nigeria, *AAPG Bulletin*, 70, 1787-1798.
- Ayinla, H.A., Abdullah, W.H., Makeen, Y.M., Abubakar, M.B., Jauro, A., Sarki Yandoka, B.M., Mustapha, K.A., & Zainal Abidin, N. S. (2017a). Source rock characteristics, depositional setting and hydrocarbon generation potential of Cretaceous coals and organic rich mudstones from Gombe Formation, Gongola Sub-basin, Northern Benue Trough, NE Nigeria. *International Journal of Coal Geology*, 173, 212-226.

- Ayinla, H.A., Abdullah, W.H., Makeen, Y.M., Abubakar, M.B., Jauro, A., Sarki Yandoka, B.M., & Zainal Abidin, N.S. (2017b). Petrographic and geochemical characterization of the Upper Cretaceous coal and mudstones of Gombe Formation, Gongola Sub-basin, Northern Benue Trough Nigeria: Implication for organic matter preservation, paleodepositional environment and tectonic settings. *International Journal of Coal Geology*, 180, 67-82.
- Ayinla, H.A., Ola-Buaimo, A.O., Adeigbe, O.C., Bankole, S.A., & Adebawale, M. (2013). Palynostratigraphy and high resolution paleoenvironmental reconstruction of part of Kemar-1 well, Bornu Basin, Northeastern Nigeria. *Journal of Research in Environmental Science and Toxicology* 2, 53-63.
- Ayok, J. (2016). Mineralogy and Geochemistry of mud rock units of the Late Cretaceous Kanawa and Gulani Formations, Eastern Gongola Basin, North-Eastern Nigeria: Implications for provenance studies. *Journal of Environment and Earth Science*, 6, 87-101.
- Barber, W. M., Tait, E.A., & Thompson, J.H. (1954): The Geology of the Lower Gongola. *Annual. Report. Geological Survey of Nigeria, 1952/53*. 18-20.
- Beckmann, B., Flögel, S., Hofmann, P., Schulz, M., & Wagner, T. (2005). Orbital forcing of Cretaceous river discharge in tropical Africa and ocean response. *Nature*, 437, 241-244.
- Benkhelil, J. (1982). "Benue Trough and Benue Chain". *Geological Magazine*. 119, 155-168.
- Benkhelil, J. (1989). The origin and evolution of the Cretaceous Benue Trough, Nigeria. *Journal of African Earth Sciences*, 8, 251-282.
- Berner, R.A. (1984). Sedimentary pyrite formation: an update. *Geochimica et Cosmochimica Acta*, 48, 605-615.
- Berner, R.A., & Raiswell, R. (1983). Burial of organic carbon and pyrite sulfur in sediments over Phanerozoic time: A new theory. *Geochimica et Cosmochimica Acta*, 47, 855-862.
- Bertrand, P.R. (1989). Microfacies and petroleum properties of coals as revealed by a study of North Sea Jurassic coals. *International Journal of Coal Geology*, 13, 575-595.
- Bhatia, M.R., & Crook, K.A.W. (1986). Trace element characteristics of graywackes and tectonic setting discrimination of sedimentary basins. *Contributions to Mineralogy and Petrology*, 92, 181-193.
- Bhatia, M.R. (1983). Plate tectonics and geochemical composition of sandstones. *Journal of Geology*, 91, 611-627.
- Bordenave, M.L., Espitalié, L., Leplat, P., Oudin, J.L., & Vandenbroucke, M. (1993). Screening techniques for source rock evaluation. In: M.L. Bordenave (Eds.), *Applied Petroleum Geochemistry* (pp. 237-255), Paris: Editions Technip.

- Brassell, S.C., Eglinton, G., Maxwell, J.R., & Philp, R.P. (1978). Natural background of alkanes in the aquatic environment. In: O. Hutzinger, I.H. Van Lelyeld & B.C.J. Zoetemin (Eds.), *Aquatic pollutants* (pp. 69-86), Oxford: Pergamon Press.
- Bray, E.E., & Evans, E.D. (1961). Distribution of n-paraffins as a clue to recognition of source beds. *Geochimica et Cosmochimica Acta*, 22, 2-15.
- Brooks, P.W. (1986). Unusual biological marker Geochemistry of oils and possible source rocks, offshore Beaufort-Mackenzie Delta, Canada. In: D. Leythaeuser & J. Rullkötter (Eds.), *Advances in Organic Geochemistry*. Oxford: Pergamon Press.
- Burke, K.C., Dessauvage, T. F., & Whiteman, A.J. (1970). "Geologic History of the Benue Valley and Adjacent Areas," In: T.F.J. Dessauvage & A.J. Whiteman (Eds.), *African Geology* (pp. 187-205). Ibadan: Ibadan University Press.
- Burnham, A.K., Braun, R.L., Gregg, H.R., & Samoun, A.M. (1987). Comparison of methods for measuring kerogen pyrolysis rates and fitting kinetic parameters. *Energy Fuels* 1, 452-458.
- Calvert, S.E., & Pedersen, T.F. (1993). Geochemistry of recent oxic and anoxic marine sediments: Implications for the geological record. *Marine Geology*, 113, 67-88.
- Carter, J.D., Barber, W., & Jones, G.P. (1963). The Geology of parts of Adamawa, Bauchi and Borno Provinces in Northeastern Nigeria, *Bulletin Geology Survey Nigeria*, 30, 53-61.
- Coal-Formation of Coal-Types of Coal (Retrieved on 10/10/2017) <https://goo.gl/images/8mBoc8>.
- Cratchley, C.R., & Jones, C.P. (1965). An interpretation of the Geology and gravity anomalies of the Benue Trough, Nigeria. *Overseas Geological. Survey Geophysical Paper. 1*, 1-26.
- Cratchley, C.R., Louis P., & Ajakaiye, D.E. (1984). "Geophysical and geochemical evidence for the Benue-Chad Basin Cretaceous rift valley system and its tectonic implications," *Journal of African Earth Science*, 2, 141-150.
- Crusius, J., Calvert, S., Pedersen, T., & Sage, D. (1996). Rhenium and molybdenum enrichments in sediments as indicators of oxic, suboxic, and sulfidic conditions of deposition. *Earth Planetary Science Letter*, 145, 65-78.
- Czochanska, Z., Gilbert, T. D., Philp, R.P., et al. (1988). Geochemical application of sterane and triterpane biomarkers to a description of oils from the Taranaki Basin in New Zealand. *Organic Geochemistry*, 12, 123-35.
- De Grande, S.M.B., Aquino Neto, F.R., & Mello, M.R. (1993). Extended tricyclic terpanes in sediments and petroleum. *Organic Geochemistry*, 20, 1039-1047.

- Dembicki Jr. H. (1993), Improved determination of source quality and kerogen type by combining Rock Eval and pyrolysis-gas chromatography results. *AAPG 1993 Annual Convention Program*, 2, 1-90.
- Dembicki, H.J. (2009). Three common source rock evaluation errors made by geologists during prospect or play appraisals. *AAPG Bulletin*, 93, 341-356.
- Dembicki, Jr., Horsfield, H.B., & Ho, T.T.Y. (1983). Source rock evaluation by pyrolysis gas chromatography. *AAPG Bulletin*, 67, 1094-1103.
- Deng, H.W., & Qian, K. (1993). Analysis on sedimentary Geochemistry and environment. *Science Technology Press, Gansu*, 15-85 (in Chinese).
- Didyk, B. M., Simoneit, B. R. T., Brassell, S. C., & Eglinton, G. (1978). Organic geochemical indicators of palaeoenvironmental conditions of sedimentation. *Nature*, 272, 216-22.
- Dieckmann, V. (2005). Modelling petroleum formation from heterogeneous source rocks: the influence of frequency factors on activation energy distribution and geological prediction. *Marine and Petroleum Geology*, 22, 375-390.
- Diessel, C.F.K. (1986). On the correlation between coal facies and depositional environments. Advances in the Study of the Sydney Basin, *Proceeding of the 20th Symposium. University of Newcastle, Australia*, 19-22.
- Diessel, C.F.K. (1992). *Coal-bearing Depositional Systems*. New York: Springer-Verlag, Berlin.
- Dike, E.F.C. (1995). Stratigraphy and structure of the Kerri-Kerri Basin, Northeastern Nigeria. *Journal of Mining and Geology*, 29, 77-92.
- Eglinton, G., & Hamilton, R.J. (1967). Leaf epicuticular waxes. *Science*, 156, 1322-1335.
- Eglinton, T.I., Sinninghe Damste, J.S., Kohnen, M.E.L., & De Leeuw, J.W. (1990). Rapid estimation of the organic sulphur content of kerogens, coals and asphaltenes by pyrolysis-gas chromatography. *Fuel* 69, 1394-1404.
- Ekweozor, C.M., & Telnaes, N. (1990). Oleanane parameter: verification by quantitative study of the biomarker occurrence in sediments of the Niger Delta. *Organic Geochemistry* 16, 401-413.
- El Diasty, W., & Moldowan, J.M. (2013). The western desert versus Nile Delta: A comparative molecular biomarker study. *Marine and Petroleum Geology*, 46, 319-334.
- El-Diasty, W., & Moldowan, J.M. (2012). Application of biological markers in the recognition of the geochemical characteristics of some crude oils from Abu Gharadig Basin, north Western Desert – Egypt. *Marine and Petroleum Geology*, 35, 28-40.

- Espitalié, Â.J., Madec, M., Tissot, B., Mennig, J.J., & Leplat, P. (1977). Source rock characterisation methods for petroleum exploration. *9th Annual Offshore Technology Conference. Houston*, 439-444.
- Falconer, J.D. (1911). *The Geology and Geography of Northern Nigeria*. London: Macmillan.
- Farhaduzzaman, M., Abdullah, W.H., Aminul Islam, M., & Pearson, M.J. (2012). Source rock potential of organic-rich shales in the Tertiary Bhuban and Boka bil Formations, Bengal basin, Bangladesh. *Journal of Petroleum Geology*, *35*, 357–375.
- Farrimond, P., Taylor, T. & Telnaes, N. (1998). Biomarker maturity parameters: the role of generation and thermal degradation. *Organic Geochemistry*, *29*, 1181–1197.
- Forsman, J.P., & Hunt, J.M. (1958). Insoluble organic matter (kerogen) in sedimentary rocks. *Geochimica et Cosmochimica Acta*, *15*, 170-182.
- Fu, X., Wang, J., Zeng, Y., Cheng, J., & Tano, F. (2011). Origin and mode of occurrence of trace elements in marine oil shale from the Shengli River Area, Northern Tibet, China. *Oil Shale*, *28*, 487-506.
- Galarraga, F., Reategui, K., Martínez, A., Martínez, M., Llamas, J.F., & Márquez, G. (2008). V/Ni ratio as a parameter in palaeoenvironmental characterization of non-mature medium-crude oils from several Latin American basins, *Journal of Petroleum Science and Engineering*, *61*, 9-14.
- Genik, G, J. (1992). Regional framework, structural and petroleum aspects of rift basins in Niger, Chad and the Central African Republic (C.A.R.). *Tectonophysics*, *213*, 169-185.
- Giraud, A. (1970). Application of pyrolysis and gas chromatography to geochemical characterization of kerogen in sedimentary rocks. *AAPG. Bulletin*, *54*, 439-451.
- Grant, N.K. (1971). South Atlantic, Bene Trough and Gulf of Guinea Cretaceous triple junction. *Bulletin of the Geological Society of America*, *82*, 2295-2298.
- Grantham, P.J., Posthuma, J., & Baak, A. (1983). Triterpanes in a number of Far-Eastern crude oils. In: M. Bjorøy, C. Albrecht, C. Cornford, et al. (Eds.), *Advances in Organic Geochemistry 1981* (pp. 675-683), New York, NY: John Wiley & Sons.
- Guiraud, R., & Maurin, J. C. (1992). Early Cretaceous rifts of Western and Central Africa: An overview. *Tectonophysics*, *213*, 153-168.
- Guiraud, M. Laborde, O., & Philp, H. (1989). "Characterization of various types of deformation and their corresponding deviatoric stress tensors using microfault analysis," *Tectonophysics*, *170*, 1-28.

- Guiraud, M. (1990). "Tectono-Sedimentary framework of the Early Cretaceous continental Bima Formation (Upper Benue Trough, NE Nigeria)," *Journal of African Earth Science*, 10, 341-353.
- Hakimi, M.H., & Abdullah, W.H. (2014). Source rock characterization and hydrocarbon generation modelling of Upper Cretaceous Mukalla Formation in the Jiza-Qamar Basin, Eastern Yemen. *Marine and Petroleum Geology*, 51, 100-116.
- Hakimi, M.H., & Abdullah, W.H. (2013). Organic geochemical characteristics and oil generating potential of the Upper Jurassic Safer shale sediments in the Marib-Shabawah Basin, western Yemen. *Organic Geochemistry*, 54, 115–124.
- Hakimi, M.H., Abdullah, W.H., Makeen, Y.M. Saeed, S.A., Al-Hakame, H., Al-Moliki, T., Al-Sharabi, K.Q., & Hatem B.A. (2017). Geochemical characterization of the Jurassic Amran deposits from Sharab area (SW Yemen): Origin of organic matter, paleoenvironmental and paleoclimate conditions during deposition. *Journal of African Earth Sciences*, 129, 579–595.
- Hakimi, M.H., Abdullah, W.H., Mustaph, K.A., & Makeen, Y.M. (2015). Oil-generation characteristics of Mesozoic syn-rift Madbi source rock in the Masila Basin, Eastern Yemen: New insights from kerogen pyrolysis and bulk kinetic modelling. *Marine and Petroleum Geology*, 59, 336-347.
- Hakimi, M.H., Abdullah, W.H., & Shalaby, M.R., (2011). Organic geochemical characteristics of crude oils from the Masila Basin, eastern Yemen. *Organic Geochemistry*, 42, 465–476.
- Han, Y., Horsfield, B., & Curry, D.J. (2017). Control of facies, maturation and primary migration on biomarkers in the Barnett Shale sequence in the Marathon 1 Mesquite well, Texas. *Marine and Petroleum Geology*, 85, 106-116.
- Harouna, M., & Philp. R. P. (2012). Potential petroleum source rocks in the Termit Basin, Niger. *Journal of Petroleum Geology*, 35, 165-185.
- Harris, N.B., Freeman, K.H., Pancost, R.D., White, T.S., & Mitchell, G.D. (2004). The character and origin of lacustrine source rocks in the Lower Cretaceous synrift section, Congo Basin, west Africa. *AAPG Bulletin*, 88, 1163–1184.
- Hartwig, A., Primio, R., Anka, Z., & Horsfield, B. (2012). Source rock characteristics and compositional kinetic models of Cretaceous organic rich black shales offshore southwestern Africa. *Organic Geochemistry*, 51, 17-34.
- Hieronimus, B., Kotschoubey, B., & Boulegue, J. (2001). Gallium behavior in some contrasting lateritic profiles from Cameroon and Brazil. *Journal of Geochemical Exploration*, 72, 147-163.
- Holba, A. G., Dzou, L. I., Wood, G. D., Ellis L., Adam, P., Schaeffer P., ... Hughes W.B. (2003). Application of tetracyclic polyprenoids as indicators of input from fresh-brackish water environments. *Organic Geochemistry*, 34, 441-469.

- Horsfield, B. (1989). Practical criteria for classifying kerogens: some observations from pyrolysis–gas chromatography. *Geochimica et Cosmochimica Acta* 53, 891-901.
- Hower, J.C., Trinkle, E.J. & Raione R.P. (2008). Vickers microhardness of telovitrinite and pseudovitrinite from high volatile bituminous Kentucky coals. *International Journal of Coal Geology*, 75, 76-80.
- Huang, W.Y., & Meinshein, W.G. (1979). Sterols as ecological indicators. *Geochimica et Cosmochimica Acta*, 43, 739-45.
- Hughes, W.B., Holba, A.G., & Dzou, L.I.P. (1995). The ratios of dibenzothiophene to phenanthrene and pristane to phytane as indicators of depositional environment and lithology of petroleum source rocks. *Geochimica et Cosmochimica Acta*, 59, 3581-3598.
- Hunt, J.M. (1991). Generation of gas and oil from coal and other terrestrial organic matter. *Organic Geochemistry*, 17, 673-680.
- Hunt, J.M. (1996). *Petroleum Geochemistry and Geology*, second edition., San Francisco, W.H, Freeman.
- International Committee for Coal Petrology-ICCP, (1963). *International Handbook of Coal Petrography*. (second ed.), CNRS. Academy of Sciences of the USSR, Paris, Moscow.
- International Committee for Coal Petrology-ICCP, (1993). *International Handbook of Coal Petrography* (3rd Supplement to 2nd ed.), University of Newcastle upon Tyne, England.
- International Committee for Coal Petrology-ICCP, (1998). The new vitrinite classification (ICCP System 1994). *Fuel*, 77, 349-358.
- International Committee for Coal Petrology-ICCP, (2001). The new inertinite classification (ICCP system 1994), *Fuel* 80, 459-471.
- Jauro, A., Agho, M.O., Abayeh, O.J., Obaje, N.G., & Abubakar M.B. (2008). Petrographic studies and coking properties of Lamza, Chikila and Lafia-Obi Coals of the Benue Trough. *Journal of Mining and Geology*, 44, 37-43.
- Jauro, A., Obaje, N.G., Agbo, M.O., Abubakar, M.B., & Tukur, A., (2007). Organic Geochemistry of Cretaceous Lamza and Chikila coals, Upper Benue Trough, Nigeria, *Fuel* 86, 520–532.
- Jia, J., Bechtel, A., Liu, Z., Susanne, A.I., Strobl, P.S., & Reinhard, F.S. (2013). Oil shale formation in the Upper Cretaceous Nenjiang formation of the Songliao Basin (NE China): Implications from organic and inorganic geochemical analyses. *International Journal of Coal Geology*, 113, 11-26.
- Jimoh, A.Y., & Ojo, O.J. (2016). Rock-Eval pyrolysis and organic petrographic analysis of the Maastrichtian coals and shales at Gombe, Gongola Basin,

- Jones, B. & Manning, D.A.C. (1994). Comparison of geochemical indices used for the interpretation of paleoredox conditions in ancient mudstone. *Chemical Geology*, *111*, 111-129.
- Jones, R.W. (1987). Organic facies. In: J. Brooks, & D. Welte (Eds.), *Advances in Petroleum Geochemistry* (pp. 1-90). London: Academic Press, Harcourt Brace Jovanovich, Publishers.
- Kaiser, H., & Ashraf, R. (1974). Gewinnug und Präparation fossiler Sporen und Pollen sowie anderer Palynomorphaeunter besonderer Betonung der Siebmethode. *Geologisches Jahrbuch*, *25*, 85-114.
- Kalaitzidis, S., Bouzinos, A., & Christanis, K. (2000). The lignite-forming palaeoenvironment before and after the volcanic tephra deposition in the Ptolemais basin, Hellas. *Mineral Wealth*, *115*, 29–42 (in Greek).
- Kalkreuth, W., & Leckie, D.A. (1989). Sedimentological and petrological characteristics of Cretaceous strandplain coals: a model for coal accumulation from the North American Western Interior Seaway. *International Journal of Coal Geology*, *12*, 381-242.
- Kalkreuth, W., Kotis, T., Papanicolaou, C., & Kokkinakis, P. (1991). The Geology and coal Petrology of a Miocene lignite profile at Meliadi Mine, Katerini, Greece. *International Journal of Coal Geology*, *17*, 51-67.
- Ketris, M.P., & Yudovich, Y.E. (2009). Estimation of Clarkes for carbonaceous biolithes: World averages for trace element contents in black shales and coals. *International Journal of Coal Geology*, *78*, 135–148.
- Killops, S.D., Vanessa J., & Killops, V.J. (2005). *Introduction to Organic Geochemistry*, (2nd Edition) UK, Blackwell Publishing Limited.
- Kim, N.S., & Rodchenko, A.P. (2016). Hopane hydrocarbons in bitumens of Mesozoic deposits of the western Yenisei–Khatanga regional trough. *Russian Geology and Geophysics* *57*, 597-607.
- King, L.C. (1950). “Outline and distribution of gondwanaland,” *Geological Magazine*, *87*, 353-359.
- Kitson, F.G., Larsen, B.S., & McEwen, C.N. (1996). *Gas Chromatography and Mass Spectrometry*. Academic Press, New York.
- Kogbe, C.A. (1976). The Cretaceous and Paleocene sediments of Southwestern Nigeria. In: C.A. Kogbe (Ed), *Geology of Nigeria* (pp. 50-61), Lagos: Elizabethan Publishing Company.

- Korkmaz, S., & Kara Gülbay, R. (2007). Organic geochemical characteristics and depositional environments of the Jurassic coals in the Eastern Taurus of Southern Turkey. *International Journal of Coal Geology*, 70, 292-304.
- Larter, S.R., & Douglas, A.G. (1980). A pyrolysis-gas chromatographic method for kerogen typing. In: A.G. Douglas & J.R. Maxwell (Eds.), *Advances in Organic Geochemistry 1979*(pp. 579-584). New York, NY: Pergamon Press.
- Larter, S.R. (1984). Application of analytical pyrolysis technique to kerogen characterization and fossil fuel exploitation. In: K. Voorhees (Ed.), *Analytical Pyrolysis* (pp. 212-275). London: Butterworths.
- Lawal, O. (1982). *Biostratigraphie, palynologie et paléoenvironnements des formations Crétacées de la Haute-Bénoué, Nigeria nord-oriental. Thèse 3e cycle Université Nice.*
- Lawal, O., & Moullade, M. (1986). Palynological Biostratigraphy of the Cretaceous sediments in the Upper Benue Basin, N.E. Nigeria. *Revue de Micropaleotologie*, 29, 61-83.
- MacDonald, R., Hardman, D., Sprague, R., Meridji, Y., Mudjiono, W., Galford, ... Kelto, M. (2010). Using Elemental Geochemistry to Improve Sandstone Reservoir Characterization: A Case Study from the Unayzah A Interval of Saudi Arabia, *SPWLA 51st Annual Logging Symposium*, 1-16.
- Makeen, Y.M., Abdullah, W.H., & Hakimi, M.H. (2015a). The origin, type and preservation of organic matter of the Barremian-Aptian organic-rich shales in the Muglad Basin, Southern Sudan, and their relation to paleoenvironmental and paleoclimate conditions. *Marine and Petroleum Geology* 65, 187-197.
- Makeen, Y.M., Abdullah, W.H., Ayinla, H.A., Hakimi, M.H., & Sia S. (2016). Sedimentology, diagenesis and reservoir quality of the upper Abu Gabra Formation sandstones in the Fula Sub-basin, Muglad Basin, Sudan. *Marine and Petroleum Geology*, 77, 1227-1242.
- Makeen, Y.M., Abdullah, W.H., Hakimi, M.H., & Mustapha. K.A. (2015b). Source rock characteristics of the Lower Cretaceous Abu Gabra Formation in the Muglad Basin, Sudan, and its relevance to oil generation studies. *Marine and Petroleum Geology*, 59, 505-516.
- Makeen, Y.M., Abdullah, W.H., Hakimi, M.H., Elhassana, O.M.A. (2015c). Organic geochemical characteristics of the Lower Cretaceous Abu Gabra Formation in the great Moga oilfield, Muglad Basin, Sudan: Implications for depositional environment and oil-generation potential. *Journal of African Earth Sciences*, 103, 102–112.
- Mangini, A. (1978). Th and U isotope analyses on meteor core 12310 northwest African continental wise. *Meteor-Forschungsergeb Reihe.C. 29*, 1-5.
- Markic, M., & Sachsenhofer, R. (1997). Petrographic composition and depositional environments of Pliocene Velenje lignite seam (Slovenia). *International Journal of Coal Geology*, 33, 229–254.

- Maynard, J.B., Valloni, R., & Yu, H.S. (1982). Composition of modern deep-sea sands from arc-related basins. In: J.K. Leggett (Eds.), *Trench and Fore-arc Sedimentation* (pp. 551-561). London: The Geological Society of London, (Special Publications 10).
- McManus, J., Berelson, W.B., Severmann, S., Poulson, R.L., Hammond, D.E., Klinkhammer, G.P., & Holm, C. (2006). Molybdenum and uranium geochemistry in continental margin sediments: paleoproxy potential. *Geochimica et Cosmochimica Acta*, 70, 4643-4662.
- McManus, J., Nagler, T.F., Seibert, C., Wheat, C.G., & Hammond, D.E. (2002). Oceanic molybdenum isotope fractionation: diagenesis and hydrothermal ridge-flank alteration. *Geochemistry, Geophysics, Geosystems*, 3, 1-9.
- Mendonça Filho, J.G.M., Menezes, T.R., Mendonça, J.O., Oliveira, A.D., Silva, T.F., Noelia Franco Rondon, N.F., & Silva, F.S. (2012). Organic Facies: Palynofacies and Organic Geochemistry Approaches. *Geochemistry – Earth's System Processes*. DOI: 10.5772/47928.
- Mohialdeen, M.J., & Raza, S.M. (2013). Inorganic geochemical evidence for the depositional facies associations of the Upper Jurassic Chia Gara Formation in NE Iraq. *Arabian Journal of Geoscience*, 6, 4755-4770.
- Moosavirada, S.M., Janardhanab, M.R., Sethumadhava, M.S., Moghadamc, M.R., & Shankara, M. (2011). Geochemistry of lower Jurassic shales of the Shemshak Formation, Kerman Province, Central Iran: Provenance, source weathering and tectonic setting. *Chemie der Erde*, 71, 279–288.
- Mukhopadhyay, P.K., Wade, J.A., & Kruger, M.A. (1995). Organic facies and maturation of Jurassic/Cretaceous rocks, and possible oil-source rock correlation based on pyrolysis of asphaltenes, Scotian Basin, Canada. *Organic Geochemistry*, 22, 85-104.
- Murray, A.P., Sosrowidjojo, I.B., Alexander, R., Kagi, R.I., Norgate, C.M., & Summon, R.E. (1997). Oleananes in oils and sediments: Evidence of marine influence during early diagenesis? *Geochimica et Cosmochimica Acta*, 61, 6, 1261-1276.
- Mustapha, K.A., Abdullah, W.H., Konjing, Z., Sia, S.G., & Koraini, A.M. (2017). Organic geochemistry and palynology of coals and coal-bearing mangrove sediments of the Neogene Sandakan Formation, Northeast Sabah, Malaysia. *Catena*, 158, 30-45.
- Nwajide, C.S. (2013). *Geology of Nigeria's Sedimentary Basins*. Lagos: CSS Bookshop Limited.
- Obaje, N.G. (2009). *Geology and Mineral Resources of Nigeria* Springer-Verlag Berlin Heidelberg (www. Springer.com).
- Obaje, N.G., Abaa, S.I., Najime, T., & Suh, C.E. (1999). Economic Geology of Nigerian coals resources-a brief review. *Africa Geoscience. Review*, 6, 71-82.

- Oikonomopoulos, I.K. Kaourasa, G. Tougiannidis, N. Rickenb, W. Gurkc, M., & Antoniadis, P. (2015). The depositional conditions and the palaeoenvironment of the Achlada xylite-dominated lignite in western Makedonia, Greece. *Palaeogeography, Palaeoclimatology, Palaeoecology*, 440, 777-792.
- Ojo, O.J., & Akande, S.O. (2004). Palynology and Paleoenvironmental studies of the Gombe Formation, Gongola Basin, Nigeria. *Journal of Mining Geology*, 40, 143-149.
- Ojo, O.M. (1982). Palaeogeographical and structural evolution of the Upper Benue Trough of Nigeria. *Cretaceous Research*, 3, 195-207.
- O'Keefe, J. M.K., Bechtel, A., Christanis, K., Dai, S., DiMichele, W.A., Eble, C.F., ... Hower., J.C. (2013). On the fundamental difference between coal rank and coal type. *International Journal of Coal Geology*, 118, 58-87.
- Okosun, E.A. (1995). Review of the Geology of the Bornu Basin. *Journal of Mining and Geology*, 31, 113-122.
- Olade, M.A. (1975). "Evolution of Nigeria's Benue Trough (Aulacogen): A Tectonic Model," *Geological Magazine*, 112, 575-583.
- Onoduku, U.S., & Okosun, E.A. (2014). Palynology, Palynostratigraphy and paleoenvironmental Analysis of Maiganga coal mine, Gombe Formation, Nigeria. *Universal Journal of Geoscience*, 2, 93-103.
- Onoduku, U.S., Okosun, E.A., & Akande, W.G. (2013). An Assessment of the hydrocarbon potential of the Gombe Formation, Upper Benue Trough, Northeastern Nigeria: Organic Geochemical point of view. *Earth Science Research*, 2, 203-213.
- Ourisson, G., Albrecht, P., & Rohmer, M. (1984). The microbial origin of fossil fuels. *Scientific American*, 251, 34-41.
- Pattan, J.N., & Pearce, N.J.G., (2009). Bottom water oxygenation history in southeastern Arabian Sea during the past 140 ka: Results from redox-sensitive elements. *Palaeogeography, Palaeoclimatology, Palaeoecology*, 280, 396-405.
- Peters, K.E. (1986). Guidelines for evaluating petroleum source rock using programmed pyrolysis. *AAPG Bulletin*, 70, 318-329.
- Peters, K.E., & Cassa, M.R. (1994). Applied source rock Geochemistry. In: L.B. Magoon & W.G. Dow (Eds.), *The petroleum system-from source to trap*, (pp. 93-120). AAPG.
- Peters, K.E., & Moldowan, J.M. (1993). *The Biomarker guide: Interpreting molecular fossils in petroleum and ancient sediments*. Prentice-Hall, Inc., Englewood Cliffs, New Jersey.

- Peters, K.E., Walters, C.C. & Moldowan, J.M. (2005). *The Biomarker guide: Biomarkers and isotopes in Environment and Human history* (second ed.) Cambridge University Press, Cambridge.
- Petersen, H., & Rosenberg, P. (2000). The relationship between the composition and rank of humic coals and their activation energy distributions for the generation of bulk petroleum. *Petroleum Geoscience*, 6, 137-149.
- Philp, R.P. (1985). *Fossil fuel Biomarkers: applications and spectra*. Elsevier Science Publishers B.V, Amsterdam.
- Pickel, W., Kus, J., Flores, D. Kalaitzidis, C, S. Christanis, K. Cardotte, B.J., ... ICCP. (2017). Classification of liptinite – ICCP System 1994). *International Journal of Coal Geology*, 169, 40 -61.
- Piper, D.Z. (1994). Seawater as the source of minor elements in black shales, phosphorites and other sedimentary rock. *Chemical Geology*, 114, 94-114.
- Popoff, M., Benkhelil, J., Simon, B., & Motte, J. J. (1983). “Approche Géodynamique du Fossé de la Bénoué (N. Nigeria a Partir des Données de Terrain et de Télédétection,” *Bulletin Des Centres de Recherches Exploration-Production Elf-Aquitaine*, 7, 323-337.
- Powell, T. G., & McKirdy, D. M. (1973). Relationship between ratio of pristane to phytane, crude oil composition and geological environment in Australia. *Nature*, 243, 37-9
- Powell, T.G., Foscolos, A.E., Gunther, P.R., & Snowdon, L.R. (1978). Diagenesis of organic matter and fine clay minerals: a comparative study. *Geochimica et Cosmochimica Acta*. 42, 1181-1197.
- Quirk, M.M., Wardroper, A.M.K., Wheatley, R.E., & Maxwell, J.R. (1984). Extended hopanoids in peat environments. *Chemical Geology* 42, 25-43.
- Ratcliffe, K.T., Wright, A.M., Hallsworth, C., Morton, A., Zaitlin, B.A., Potocki, D., & Wray D.S. (2004). Alternative correlation techniques in the petroleum industry: An example from the (Lower Cretaceous) Basal Quartz, Southern Alberta. *AAPG Bulletin*, 88, 419-432.
- Reimann, C., & De Caritat P. (1998). *Chemical Elements in the Environment*. New York, NY: Springer-Verlag.
- Reyment, R.A. (1965). *Aspects of the Geology of Nigeria*. Nigeria: University of Ibadan Press.
- Rojas, K.M.K., Niemann, M., Palmowski, D., Peters, K., & Stankiewicz, A. (2011). Basic Petroleum Geochemistry for Source Rock Evaluation *Oilfield Review Summer* 23, 32-43.
- Roser, B.P., & Korsch, R.J. (1986). Determination of tectonic setting of sandstone-mudstone suites using SiO₂ content and K₂O/Na₂O ratio. *Journal of Geology*, 94, 635-650.

- Ross, D.J.K., & Bustin, R.M. (2009). Investigating the use of sedimentary geochemical proxies for palaeoenvironment interpretation of thermally mature organic-rich strata: examples from the Devonian-Mississippian shales, Western Canadian Sedimentary Basin. *Chemical Geology*, 260, 1-19.
- Roy, D.K., & Roser, B.P. (2013). Climatic control on the composition of Carboniferous-Permian Gondwana sediments, Khalaspir basin, Bangladesh. *Gondwana Research* 23, 1163-1171.
- Ruebsam, W., Dickson, A.J. Hoyer, E. M., & Schwark. L. (2017). Multiproxy reconstruction of oceanographic conditions in the southern epeiric Kupferschiefer Sea (Late Permian) based on redox-sensitive trace elements, molybdenum isotopes and biomarkers. *Gondwana Research*, 4, 205-218.
- Sarki Yandoka, B.M., Abdullah, W.H., Abubakar M.B., Hakimi, M.H., & Adegoke, A.K. (2015a). Geochemistry of the Cretaceous coals from Lamja Formation, Yola Sub-basin, Northern Benue Trough, NE Nigeria: Implications for paleoenvironment, paleoclimate and tectonic setting. *Journal of African Earth Sciences*, 104, 56-70.
- Sarki Yandoka, B.M., Abdullah, W.H., Abubakar, M.B., Hakimi, M.H., Jauro, A., & Adegoke, K.A. (2016). Organic geochemical characterisation of shallow marine Cretaceous formations from Yola Sub-basin, Northern Benue Trough, NE Nigeria. *Journal of African Earth Sciences*, 117, 235-251.
- Sarki Yandoka, B.M., Abdullah, W.H., Abubakar, M.B., Hakimi, M.H., Jauro, A., & Adegoke, K.A. (2014). Facies analysis, palaeoenvironmental reconstruction and stratigraphic development of the Early Cretaceous sediments (Lower Bima Member) in the Yola Sub-basin, Northern Benue Trough, NE Nigeria. *Journal of African Earth Sciences*, 96, 168-179.
- Sarki Yandoka, B.M., Abubakar, M.B., Abdullah, W.H., Maigari, A.S., & Aliyu, A.H. (2015b). Sedimentology, geochemistry and paleoenvironmental reconstruction of the Cretaceous Yolde formation from Yola Sub-basin, Northern Benue Trough, NE Nigeria. *Marine and Petroleum Geology*, 67, 663-677.
- Scalan, R.S., & Smith, J.E. (1970). An improved measure of the odd-to-even predominance in the normal alkanes of sediment extracts and petroleum. *Geochimica et Cosmochimica Acta*, 34, 611-620.
- Schenk, H.J., Horsfield, B., Krooss, B., Schaefer, R.G., & Schwochau, K. (1997). Kinetics of petroleum formation and cracking. In: D.H. Welte, B. Horsfield, & D.R. Backer (Eds.), *Petroleum and Basin Evolution; Insights from Petroleum Geochemistry, Geology and Basin Modeling*. Berlin: Springer.
- Seifert, W.K., & Moldowan, J.M. (1981). Paleoreconstruction by biological markers *Geochimica et Cosmochimica Acta*, 45, 783-794.

- Seifert, W.K., & Moldowan, J.M. (1986). Use of biological markers in petroleum exploration. In: R. B. Johns (Eds), *Methods in Geochemistry and Geophysics*. (pp. 261–290), Amsterdam: Elsevier.
- Shu, T., Dazhen, T., Hao, X., Jianlong, L., & Xuefeng, S. (2013). Organic geochemistry and elements distribution in Dahuangshan oil shale, southern Junggar Basin: Origin of organic matter and depositional environment. *International Journal of Coal Geology* 115, 41–51.
- Sia, S.G., & Abdullah W.H. (2012). Geochemical and petrographical characteristics of low-rank Balingian coal from Sarawak, Malaysia: Its implications on depositional conditions and thermal maturity. *International Journal of Coal Geology*, 96-97, 22-38.
- Simoneit, B. R. T., Otto, A., & Wilde, V. (2003). Novel phenolic biomarker triterpenoids of fossil laticifers in Eocene brown coal from Geiseltal, Germany. *Organic Geochemistry*, 34, 121-129.
- Singh, P.K., Singh, V.K., Rajak, P.K., Singh, M.P., Naik, A.S., Raju, S.V. & Mohanty, D. (2016). Eocene lignites from Cambay basin, Western India: An excellent source of hydrocarbon. *Geoscience Frontiers*, 7, 811-819.
- Singh, P.K., Singh, M.P., Prachiti, P.K., Kalpana, M.S., Manikyamba, C., Lakshminarayana, G., Singh, A.K., & Naik, A.K. (2012). Petrographic characteristics and carbon isotopic composition of Permian coal: Implications on depositional environment of Sattupalli coalfield, Godavari Valley, India. *International Journal of Coal Geology*, 90-91, 34-42.
- Solarin, S.A., & Ozturk, I. (2016). The relationship between natural gas consumption and economic growth in OPEC members. *Renewable and Sustainable Energy Reviews*, 58, 1348-1356.
- Solli, H., BJORØY, M., LEPLAT, P., & HALL, K. (1984). Analysis of organic matter in small rock samples using combined thermal extraction and pyrolysis-gas chromatography. *Journal Analytical and Applied Pyrolysis*, 7, 101-119.
- Spackman, W. (1958). Section of Geology and Mineralogy: the maceral concept and the study of modern environments as a means of understanding the nature of coal. *Transactions of the New York Academy of Sciences*, 20, 411-423.
- Stach, E., Mackowsky, M-Th., Teichmuller, M., Taylor, G.H., Chandra, D., & Teichmuller, R. (1982). *Coal Petrology*. Gebruder Borntraeger, Berlin – Stuttgart.
- Stoneley, R. (1966). The Niger Delta region in the light of the theory of continental drift. *Geological Magazine*, 103, 386-397.
- Stopes, M.C. (1935). On the petrology of banded bituminous coals. *Fuel*, 14, 4-13.
- Suárez-Ruiz, I., Flores, D., Mendonça Filho, J.G., & Hackley P.C. (2012). Review and update of the applications of organic petrology: part 1, geological applications. *International Journal of Coal Geology*, 99, 54-112.

- Suttner, L.J., & Dutta, P.K. (1986). Alluvial sandstone composition and palaeoclimate. 1. Framework mineralogy. *Journal of Sedimentary Research*, 56, 329-345.
- Swaine, D.J. (1990). *Trace Elements in Coal*. London: Butterworths.
- Sykorova, I., Pickel, W., Christanis, K., Wolt, M., Taylor, G.H., & Flores, D., (2005). Classification of huminite- ICCP system 1994. *International Journal of Coal Geology*, 62, 85-106.
- Talbot, M.R. (1988). The origins of lacustrine oil source rocks: evidence from the lakes of tropical Africa. *Geological Society, London, Special Publications* 40, 29-43.
- Tao, H., Wang, Q., Yang, X., & Jiang, L. (2013). Provenance and tectonic setting of Late Carboniferous clastic rocks in West Junggar, Xinjiang, China: A case from the Hala-alat Mountains. *Journal of Asian Earth Sciences*, 64, 210-222.
- Tao, S., Wang, C., Du, J., Liu, L., & Chen, Z. (2015). Geochemical application of tricyclic and tetracyclic terpanes biomarkers in crude oils of NW China. *Marine and Petroleum Geology*, 67, 460-467.
- Taylor, G.H., Teichmuller, M., Davis, A., Diessel, C.F.K., Littke, R., & Robert, P. (1998). *Organic Petrology*. Gebrüder Borntraeger, Berlin.
- Teichmuller, M. (1989). The genesis of coal from view point of coal petrology. *International Journal of Coal Geology*, 2, 1-87.
- Thomas, D. (1996). Benue and Mid-African rift system: oil and gas exploration (Nigeria, part 5). <http://www.ogj.com/...5/.../exploration/nigeria-5-benue-trough-and-the-mid-af>
- Thompson, J.H. (1958). The Geology and Hydrology of Gombe, Bauchi Province. *Rec. geological. Survey. Nigeria, Kaduna, 1956*: 46-65.
- Tissot, B., Demaison, G., Masson, P., Delteil, J.R., & Combaz, A. (1980). Paleoenvironment and Petroleum Potential of Middle Cretaceous black shales in Atlantic basins: *American Association of Petroleum Geologists Bulletin*, 64, 2051-2063.
- Tissot, B.P., & Welte, D.H. (1984). *Petroleum Formation and Occurrence*, second ed. New York: Springer.
- Traverse, A. (1988). *Paleopalynology*. Boston Unwin Hyman, London Sydney Wellington.
- Tribovillard, N., Ramdani, A., & Trentesaux, A. (2005). Controls on organic accumulation in Late Jurassic shales of northwestern Europe as inferred from trace-metal geochemistry. In: N. Harris (Eds.), *The Deposition of Organic-Carbon-Rich Sediments: Models, Mechanisms, and Consequences*. SEPM Special Publication 821, 45-164.

- Tyson, R. V. (1995). *Sedimentary organic matter, organic facies and palynofacies*. Chapman and Hall. Longman.
- Van Aarssen, B.G.K., Hessels, J.K.C., Abbink, O.A., & De Leeuw, J.W. (1992). The occurrence of polycyclic sesqui-, tri-, and oligo terpenoids derived from a resinous polymeric cardinene in crude oils from Southeast Asia. *Geochimica et Cosmochimica Acta*, 56, 1231-1246.
- Van Krevelen, D.W. (1961). *Coal*: New York, NY: Elsevier.
- Volkman, J.K. (1988). Biological marker compounds as indicators of the depositional environments of petroleum source rocks. In: A.J. Fleet, K. Kelts & M.R. Talbot *Lacustrine Petroleum Source Rocks* (pp. 103-122). Oxford: Blackwell.
- Volkman, J.K. (1986). A review of sterol biomarkers for marine and terrigenous organic matter. *Organic Geochemistry*, 9, 83-89.
- Wan Hasiah, A. (2002). Organic petrological characteristics of limnic and paralic coals of Sarawak. *Bulletin of the Geological Society of Malaysia*, 45, 65-69.
- Wang, A.H. (1996). Discriminant effect of sedimentary environment by the Sr/Ba ratio of different existing forms. *Acta Sedimentologica Sinica*, 14, 168-173.
- Wang, S., Dong, D., Wang, Y., Li, X., Huang, J., & Guan Q. (2016). Sedimentary geochemical proxies for paleoenvironment interpretation of organic-rich shale: A case study of the Lower Silurian Longmaxi Formation, Southern Sichuan Basin, *China Shufang Journal of Natural Gas Science and Engineering*, 28, 691-699.
- Waples, D.W., & Machihara, T. (1991). *Biomarkers for Geologists*. AAPG, Tulsa, Oklahoma.
- White, D., & Thiessen, R. (1913). *The origin of coal*. U.S. Bureau of Mines Bulletin, 38, 390.
- Wilkins, R.W.T., & George S.C. (2002). Coal as a source rock for oil: a review. *International Journal of Coal Geology*, 50, 317-361.
- Wood, D.G., Gabriel, A.M., & Lawson, J.C. (1996). Palynological techniques - processing and microscopy. In: J. Jansonius, & D.C. McGregor, (Eds.), *Palynology: Principles and applications* (pp. 29-50), AASP Foundation.
- Yang, J., Kunito, T., Anan, Y., Tanabe, S., & Miyasaki, N. (2004). Total and subcellular distribution of trace elements in the liver of a mother-fetus pair of Dall's porpoises (*Phocoenoides dalli*). *Marine Pollution Bulletin*, 48, 1122-1129.
- Yi, L., Feng, J., Qin, Y.H., & Li, W.Y. (2017). Prediction of elemental composition of coal using proximate analysis. *Fuel*, 193, 315-321.
- Zaborski, P.M. (2003). "Guide to the Cretaceous System in the Upper Part of the Upper Benue Trough, Northeastern Nigeria," *African Geosciences Review*, 10, 13-32.

- Zaborski, P.M., Ugoduluwa, F., Idornigie, A., Nnabo, P., & Ibe, K. (1997). Stratigraphy and structure of the Cretaceous Gongola Basin, Northeastern Nigeria. *Bulletin des Centres de Recherches Exploration-Production Elf – Aquitaine*, 21, 153-185.
- Zonneveld, K.A.F., Versteegh, G.J.M., Kasten, S., Eglinton, T.I., Emeis, K.C., Huguet, C., Wakeham, S.G. (2010). Selective preservation of organic matter in marine environments: processes and impact on the sedimentary record. *Biogeosciences* 7, 483-511.
- Zulkifley, M.T.M., Ng, T.F., Abdullah, W.H., Raj, J.K., Param, S.P., Hashim, R., & Ashraf, M.A. (2013). Distribution, Classification, Petrological and Related Geochemical (SRA) Characteristics of a Tropical Lowland Peat Dome in the Kota Samarahan-Asajaya area, West Sarawak, Malaysia. *Central European Journal of Geosciences*, 5, 285-314.
- Zulkifley, M.T.M., Ng, T.F., Abdullah, W.H., Raj, J.K., Shuib, M.K., Ghani, A.A., & Ashraf, M.A. (2015). Geochemical characteristics of a tropical lowland peat dome in the Kota Samarahan-Asajaya area, West Sarawak, Malaysia. *Environmental Earth Science*, 73, 1443-1458.

University of Malaysia

LIST OF PUBLICATIONS AND PAPERS PRESENTED

The following is the list of published papers pertaining to this thesis research topic:

1. Ayinla, H.A., Abdullah, W.H., Makeen, Y.M., Abubakar, M.B., Jauro, A., Sarki Yandoka, B.M., Mustapha, K.A., & Zainal Abidin, N. S. (2017a). Source rock characteristics, depositional setting and hydrocarbon generation potential of Cretaceous coals and organic rich mudstones from Gombe Formation, Gongola Sub-basin, Northern Benue Trough, NE Nigeria. *International Journal of Coal Geology*, 173, 212-226.
2. Ayinla, H.A., Abdullah, W.H., Makeen, Y.M., Abubakar, M.B., Jauro, A., Sarki Yandoka, B.M., & Zainal Abidin, N.S. (2017b). Petrographic and geochemical characterization of the Upper Cretaceous coal and mudstones of Gombe Formation, Gongola Sub-basin, Northern Benue Trough Nigeria: Implication for organic matter preservation, paleodepositional environment and tectonic settings. *International Journal of Coal Geology*, 180, 67-82.